

~~SECRET~~ [REDACTED]

14 000231560

[REDACTED]

FEASIBILITY STUDY FINAL REPORT

**GEODETTIC ORBITAL
PHOTOGRAPHIC
SATELLITE SYSTEM**

VOLUME 2 DATA COLLECTION SYSTEMS

JUNE 1966

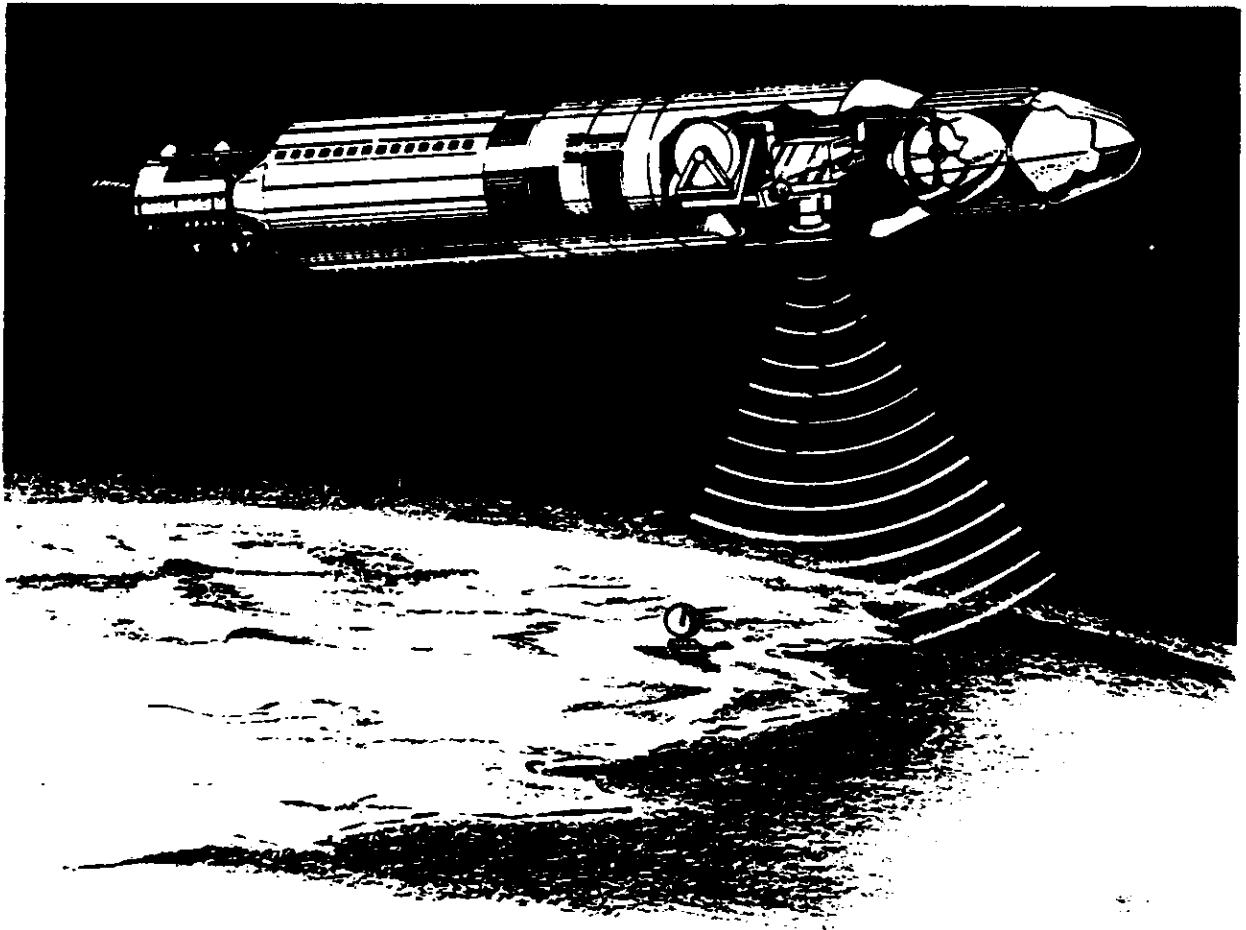
Declassified and Released by the N R O

In Accordance with E. O. 12958

on NOV 26 1997

~~SECRET~~ [REDACTED]

~~SECRET~~



Geodetic Orbital Photographic Satellite System

~~SECRET~~

CONTENTS

	Page
2.1	Introduction 2-1
2.2	Data Collection Subsystems 2-3
2.2.1	Photo-Optical Sensor 2-3
2.2.1.1	Lens Design, Fabrication, and Test 2-3
2.2.1.1.1	Lens Design 2-3
2.2.1.1.2	Lens Fabrication and Test 2-22
2.2.1.2	Photo-Optical System Analysis 2-33
2.2.1.2.1	Terrestrial Camera Performance 2-34
2.2.1.2.2	Stellar Camera Performance 2-68
2.2.1.2.3	Experimental Investigations 2-78
2.2.1.2.4	Influence of Image Quality on Measurement Accuracy 2-93
2.2.1.3	Photo-Sensor Preliminary Design 2-103
2.2.1.3.1	Photo-Sensor Description 2-103
2.2.1.3.2	Photo-Sensor Subsystems 2-103
2.2.1.4	Auxiliary Systems 2-180
2.2.1.4.1	TRANSIT Transmitter 2-181
2.2.1.4.2	General Description—SCI Radar Altimeter 2-182
2.2.1.4.3	Accelerometer 2-184
2.2.1.4.4	System Clock 2-189
2.2.1.4.5	Data Recording Systems 2-190
2.2.1.4.6	System Performance Monitoring (Confidence Module) 2-197
2.3	GOPSS System Integration 2-201
2.3.1	System Configuration 2-201
2.3.1.1	Orbital Control Vehicle 2-201
2.3.1.2	Data Collection Module 2-203
2.3.1.3	Recovery Section 2-204
2.3.2	Mission Operation and Coverage 2-211
2.3.2.1	Mission Modes 2-211
2.3.2.2	Mission Coverage 2-214
2.3.3	System Power Budget 2-216
2.3.4	System Weight and Balance 2-218
2.3.4.1	System Weight 2-218
2.3.4.2	System Centers of Gravity and Inertias 2-218
2.4	Supporting Studies 2-223
2.4.1	Payload Structural Study 2-223
2.4.1.1	Recovery Section 2-223

	Page
2.4.1.2 Data Collection Module	2-224
2.4.1.3 Camera Support	2-224
2.4.1.4 Film Supply Cassette	2-225
2.4.1.5 Terrestrial Camera Platen and Pressure Mechanism	2-225
2.4.2 Thermal Analysis	2-226
2.4.2.1 Summary	2-226
2.4.2.2 Results	2-226
2.4.2.3 Analytical Methods	2-226
2.4.2.3.1 Nodal Program	2-226
2.4.2.3.2 Nodal Models	2-227
2.4.2.4 Environment	2-228
2.4.2.5 Analytical Studies	2-236
2.4.2.5.1 Terrestrial Camera	2-236
2.4.2.5.2 Stellar Camera	2-245
2.4.2.5.3 Data Collection Module (DCM)	2-249

FIGURES

	Page
2-1	GOPSS Lens Design 2-7
2-2(a)	Ray Trace Plots for GOPSS Lens Design (On-Axis to 4 Inches Off-Axis) 2-8
2-2(b)	Ray Trace Plots for GOPSS Lens Design (6 Inches to 10 Inches Off-Axis) 2-9
2-3	Distortion Plot. 2-10
2-4(a)	Geometrical Frequency Response: Semifield Height = 10.0 Inches, Deflection = +0.002 Inch, Spectral Region = 0.60 to 0.70 Micron 2-11
2-4(b)	Geometrical Frequency Response: Semifield Height = 8.5 Inches, Deflection = +0.002 Inch, Spectral Region = 0.60 to 0.70 Micron 2-12
2-4(c)	Geometrical Frequency Response: Semifield Height = 7.0 Inches, Deflection = +0.002 Inch, Spectral Region = 0.60 to 0.70 Micron 2-13
2-4(d)	Geometrical Frequency Response: Semifield Height = 3.5 Inches, Deflection = +0.002 Inch, Spectral Region = 0.60 to 0.70 Micron 2-14
2-4(e)	Geometrical Frequency Response: Semifield Height = 0.0 Inch, Deflection = +0.002 Inch, Spectral Region = 0.60 to 0.70 Micron 2-15
2-5	Effects of Change in Position of the Front Element. 2-16
2-6	Effects of Change in Position of the Front Half of the Lens 2-17
2-7	Effects of Change in Position of Lens Relative to the Platen 2-17
2-8	Thermal Behavior of Terrestrial Camera in Vacuum (Cell Material-Beryllium) 2-20
2-9	Special Center-Thickness Measuring Fixture 2-23
2-10	Image Sensitivities Relative to Present Measuring Techniques (Assuming 30-Microinch Gauge Error and 25-Microinch Table Run-Out Error) 2-24
2-11	Positioning of Triplet Elements During Cementing Process (Computer- Generated Drawing) 2-25
2-12	Element Fabrication 2-27
2-13	Aspheric Measuring Machine 2-28
2-14	Aspheric Measuring Machine, Overall Setup 2-29
2-15	Aspheric Measuring Machine, Servo Block Diagram 2-30
2-16	Cementing Jigs and Fixtures 2-31
2-17	Resolution and Distortion Measuring Bench 2-35
2-18	Allowable Amplitude of Single-Frequency Vibrations (Based on ± 1 Percent of V/h Allowable Blur Rate; $fV/h = 7.9$ Millimeters Per Second; Exposure Time = 11.5 Milliseconds) 2-39
2-19	Image Motion Variations Along the Fore and Aft Axis From Distortion and Platen Motion as a Function of Image Position in Format 2-41

2-20 Maximum and Minimum Image Velocity Variations Along- and Across-Track, as Functions of Fore and Aft Format Position From Distortion, Platen Motion, and Earth's Curvature (160-Nautical Mile Altitude) 2-42

2-21 Systematic Image Velocity Variations Along- and Across-Track From Distortion, Platen Motion, and Earth's Curvature as a Function of Radial Position in Image Plane (160-Nautical Mile Altitude) 2-43

2-22 Required Exposure Times for a T/12 System With a W-25 Filter 2-47

2-23 Resolution Versus Blur 2-49

2-24 Image Plane Resolution Versus Image Position for Final Design 2-50

2-25 Ground Resolved Distance as a Function of Format Position 2-51

2-26 Effective AIM Curves for EK Type 3400 Film, Modified for Contrast Level and Blur Superimposed Upon Final Design Transfer Function 2-52

2-27 Spectral Reflectance Properties of Natural Formations (From E. L. Krinov) 2-55

2-28 Relative Intensity Profiles for Monochromatic Objects to Shadows on Grass, Snow, and a Neutral Surface 2-57

2-29 Cumulative Distribution of Stars by Visual Magnitude 2-67

2-30 Effect of Varying Roentgen Dosage on Kodak Royal-X Pan Film, 1000 kvp Hardened X-Rays 2-69

2-31 Effect of Varying Roentgen Dosage on Kodak Plus-X Aerecon Film, 1000 kvp Hardened X-Rays 2-70

2-32 Accuracy of Orientation in Pointing Determined by a Stellar Camera as a Function of the Number of Stars Recorded and Measured 2-72

2-33 Wild Falconar 250 Lens 2-74

2-34 Recordable Star Magnitudes for 45-Degree Stellar Camera Orientation 2-77

2-35 Test Results of AIM Curve Extension 2-81

2-36 Photograph of Stars in Pleides 2-83

2-37 Stars in Pleides From Star Catalog 2-84

2-38 Experimental Setup for Observing Film Topograph 2-86

2-39 Film Topograph of EK Type 4400 Film: 30 Durometer Rubber Pressure Pad; 0.3 psi Pressure 2-87

2-40 Topograph of EK Ultraflat High Resolution Plate 2-89

2-41 Vacuum Test Apparatus Setup 2-90

2-42 Topograph of 70-Millimeter EK Type 3404 Film: 18 Durometer Rubber Pressure Pad; 0.3 psi Pressure 2-91

2-43 Topograph of 70-Millimeter Ultrathin Base Film: 18 Durometer Rubber Pressure Pad; 0.3 psi Pressure 2-92

2-44 Topograph of EK Type 3404 Film: Optical Glass, Flat Pressure Pad; 1.5 psi Pressure 2-94

2-45 Contact Print of Target Area (Detail Reversed Right to Left) 2-95

2-46 Diagram of Photographic System 2-97

2-47 Image Photometric Functions 2-102

2-48 Primary and Secondary Camera Assembly 2-105

2-49 Platen and Pressure Plate Mechanism 2-111

	Page
2-50	IMC Drive Assembly 2-113
2-51	Terrestrial Camera Shutter 2-116
2-52	Shutter Operation 2-119
2-53	Arming Motor Loading Cycle 2-122
2-54	Stress Levels Versus rpm for Steel, Aluminum and Beryllium 2-123
2-55	Location of Critical Frequencies, Terrestrial Shutter 2-125
2-56	Synchronization and Control Block Diagram for Terrestrial and Stellar Cameras 2-126
2-57	Intervalometer Servo Schematic 2-130
2-58	Platen Servo Schematic 2-131
2-59	Shutter Servo Schematic 2-134
2-60	Terrestrial Camera Fiducial Marker 2-137
2-61	Stellar Camera Configuration 2-139
2-62	Stellar Shutter 2-143
2-63	Acceleration Rates of Stellar Shutter Motors Considered 2-146
2-64	Terrestrial Film Transport System, Block Diagram 2-149
2-65	Stellar Film Transport System, Block Diagram 2-151
2-66	Supply Cassette 2-154
2-67	Spool Power Drive 2-155
2-68	Spool Brake System 2-156
2-69	Takeup Cassette 2-159
2-70	Stellar Camera Thermal Shutter 2-161
2-71	Camera Control and Synchronization System Block Diagram 2-167
2-72	Camera System Functional Schematic 2-171
2-73	Mode I Operation Timing Diagram; Frame Time: 14.45 Seconds 2-175
2-74	Mode I Operation Timing Diagram; Frame Time: 22.0 Seconds 2-176
2-75	Mode IV Operation Timing Diagram; Frame Time: 14.45 Seconds 2-177
2-76	Radar Altimeter Block Diagram 2-183
2-77	Primary Mechanical Elements - MESA 2-186
2-78	Pickoff System - MESA 2-186
2-79	Optical Recorder Assembly 2-193
2-80	Mission Data Block Recorder 2-195
2-81	In-Flight Confidence Block Diagram 2-198
2-82	System Configuration 2-202
2-83	Data Collection Module (DCM) 2-205
2-84	Recovery Vehicle Inline Configuration 2-207
2-85	Recovery Vehicle, Canted Configuration 2-209
2-86	Cutter/Sealer Assembly 2-212
2-87	Terrestrial Camera Nodal Model 1 2-229
2-88	Terrestrial Camera Nodal Model 2 2-230
2-89(a)	Terrestrial Camera Nodal Model 3, Primary Camera 2-231
2-89(b)	Terrestrial Camera Nodal Model 3, Primary Shutter 2-233
2-90	Stellar Camera Nodal Model 2-234
2-91	Simplified DCM Thermal Model 2-235
2-92	Temperature of Element Number 1 When Subjected to Infrared Heat Flux 2-237
2-93	Lens System Temperature Response for Model 1 (Fig. 2-87) 2-238



		Page
2-94	Lens System Temperature Response for Model 1 (Fig. 2-87)	2-239
2-95	Lens System Temperature Response for Model 1 (Fig. 2-87)	2-240
2-96	Lens System Temperature Response for Model 2 (Fig. 2-88)	2-241
2-97	Lens System Temperature Response With Thermal Shutter	2-243
2-98	Terrestrial Camera Shutter and Motor Temperatures	2-246
2-99	Lens Element 1 Nodal Scheme	2-247
2-100	Lens Element 1 Radial Temperature Gradients	2-248
2-101	Lens Element 1 Temperature Gradient After Each 90-Minute Cycle	2-250
2-102	Camera Box Temperature Response, Case 142	2-251
2-103	Camera Box Temperature Response, Case 3	2-252



TABLES

	Page
2-1	Comparison of Proposed and Final GOPSS Lens Design 2-4
2-2	Final Lens Design Specification Sheet (9240 Wide Angle System, Melt 1A) 2-6
2-3	Effects of Tilt, Decenter, and Spacing Error 2-16
2-4	Blur Budget for Terrestrial Camera ($V/h = 0.035$ rad/sec) 2-37
2-5	Summary of Systematic Image Motions 2-44
2-6	Exposure Times for a 20-Degree Scan Angle 2-46
2-7	Resolution Values 2-54
2-8	Camera Mechanism Tolerances 2-58
2-9	RSS Random Image Position Errors at Various Format Positions and Orientations, Microns 2-58
2-10	Terrestrial Camera Image Position Errors From Camera Geometry Changes 2-61
2-11	Thermal Tolerance Budget for the Terrestrial Camera 2-65
2-12	Resolution at High Contrast for Gevapon 30 Film 2-75
2-13	Resolutions Obtained on EK 3401 High Contrast Film 2-75
2-14	Test Results of AIM Curve Extension 2-80
2-14(a)	Stereoscopic Pair 2-99
2-15	Terrestrial Camera Leading Particulars 2-107
2-16	Stellar Camera Leading Particulars 2-108
2-17	Performance Specifications for the Terrestrial Camera Control System 2-129
2-18	Photographic System Modes of Operation 2-166
2-19	Comparison of Data Recorders 2-191
2-20	Dual Mark V Recovery System Coverage 2-215
2-21	Dual Mark VIII Recovery System Coverage 2-215
2-22	System Weight—Canted Configuration 2-220
2-23	System Weight—Inline Configuration 2-221
2-24	Terrestrial Camera Lens Temperatures With Thermal Shutter Cycling 2-244
2-25	Terrestrial Camera Lens and Lens Cell Temperatures With Thermal Shutter Cycling 2-244
2-26	Stellar Camera Temperatures 2-250

PREFACE

The objective of the Geodetic Orbital Photographic Satellite System (GOPSS) is to accurately determine the location of landmarks widely distributed over the earth's surface and provide better information concerning the geophysical parameters which affect this system and other systems operating at similar altitudes. The means chosen to accomplish this objective is to orbit a series of data acquisition systems supported by ground-based instrumentation. The data gathered by this system is incorporated into a sophisticated data reduction scheme which determines the geodynamic parameters and landmark locations.

Detailed studies were conducted to determine the feasibility of the GOPSS. The study period was designated as Phase I, and the results of these studies have been compiled into five volumes for reader convenience.

This volume describes the effort for implementation of the data acquisition requirements for the GOPSS program. This volume presents the preliminary design which defines and describes the various sensors, considers their functional interdependencies, and shows their evolution into an integrated GOPSS.

The division of the remaining volumes and their content are now briefly described for information and reference purposes.

Volume 1, Program Compendium and Conclusions, was prepared to provide briefly the details essential to a comprehensive understanding of the effort conducted during Phase I of the GOPSS feasibility study. System concept and objectives are described plus conclusions which concern the attainment or modification of the initial objectives, along with recommendations for a system configuration and a solution of the attendant data handling problems.

Volume 3, Data Reduction, Part 1, considers the photogrammetric data subject to constraints imposed by orbital and auxiliary data, the mapping capabilities of the system, and ground handling of mission photography.

Volume 4, Data Reduction, Part 2, discusses orbital considerations affecting the feasibility of the GOPSS. Physical models and computational procedures are reviewed and error studies involving typical sensor and model inaccuracies are described. Based on these studies, recommendations are made for tracking networks, auxiliary on-board sensors, and detailed orbit plans. In addition, the data reduction procedure whereby the acquired data are simultaneously located to yield geodynamic parameters and landmark locations is considered.

Volume 5, Program Plan, Phases II-V, describes the planning activity as it has been programmed through Phases II to V for the engineering, fabrication, and operational support for the delivery of five systems. Continuing studies which are required are also recommended in this volume.

SUMMARY

A data collection system implements the data gathering phase of the GOPSS program through the use of an orbiting metric camera which photographs all continental land masses and islands, and through auxiliary satellite sensors to provide detail data on satellite position supported by ground based tracking instrumentation.

A preliminary design of the data collection system was completed during the feasibility study. Individual tasks which were accomplished during the study were: (1) the design of a metric lens (fabrication and test are scheduled for completion in February 1967); (2) the preliminary design of a photo-sensor system; (3) a photo-optical analysis to determine the performance of the camera system; (4) an evaluation and selection of auxiliary satellite sensors; and (5) the preliminary design of a recovery section to provide a means of retrieval for photographic data.

The final task was the integration of the sensors into a data collection module, ensuring its design integrity with the recovery section which contains the recovery vehicles, and the interface of both these subsystems to the orbiting control vehicle to accomplish the required system performance.

To establish the required photogrammetric capability, a wide-angle lens has been designed and is being fabricated for the camera system. Lens design progressed through four versions of a 300-millimeter focal length, 80-degree field system. The final selected configuration has three aspheric surfaces, and will yield a 70-line per millimeter AWAR at 1.6:1 contrast on EK type 3404 film.

The resultant photo-sensor system consists of a terrestrial photogrammetric camera and a twin stellar camera which provides a precise attitude reference for the photo-sensor system.

The terrestrial camera consists of the Itek-designed 300-millimeter focal length, $f/6.0$, wide-angle lens, shutter, IMC drive, platen assembly, film transport assembly, and connecting structure. The twin stellar camera, constructed as a single unit, uses two 250-millimeter focal length, $f/1.8$ modified Wild Falconar lens assemblies, and is bolted directly to the terrestrial central cell section with the rigidity required to maintain the calibrated knee angles between all three lenses. The stellar lenses are 90 degrees apart, ± 45 degrees from the roll axis; they are pointed forward and are elevated 10 degrees with respect to the horizontal.

Lens and camera design factors and environmental factors were analyzed to determine photogrammetric accuracy predictions from all contributing sources. These errors are reflected in an overall system performance estimate. Experimental investigations were also conducted concerning the extension of the ADM curves, film flatness, experimental star recording, and the influence of image quality on measurement accuracy.

The detailed photo-optical analysis of the camera system performance indicates that a minimum resolution of 40 lines per millimeter will be maintained at a 20-degree sun angle on EK 4404 and that 30 lines per millimeter will be maintained at a 5-degree sun angle with EK 3400.

The auxiliary equipment required to implement to the GOPSS operation are configured into the overall payload package. These equipments are the TRANSIT transmitter, radar altimeter, low-g accelerometer, precision clock, and mission data recorder.

Inclusion of the TRANSIT transmitter in the orbiting package allows Doppler tracking by the TRANSIT network. The use of low-g accelerometers aboard the satellite will provide direct information on nongravitational forces acting on the vehicle. The radar altimeter is a complete on-board tracking system which provides an altitude measurement to an accuracy of 10 meters, providing needed information to the photogrammetry and measurement of the geoid fluctuations over the surface of the oceans. The recorder stores time, altitude, and other mission data which will serve as inputs in the data reduction scheme, and has the capability to collect a large quantity of information in small increments. The system clock is a precision oscillator which provides an absolute time reference of less than 1-millisecond error over the entire mission.

The subsystems which comprise the photographic satellite system (see frontispiece) consist of the Orbiting Control Vehicle (OCV), Data Collection Module (DCM), and the Recovery Section (RS).

The OCV provides the required on-orbit propulsion, satellite stability, payload power, and mission control. The OCV sensors provide the signals from which the vehicle is stabilized in roll and yaw, and pitched at a controlled rate. The OCV programmer operates the subsystem equipments through the use of mode signals in any one of four data gathering modes. Two additional photosensor signals, V/h and exposure (t_e), are also supplied from the OCV.

The DCM is connected directly to the front of the OCV and contains the photosensors, radar altimeter, TRANSIT transmitter and clock, and houses the film supply spools. The DCM bay is a cylindrical structure of monocoque design, which is thermally insulated and contains fore and aft fiberglass bulkheads for thermal and light sealing purposes. The payload electronics, radar altimeter, and transponder are packaged as modular units and mounted to the DCM structure. The radar altimeter antenna is mounted below the supply cassettes with its axis pointed down along a yaw axis.

The RS is attached to the forward end of the DCM structure. This section contains the recovery vehicles (RV), each with a recoverable film payload. Two RV configurations were developed, one which has the RV's in line along the roll axis, and the other, the "canted," which has each RV pointed down 60 degrees from the horizontal and aft; the "canted" configuration eliminates the necessity of adjusting the pitch of the vehicle prior to recovery. Each RV contains a recoverable payload consisting of a takeup cassette with spools for 9 1/2-inch wide terrestrial film and 70-millimeter stellar film, and a recorder for electronic data storage. A combination cutter and seal is mounted on the bulkhead of each RV to cut the film path and seal the water-tight compartment.

2.1 INTRODUCTION

A data collection system is required to gather inputs for the implementation of the objectives of the GOPSS program. This system consists of both satellite-borne sensors and ground tracking instrumentation which supplement each other in orbit determination and in determining the precise location of ground points which will be compiled into a landmark catalog.

Based on the input data determined to be required by the systems analysis of this study, a data collection system was developed which defined the employment of a photosensor, the auxiliary sensors and the ground-based instrumentation that would be necessary and compatible within the prescribed operational environment. Specifics were generated for the individual sensors, functional interdependencies of these sensors were considered, and finally but most important, was the evolution of the satellite-borne sensors into an integrated payload, properly interfaced with the orbital control vehicle.

Within this integrated concept, Itek developed a payload system responsibility which considered all equipment forward of the orbiting control vehicle as a single assembly. This assembly comprises the section containing the data collection sensors and a recovery section.

Specifically, the data collection module (DCM), contains the photosensor, radar altimeter, TRANSIT transmitter, and a precision clock. The film supply spools are also located in the DCM. The photosensor is composed of a terrestrial photogrammetric camera and twin stellar camera configuration. Detailed tasks performed in this area were the design, fabrication, and test of a suitable lens for the terrestrial camera, and a photo-optical analysis to determine the performance of the photosensor system. Lens and camera design factors and environmental factors were analyzed to determine photogrammetric accuracy from all contributing sources.

The recovery section (RS), attached to the forward end of the DCM structure, contains two recovery vehicles (RV). The RV's contain a recoverable film payload which is spooled into a takeup cassette, and a mission data recorder. A combination cutter and seal on the RV cuts the film and seals the RV to ensure a water-tight compartment.

This volume then describes the effort for implementation of the data collection requirements for the GOPSS program.

2.2 DATA COLLECTION SUBSYSTEMS

2.2.1 Photo-Optical Sensor

2.2.1.1 Lens Design, Fabrication, and Test

2.2.1.1.1 Lens Design

1. Design Evaluation

The objective of the lens design task was to design a high resolution, wide angle optical system. Photogrammetric and operational considerations prescribed a lens with a 12-inch focal length and 80-degree field, and a resolution satisfactory to achieve the feasibility program objectives. With this in mind, detail objectives were established and are listed in Table 2-1.

To attain these objectives, the lens design has evolved from the proposal stage to the final GOPSS design through a succession of significant changes and refinements, with associated upgrading of performance predictions. Initial design effort considered a potential modification of the Geocon design by J. G. Baker. This was the only lens in the patent literature that: (1) included a reseau plate, (2) had a field greater than 80 degrees, (3) was faster than $f/6.0$, (4) was shorter than three focal lengths, and (5) had a potential of meeting a minimum low contrast resolution of 25 lines per millimeter. It was setup as described in the patent literature; it was scaled to a focal length of 12.0 inches, the aperture was reduced from $f/3.5$ to $f/6.0$, and the field decreased from 94 to 80 degrees. The geometrical transfer functions were solved in three colors from 0.54 to 0.70 micron. The computed AWAR of the lens was approximately 33 lines per millimeter, and the minimum resolution, at the worst orientation point, was 7 lines per millimeter at 1.6:1 contrast on Eastman Kodak (EK) type 3404 film. This lens was designed for negligible distortion and a flat field. Relaxing these requirements as well as optimizing for the lens f /number, field, spectral range, and film choice resulted in an increase in AWAR from 33 to 75 lines per millimeter at the expense of a 0.2-inch deformed image and 0.2-inch distortion. The minimum resolution remained at 7 lines per millimeter because of an oversight concerning the control of rays outside the sagittal and tangential fans. The new lens had the original high index glasses in the optical elements which are not available in the size necessary for a 12-inch focal length objective.

The first configuration studies made after the contract was awarded utilized negative elements on the outside, as exemplified by Bertele's Aviogon, Roosinov's patent, and Gray's work during World War II. A reseau plate, aspherics adjacent to the stop, and an aspheric image were utilized. The starting point was an 11-element Bertele design with a flat field, no aspherics, and minimum monochromatic resolution of 7 lines per millimeter. This design had low index glass for the outer elements and approximately $\cos^3 \theta$ illumination drop-off. The Preliminary I (P-I) design indicated that with BK-7 used in the outer elements, minimum resolutions exceeding 25 lines per millimeter would be obtained; for this reason, the Geocon approach was abandoned.

Table 2-1 — Comparison of Proposed and Final GOPSS Lens Design

	Objective	Final GOPSS Design
1. Focal length	300 millimeters	300 millimeters
2. f-ratio	f/6.0	f/6.0
3. Format	230 by 460 millimeters	230 by 460 millimeters
4. Total field angle	80 degrees	80 degrees
5. Spectral region	0.54 to 0.70 micron	0.60 to 0.70 micron
6. Film	EK 3404	EK 3400
7. Glass reseau plate	Provided	Provided
8. Reseau back and film surface	Aspheric	Flat
9. Maximum distortion	0.10 inch	0.055 inch
10. Minimum relative illumination	40 percent	40 percent
11. Elements (without reseau)	10 to 12	10
12. Aspheric surfaces	3	3
13. Low contrast (1.6:1) resolution, lines per millimeter		
a. On-axis	3404	125
	3404	64
b. Minimum over	3404	25 lines per millimeter
entire format	3400	40
		30
c. AWAR	3404	≈ 70
	3400	≈ 48
14. High contrast resolution, lines per millimeter		
a. On-axis	3404	180
	3400	112
b. Minimum over	3404	greater than 50
entire format	3400	greater than 50
c. AWAR	3404	≈100
	3400	≈ 70

The completed Preliminary II (P-II) design had a minimum resolution in all orientations, and fields of 30 lines per millimeter on a 0.012-inch sag from aspheric image surface, which was significantly flatter than the proposed value of 0.12 inch. The distortion, as measured on a flat field, was approximately 0.12 percent. Optical glass was ordered for lens fabrication specifying oversize blanks for the elements in this design.

The reduction in aspheric field sag from 0.5 inch in the proposal to 0.012 inch for the P-II design, raised the minimum resolution from 7 to 30 lines per millimeter and indicated that a 25-line per millimeter minimum on a flat field might be attainable.

The aspheric surface on the reseau plate was placed on the side opposite the film, permitting a flat field. This configuration (P-III) resulted in the first flat field design having a minimum resolution that exceeded 25 lines per millimeter (Modulation = 0.12) on EK type 3404 film at 1.6:1 contrast with a 0.54- to 0.70-micron spectral range.

To reduce the metric errors caused by the secondary lateral color blur which is proportional to the square of the spectral bandwidth, the region was reduced from the old value of 0.54 to 0.70 micron to 0.60 to 0.70 micron. This reduction in spectral bandwidth also improved the lens modulation transfer function at frequencies of 20- to 30-line per millimeter resolution.

2. Final GOPSS Lens Design

The final GOPSS Design utilizes the 0.60- to 0.70-micron spectral region and EK type 3400 film (refer to Figure 2-1). The specifications for the final lens design are given in Table 2-2. The minimum resolution on EK type 3404 film is 40 lines per millimeter on a flat field compared to the proposal estimate of 25 lines per millimeter on EK type 3404 film using a 0.1-inch deformed image surface; on-axis performance is 125 lines per millimeter with an AWAR of 70 lines per millimeter. Table 2-1 lists the performance of the final design in comparison with the initial goals. Ray-trace results and geometric transfer functions (Figures 2-2 through 2-4) show reduced higher order aberrations and chromatic blur, as well as the increased contrast in the transfer function.

3. Optical System Studies

a. Image Position Displacements Caused by Mechanical Changes

Calculations were made to determine the sensitivity of the camera calibration to small displacements of the optical components. Changes in tip, decentering, and spacing were studied (see Table 2-3). Three cases were taken as being representative: (1) the movement of the front element within its cell, (2) the movement of the front half of the lens with respect to the rest of the camera, and (3) the movement of the entire lens with respect to the platen. The front element is considered to be the most sensitive single element because of its power, size, and distance from the stop. Since the two halves of the lens cell and the platen are different structural units, the possibility of their moving relative to each other was considered.

Calculations were made, using computer ray traces where necessary, to determine the effects of 0.0001-inch decentering, 5×10^{-6} radian tip (0.0001-inch at a radius of 20 inches), and 0.0001-inch spacing change. The maximum radial image shifts are plotted as functions of image position for the three separate cases shown in Figures 2-5, 2-6, and 2-7.

Table 2-2 — Final Lens Design Specification Sheet (9240 Wide Angle System, Melt 1A)

Element Number	Surface Number	Radius, inches	Radius Tolerance, ± inches	Thickness, inches	Thickness Tolerance, inches	Airspace, inches	Airspace Tolerance, inches	Clear Aperture, inches	n*	v†	Glass Type and Melt
I	1	27.7896	0.0072	0.8000	0.0050			12.769	1.51514	64.02	BK-7 14097
	2	6.5414	0.0010			1.8500	0.0040	9.976	Air		
II	3	12.0615	0.0021	0.9437	0.0050			9.715	1.51416	64.07	BK-7 14176
	4	9.5482	0.0014			2.1725	0.0030	8.918	Air		
III	5	7.5519	0.0013	3.0022	0.0030			7.580	1.71673	50.35	LAK-10 80980/1
	6	2.5844	0.0006	0.0004				4.659	1.55063		Cement M62
IV	7	2.5844	0.0006	2.3692	0.0020			4.659	1.61508	49.72	SSK-8 310543/44
	8	-4.9491	0.0017	0.0004				4.377	1.55063		Cement M62
V	9	-4.9491	0.0017	0.9493	0.0020			4.377	1.60281	40.28	BaSF-3 13893
	10*	29.3694				0.7742		3.272	Air		
	11	-		Aperture stop		0.5602	to be adjusted	2.388	Air		Aperture stop
VI	12*	18.6093		0.5016	0.0040			3.325	1.55083	51.22	BaLF-8 13906
	13	5.5566	0.0030	0.0004				3.884	1.55063		Cement M62
VII	14	5.5566	0.0030	2.1803	0.0040			3.885	1.61079	51.24	SSK-3 330763/1
	15	-2.9840	0.0010	0.0004				4.435	1.55063		Cement M62
VIII	16	-2.9840	0.0010	0.5000	0.0020			4.435	1.71136	29.48	SF-1 340756/29, 32
	17	-6.2808	0.0020			5.8752	0.0020	5.120	Air		
IX	18	-4.9664	0.0008	0.6713	0.0040			7.876	1.51416	64.07	BK-7 14176
	19	-10.5045	0.0016			1.9500	0.0030	9.562	Air		Air
X	20	-8.3356	0.0010	0.7326	0.0040			10.202	1.51514	64.02	BK-7 14097
	21	-11.8946	0.0011			1.9255		12.640	Air		Air
XI	22†	226.1301		0.7099	0.0050			19.158	1.51483	64.06	BK-7 14102
	23	-				0.0001		20.145	Air		Air
	24	-		Image plane				20.144			

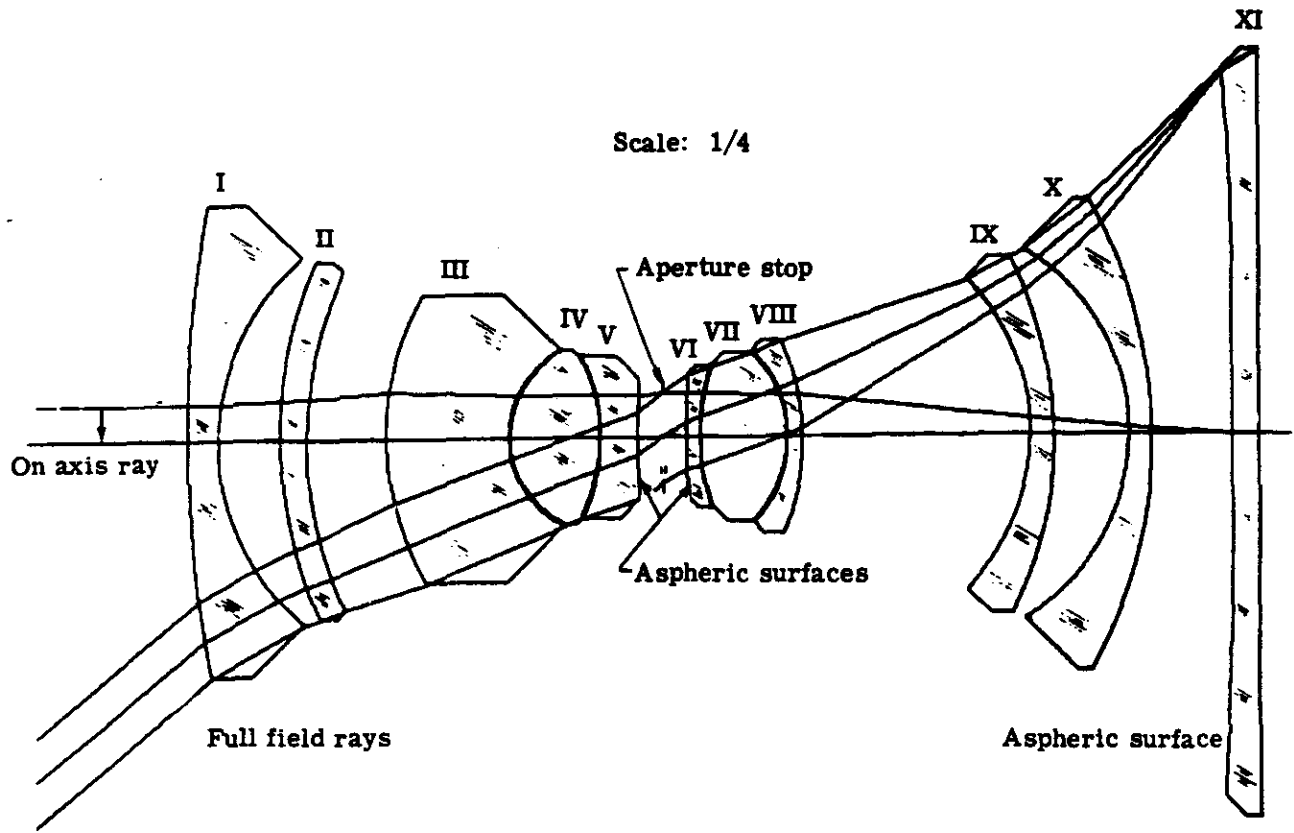
* Refractive index at 6500 angstroms

† Reciprocal dispersive power at 5876 angstroms

‡ Aspheric with coefficients as follows:

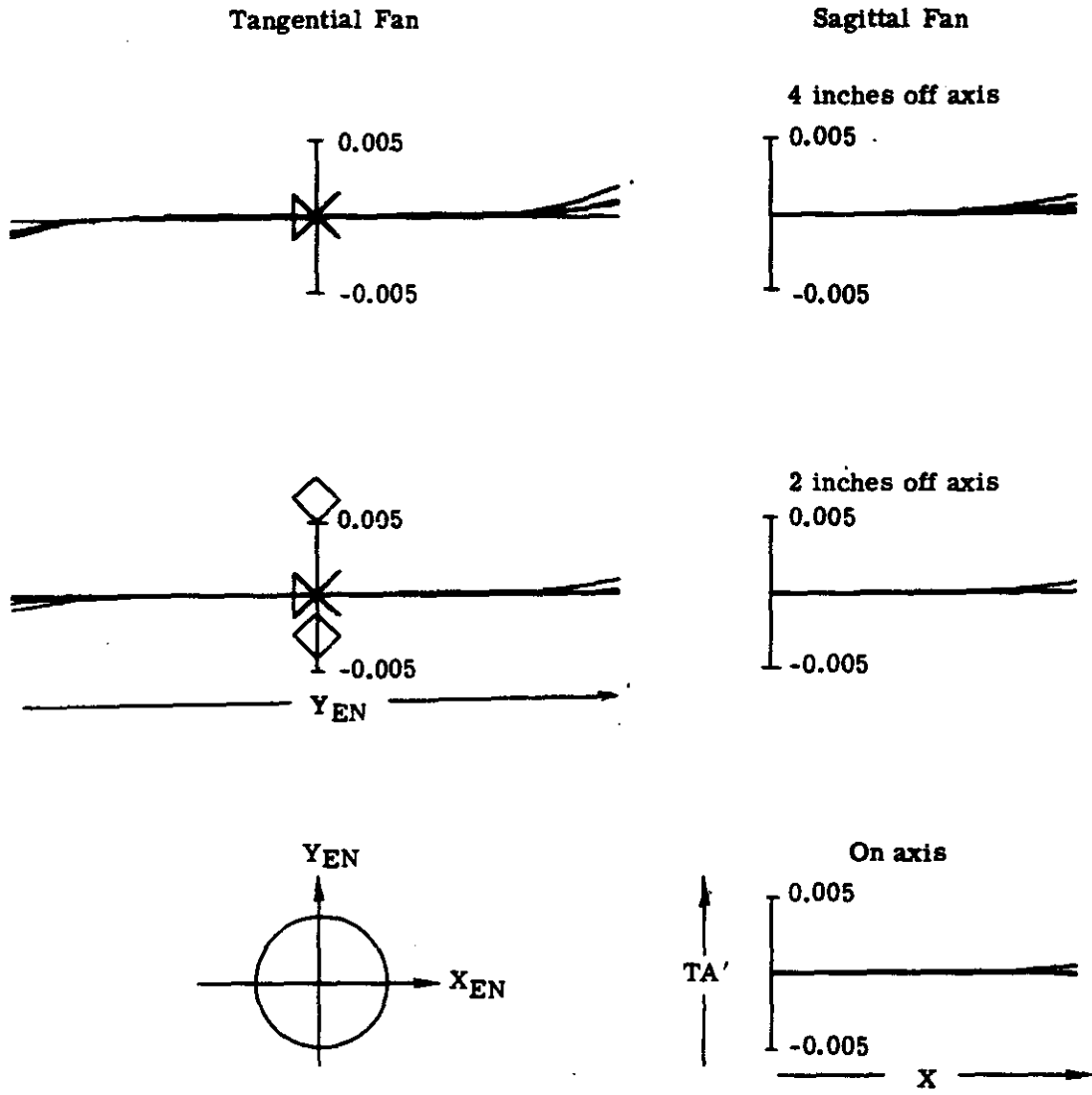
	Fourth Order	Sixth Order	Eighth Order	
Surface 10	$+2.566 \times 10^{-4}$	-7.086×10^{-5}	-1.180×10^{-5}	-7.537×10^{-7}
Surface 12	$+4.960 \times 10^{-4}$	$+1.113 \times 10^{-5}$	-2.120×10^{-6}	$+3.547 \times 10^{-7}$
Surface 22	-1.111×10^{-4}	$+5.840 \times 10^{-7}$	$+8.031 \times 10^{-10}$	0.0

§ The airspace thicknesses given will be subject to change in a redesign after the test spheres are made and measured. Elements I, II, IX, X, XI may be completely fabricated at this time using the above data. The inside triplet elements are subject to changes in central thicknesses; therefore, only one surface per element may be completely fabricated at this time.



Element	I	II	III	IV	V	VI	VII	VIII	IX	X	XI
Glass Type	BK7	BK7	LAK10	SSK8	BaSF3	BaLF8	SSK3	SF1	BK7	BK7	BK7

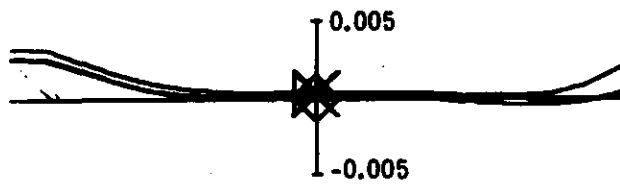
Fig. 2-1 — GOPSS lens design



NOTE: TA' = transverse aberration

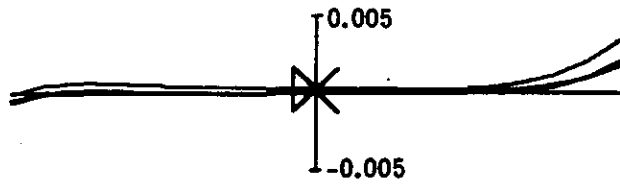
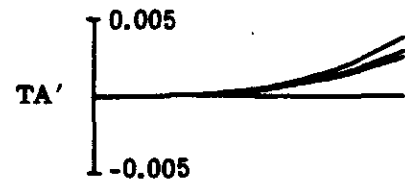
Fig. 2-2(a) — Ray trace plots for GOPSS lens design (on-axis to 4 inches off-axis)

Tangential Fan

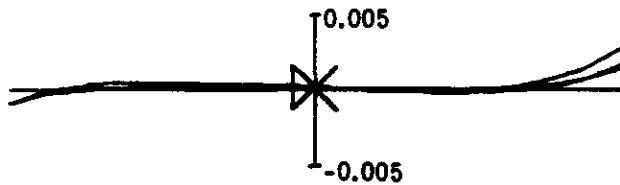
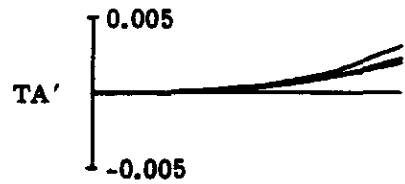


Sagittal Fan

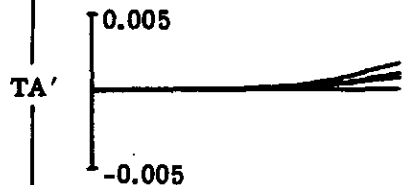
10 inches off axis



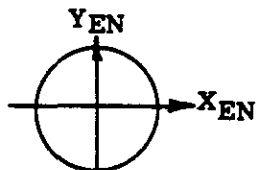
8 inches off axis



6 inches off axis



Y_{EN}



NOTE: TA' = transverse aberration

Fig. 2-2(b) — Ray trace plots for GOPSS lens design (6 inches to 10 inches off-axis)

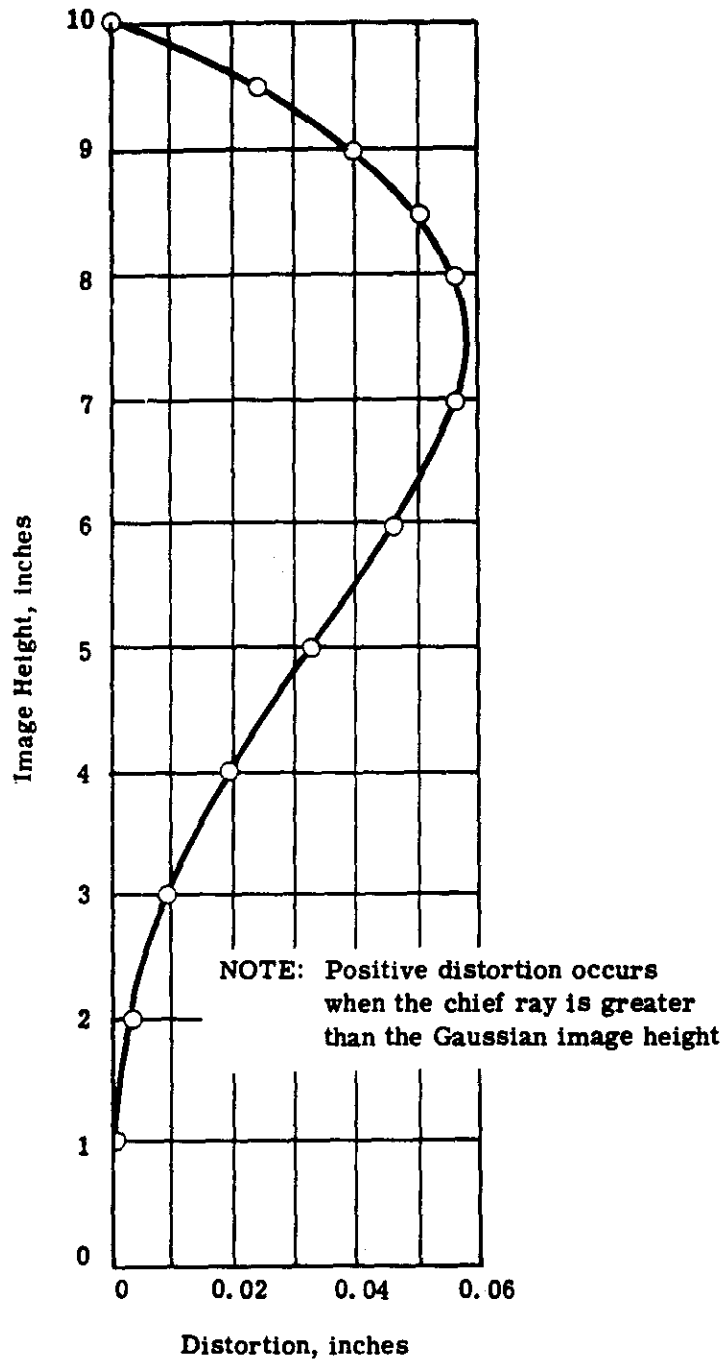


Fig. 2-3 — Distortion plot

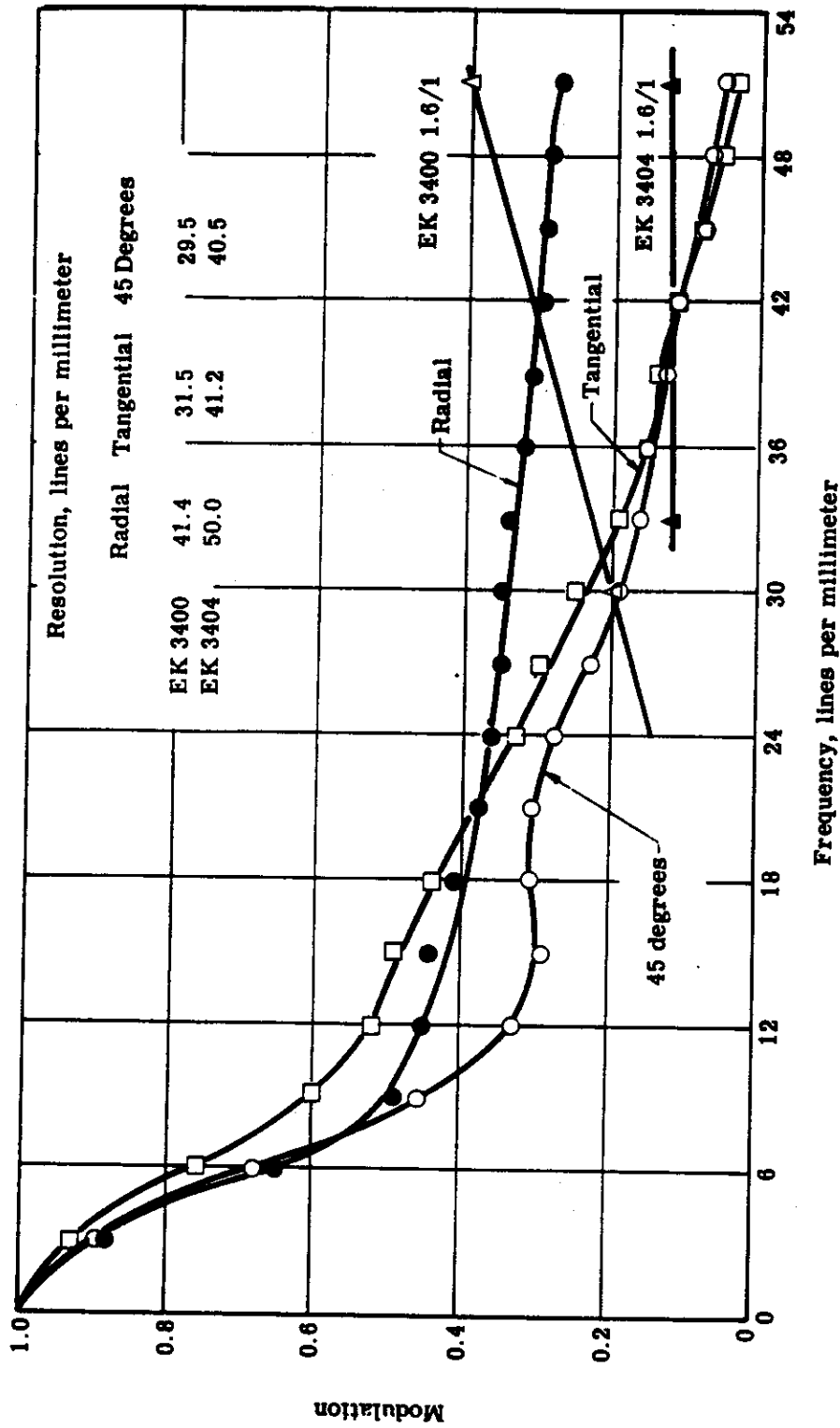


Fig. 2-4(a) — Geometrical frequency response: semifield height = 10.0 inches, deflection = +0.002 inch, spectral region = 0.60 to 0.70 micron

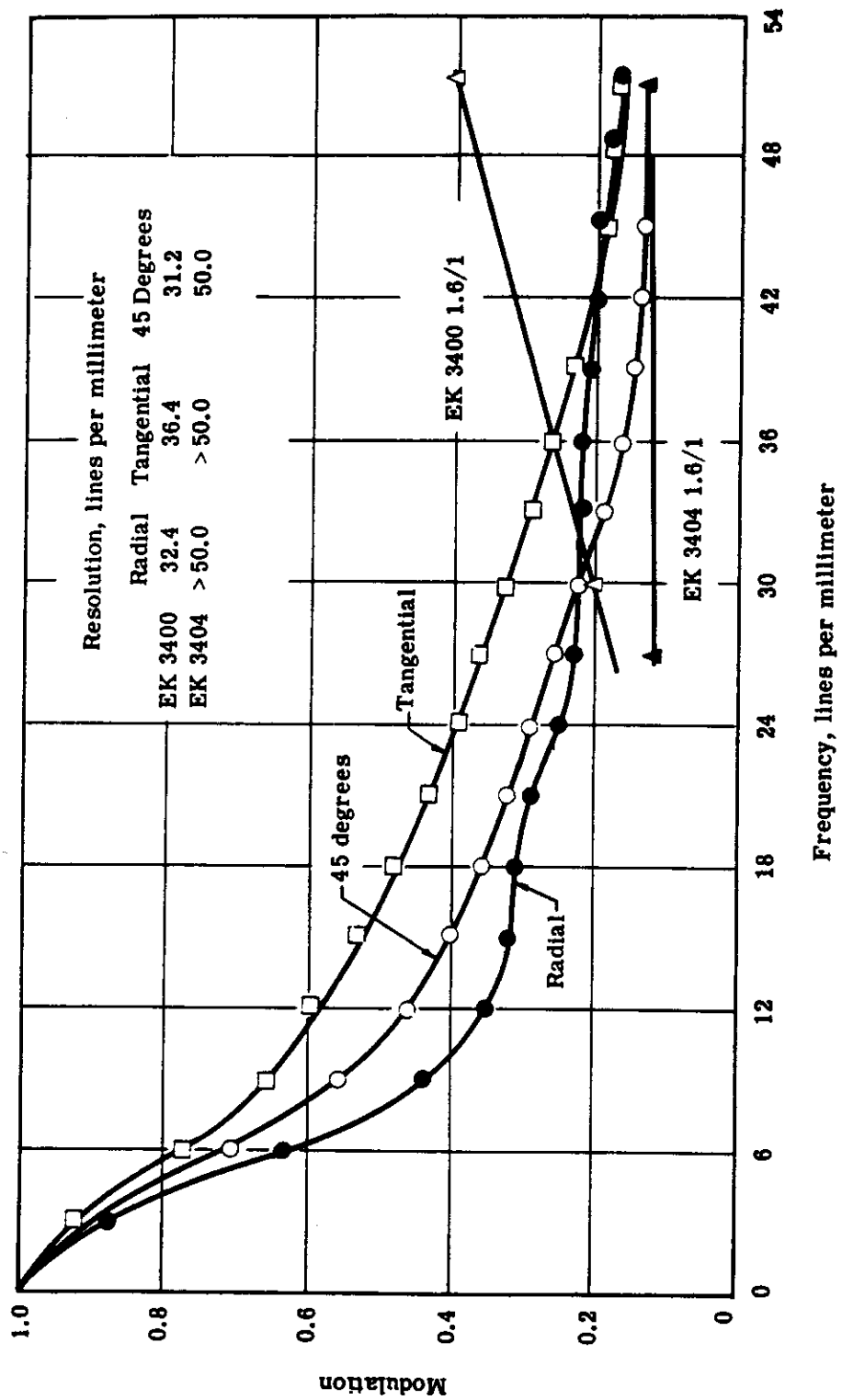


Fig. 2-4(b) — Geometrical frequency response: semifield height = 8.5 inches, deflection = +0.002 inch, spectral region = 0.60 to 0.70 micron

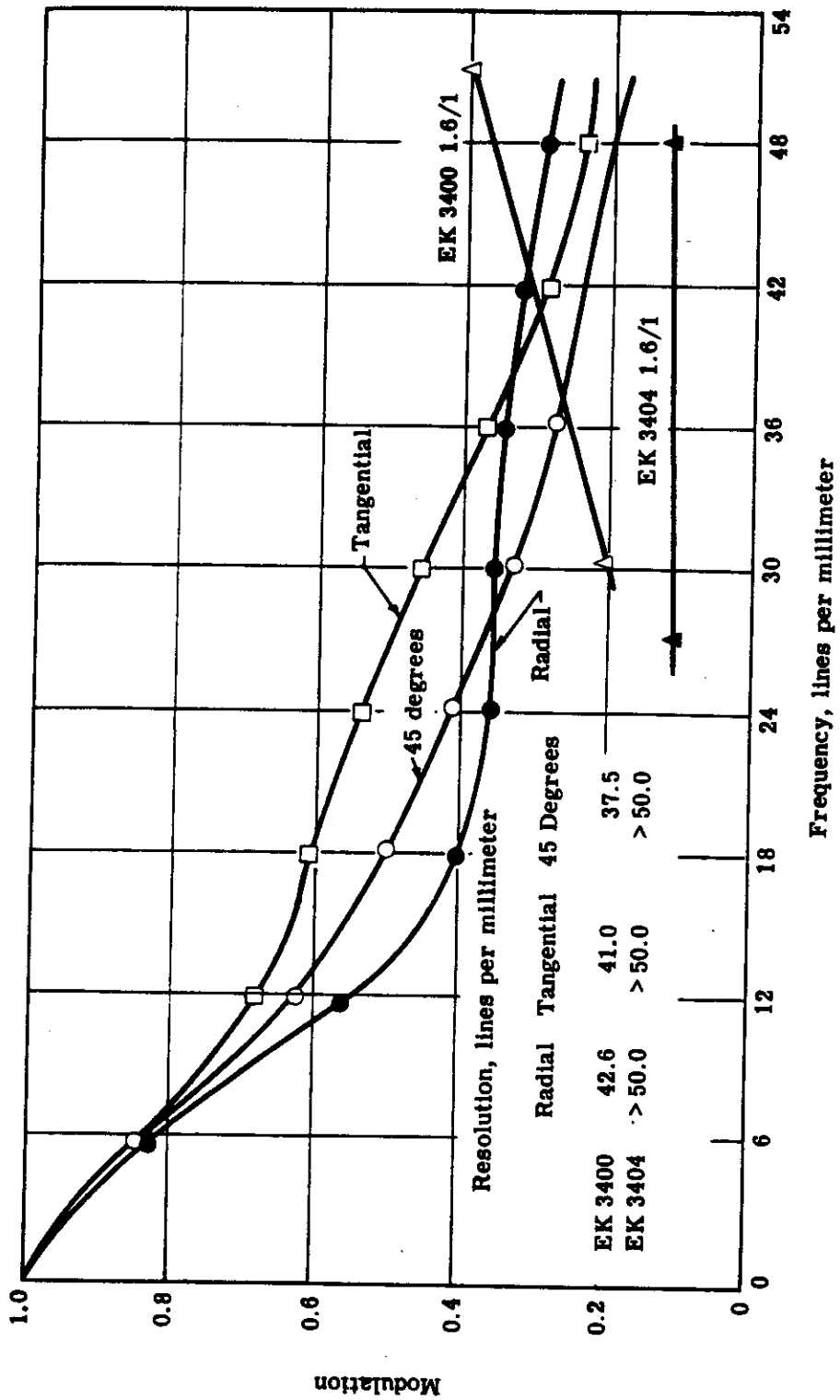


Fig. 2-4(c) — Geometrical frequency response: semifield height = 7.0 inches, deflection = +0.002 inch, spectral region = 0.60 to 0.70 micron

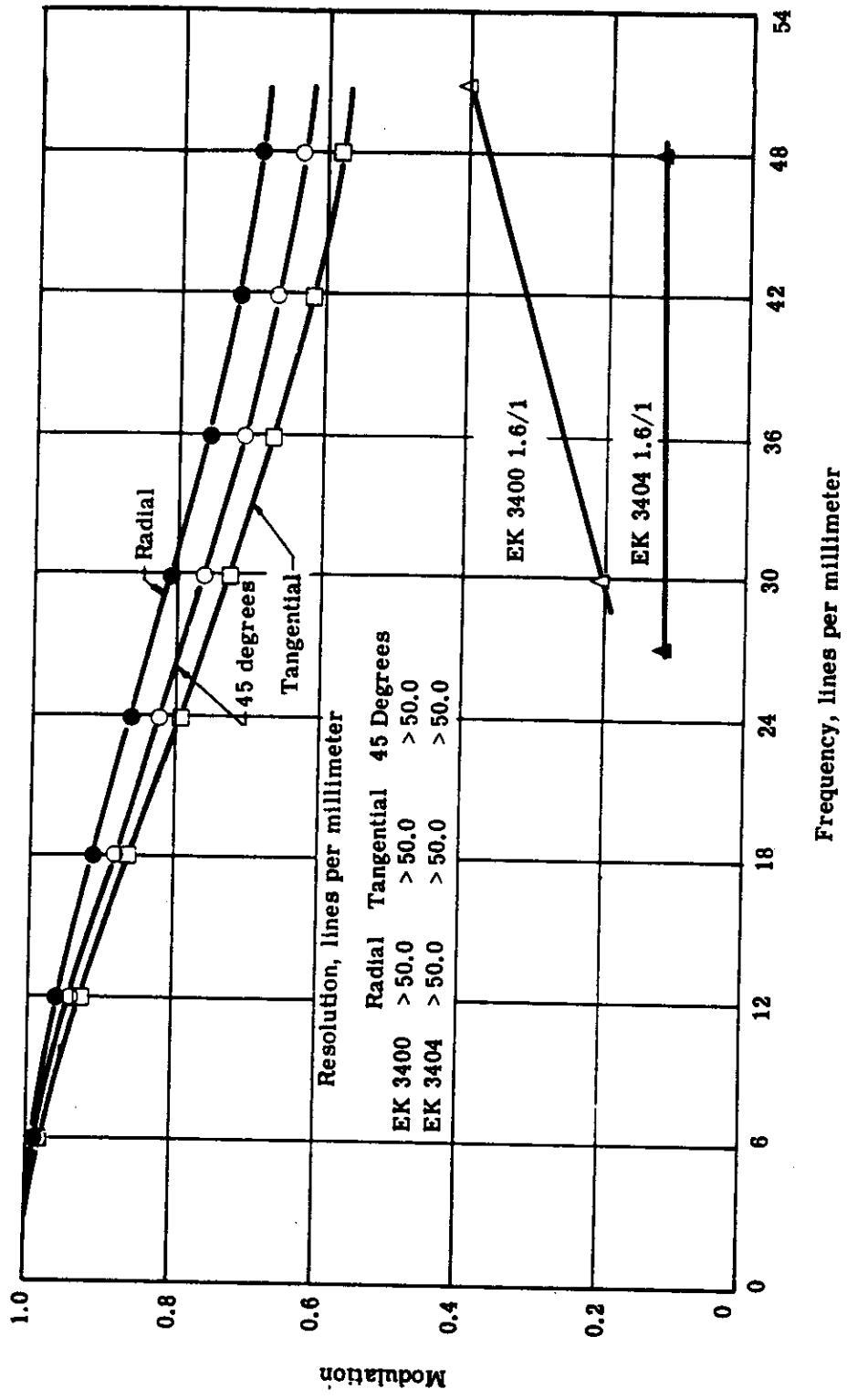


Fig. 2-4(d) — Geometrical frequency response: semifield height = 3.5 inches, deflection = +0.002 inch, spectral region = 0.60 to 0.70 micron

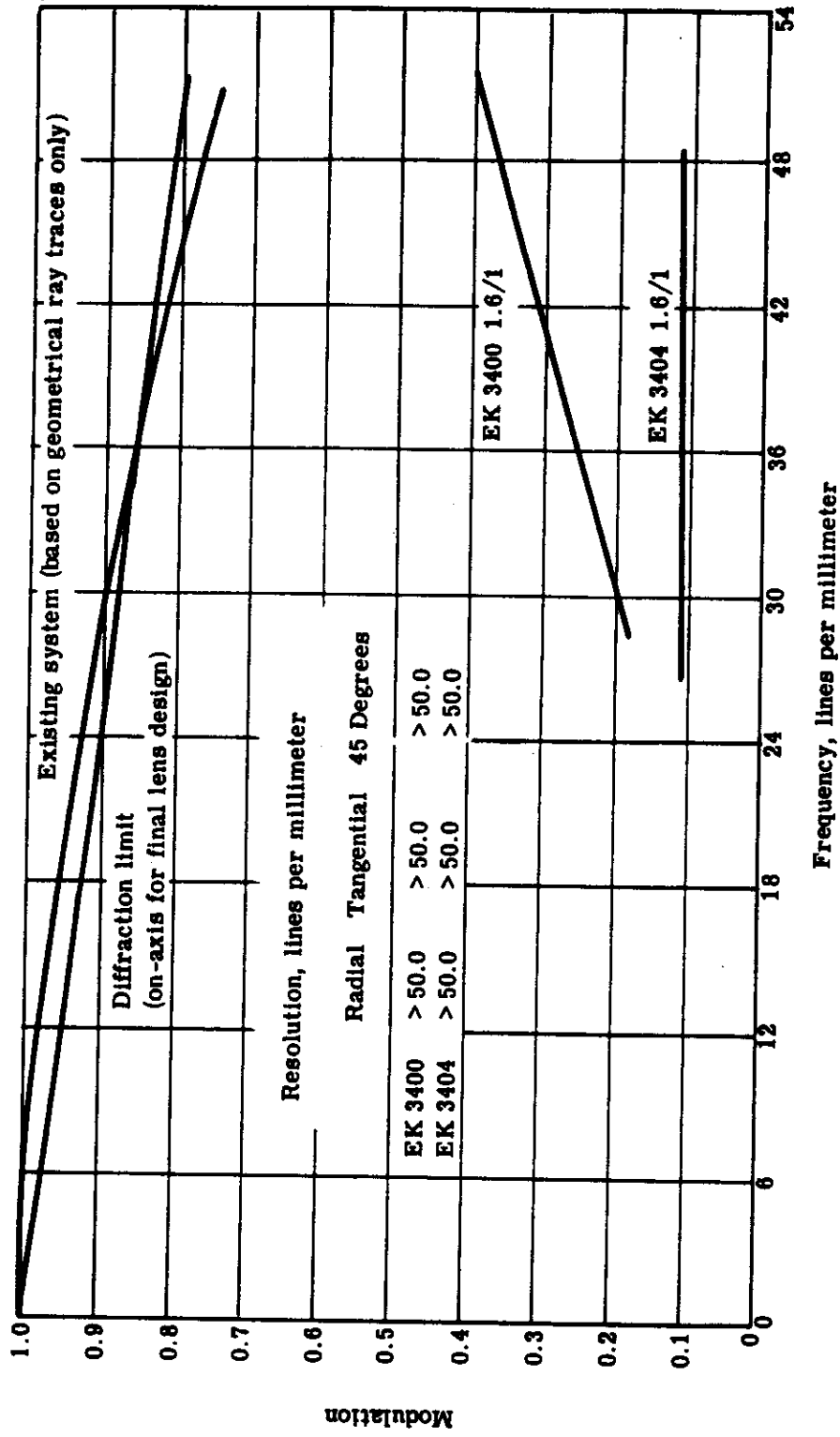


Fig. 2-4(e) — Geometrical frequency response: semifield height = 0.0 inch, deflection = +0.002 inch, spectral region = 0.60 to 0.70 micron

Table 2-3 — Effects of Tilt, Decenter, and Spacing Error

\bar{H}	Nominal System		Element I		First Half of System		Element I		First Half of System	
	Distortion	Chief Ray Height	Chief Ray Height	Chief Ray Height	Chief Ray Height	Chief Ray Height	Chief Ray Height	Chief Ray Height	Chief Ray Height	Chief Ray Height
0.0	0.0	0.0	-0.0007132	-0.0003712	-0.0002435	-0.0007169	0.0	0.0	0.0	0.0
0.2	0.0027414	2.0165335	2.0157966	2.0161511	2.0162714	2.0157965	2.0163566	2.0164847	2.0163566	2.0164847
0.4	0.0187631	4.0463473	4.0455404	4.0459312	4.0460293	4.0455503	4.0459772	4.0462326	4.0459772	4.0462326
0.6	0.0455573	6.0869336	6.0860195	6.0864673	6.0865210	6.0860490	6.0863379	6.0867207	6.0863379	6.0867207
0.7	0.0551399	7.1034122	7.1024353	7.1029167	7.1029382	7.1024794	7.1026889	7.1031347	7.1026889	7.1031347
0.8	0.0549699	8.1101383	8.1090947	8.1096122	8.1095946	8.1091533	8.1092840	8.1097807	8.1092840	8.1097807
0.9	0.0385507	9.1006151	9.0995026	9.1000580	9.0999947	9.0995801	9.0996315	9.1001666	9.0996315	9.1001666
1.0	-0.0000327	10.0689276	10.0677461	10.0683393	10.0682246	10.0678448	10.0678439	10.0683769	10.0678439	10.0683769

Maximum Radius Deviation of 30 Percent Spot Size (tolerance is 0.00003 inch)

	Decenter, 0.001 inch	Tilt, 0.00005 radian	Δ Air Space, 0.001 inch	Deflection for Δ Air Space
Element I	-0.00011108	-0.00008469	-0.00004248	-0.0010370
First half of system	-0.00030872	-0.00006206	-0.00018690	-0.0002785

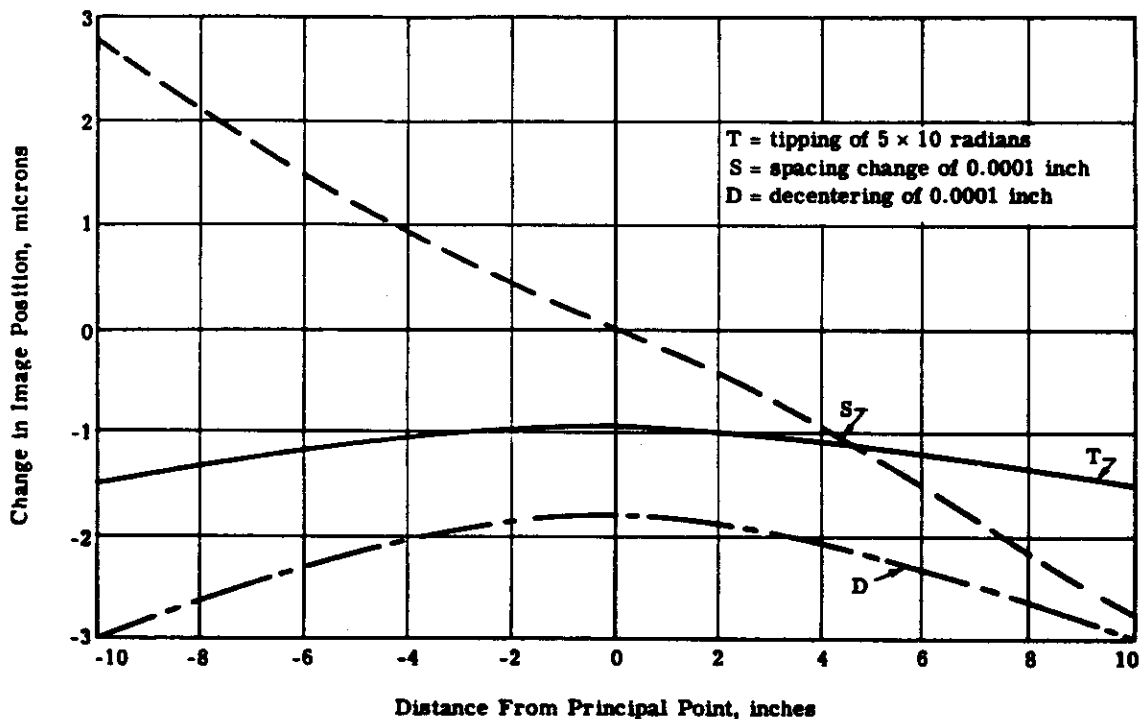


Fig. 2-5 — Effects of change in position of the front element

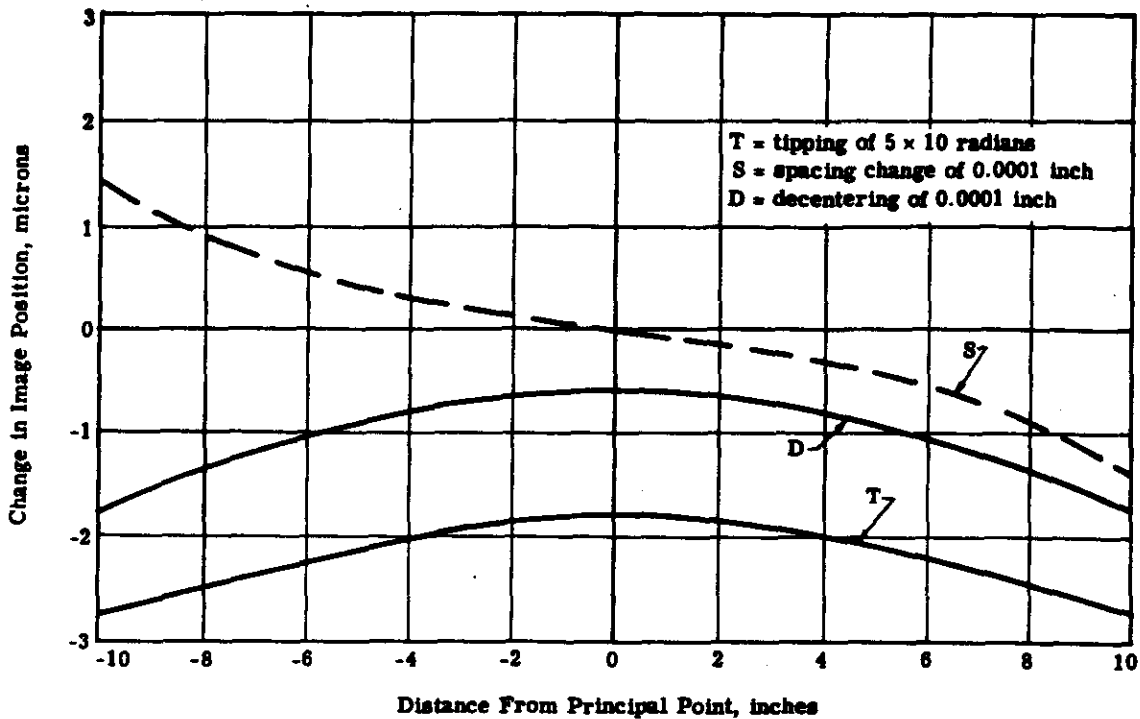


Fig. 2-6 — Effects of change in position of the front half of the lens

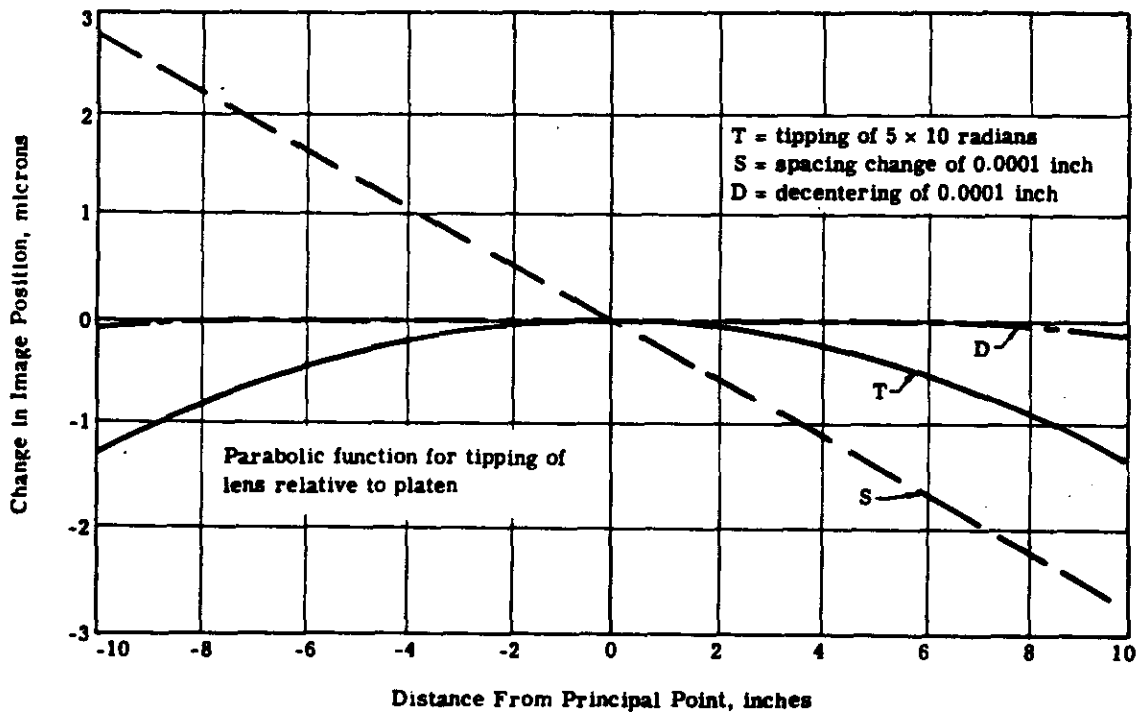


Fig. 2-7 — Effects of change in position of lens relative to the platen

Examination of these curves indicates the degree to which changes in the lens distortion pattern after calibration can be corrected by on-orbit recalibration. The errors produced by spacing changes can be partially removed by focal length recalibration done from on-orbit star photographs. In the case of movement of the front element alone, shown in Figure 2-5, the image displacements are almost exactly proportional to the image heights. This indicates a simple magnification change and is removed almost completely by focal length recalibrating. In this case, the residual error, or uncompensated change in the distortion, is less than 0.1 micron. In the case of a change of the central air spacing (refer to Figure 2-6), the residual error after focal length recalibration would be about 0.3 micron. Axial movement of the platen produces very nearly pure scale change (refer to Figure 2-7). Again, the residual error after focal length recalibration is less than 0.1 micron.

Tip and decentering cannot be compensated by scale recalibration since, as shown by the curves, the image is shrinking in one half of the format but expanding in the other half. This effect is similar to the effects of tipping the camera slightly away from vertical, with the resulting increase in scale factor in one half the picture and decrease in the other half. In fact, tip of the platen has exactly the effect of tilting the camera out of vertical. In each case, the image movement is a parabolic function of image height in the format. By comparison with the platen tip curve, the tip and decentering functions of the front element and the front half of the lens are also seen to be very close to the parabolic form of the function for tilting of the camera. This apparent tilt of the camera should become evident from the photogrammetry or, for that matter, from the on-orbit stellar photographs used for the focal length recalibration; it can be corrected, except for residuals on the order of 0.1 micron, the amount by which the tip and decentering curves deviate from a true parabola.

The tip and decentering curves for the front element and the front half of the lens show, as well as a parabolic form, a constant displacement from the origin. This movement of the image at the center of the format is a shift of the principle point, and gives, when multiplied by the focal length, an apparent change in the pointing angle of the camera relative to the rest of the system. This change can be compensated, therefore, by recalibration of the knee angle with the on-orbit stellar photographs.

In conclusion, it is seen that the camera can suffer surprisingly large changes in its structural dimensions without any serious impairment of its photogrammetric capabilities. While changes in the positions of the elements on the order of 0.0001 inch, and tips on the order of 5×10^{-6} micron, are intolerable if uncalibrated, it appears (for the cases examined) that all but a few tenths of a micron distortion can be compensated, because changes in the image caused by movements of the individual elements all fall into the same basic pattern. Complete distortion recalibration is therefore unnecessary; measurements of image position movements at a relatively few points are sufficient, and several on-orbit star photographs should be sufficient to make the corrections.

b. Lens Cell Materials

Studies have been made to determine the material with the optimum thermal characteristics for the lens cell. Three materials with a widely different coefficient of expansion were considered for the lens cell/camera construction. Cameras of all invar, all beryllium, and all aluminum construction were analyzed. The metric fidelity of the camera was found for (1) a uniform change in temperature of the whole camera system, (2) a change in temperature of the front half of the lens, and (3) a change in temperature of the front element only.

Of the three materials studied, only beryllium appeared to provide a real advantage for the present system. The change of image size with temperature level for an all beryllium camera construction is closely matched by the change in size of the reseau plate. For this type of change the camera can be expected to keep its calibration regardless of operating temperature. Figure 2-8 shows the plots for beryllium construction.

When the front half of the system was raised 10 °F above the rest of the camera, an image point at the corner of the format moved about 7 microns toward the center. When the front element alone was raised in temperature by 10 degrees, the image at the corner moved toward the axis by about 6 microns. Invar construction for the system reduced the error in the former case from 7 to 5 microns, but had no effect on the change caused by temperature difference of the front element.

While it is theoretically possible to provide a system which is insensitive to these temperature differences, as well as being insensitive to overall temperature level, the construction would require materials of several different coefficients of expansion. In this construction it appears likely that the fit of the lens elements in their cells would suffer. The mechanical errors would then become far more serious than the thermal errors. On this basis, the better procedure appears to be the controlling of the temperature difference throughout the system. This is the approach presently planned.

c. Shift of Focus Corrections

The camera will be fabricated, assembled and tested under normal atmospheric temperature and pressure. The final focusing, however, must be correct for the operational environment in which the system will operate. The focus changes to be expected between atmospheric pressure and vacuum have been calculated. In addition, the temperature shift of focus under vacuum conditions has been determined. These values are as follows:

Condition	Shift of Focus, inches
Change of pressure of 1 atmosphere	-0.017
Camera system temperature of +10 °F	+0.001
Front half of system raised +10 °F	+0.001
Front element raised +10 °F	+0.0001

With the exception of the pressure shift, the focal shifts appear to be insignificant in terms of their effect on image quality.

d. Thermal Gradients in the Front Element

Because this design requires front elements which are considerably larger in diameter than the entrance pupil, the image forming rays for different field points will pass through different sections of the front element. Therefore, a change at one edge of the front element can shift the image points at one edge of the format without changing the position of image points over the rest of the format. This shift appears as a measurement error.

If this error is radially symmetrical and constant, it may be partially removed through stellar recalibration of the scaling factor, or calibrated equivalent focal length. Since it is probable that the gradient will not be constant and possibly not completely symmetrical, a limit as to the permissible gradient has been determined.

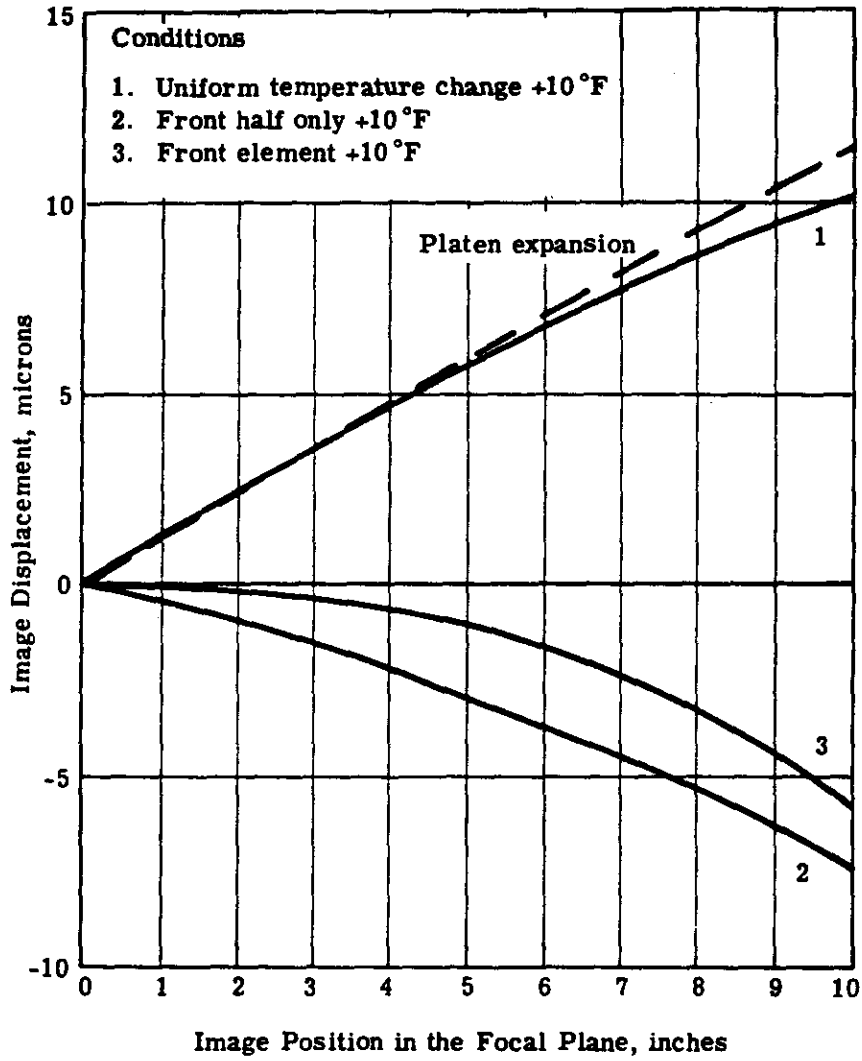
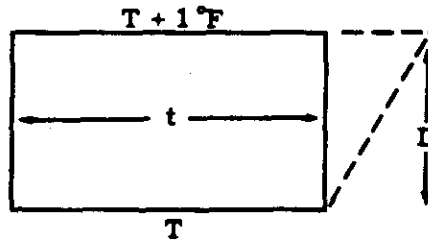


Fig. 2-8 — Thermal behavior of terrestrial camera in vacuum (cell material-beryllium)

~~SECRET~~

The gradient, by differential thermal expansion of the glass, generates a slight wedge; in addition, by the change of index of refraction with temperature it produces a gradient of index in the piece which also deviates the light rays. These effects are additive. Generally, the effect of the thermal expansion is the major source of trouble, being several times as large as the effect of the index gradient.

The calculation for the effect of a 1 °F per inch gradient in a block of glass is shown below.



The expansion of BK-7 glass per degree Fahrenheit is $\alpha = 4.6 \times 10^{-6}/^\circ\text{F}$. The deviation caused by this expansion is

$$\delta_1 = \frac{t}{D} \alpha (n - 1) = \frac{t}{D} [4.6 \times 10^{-6} (0.516)]$$

The effect of change of index with temperature $0.84 \times 10^{-6}/^\circ\text{F}$ is to retard the wavefront at one side by an amount equal to $t\Delta n$.

The deviation caused by this retardation is directly

$$\delta_2 = \frac{t}{D} \Delta n = \frac{t}{D} (0.84 \times 10^{-6})$$

Or the total deviation is equal to

$$\delta = \delta_1 + \delta_2 = \frac{t}{D} [4.6 \times 10^{-6} \times (0.516) + 0.84 \times 10^{-6}]$$
$$\delta = \frac{t}{D} (3.2 \times 10^{-6})$$

The thickness of glass for the front element for the principal ray at the 40-degree field angle is 2.2 inches. The deviation of this ray produced by a lateral 1 °F per inch temperature gradient is then

$$\delta = \frac{2.2}{1.0} (3.2 \times 10^{-6}) = 7.0 \times 10^{-6} \text{ radian}$$

The displacement in the focal plane caused by this deviation is

$$s = \delta f / \cos^2 40$$

$$s = 7.0 \times 10^{-6} \times 305 \times 10^3 \times 1/0.586 \text{ (microns)}$$

$$s = 3.6 \text{ microns}$$

~~SECRET~~

SECRET

Results indicate a thermal gradient of one Fahrenheit degree per inch will cause a maximum image point shift of 3.6 microns.

2.2.1.1.2 Lens Fabrication and Test

1. Tolerances

A thorough investigation into optical alignment and fabrication procedures required to achieve a complete system commensurate with the optical design effort has been conducted jointly by the Itek optical design department, the optical shop engineers, and the system engineers. Image sensitivity to element tilts, decenters, central thicknesses, air space thicknesses, and surface radii require the tolerancing of some 60 odd parameters. The feasibility of maintaining these tolerance requirements has been examined.

The radius, decenter (or wedge), and tilt tolerances can be maintained through normal shop procedures. However, the central thickness tolerances of the elements are extremely tight and require a modification of normal procedures, but can be met. A special center-thickness measuring fixture has been designed and built to ensure sufficiently accurate control of the element center thickness (see Figure 2-9). The generation of exact tolerance values for all the above mentioned parameters has been completed for the final optical design.

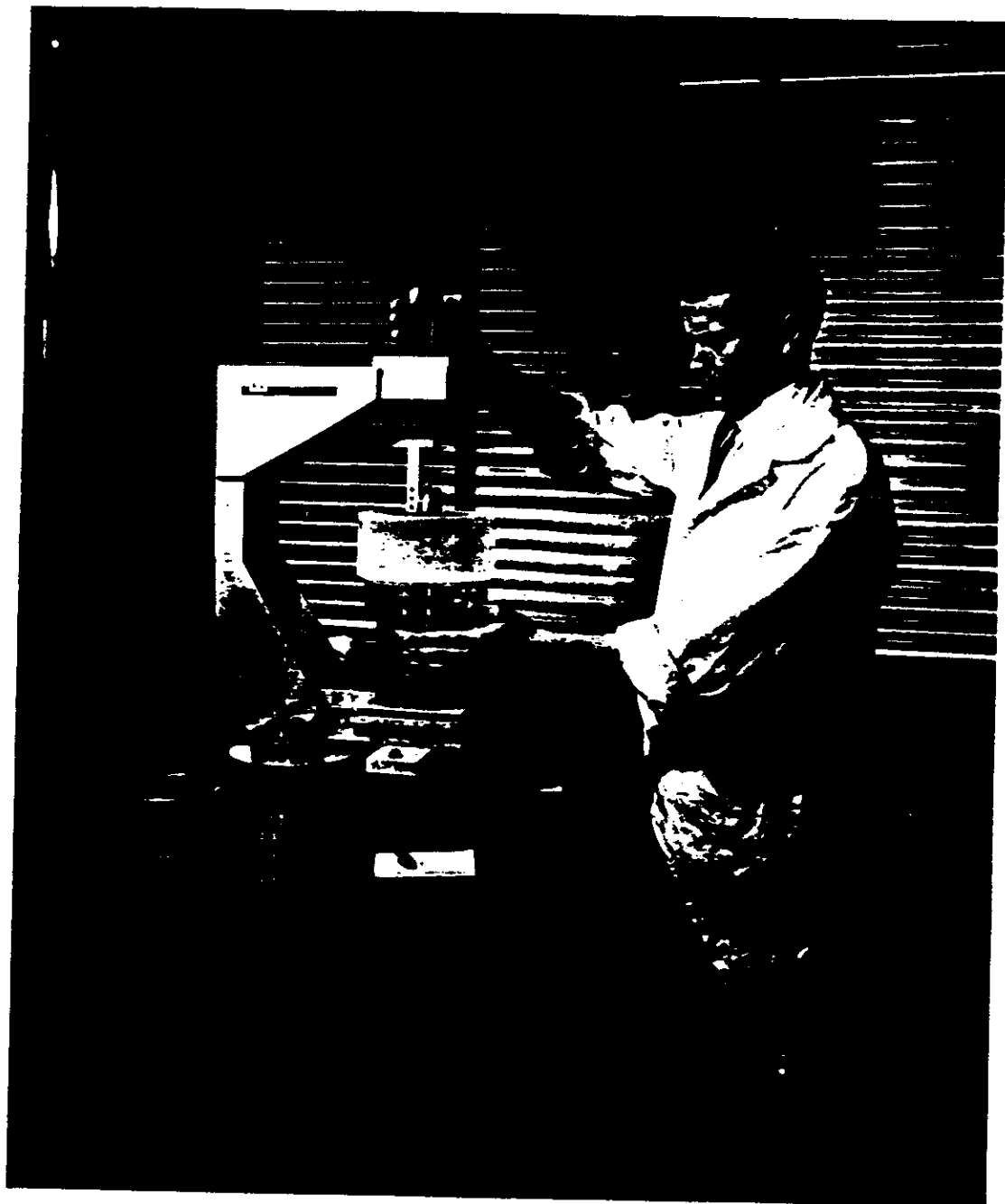
Image quality sensitivity to misalignment errors and to central thickness errors for the final design has been studied. Image quality for static environment is based upon a 30 percent allowable increase in image spot size throughout the field. Image quality for the dynamic case (fixed image plane) is based largely upon the effect on variation of distortion. The tolerancing has been concentrated on the elements in the two cemented triplets since image quality is more sensitive to their alignment. The procedure given in the following paragraph minimizes these errors. The bar graphs in Figure 2-10 illustrate the combined effect to image quality due to alignment errors and to inherent mechanical errors in fabricating these elements.

During the cementing process, the triplet elements will be positioned utilizing either an air or electronic gauge to read total indicated run-out normal to the exposed surface of the rotating element as shown in Figure 2-11. In addition to an approximately 30-microinch decentering error in either gauge, there is also a mechanical error inherent in the present edging table resulting in a possible 25-microinch decentering error in each element. These error values are used through analytical equations to determine the maximum possible error which may exist in the triplets after cementing. Each element is then decentered and/or tilted by these calculated values and then ray-traced to determine the effect on image quality.

The major aberration due to a change in central thickness of an element is astigmatism, which increases as the square of the field angle. The wide field angle of this system thus increases the requirement in the fabrication of central thicknesses within allowable tolerances. However, the number of elements requiring this extreme accuracy in measuring may be greatly minimized or even eliminated by the following procedure. After each element is completed, its central thickness is measurable to 5×10^{-5} inch which is within the required accuracy.

The system is then melt-designed using these new values. This procedure is followed after the completion of certain key elements. At most, the last melt design will require a very tight central thickness tolerance on the last completed element. Since the now existing automatic lens design program on the IBM-7094 decreases the melt design computer time by a factor of 20, the above procedure requires only approximately one day for each melt design.

SECRET



11,448

Fig. 2-9 — Special center-thickness measuring fixture

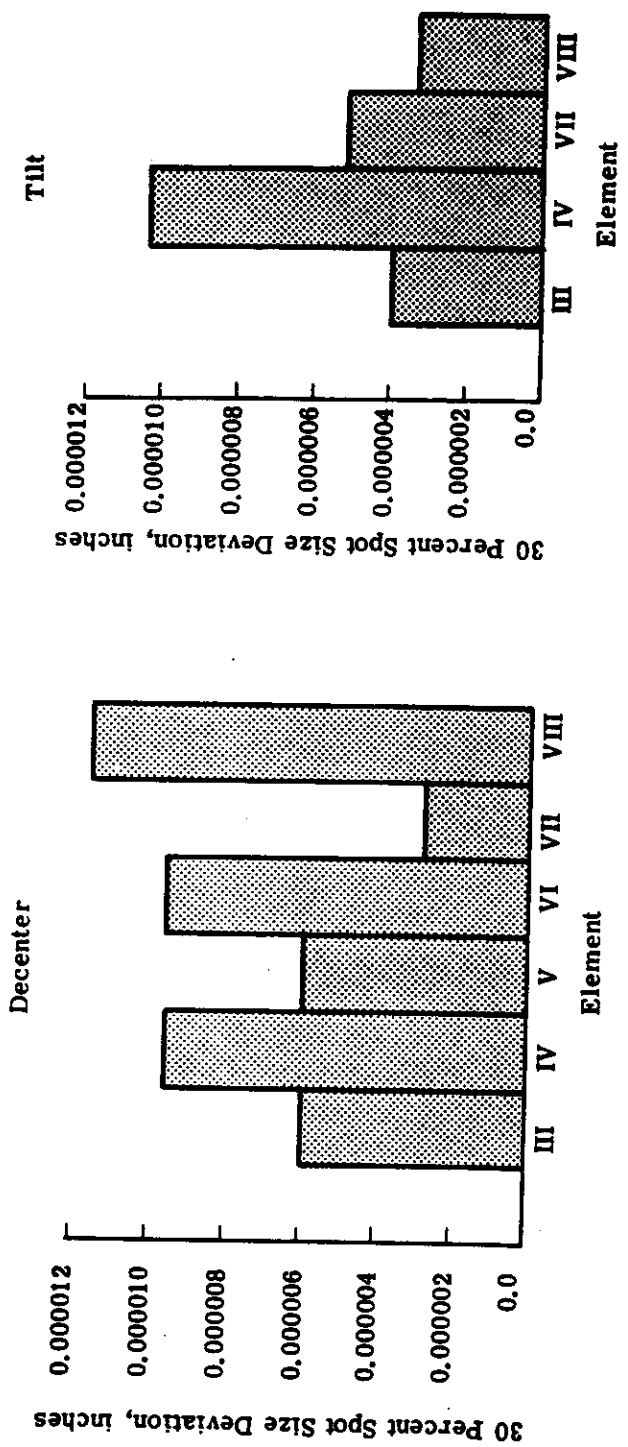


Fig. 2-10 — Image sensitivities relative to present measuring techniques (assuming 30-microinch gauge error and 25-microinch table run-out error)

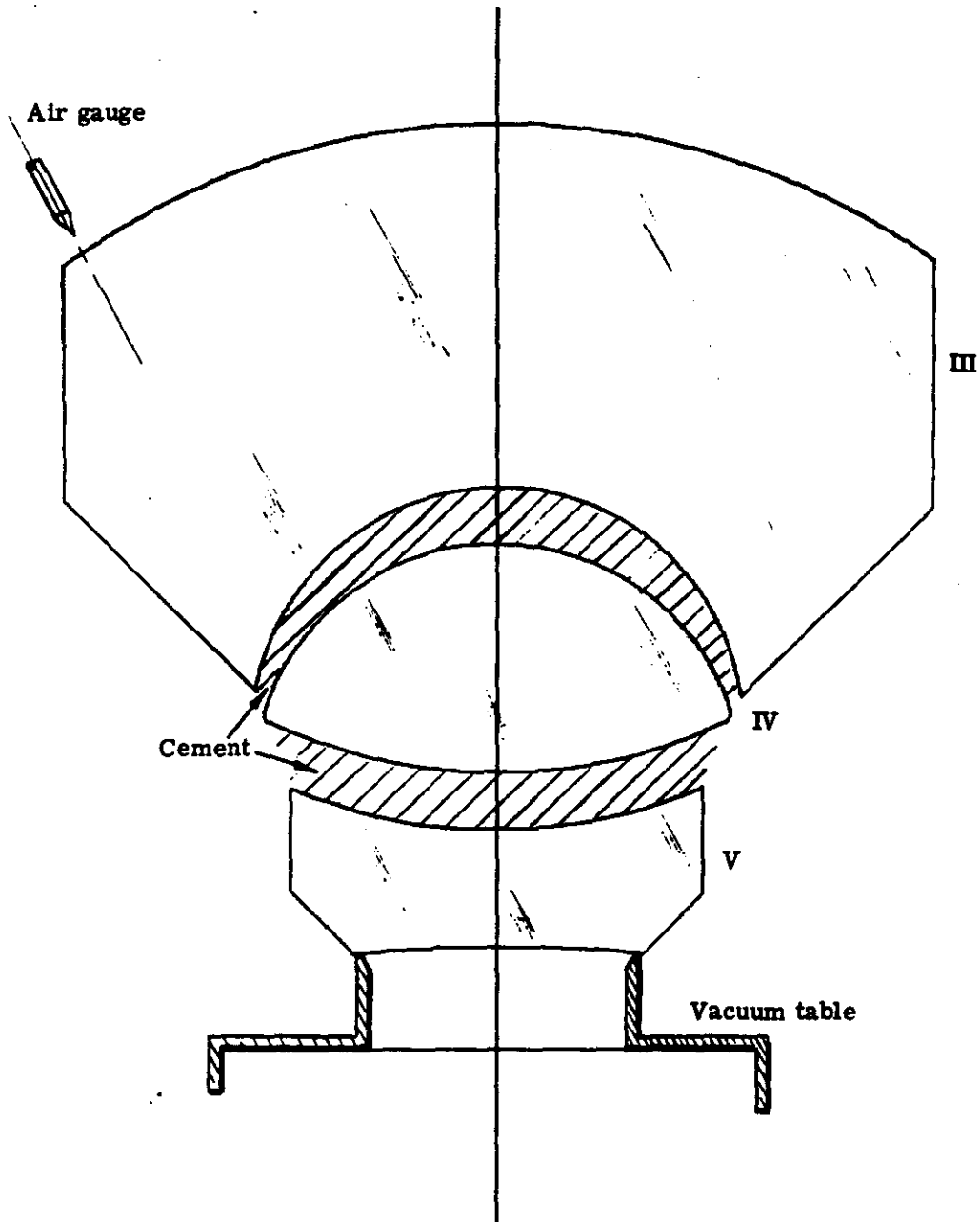


Fig. 2-11 — Positioning of triplet elements during cementing process (computer-generated drawing)

2. Element Fabrication

Test plate sets for all surfaces have been fabricated. The elements have been generated, and are presently in the polishing and figuring stages. Figure 2-12 illustrates the lens elements going through the various fabrication processes.

3. Aspheric Measuring Machine

The aspheric measuring machine (Figures 2-13, 2-14, and 2-15) is the measuring stick for the Itek optical shop personnel who hand-figure the aspheric elements to better than the 1λ (20×10^{-6} inch) tolerance set by the optical design. This machine is an automatic x-z coordinate measuring device which measures the profile of the aspheric surface.

An x-z coordinate tabulation will be generated for each aspheric by the optical designer. These coordinates will be punched onto paper tape for input into the machine. The paper tape reader will drive the x-lead screw by fixed controllable increments. A servo device will drive the z-coordinate drum micrometer until the electronic pick-up on the micrometer tip has reached a null position. At that time, a 2000-count-per-turn angular encoder connected to the micrometer shaft will input its count into a recorder. The actual z-coordinate measured, and the correct z-coordinate as read from the punched paper tape will then be compared, and the difference automatically plotted out on a recorder. The tape reader will advance to the next set of coordinates, and the second point will be plotted, and so on until the whole aspheric contour has been established.

Present error analysis shows that the machine will measure accurately to better than 10×10^{-6} inch. Absolute calibration can be obtained against known optical flats or spheres when the device becomes fully operative. Optical tolerance analysis indicates that this degree of measuring accuracy should be entirely adequate for the production of the central aspherics.

Calibration of this machine against a known flat shows that the horizontal slide humps 70 microinches across a $3\frac{1}{2}$ -inch diameter test flat. However, this error is reproducible to 8 microinches, and can be corrected by altering the input tape accordingly.

The final electronic input and output devices are presently being tested and debugged.

4. Cementing

Itek's present edging equipment allows elements to be edged round with a total indicator run-out error of only 40×10^{-6} inch, and the mounting flats can be ground relative to the polished surfaces of the elements to better than 1 second of arc. The final optical tolerance analysis indicates that this will be sufficiently accurate to allow edge centering in the cementing operation.

A set of cementing jigs and fixtures have been designed and are presently being built to facilitate the alignment of the elements as they are cemented. These fixtures will be attached to the Trans-o-Round roundness checker which will be used to actually make the alignment.

The fixtures will basically consist of a set of nested tubular rings containing differential adjusting screws as shown in Figure 2-16. The differential screw will be used to obtain very fine control in the alignment process.

The bottom element (Number 5) will be aligned using the roundness checker with two electronic gauges (one for the top surface and one for the edge) and a dual channel recorder. The top element (Number 4) would then be placed in position, the gauges would be removed from the bottom element and placed on the edge and top surface of the top element (see Figure 2-9).



Polishing process



Final figuring process

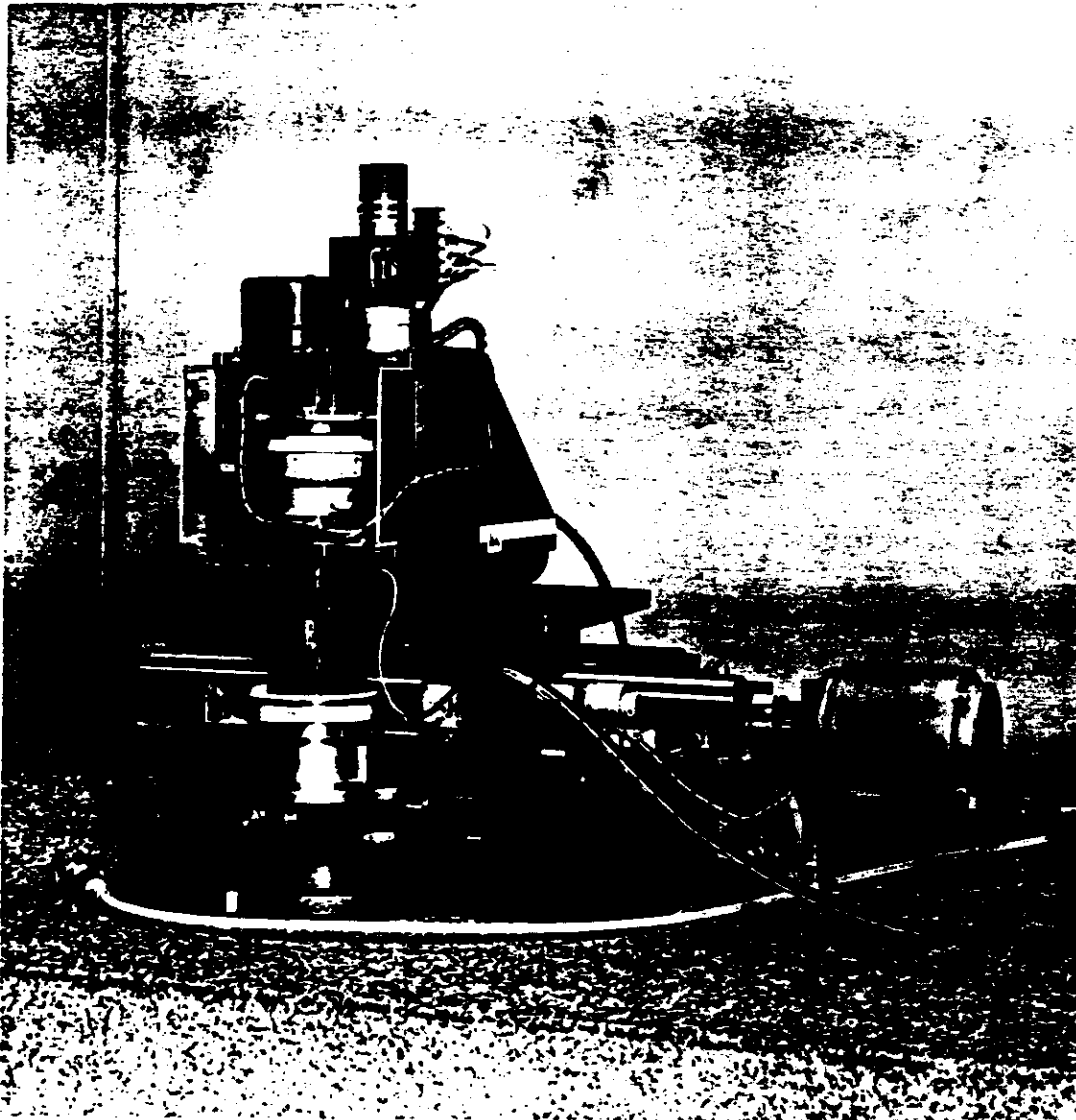


Examining lens element for visible imperfections



Making a test plate match

Fig. 2-12 — Element fabrication



11,400

Fig. 2-13 — Aspheric measuring machine



11,447

Fig. 2-14 — Aspheric measuring machine, overall setup

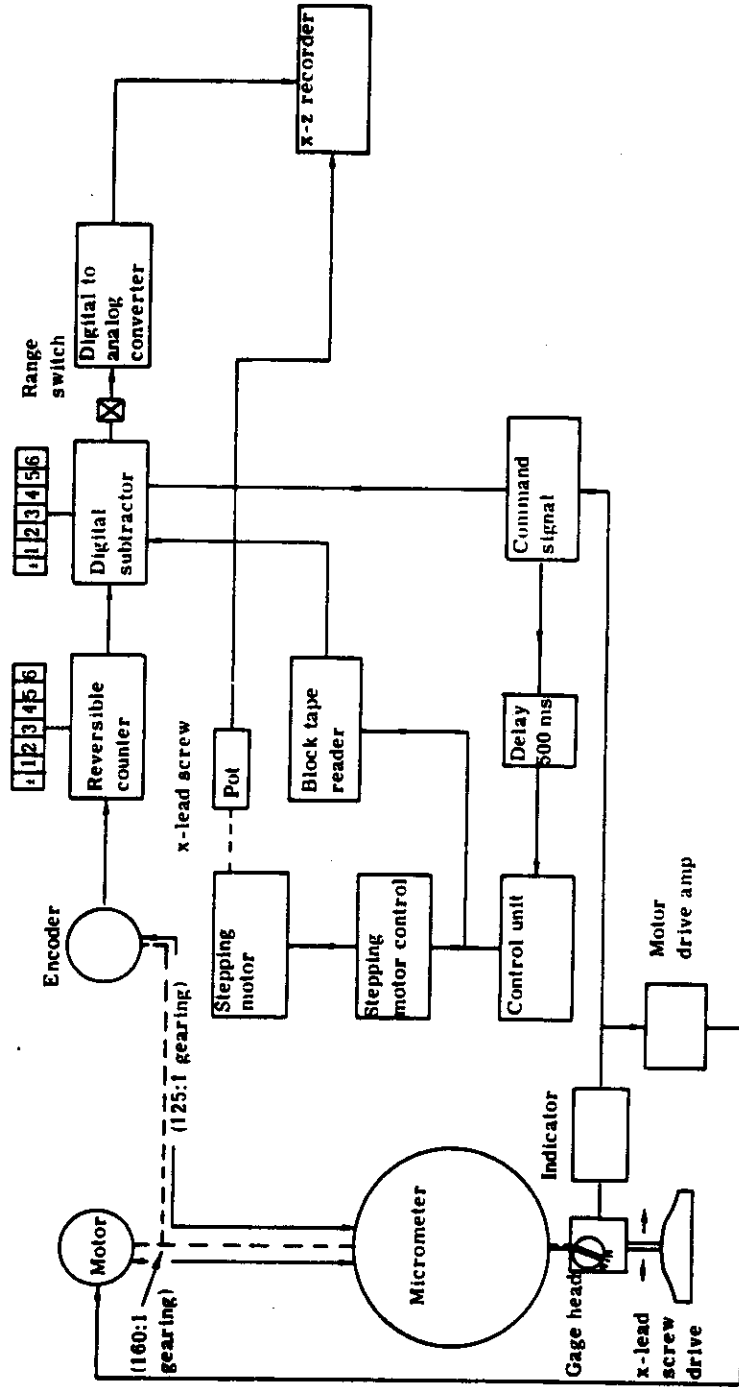


Fig. 2-15 — Aspheric measuring machine, servo block diagram

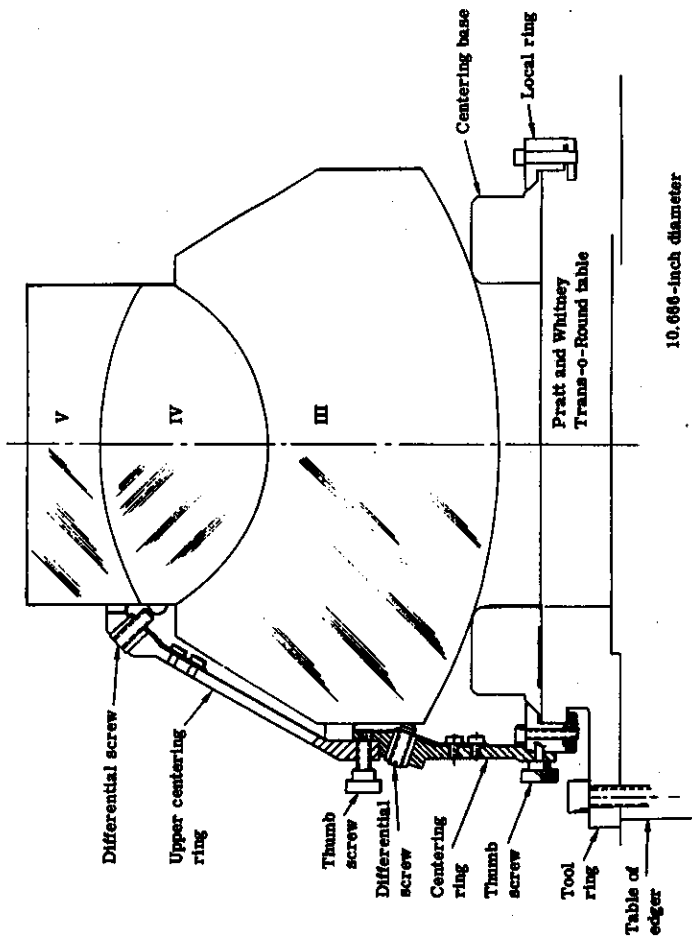
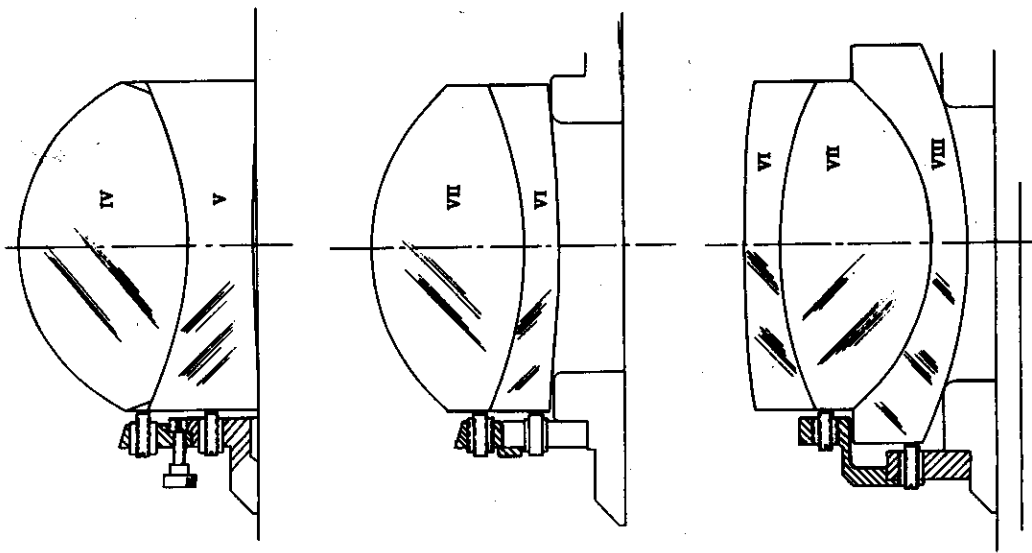


Fig. 2-16 — Cementing jigs and fixtures

~~SECRET~~

The top element could then be aligned relative to the axis of the roundness checker as had been done for the bottom lens. The two elements would then be held in position by specially designed jigs and fixtures and the cement allowed to cure.

When the elements have been cemented, the thickness of the cement layers will be measured. The elements will be tested for strain and birefringence, subjected to controlled thermal environments, and mounted in a cell using techniques similar to those planned for use in the final system and checked for the strength of the bond for various levels of shock and vibration.

5. Resolution and Distortion Measuring Bench

The resolution and distortion measuring bench (Figure 2-17) serves a twofold purpose. It will present to the lens a set of resolution targets emanating from infinity and spaced at various representative field angles. This is accomplished by a horizontal fan of seventeen 3-inch aperture, 24-inch focal-length collimators, spaced every 5 degrees from the optical axis out to ± 40 degrees. The lens is mounted in a drum which will be rotatable about the optical axis to allow the single fan of collimators to appear as any diagonal in the image plane of the lens.

To convert the resolution measuring bench to a distortion measuring bench, the resolution targets are replaced by distortion targets, and the angles between the collimators and the angular rotation of the lens supporting drum are measured to better than one second of arc.

The design of the resolution and distortion measuring bench is progressing on schedule. The angle between various optical components of the distortion measuring system will be known to better than 1 arc-second. All components will be made as stable as possible but they will be rechecked and realigned if necessary before each distortion calibration. Present plans call for the fabrication of a massive T-shaped, two-level, vibration isolated cement block. Into the top level will be set (grouted in) a granite surface plate upon which the bank of collimators will be mounted. Into the bottom level will be set a long, narrow, thick granite beam which will act as the bench, and upon which will be mounted the lens cradle, the reference autocollimators, traveling microscope assembly, etc.

2.2.1.2 Photo-Optical System Analysis

The objective of this task was to establish a detailed analysis of the camera system to determine the performance of both the terrestrial and stellar cameras.

The terrestrial camera required an analysis of resolution and those operating conditions which affect the photogrammetric accuracy of the system. Resolution is determined basically by the transfer characteristics of the lens in conjunction with the resolution limits of the film, but is degraded by the effects of uncompensated image motion. Therefore, a study was made to predict the blur likely to occur in operation from this motion. This resulted in the compilation of a budget of the different contributing sources of blur within the camera design.

Direct metric errors, that is, errors in the format position at which the image forms as opposed to the resolution loss from movement of the image during exposure, are attributable to three causes: (1) operation of the camera mechanism, (2) changes in optical dimensions as a result of launch and ageing, and (3) camera temperature variations and gradients during operation. These effects were studied and are tabulated in this section.

The possibility of on-orbit recalibration of the terrestrial-stellar camera knee-angle and the terrestrial camera scale using on-orbit star photographs was studied to see if such a procedure could be used to minimize the effects of launch and the effects of thermal variations.

The stellar camera analysis was concerned with lens choice, configuration analysis, camera motion, recordable star magnitudes, and a survey of star populations.

In addition to these tasks, several experimental studies were conducted, which are briefly summarized as follows:

1. Extension of the AIM curve—this study was conducted to determine the feasibility of lowering the minimum detectable modulation level by printing the negative on a high gamma, high resolution material
2. Experimental star recording— this study was performed to determine the recordable star magnitudes for the proposed system
3. Film flatness—a laboratory experiment conducted to determine the localized variations in film flatness under simulated operational conditions
4. Modulation transfer function versus point transfer accuracy—this experiment examined the photogrammetric measurement capability as a function of the photo-optical modulation transfer function

These experiments are discussed in detail in the text of this section.

2.2.1.2.1 Terrestrial Camera Performance

1. Operation Resolution

This section first discusses, in detail, the factors affecting the operational resolution of the terrestrial camera: motion errors, focusing, and the choice of exposure time and film. These factors are then considered together with the lens characteristics for an estimation of the operational resolution.

a. Factors Affecting Operational Resolution

(1) Motion Errors

In order to determine the amount of blur likely to degrade the image and the resolution, a blur budget was made. Table 2-4 contains the blur budgets, followed by more detailed descriptions of some of the items in the budget. In summary, the total expected blur rates, including the effects of random and systematic errors are as follows:

Center of Format	V/h, percent
Along-track	±4.2
Across-track	±4.9
Corners	
Along-track	±4.3
Across-track	±6.5

The target blur rate was 5 percent V/h.

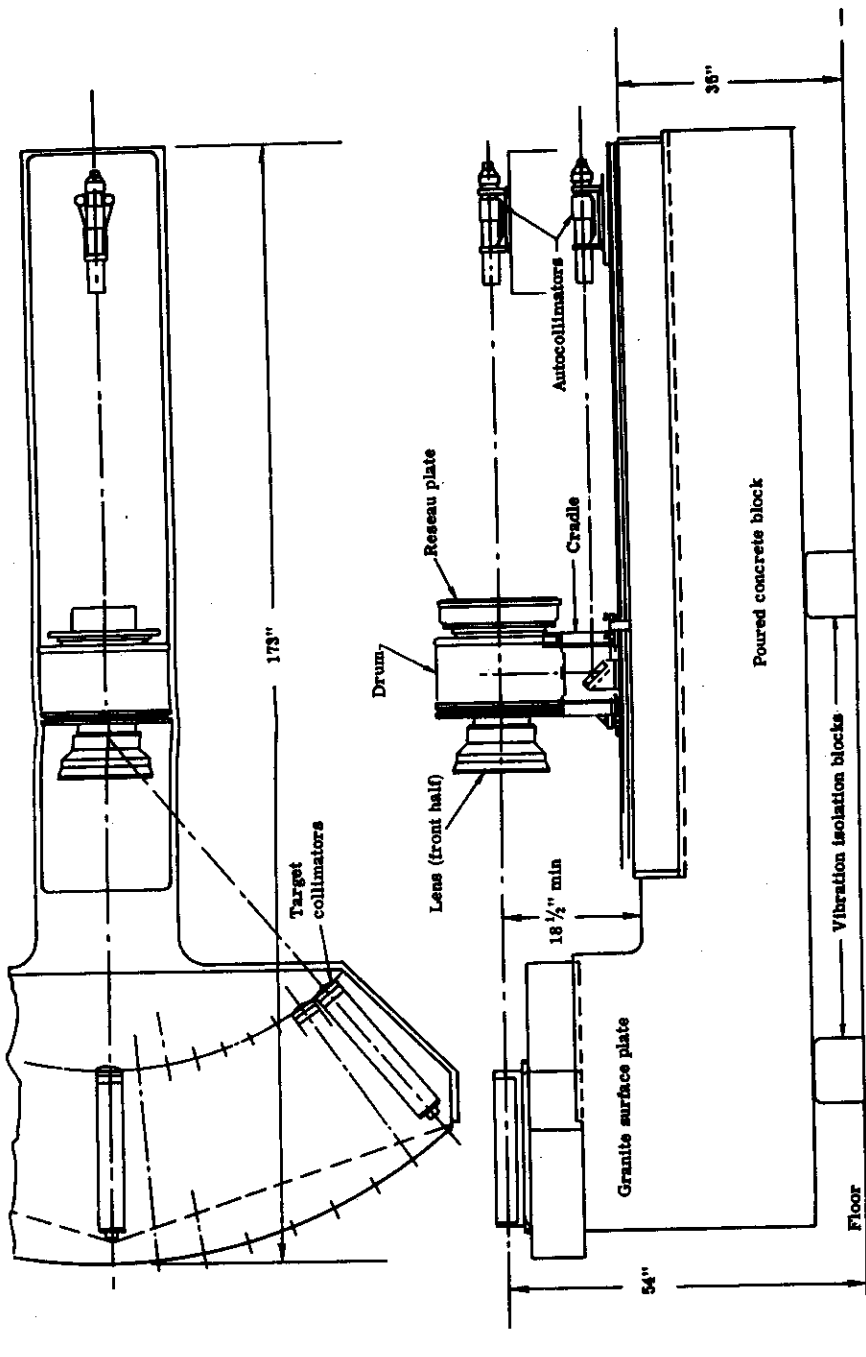


Fig. 2-17 — Resolution and distortion measuring bench

~~SECRET~~

Table 2-4 — Blur Budget for Terrestrial Camera
(V/h = 0.035 rad/sec)

Random Errors	Blur Rate, millimeters per second Along-Track		Blur Rate, millimeters per second Across-Track	
	Corners	Center	Corners	Center
IMC servo error 0.66 percent fV/h*	0.050	0.050	0	0
Platen across-track motion ± 1 micron	0	0	0.087	0.087
Focal length knowledge error f = 60μ (20 percent greater than Rayleigh tolerance)	0.0019	0.0019	10 ⁻⁴	10 ⁻⁴
Vibration 1 percent fV/h	0.085	0.085	0.085	0.085
Camera-vehicle alignment ± 0.1 degree (sensitive in pitch along-track, yaw across-track)	0.028	0	0.013	0.013
Vehicle attitude errors				
Roll: r = 3.2 × 10 ⁻³ radian	0.013	0	0.0008	0
Pitch: p = 3.2 × 10 ⁻³ radian	0.05	0	0.013	0
Yaw: q = 4.1 × 10 ⁻³ radian	8 × 10 ⁻⁵	8 × 10 ⁻⁵	0.043	0.043
Vehicle rate errors				
Roll: r = 0.14 × 10 ⁻³ rad/sec	0.012	0	0.046	0.040
Pitch: p = 0.105 × 10 ⁻³ rad/sec	0.049	0.03	0.009	0
Yaw: q = 0.105 × 10 rad/sec	0.012	0	0.024	0
Terrain height variation in format h = ± 3000 feet	0.020	0.020	0.0006	0.0006
V/h command error ± 1.5 percent fV/h	0.12	0.12	0.003	0.003
RSS random error (1σ) (Percent fV/h)	0.17 (2.2)	0.16 (2.0)	0.14 (1.8)	0.13 (1.7)
Systematic errors				
Lens distortion, platen motion and earth's curvature	-0.17	+0.17	± 0.11	0
Crab velocity (halved by initial setting)	0	0	± 0.26	± 0.26
Total equivalent blur rate				
RSS random plus systematic errors (Percent fV/h)	0.34 (4.3)	0.33 (4.2)	0.51 (6.5)	0.39 (4.9)

*Δ = error h = vehicle altitude r = roll angle q = yaw angle
V = vehicle velocity f = focal length p = pitch angle

~~SECRET~~

A detailed description of budget items is given in the following paragraphs.

(a) IMC Servo Error

The servo design analysis indicates that a tolerance of 0.66 percent fV/h is presently feasible. The design target was ± 1 percent fV/h.

(b) Vibration

Vibration sources within the camera are the shutters, the IMC servo, and the film advance mechanisms. Excessive vibration can probably be reduced to a sufficiently low level by design modifications in the breadboard stage. An initial vibration tolerance of ± 1 percent fV/h (same order as the IMC servo tolerance) was set. At high frequencies, this tolerance converts to an amplitude tolerance because a half cycle or more can occur within the exposure time. In this case, high frequency is 43 cps for an 11.5-millisecond exposure time. Figure 2-18 gives allowable amplitude versus frequency of vibration for vibration at a single frequency. This case is unrealistic but serves as a guideline.

(c) Camera-Vehicle Alignment

Misalignment of the camera within the vehicle is equivalent to a vehicle attitude error. It is, in a strict sense, a systematic error in any given vehicle, but because of its random value, it does not add directly to the other systematic errors. Furthermore, with a ± 0.1 degree alignment tolerance the blur effect is almost negligible, so this error has been placed with the time-varying random errors.

(d) Vehicle Attitude and Rate Errors

The equations for blur sensitivity to attitude and rate errors are given in the budget. The one-sigma error values for the Agena-D vehicle were used in the budget.

(e) V/h Command Error

A one-sigma value of ± 1 percent for V/h knowledge relative to mean sea level was used. A ± 3000 -foot terrain height variation was added to this to obtain the value for V/h knowledge used in the budget.

(f) Platen Across-Track Motion

A tolerance of ± 1 micron of across-track travel for any part of the platen was used; this includes platen rotation as well as across-track translation during the IMC stroke. This is equivalent to a velocity during exposure of 1 percent fV/h.

(g) Systematic Image Velocity Variations

The image motion at different positions in the image plane varies from the nominal fV/h value and is compensated by motion of the platen. Slight radial lens distortion causes a variation of scale in the format or, from a different viewpoint, a slightly varying focal length. Because of this, a constant velocity of the object in a flat object plane does not produce a corresponding constant image velocity. The IMC motion of the platen itself causes image motion variations because the front surface of the platen is aspherically curved. Because of the curvature of the earth's surface, the scale at large field angles is decreased and the image velocity is slowed, resulting in another variation from a constant nominal value.

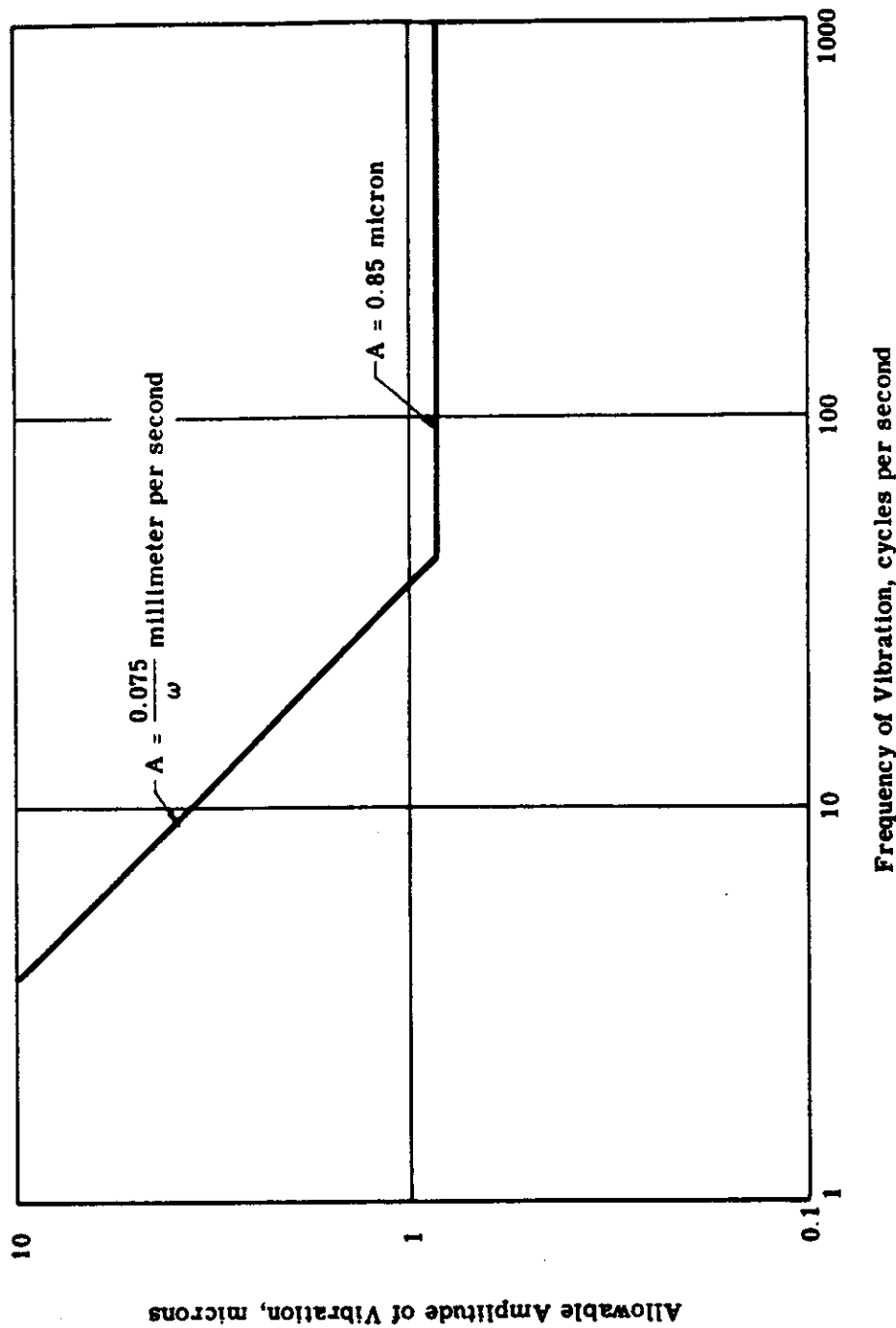


Fig. 2-18 — Allowable amplitude of single-frequency vibrations (based on ± 1 percent of V/h allowable blur rate; $f V/h = 7.9$ millimeters per second; exposure time = 11.5 milliseconds)

With data provided for the final lens design and for an operating altitude of 160 nautical miles, the effects of these blur sources were analyzed and combined. To indicate the magnitude of the motion variations from distorting and platen motion alone, curves provided by the lens designer which show the effects of platen movement and distortion upon image motion along the fore-and-aft axis are given in Figure 2-19.

The blur rates determined in the analysis are plotted in Figures 2-20 and 2-21 in different forms. Figure 2-20 gives the along-track and the across-track image motion variations as functions of the fore-and-aft position (x) in the image plane. The curves show maximum and minimum values at each x position. The motion variations at all points in the format fall within the closed curves.

The predominant portion of the maximum values shown on these curves is determined by the earth's curvature. Since the effect of the earth's curvature is proportional to the altitude, these curves can also be scaled in proportion to altitude. In terms of actual linear image motion, there is little effect of altitude, since fV/h is inversely proportional to altitude.

The along-track curves are even functions and have a peak-to-peak value of 4.1 percent fV/h at a 160-nautical mile altitude. This blur can be halved by adjustment of the IMC. To do this, the IMC rate should be reduced by about 1.9 percent or, for the same effect, adjustment to zero at format positions of about $7\frac{1}{2}$ inches along the fore-and-aft axis.

For across-track, the blur is an odd function with the curves having a peak-to-peak value twice the maximum amplitude from zero, which is ± 1.4 percent fV/h at 160 nautical miles.

Further optimization of the IMC adjustment can be made by choosing a criterion which considers the system resolution versus radius characteristics. For this kind of optimization, the systematic image motion variations are best given as functions of the radial position in the format as shown in Figure 2-21.

An investigation showed that if the systematic forward direction IMC error is made zero at the format corners by IMC adjustment, the worst resolution level is raised slightly at the expense of on-axis resolution. In terms of the performance predictions the gain is insignificant because in the present design the total across-track blur, which is not affected by IMC adjustment, is as large as the along-track blur, chiefly because of the uncompensated crabbing. If a device to compensate the crabbing is incorporated into the design, the improvement for worse-case resolution is no more than 1 line per millimeter with 3400 film and no more than 5 lines per millimeter with 3404 film.

The results of the systematic image motion analysis are summarized in Table 2-5.

(2) Focus Budget for the Terrestrial Camera

Defocusing is a source of blur because a change in f causes a change in fV/h . For a diffraction limited lens, the depth of focus is commonly given as the Rayleigh limit, $2\lambda f^2/\text{number}$. This gives approximately the defocus of a lens at which image degradation becomes just perceptible. In the case of the terrestrial camera, the use of the Rayleigh limit as the depth of focus is conservative, since the lens is not diffraction limited at most points in the field. The Rayleigh tolerance for an $f/6$ lens at 650-millimicron wavelength is about 50 microns.

One source of defocus is the initial location of the best-focus position. If focusing is done with a fine-grained film, best focus possibly can be determined within one-half Rayleigh limit, or 25 microns.

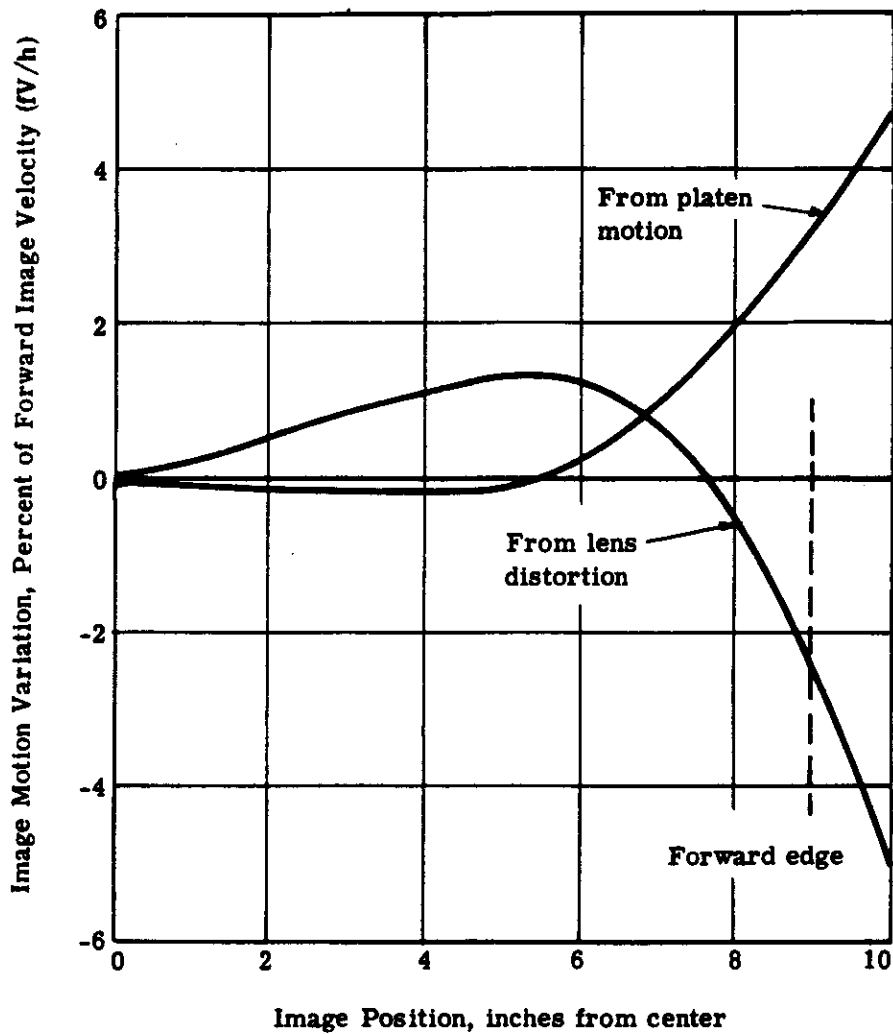


Fig. 2-19 — Image motion variations along the fore and aft axis from distortion and platen motion as a function of image position in format

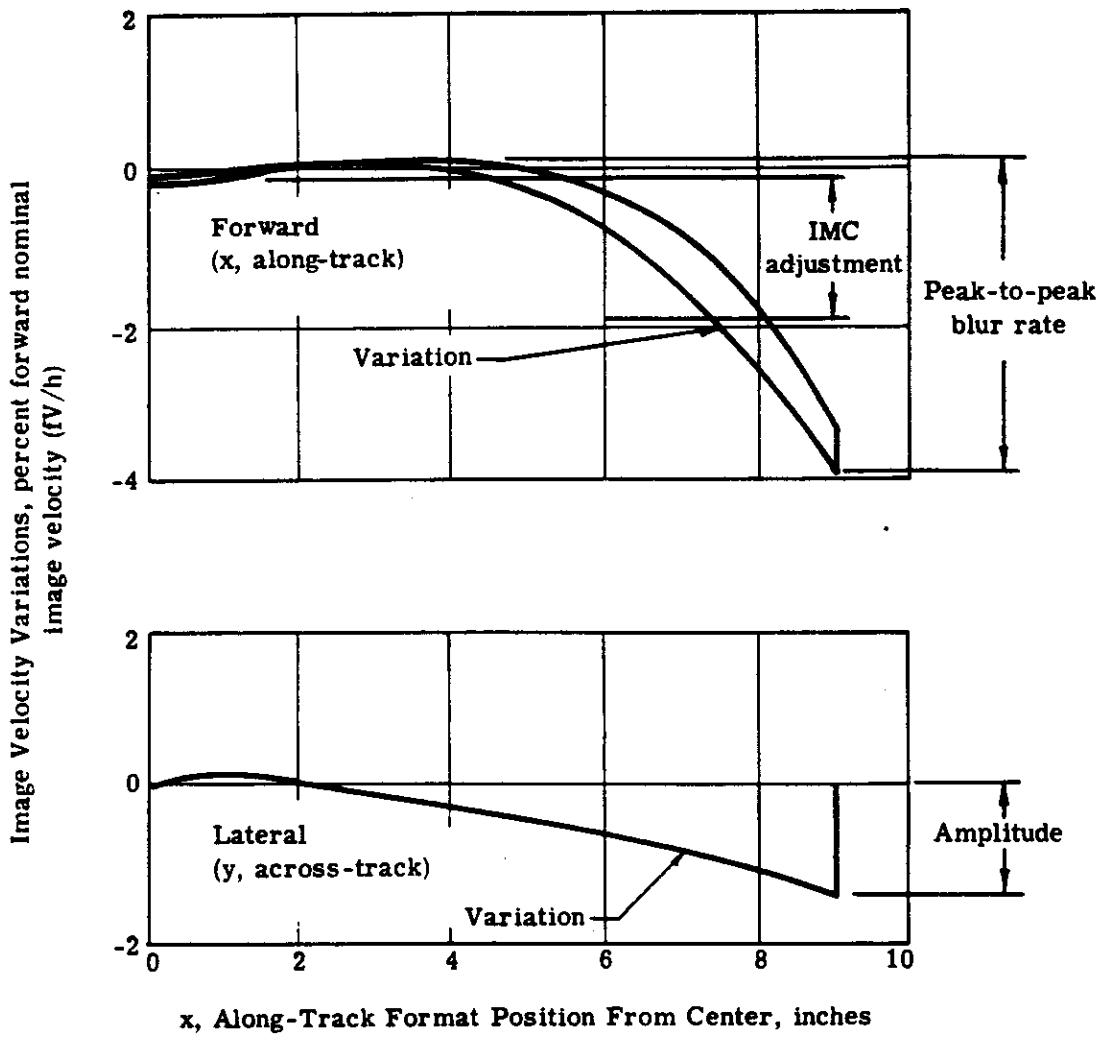
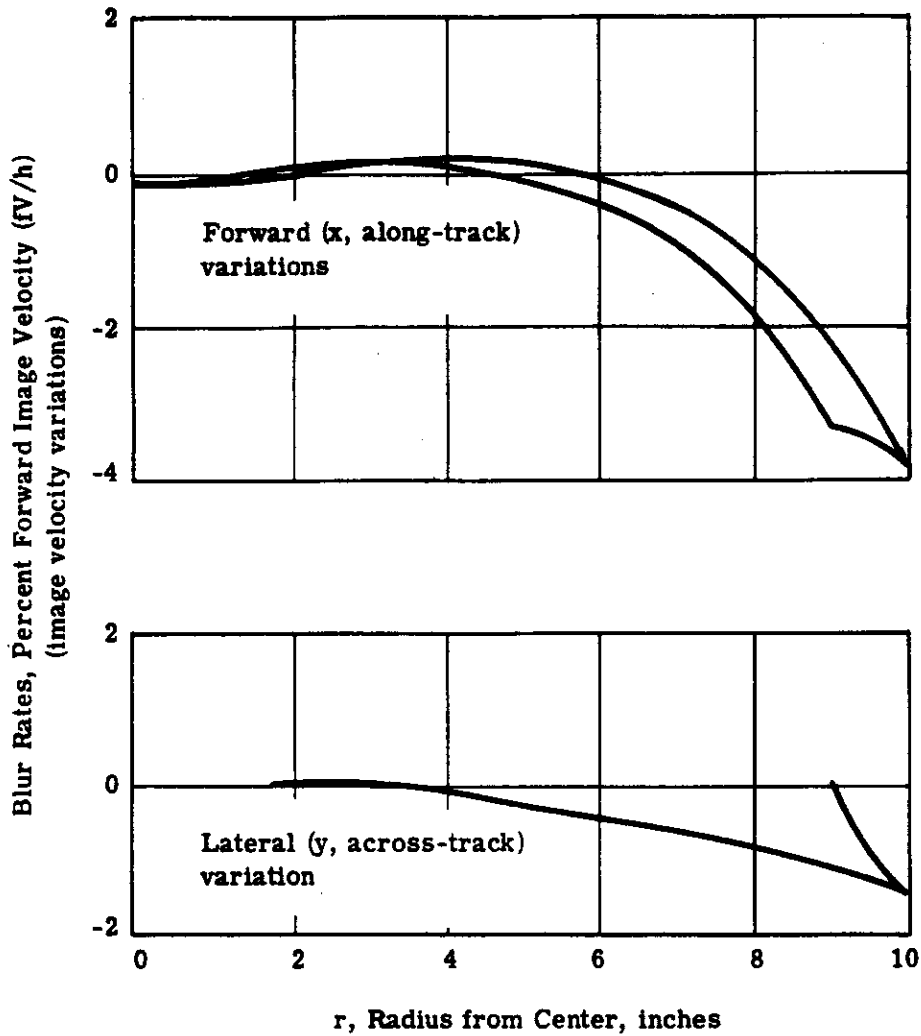


Fig. 2-20 — Maximum and minimum image velocity variations along- and across-track, as functions of fore and aft format position from distortion, platen motion, and earth's curvature (160-nautical mile altitude)



NOTE: Curves show maximum and minimum values at each radius. Blurs at all points in the format fall within the closed curves.

Fig. 2-21 — Systematic image velocity variations along- and across-track from distortion, platen motion, and earth's curvature as a function of radial position in image plane (160-nautical mile altitude)

Table 2-5 — Summary of Systematic Image Motions

Image Motion	Percent IV/h, 160-nautical mile altitude
Along-track blur rate	
Distortion, platen motion, and earth's curvature halved by IMC adjustment	± 2.1
Across-track blur rate	
Distortion, platen motion, and earth's curvature	± 1.4
Crab motion from earth's rotation halved by initial camera setting	± 3
Worst total across-track	± 4.4

A conservative value for defocus as an effect of the launch environment can be taken from the greatest nodal point shift found by previous experiments which is 50 microns. This is discussed in detail in the following section dealing with the metric accuracy of the system.

The sag of the platen from the pressure applied to the film was calculated to be about 2 microns for 0.3 psi pressure. This can be taken into account in the lens design and thus does not affect the focus.

Other factors which influence focus are axial platen motion during IMC, platen deflection variation with pressure variation, platen tilt and film/platen contact irregularities. Each of these factors must be kept on the order of 1 micron for photogrammetric reasons; they are not significant defocus sources.

The RSS value of the two significant defocus sources is about 60 microns (0.0023 inch), or about 20 percent greater than the Rayleigh tolerance. Direct image degradation from this amount of defocus is negligible.

(3) Exposure Time Determinations

Exposure times have been calculated by two methods: (1) the radiant energy method, and (2) using the Eastman Kodak exposure value (EV) numbers derived from field experience for the several films considered for use in the terrestrial camera.

The exposure times computed by the radiant energy method are not in agreement with exposure times computed from Eastman Kodak EV numbers for these films and maximum processing conditions. A comparison of the exposure times indicated by the two methods is given for a 20-degree scan angle in Table 2-6.

The calibration of exposure by the exposure value method is based on experimental results. It is a more conservative approach. Because of familiarity with the EV system and its results, it is planned to use these exposure times. They are shown in Figure 2-22 as a function of solar elevation. In addition, the error budget has shown that the system can perform with the exposure times given by the EV calculation. If subsequent information shows that shorter exposures or a finer grain film can be used, this will provide an added advantage to the system.

(4) Film Choice

The exposure time plots in Figure 2-22 show that EK type SO-206 offers negligible speed advantage over the improved EK type 3404 film. In addition, experience and laboratory tests have shown that it gives an appreciably grainier image and poorer resolution.

Preliminary system calculations have also shown that EK type 3401 film with its much higher speed offers no advantage. The reason for this is that its much lower inherent resolving power capability loses more image detail than is gained by its reduction of motion blur.

The two remaining films, EK type 3404 with its extremely fine grain but low inherent speed, and EK type 3400 film with moderate grain and a factor of three times speed increase, are good possibilities. The following system calculations show that they perform almost equally well at a 20-degree solar elevation with the predicted motion error of the system.

b. Operational Resolution Prediction

The operational resolution of the terrestrial camera is now estimated using the previously calculated lens transfer functions, image motions, and exposure times. The resolution was

Table 2-6 -- Exposure Times for a 20-Degree Scan Angle

Film	Exposure Time Radiant Energy Calculation, milliseconds	Exposure Value Calculation for 20 Degrees Solar Elevation, milliseconds
3401	1.6	3.9
3400	4.4	11.4
SO-206	11	25
3404	22	29

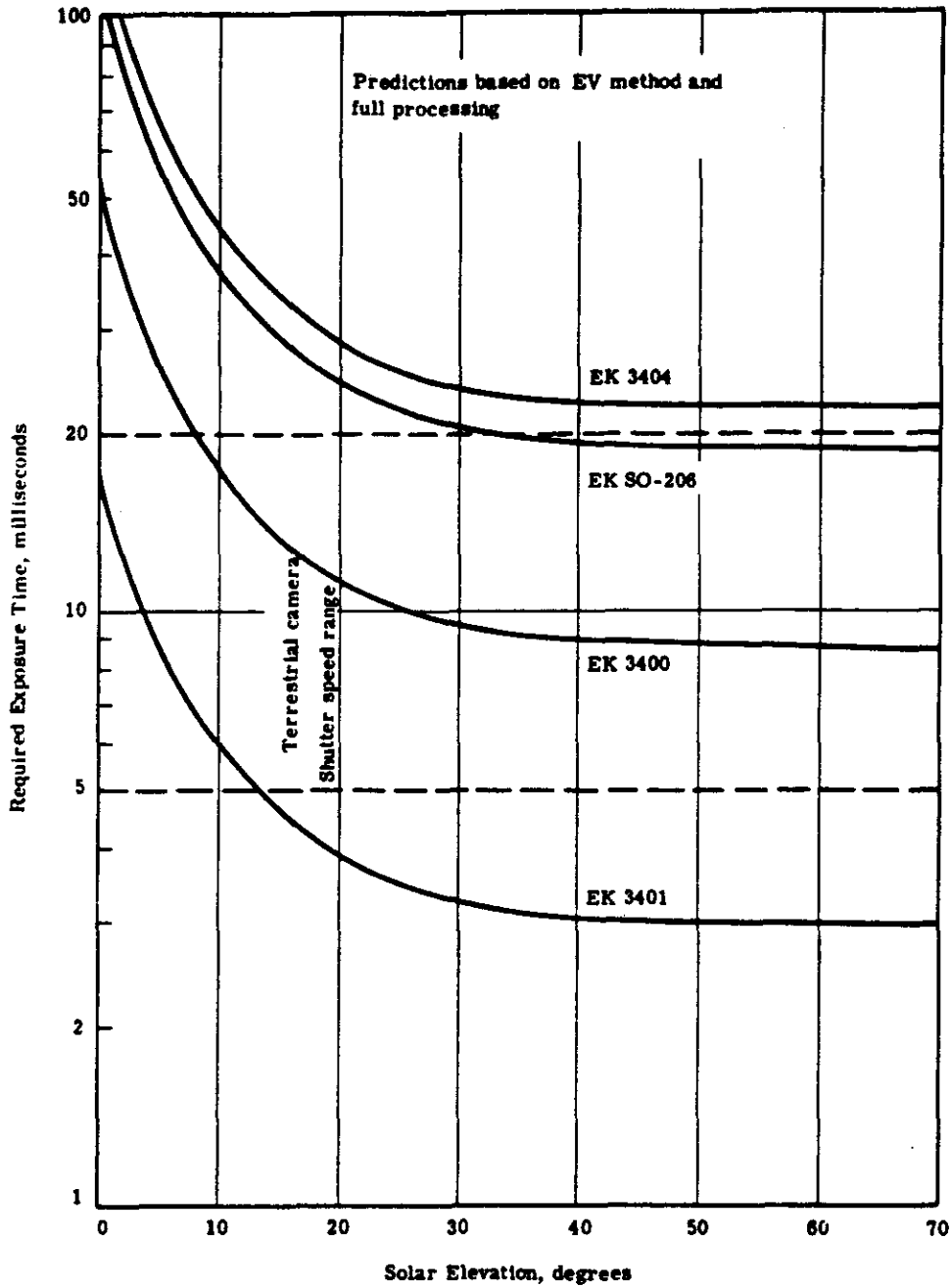


Fig. 2-22 — Required exposure times for a T/12 system with a W-25 filter

determined by finding the intersection of the aerial image modulation curve with the product function of the ground scene modulation (1.6:1 contrast), the lens transfer function, and the blur transfer function (blur = IMC error exposure time). The EK AIM curves for 3400 and 3404 films were extrapolated at low frequencies to a modulation limit of 0.015, the eye threshold divided by the contrast enhancement (γ) of the film. The results of the analysis are given graphically in Figures 2-23, 2-24, and 2-25.

The curves are for the specific altitude of 160 nautical miles and for the specific solar elevation of 20 degrees. The use of a log-log scale allows the curves to be linearly translated left or right to represent the situation at different altitudes or solar elevations. The amount of translation for a different sun angle is proportional to the ratio of the exposure time at the new sun angle to the exposure time for a 20-degree sun angle. Exposure time as a function of sun angle has been given in Figure 2-22. The location of the 6.5 percent IMC error point at 5-degree sun angle is shown in Figure 2-23. The amount of translation for a different altitude is proportional to the ratio of the new V/h to the old, or effectively, the old altitude to the new.

Figure 2-24 takes into account the lens transfer function at interior points in the format and gives resolution as a function of the image position in the format. This figure has been drawn for the specific case of a 160 nautical mile altitude, with the 6.5 percent maximum IMC error obtained in the blur budget, and for EK type 3400 film, which has the flatter response in the operating region as shown in Figure 2-23.

Figure 2-25 is Figure 2-24 converted to ground resolved distance.

Figure 2-26 was made to show directly the effect of blur upon the solution. There, the AIM curve for 3400 film has been divided by the ground scene modulation and the blur transfer function and then superimposed upon the lens transfer function as given in the section on the lens design.

Figure 2-23 gives the resolution predictions as functions of the uncompensated image motion in percent of fV/h . This figure shows the best and the worst resolution levels in the format. On-axis resolution and corner resolution in the radial, tangential, and 45-degree-to-radius directions in the film plane are given for both 3400 and 3404 films. At the left-hand side in Figure 2-23, each curve asymptotically approaches its own blur-free resolution level. At the right-hand side, image motion limits the resolution. Since the blur-limited resolution is the reciprocal of the image movement during exposure, the right-hand asymptote on a log-log scale is a negatively-sloping 45-degree line whose position depends upon the exposure time and the fV/h rate, but not the lens transfer function.

With regard to film, both EK type 3400 and 3404 have advantages for use under certain operational conditions, as shown by the curves of Figure 2-22. At the nominal operation conditions of 160-nautical mile altitude and 20-degree solar elevation, 3404 film has a minimum resolution about 6 lines per millimeter higher than that of 3400 film. The maximum resolutions are about the same. But if the useful range of operation is extended to include photography at 5-degree solar elevation, the 3400 minimum resolution is shown to be superior to the 3404 resolution at all points in the field. The advantages of each of the films, in relation to the nominal operating conditions of 160-nautical mile altitude and 20-degree solar elevation, can be summarized as follows:

EK type 3404 (finer-grained film, but slower) superior for operation at:

1. Higher sun angles
2. Higher altitudes

Conditions:

- 160-nautical mile altitude
- 20 and 5-degree solar elevation
- 1.6:1 contrast in ground scene
- 3400 and 3404 films
- W-25 filter

Curve Designations:

- OA = on axis
- R = radial
- T = tangential
- 45° = 45 degrees to radius } at format corners

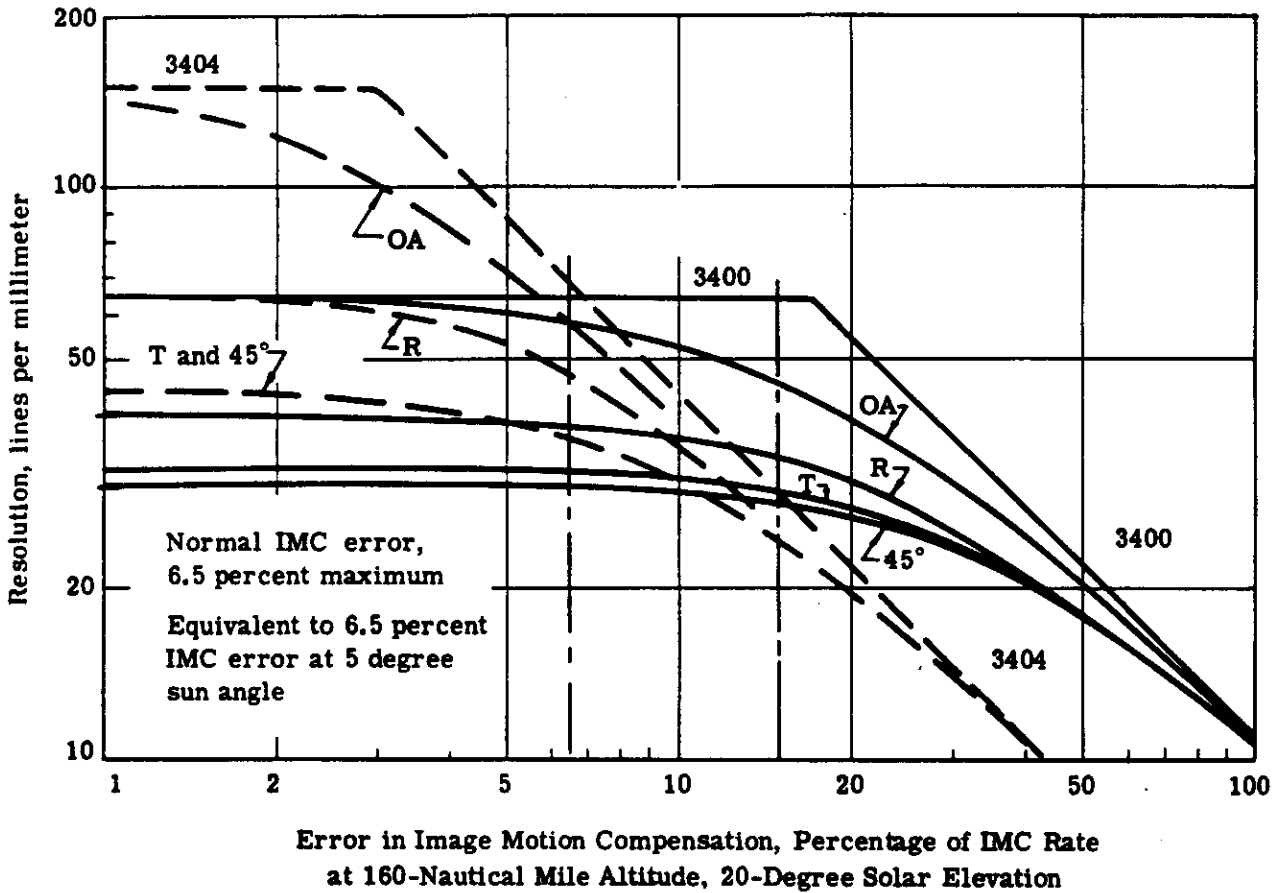


Fig. 2-23 — Resolution versus blur

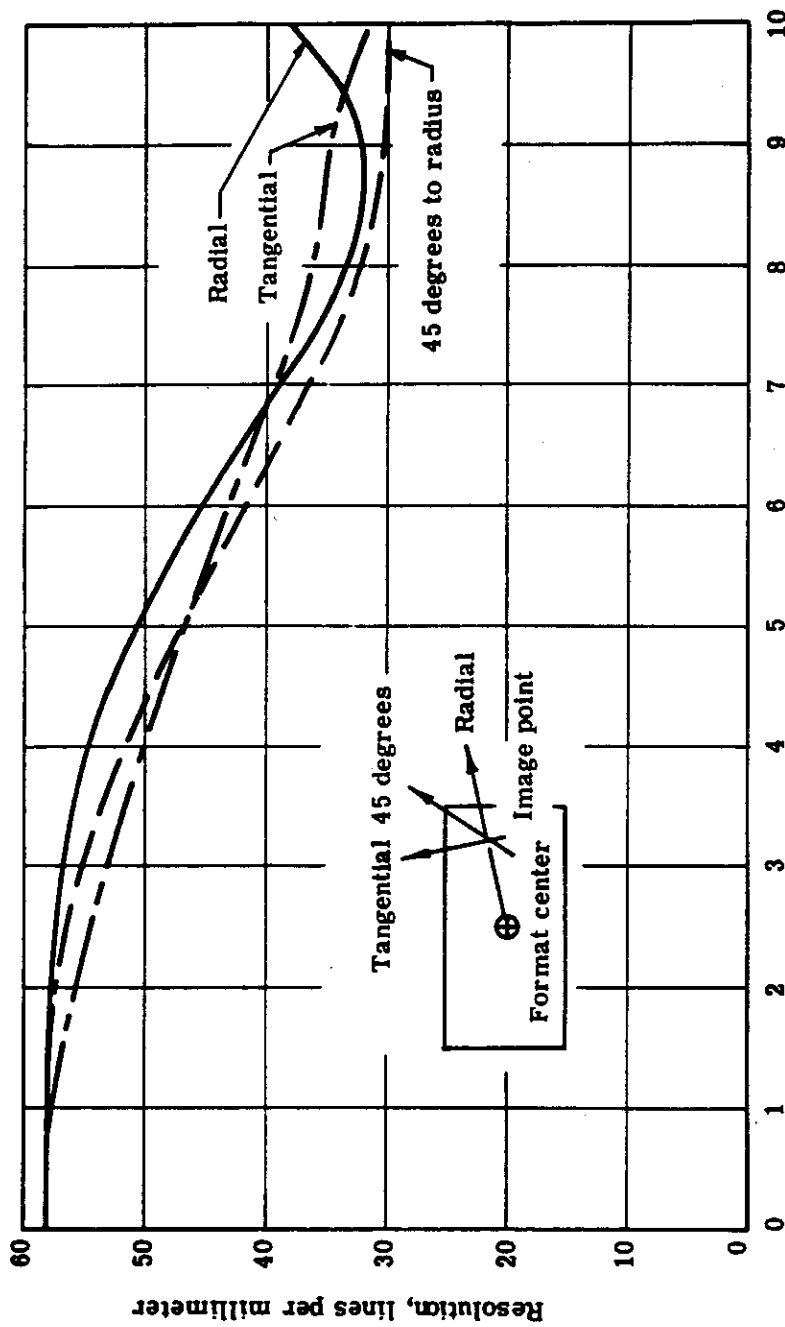


Image Position in Film Plane Measured From Center, inches

Fig. 2-24 — Image plane resolution versus image position for final design

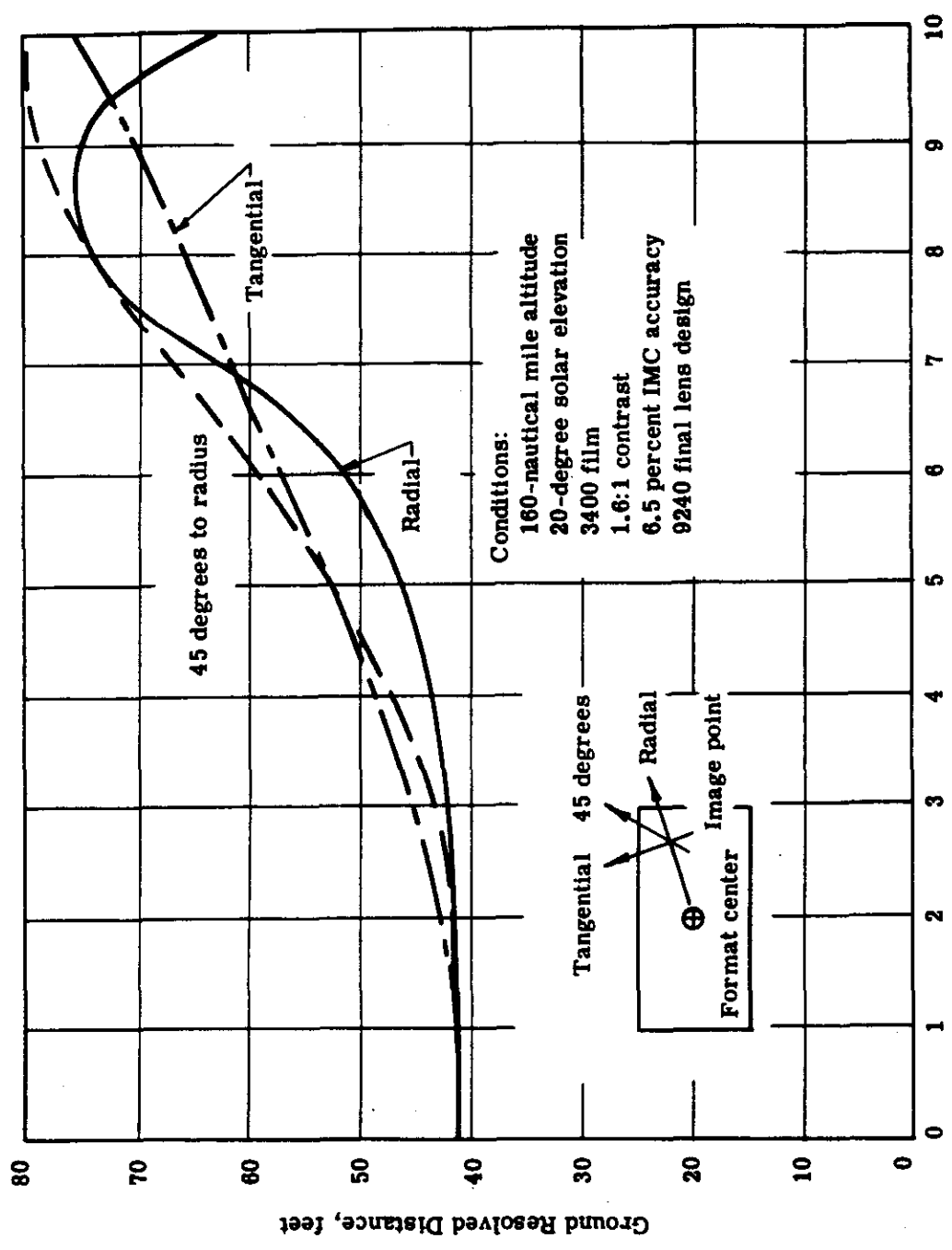


Image Position in Film Plane Measured From Center, inches

Fig. 2-25 — Ground resolved distance as a function of format position

Conditions:

- 1.6:1 contrast
- 20 degrees solar elevation
- 160-nautical mile altitude
- W-25 filter
- 11.4 millisecond exposure time

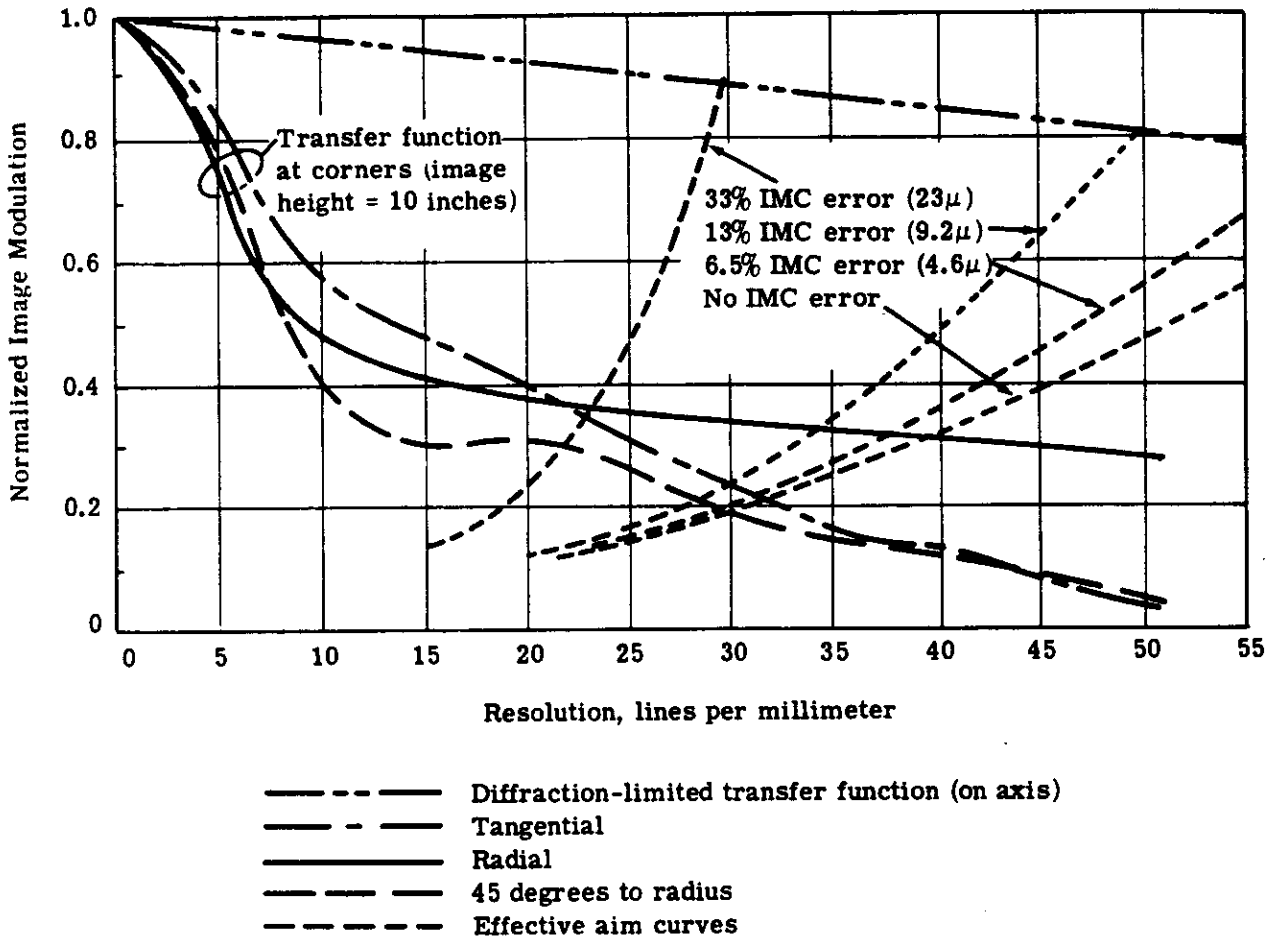


Fig. 2-26 — Effective AIM curves for EK type 3400 film, modified for contrast level and blur superimposed upon final design transfer function

EK type 3400 (coarser-grained film, but faster) superior for operation at:

1. Lower sun angles
2. Lower elevations

Another film, whose characteristics lie between those of the 3404 and 3400 film and which might be investigated at a later time, is SO-362.

Because of its usefulness over a greater range of sun angles, 3400 seems to be the most likely choice for general case, and its use has been emphasized in the resolution study. However, the final choice may be dependent upon the details of the mission.

From Figure 2-23 and using 3400 film in the terrestrial camera at a 160-nautical mile altitude with a 20-degree solar elevation, and 1.6:1 contrast in the ground scene, the values of resolution are given in Table 2-7.

2. Metric Accuracy

The geometric fidelity of the camera system is affected by its design and its environment. These factors are described in this section; also described is on-orbit calibration by which many of the launch and environment limitations to geometric fidelity can be minimized.

a. Factors Affecting Metric Accuracy

(1) Image Character - Lens Color Error

Investigations of effects of image character were, for the most part, conducted experimentally but an analytical study was performed to estimate the effects of lens color error.

The terrestrial camera has a secondary lateral color blur at large field angles. At the format corners, a point of light is blurred. The yellow portion of the spectral band falls nearest the axis of the lens, and the red and green portions fall farthest from the axis. The color shift is approximately a parabolic function of wavelength. The final lens design shows that the maximum color blur at both ends of the spectrum is about 10 microns.

The effect of the color blur is to give objects of different color different image positions. For analysis, the problem is represented here as the determination of the image position variations of shadow detail in various natural scenes as the scene color varies.

The color of the scene depends upon the spectral reflectance of the scene, the spectral distribution of the energy of the illumination, and the spectral response of the film, the filter and the lens. Figure 2-27 gives the spectral reflectances of some natural objects.*

The analysis described in the following paragraphs was made for the lens design which preceded the final design. The spectral bandwidth for this design was larger than for the final lens design, and the maximum color blur was 25 microns as opposed to about 10 microns for the

* Krinov, E. L., "Spectral Reflectance Properties of Natural Formations," Technical Translation II-439, National Research Council of Canada, Ottawa, 1953.

Table 2-7 — Resolution Values

Resolution	6.5 Percent IMC Error, lines per millimeter	Motionless, lines per millimeter
Maximum resolution, on-axis	58	64
Minimum resolution, 45 degrees to radius at corners	29	30
Minimum average resolution at corner	32	34
$\frac{R + 2R + R}{4}$		
AWAR	45	48

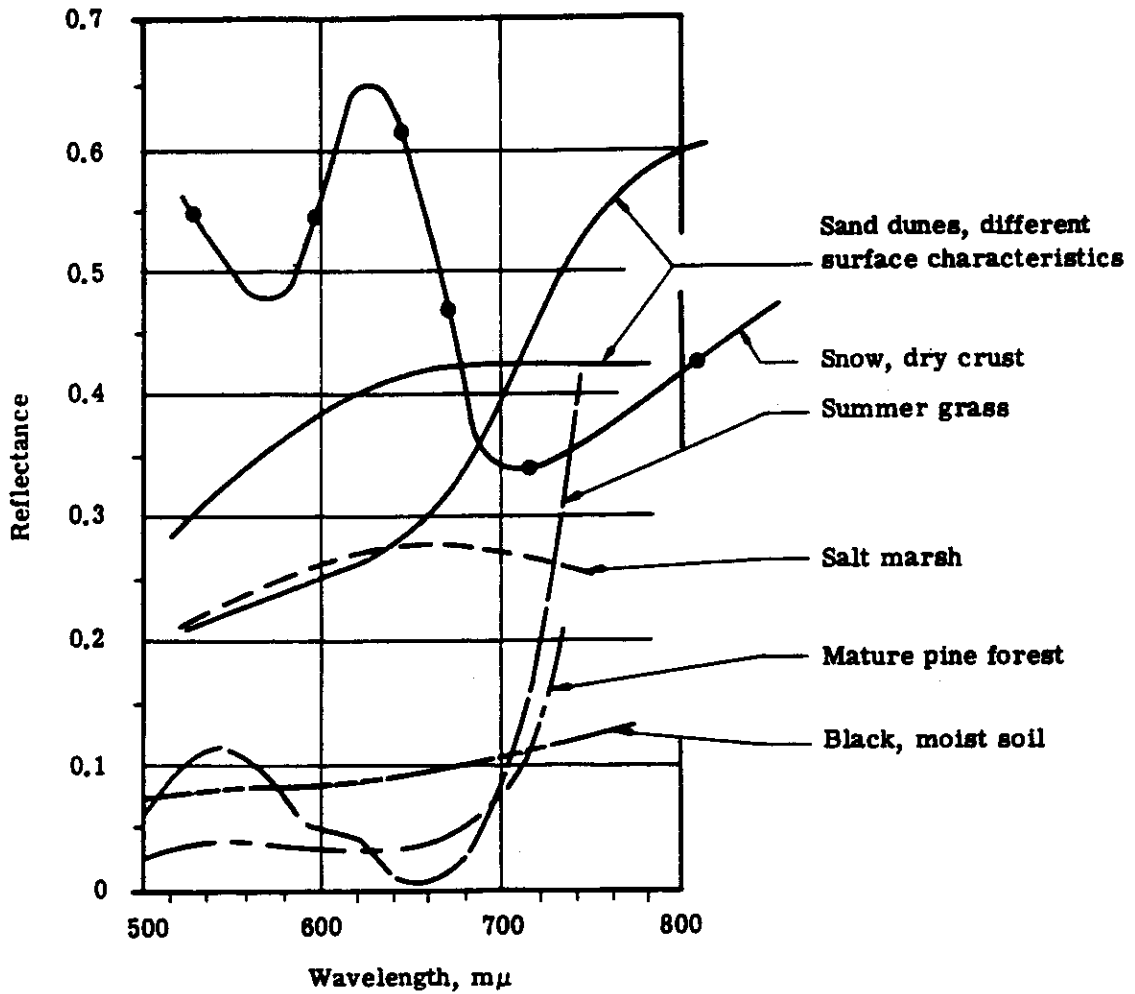


Fig. 2-27 — Spectral reflectance properties of natural formations (from E. L. Krinov)

final design as indicated by the ray trace results. Consequently, the color error in the final design is roughly 10/25 that found for the previous design.

From the data expressed in Figure 2-27, relative intensity profiles for shadow edges (shadows on a neutral surface, on summer grass, and on snow have been taken as representative of the mean and the extreme cases) have been determined and are plotted in Figure 2-28. The edges in the ground scene have been transformed into equivalent monochromatic object intensity profiles which replace the actual objects and which, when presented to a camera without the color blur, give the actual images in the real camera. The abscissa might be given as distance on the ground, but it has been expressed as distance on the film for convenience in interpreting the graphs.

In other words, when acted upon by the monochromatic transfer function of the lens, the curves of Figure 2-28 become the intensity profiles which are presented to the film. Conversely, from the actual exposure profiles presented to the film and the lens monochromatic transfer functions, the equivalent object profiles can be derived, which is how these curves were obtained.

The relative intensities in Figure 2-28 are plotted on a log scale, which more closely approximates the response of the eye than does a linear scale. The curves for snow and summer grass which are the extreme cases are generally displaced from the curve for a neutral surface by 1.5 to 2 microns. However, the points chosen by the eye as being the location of the edges may be in the regions where the slopes of the curves are greatest at the left-hand side of the curves. Because of the smoothing effect of the lens-film transfer function, the points of maximum slope on the curves are not at the extreme left but are shifted somewhat to the right, where there is some separation between the curves. Thus, the curves in this figure show that in the extreme cases, color errors of ± 1 micron are likely but in any case will not exceed ± 2 microns for the former lens design. For the final lens design, since the color error is a little less than half the amount used in this analysis, color errors of ± 0.4 micron may be expected.

(2) Camera Component Factors

In order to estimate the effect of the operation of the terrestrial camera mechanism upon image position accuracy, a budget was made containing the effects of operation of the major camera components. The composition of the budget is given in Table 2-8 in a form that permits the determination of the RSS random image position error at any position and orientation in the format. Table 2-9 gives the RSS image position errors at the format corners and at the center. The following text describes in more detail the various error sources.

(a) Platen Lateral Position Error

Because the platen has a curved front surface, the distortion pattern of the whole system depends in part upon the lateral IMC position of the platen. In order that a single set of distortion data be valid for the camera under all conditions, a restriction must be placed upon variations in the platen position from exposure to exposure. This restriction then dictates what positional accuracy must be maintained by the mechanism which moves the platen for IMC.

The distortion variation arising from a platen positioning error can be obtained from Figure 2-19 in the previous section dealing with the image motion analysis, which shows that at a point 10 inches forward of the center of the format, a given platen displacement produces an image movement of 4.6 percent of the platen movement. Although the platen actually extends forward only 9 inches at that point, it turns out that the 4.6 percent value for the 10-inch point becomes the value at the format corner when multiplied by the cosine² of the azimuth angle to the corner.

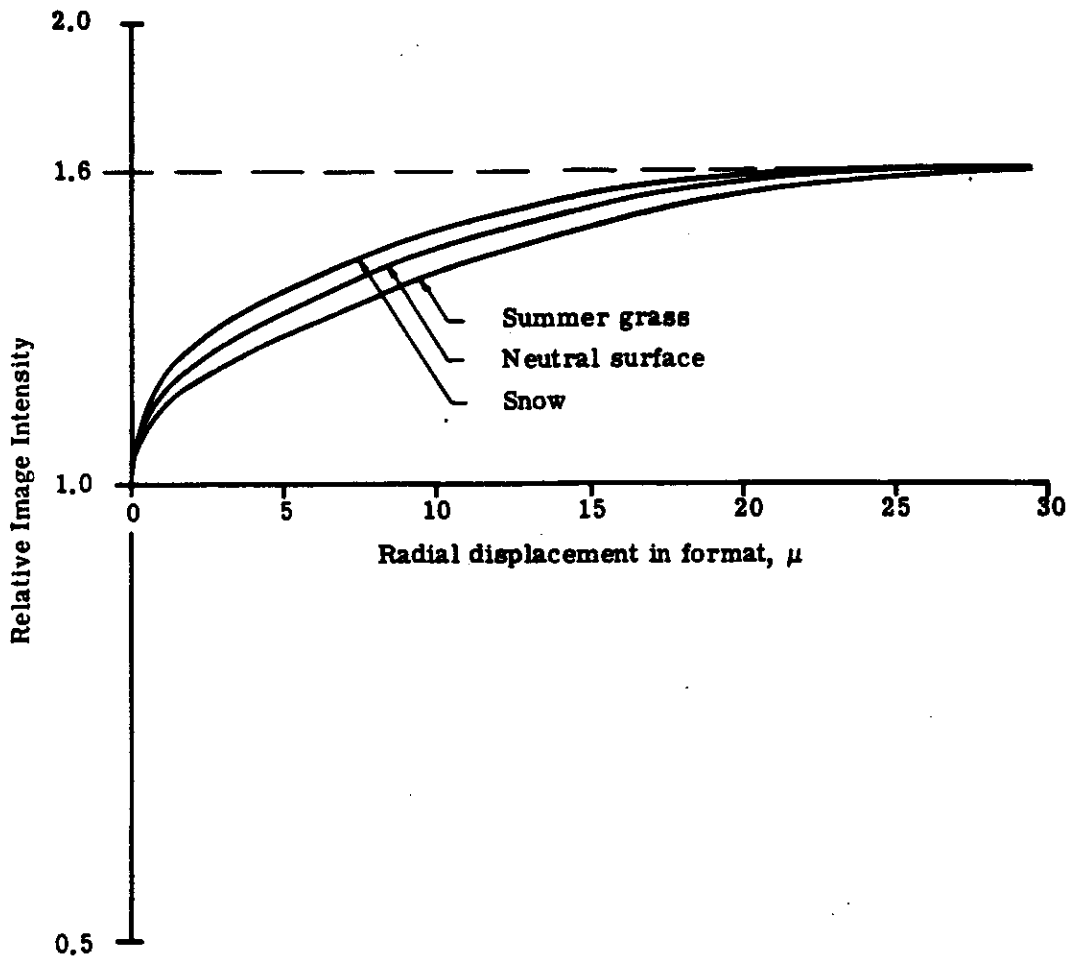


Fig. 2-28 — Relative intensity profiles for monochromatic objects to shadows on grass, snow, and a neutral surface

Table 2-8 — Camera Mechanism Tolerances

Source of Image Position Error	Error, microns	Direction
Platen lateral position error		
Shutter/platen synchronization $\pm 80 \mu$	0.5	Along-track; constant over format
Positioning error across-track	negligible	
Platen rotation about optical axis during IMC	0.4	Tangential, proportional to radius
Platen pressure variation, ± 0.03 psi, $\pm 0.2 \mu$ deflection variation	negligible	
Shutter/fiducial synchronization error $\pm 3 \times 10^{-5}$ seconds	0.3	Along-track; constant over format
Contact irregularities between film and platen $\pm 1.2 \mu$	1	Radial, proportional to radius
Image motion errors; nonlinearity of image motion		
Platen servo velocity variation during exposure ± 0.1 percent fV/h	0.025	Along-track; constant over format
Vibration ± 1 percent fV/h		
rotational	0.4	Tangential proportional to radius
translational	0.4	Any direction; constant over format
Nonlinearity of blur from distortion and platen curvature	10^{-5}	
Platen axial motion during IMC	negligible	

Table 2-9 — RSS Random Image Position Errors
at Various Format Positions and Orientations,
Microns

Corners	
Radial	Tangential
± 1.2	± 0.7
Center	
Along-Track	Across-Track
± 0.7	± 0.4

This is the maximum distortion variation in the format and is 3.7 percent of the forward-direction platen positional error. Allowing a maximum distortion variation of ± 0.5 micron, the platen servo positioning tolerance becomes ± 18.5 microns. It should be kept in mind that a reasonable alternative to maintaining this tolerance is adding to the distortion calibration a correction based upon the actual platen position at the center of the exposure. This position is always known within a micron, although it cannot be controlled that closely. Since the maximum corrections would be on the border of 3 microns (for platen positioning errors up to one-half the total IMC stroke), it could easily be computed with sufficient accuracy; there would be no need for an experimental evaluation of the distortion variations.

Thus, whether or not the actual positioning tolerance is held with ± 18 microns, makes little difference in the camera performance if distortion correction for distortion variation remains a possibility in the data handling program. It is expected that ± 18 -micron tolerance can be met without difficulty.

In the blur budget, allowable platen across-track motion during IMC was 1 micron. Mid-exposure position across-track will vary less than this amount and much less than the 18-micron position variation allowed along-track. The across-track positioning error is insignificant in terms of image position error.

(b) Platen Rotation about Optical Axis during IMC

The flexure mounting for the platen is symmetric by design, but very likely it will have some slightly nonsymmetric properties which would cause the platen to move in a curved rather than straight line. Application of the IMC driving force off center will also have this effect. If a rotation of the platen reseau relative to the fiducial marks is accounted for in the data reduction program, no error will arise. On the other hand, if the platen rotation is kept small enough, the error will be insignificant and no provision for rotation will be needed in the program. The error in image position arises in conjunction with the 80-micron tolerance for platen position at the center of exposure.

The maximum IMC stroke is about 200 microns at low sun angles, so the variation in mean rotational position from frame to frame is $\pm 18/200$, or 0.1 times the total rotational motion during the IMC stroke. In the blur budget, a 1-micron across-track motion of the platen is allowed during an IMC stroke of 100 microns, or 2 microns for a 200-micron stroke. This can conveniently be divided into a 1-micron lateral motion at the platen center and a 1-micron rotational motion at the ends of the platen. (The two motions are likely to be interdependent and add directly to fill the 2-micron blur tolerance.) From this, a 0.4-micron tangential error is likely at the ends of the platen, which is proportional to the radial distance from center.

(c) Platen Pressure Variation

The 0.3 psi pressure used to hold the film against the platen may vary slightly from frame to frame or over a long period of time. Variations in pressure cause the platen deflection to vary from its value at calibration. The formula for the deflection of a flat plate simply supported on all edges shows that deflection of the platen is about 6 microns per psi of pressure applied. If the pressure is allowed to vary by ± 10 percent, or ± 0.03 psi, the center deflection will vary by ± 0.18 micron. The deflection will decrease toward the edges of the platen and become zero at the edges. The 0.18-micron deflection variation will cause no image position error on axis, very slight (0.05 micron) errors at intermediate format positions, and no error at the format edges.

(d) Shutter/Fiducial Synchronization Error

The fiducial marks are flashed onto the film at the center of the exposure time to indicate the position of the platen at midexposure. An error in the shutter/fiducial synchronization causes a frame-to-frame time measurement error which is equivalent to an image position error constant over the format in the fore-and-aft direction. Inaccuracies in the gear train connecting the shutter discs causes variations in the time of coincidence of the shutter disc openings which trigger the fiducial marks. The total synchronization error from gear error, for precision-1 gearing, is about 2.8×10^{-5} second, or a ± 0.28 micron image position error. In addition, there exist variations in the triggering threshold of the fiducial actuator. By design, this error can be kept small enough so that the total synchronization error will be within 3×10^{-5} second, or ± 0.3 micron of position error. In addition to the random synchronization errors, there is a systematic error arising from error in the placement of the shutter disc openings and in the location of the mean fiducial triggering threshold relative to the coincidence of the shutter disc openings which trigger the fiducials. This error, which may be as much as 1 micron, is eliminated in calibration of the terrestrial-stellar camera alignment.

(e) Contact Irregularities Between Film and Platen

If there is a slight space between the film surface and the platen surface, there will be an image position error equal to the spacing times the tangent of the angle of the light incident on the film at that point. The film flatness experiment (reported in the experimental investigations at the end of this section) has indicated that a one-sigma deviation from flatness of about 0.6 micron is attainable under good conditions.

It would be too optimistic at this time to assume that this result can be repeated consistently, so in this allocation of tolerances, twice that value has been used, 1.2 microns. The angle of incidence of the light at the format corners is about 40 degrees, so the image position error at the format corners may be about ± 1 micron. This error is radial and proportional to the distance from the center of the format.

(f) Image Motion Errors—Nonlinearity of Image Motion

If there is a slight increase in the platen velocity during the exposure time, it can be shown that the resulting image position error from this velocity variation is no greater than a quarter of the product of the exposure time and the velocity variation from the beginning of the exposure to the end.

(g) Platen Servo Velocity Variation during Exposure

The platen servo velocity tolerance is about 1 percent fV/h. The servo bandwidth is about 10 radians per second, so the maximum rate of change of velocity of the platen is on the order of the bandwidth frequency times the velocity variation amplitude, or 10 percent fV/h per second. The possible variation of platen velocity during exposure is this rate of change times the exposure time, about 0.1 percent fV/h for an exposure time of 10 microseconds. This produces no more than an 0.25-micron image position error.

(h) Vibration

The greatest image position error from vibration is possible with high-frequency vibration for which a complete reversal of the direction of vibration motion is possible during the exposure time. In this case an image position error of half the peak-to-peak vibration amplitude is

possible. For an 11.4-millisecond exposure time, high-frequency is 43 cps or greater. In the blur budget, a vibration tolerance of 1 percent fV/h was used. This is equivalent to a 0.85-micron blur from high-frequency vibration and can cause a 0.4-micron image position error. Vibration might result in linear blur across the format or tangential blur about the optical axis. It is assumed that the image position error at the format corners is composed of equal portions of translational and rotational vibration; a 0.3-micron error from each yields a total RSS of 0.4 micron.

(i) Nonlinearity of Blur From Distortion, Platen Curvature, and Earth's Curvature

Linearized equations were used to compute the IMC error caused by distortion and by platen curvature. The linearized equations are in error by no more than 0.5 percent over the IMC stroke distance. The blur from these sources was 1.6 percent fV/h, so the change in the blur velocity during the IMC strike is 0.5 percent of 1.6 fV/h. The resulting image displacement error is less than 10^{-5} micron.

(j) Platen Axial Motion During IMC

The flexures carrying the platen have an effective length of about 3.5 inches. The IMC motion is about 0.004 inch on either side of dead center. The resulting axial motion of the platen, which is toward the nodal point on both sides of midexposure, is 2.7 microinches, or 0.058 micron, and is insignificant.

Table 2-10 summarizes the effects of camera geometry change from the different sources, assuming on-orbit calibration.

Table 2-10 — Terrestrial Camera Image Position Errors From Camera Geometry Changes

Source of Image Position Error	Image Position Error, microns			
	Corners		Center	
	Radial	Tangential	Along-Track	Across-Track
Color error	0.4	0	0	0
Camera mechanism errors	1.2	0.7	0.7	0.4
Launch effects and dimensional instability	1	1	negligible	negligible
Thermal variations during operation	1	negligible	negligible	negligible
RSS	1.6	1.2	0.7	0.4

(3) Environmental Factors Affecting Calibration

(a) Launch Effects and Dimensional Instability

Changes in the distortion characteristics and the focal length of the camera may occur after ground calibration as the effects of the launch environment. The distortion and focal length changes are, more directly, the result of changes in the dimensions of the lens cell and structure connecting the lens cell and the platen.

Previous experience with an 18-inch focal length Topar lens indicate that some form of recalibration after launch is highly desirable. This experiment showed a maximum nodal point shift of approximately 50 microns. Scale recalibration of the terrestrial camera, either from ground photographs or stellar photographs will correct for the scale changes and partially compensate the axi-symmetric distortion changes. Stellar-terrestrial camera alignment recalibration is necessary to correct positional shifts of the fiducial markers; this factor is properly considered with other stellar-terrestrial camera alignment factors.

To estimate the amount of relative motion likely between some of the elements, consider a change in position of the platen relative to the rest of the camera. The platen is the most massive single element, its supports are least rigid, the separation between it and the lens is the greatest element-to-element separation in the camera, and the stainless steel structure supporting the platen is slightly less stable dimensionally than the beryllium lens cell structure. For a micro-strain rate for stainless steel of 5 inch/inch and a 12-inch stainless steel structure between the platen and the lens nodal point, the estimated shift in platen position is 1.5 microns. The result might be in the form of tilt, despacing, or rotation. In the optics section, it is shown that for element movements of this magnitude, the only image position changes which are not equivalent to a combination of simple movements of the camera itself, are on the order of a few tenths of a micron. From motions of all the elements, therefore, the total variation in the radial lens distortion which cannot be compensated without a complete distortion recalibration certainly amounts to less than a micron. Although the tangential distortion induced by element shifts was not studied, it can be expected to be of the same order of magnitude as the radial distortion changes, a micron or less after stellar recalibration.

(b) Thermal Variations During Operation

A thermal analysis of the system was made to determine what thermal changes were likely to occur during operation (see Section 2.4.2). Coupled with the estimated sensitivity of the optics to thermal changes in selected parts of the lens, a thermal variations budget was devised which is thought to be realizable but sufficiently tight to keep the image position errors within acceptable limits.

In determining what factors needed study, the nature of the thermal inputs was considered. It is likely that, over a long period of the time, the whole camera may undergo a temperature change with consequent growth, and so the effect of overall temperature change was investigated. The exposure shutter isolates the rear half of the lens cell and the platen from the incident earthshine, albedo, and sunlight, so it seems likely that changes in the temperature of the front half of the lens will occur apart from those in the rest of the camera. The front element radiates directly to ground and absorbs most of the incoming infrared. Hence temperature level variations and gradients are most likely in the first element.

The sensitivities study was made for the final design lens, but the computer program used was designed for a slightly different lens. The data are approximate, but are certainly representative. Data extracted from this study are given in the following paragraphs.

(c) Overall Temperature Level Change

The sensitivity to changes in camera temperature is found in the difference between the platen expansion curve and the lens expansion curve for a 10°F temperature change, maximum image displacement is about 1.4 microns. Figure 2-8 is printed on the following page for the reader's convenience. The coincidence of these two curves will be dependent upon the accuracy with which the thermal coefficient of the stainless steel camera structure can be matched to the desired value. By adjustment of the thermal coefficients, the matching of the curves can be optimized so that the residual image displacement is halved to 0.7 micron for a 10°F temperature change. If the accuracy of prediction of these curves is only 5 percent for each one, the RSS error is an additional 0.7 micron, so the overall error is back to 1.4 microns.

If a tolerance of 0.5 micron for each thermally caused image position error is considered acceptable, overall temperature tolerances can be set. Since scale change can be corrected by the on-orbit calibration, a ±3.5°F temperature change is acceptable after on-orbit calibration. The nonlinearity of the scale change is difficult to take into account in on-orbit calibration. This nonlinearity amounts to ±0.4 micron for a ±10°F temperature change. The camera temperature on-orbit can be predicted to within ±10°F, so for this much temperature change between ground calibration and orbital operation, the effect of nonlinearity of the scale change remains within acceptable limits. If the on-orbit camera equilibrium temperature cannot be predicted within ±10°F, it may be necessary to calibrate the camera on the ground at two temperatures.

(d) Temperature Difference Between Front Half of Cell and Rest of Camera

Figure 2-8 shows that a ±10°F difference between the front half of the lens cell and the rest of the camera results in a distortion variation of ±7.4 microns. The 0.5 micron tolerance thus permits a temperature difference of ±0.7°F. The thermal analysis shows that because of absorption of light and reradiation of infrared by the shutter, a maximum difference in temperature between the front and the rear portions of the front half lens cell is about 0.9°F. By silvering the front surface of the front shutter disc, most of that energy can be reflected back out rather than be absorbed. This represents one of the important sources of gradient, and indicates that the ±0.7°F tolerance is reasonable, although other sources of gradients, such as the shutter motor, have not been examined.

(e) Temperature Difference Between Front Element and Rest of Front Half of Lens Cell

Figure 2-8 shows that a 10°F difference between the front element and the rest of the camera results in a maximum distortion change of 6 microns. The thermal analysis predicts that within each orbit, the front element bulk temperature will depart from the camera temperature by about 0.6°F. Thus, a 0.36-micron distortion change can be expected.

Long term temperature drift was not analyzed, but it can be controlled if necessary by employing a heater on the thermal shutter.

(f) Gradient in the Front Element

In Section d. (page 2-19) it is shown that a radial gradient in the front element of 1 °F per inch might produce an image shift of 3.6 microns. Such a gradient is likely to arise because the front element is not of uniform thickness but during photography radiates energy uniformly over its surface. If the gradients can be kept to within 0.1 °F per inch, the distortion will be acceptable. Because the 13-inch diameter lens varies in its bulk temperature during each orbit by 0.6 °F, it might be found necessary to use a heater on the thermal shutter that would operate during the photographic portion of the orbit in order to keep the gradients within 0.1 °F per inch. During each 12-second period in which the shutter is closed, this heater would replace the heat lost during the 2-second open period. About 1.2 watts distributed uniformly over the front element surface would be required for this.

(g) Thermal Tolerance Budget

As a summary to this section, a thermal tolerance budget is compiled from the preceding paragraphs and given in Table 2-11. The RSS result from this budget indicates that the image position errors resulting from thermal variations in the camera can be kept to within ±1 micron. This value is used in the image position error budget, Table 2-10. Most of the items discussed here are most serious at the format corners, so the ±1-micron error at the corner can be roughly scaled according to the radius of the image position in the format.

(4) On-Orbit Camera and Knee Angle Calibration

Because of the probability of minor changes in the calibrated focal length of the terrestrial camera system and in the knee angle either from the launch environment or the orbital environment, calibration of the system is recommended at least once on orbit. In addition, periodic on-orbit calibration in the first flight to determine system behavior is considered highly desirable. Checks would be desirable immediately before and after possibly 15 photographic passes. In possibly five of these passes, a calibration check would be required in the middle of the photographic pass. The data so obtained would provide the photogrammetrist with the needed information as to the degree of accuracy he can obtain from the system.

For this recalibration, the vehicle would be rolled into such a position that the terrestrial camera axis is near the plane of the galactic equator in order for the camera to see the optimum population of stars. The best time of year with regard to having the brighter stars available for calibration during the middle of a photographic pass would appear to be when the sun is farthest from the galactic equator. This would appear to be at either the vernal or the autumnal equinox. During calibration, it is probable that only one stellar camera will see a usable star field. However, this is sufficient since these cameras calibrate their own knee angle with every operational photograph.

(a) Population of Stars in the Terrestrial Camera Photograph
(On-Orbit Calibration)

In photographing extended objects, the terrestrial camera has a loss of illumination approximately equivalent to the cosine³ θ of the field angle. The reason it does not follow the classical cosine⁴ law is that the large negative elements in the front and the rear of the system expand the image of the stop so that it presents the same projected area to all parts of the film. This eliminates the cosine loss from having the aperture at an angle to the incoming light.

Table 2-11 — Thermal Tolerance Budget for the Terrestrial Camera

	Thermal Tolerance	Radial Image Position Error at Full Field, microns
Overall temperature change from conditions during on-orbit calibration	± 3.5 °F	± 0.5
Overall temperature change from conditions during ground calibration (not correctable by on-orbit calibration)	± 10 °F	± 0.4
Temperature difference between front half of cell and rest of camera	± 0.7 °F	± 0.5
Temperature difference between front element and rest of front cell	± 0.6 °F	± 0.36
Gradient within front element	0.1 °F/inch	± 0.36
RSS image position error		<u>± 0.96</u>

The other three cosines in the cosine⁴ law arising from the increase in slant distance from the aperture to the film and the angle of projection of the light onto the film still apply. The illumination decreases with the square of the distance to the aperture, accounting for a cosine² effect, and it decreases with the cosine of the angle of incidence of the light to the film. These two effects, accounting for cosine³ loss in illumination for extended objects, have no effect on star imagery. The star is well below the limit of resolution, and the lens concentrates all the energy passing through the aperture from the star into a point which is acceptably small for the emulsion. The terrestrial camera, with no vignetting correction, should record stars equally over the field, when there is no motion error.

While there are some minor losses from the poorer imagery given by the lens at large field angles and from the loss of light by reflection at the emulsion surface at large angles of incidence, the major loss of stars involves the motion of the star images during calibration.

This loss arises from a decrease in effective exposure time as the point image trails across the emulsion surface. The trailing motion is caused by angular instability of the spacecraft during the calibration exposure. The trailing motion is the smallest near the center of the format. In this location residual angular rates in pitch and roll are multiplied directly by the focal length to produce image motion. In the outer portions of the field of the system, the lever arm by which the angular rates are multiplied increases. The maximum motion effect appears in a radial direction. Here the lever arm has increased to the slant focal distance $f/\cos \theta$ and there is an additional $\cos \theta$ increase in motion by the projection angle onto the format. From this cause there is a $\cos^2 \theta$ loss in exposure for images in the field. This represents a maximum loss in effective exposure of less than a factor of 2 between the center and the edge. And indeed, even when motion components of roll and pitch are combined for images near the axis and roll, pitch, and yaw components are combined for the field points, the ratio of exposure between center and corner of format remains less than a factor of 2.

Since the system is being provided with an approximate cosine³ θ antivignetting filter to equalize the exposure for terrestrial detail, and since this filter is to be left in place for star calibration, it is evident that the star field at the extremes of the format for this system will contain stars of magnitudes equal to those recorded at the center of the format.

(b) Recordable Star Magnitudes

Experimental star recording tests (Subsection 2, page 2-79) have shown that the terrestrial camera using a red filter and 2475 film (Royal X Pan type with extended red sensitivity) will be able to record usable stars up to a magnitude somewhat beyond 4.

Figure 2-29 shows a cumulative distribution of the number of stars in the sky by magnitude. There are about 530 stars in the sky of fourth magnitude or brighter. The field of the terrestrial camera covers about 0.9 steradian. If stars were randomly distributed, about 38 stars would be recorded. However, the star population is considerably denser in the region of the Milky Way on the galactic equator. Thus, if the camera axis can be oriented so that it is in the plane of our galaxy, about 80 stars can be expected on the format. In the poorest portion of the sky, it is possible that only 15 stars would be available.

But to obtain a recalibration of the type discussed (Subsection 3, page 2-85) on the effects of tip, spacing changes, and decentering of the elements, theoretically only 5 well-distributed stars would need to be recorded in any given photograph, since the expected changes in the original

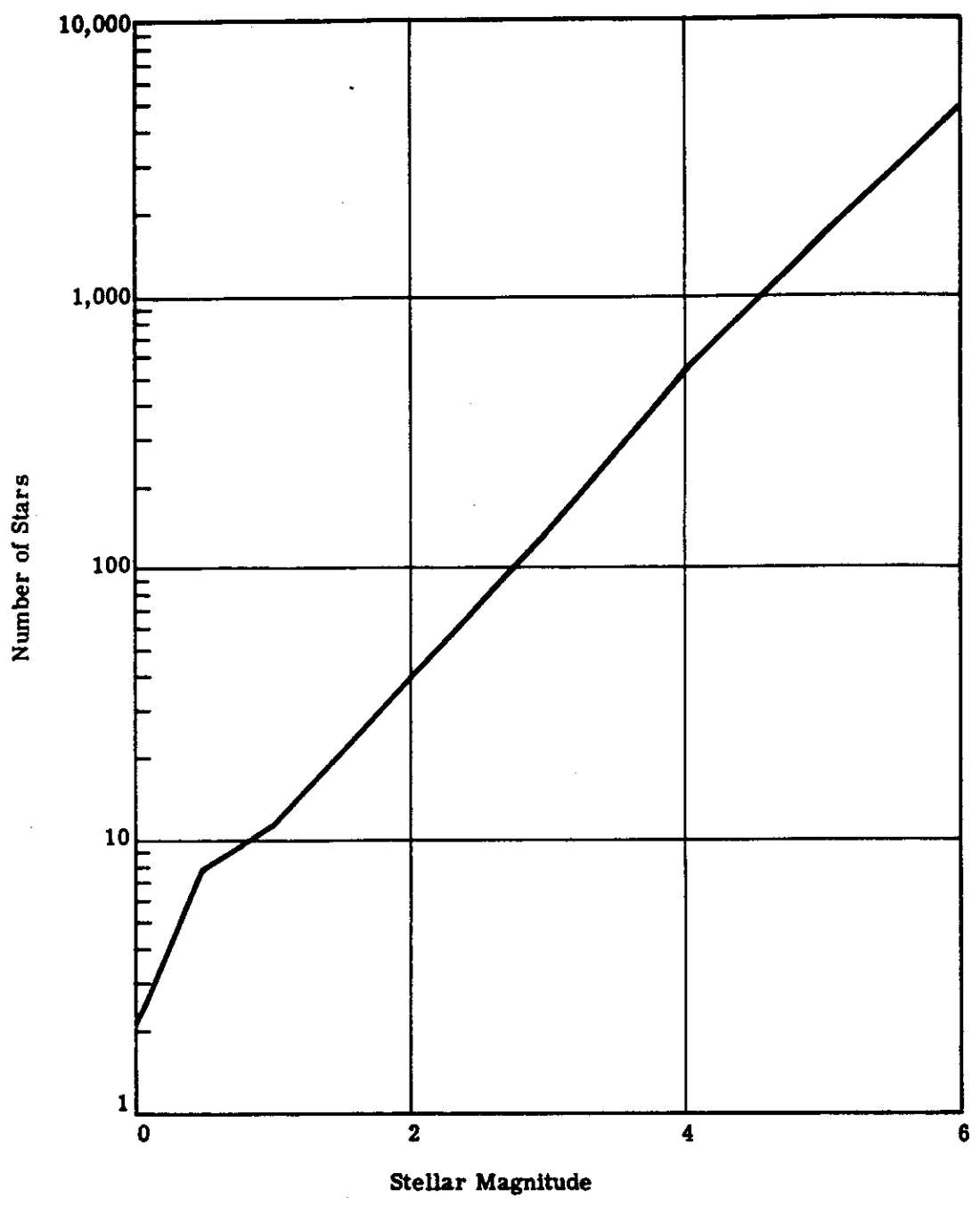


Fig. 2-29 — Cumulative distribution of stars by visual magnitude

distortion calibration are essentially equivalent to a combination of camera movements and can thus be detected photogrammetrically. For improved change-of-calibration accuracy, a series of stellar photographs, each with a minimum of 5 well-distributed stars, could be used to calibrate changes in the knee angle, focal length, and lens distortion function to within 1 micron.

(c) Radiation Effects on Royal X Pan Type Film

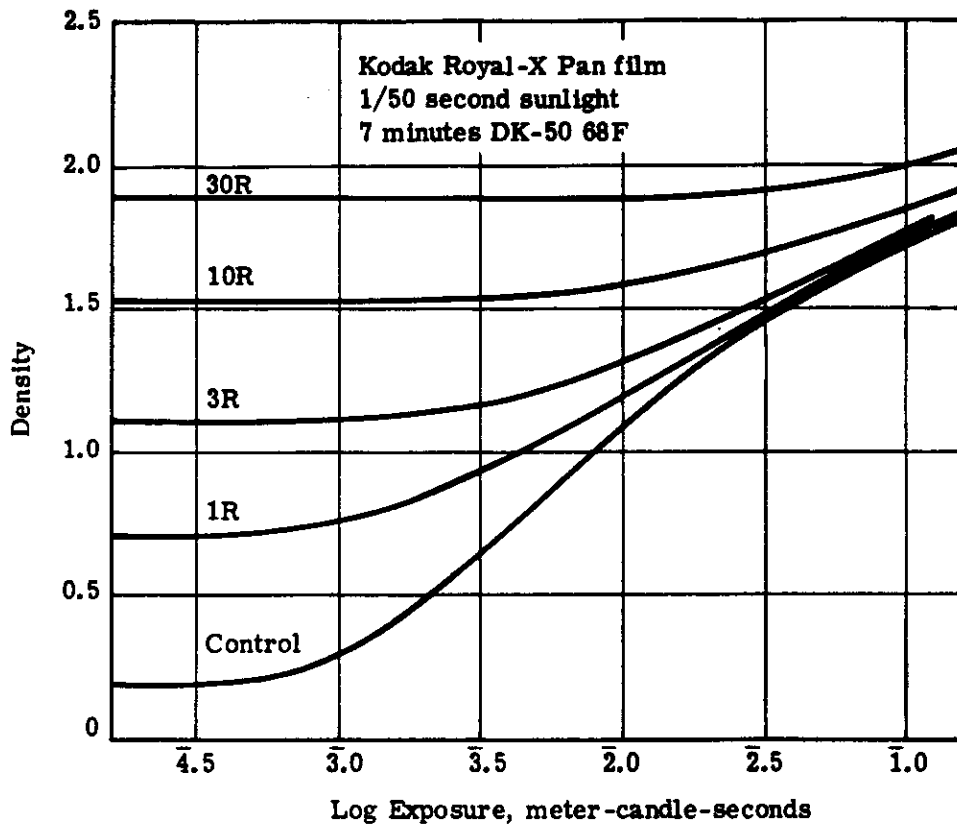
To obtain useful operational stellar calibration data for the terrestrial camera, the 2475 emulsion is necessary. There is some chance that this emulsion would be fogged during a period of intense solar flares. Under these conditions, high energy radiation increases. Plots made by [REDACTED] of Eastman Kodak (Figures 2-30 and 2-31) show the effects of radiation on Royal and Plus-X-Aerecon film. From Figure 2-30, it can be seen that 1 Roentgen raises the base fog level of Royal-X Pan from 0.20 to 0.71. At this level the ability of the film to record stars is somewhat decreased. A safe level of dosage would be 0.5 Roentgen. Additionally, in a recent space experiment Royal-X Pan film was carried on a 150-mile altitude mission for one week without special shielding. The measured increase in fog level was 0.10. Since Royal-X Pan is similar to 2475, the orbit life of 15 days and the nominal radiation environment appear to allow the use of 2475 film for calibration, when some shielding against sun flare activity is employed for safety. Incidentally, the normal terrestrial camera emulsion 3400 and the normal stellar camera 3401 Plus-X-Aerecon appear to be completely unaffected at the expected radiation levels.

2.2.1.2.2 Stellar Camera Performance

1. Choice of Configuration

The stellar camera determines the angular position of the terrestrial camera in space at the moment a photograph is taken. To do this, the stellar camera must photograph a star pattern of at least 2 known stars. In the simplest case, with no instrument or measuring errors, and the stars spaced at the extremes of the format, 2 stars are sufficient for calculating roll, pitch and yaw angles from one photograph. However, in practice, it is extremely difficult to recognize only 2 stars, especially when the positions of the stars are somewhat uncertain because of changing lens distortions. In addition to these, there are the measuring errors arising from film granularity and lack of precise knowledge of star positions. Therefore, it is desirable to measure more than 2 stars to determine the three attitude angles. Generally, the analyst desires 20 to 60 stars in his format to make the orientation determination.

The analyst's accuracy in determining the three angles depends on the accuracy with which he can measure the image positions and the optical lever arm which placed the images on the film. For motions in the focal plane produced by a change in the pointing direction of the optical axis, the lever arm is the focal length of the system. However, for motions in the focal plane produced by a rotation of the camera about the optical axis, the lever arm is the maximum distance between 2 stars in the format. This dimension, for large aperture lenses which are required for recording weak stars, is smaller than the focal length; the result is that the attitude angle around the optical axis is measured with less accuracy than the other two. On the other hand, the photogrammetrist needs more help in finding pitch and roll than the yaw direction. These conditions would dictate that the optical axis of the stellar recording system be on the vertical which, of course, is not practical during the daytime.



Data:

Eastman Kodak Co.

R	Total Fog*	Graininess†
30	1.90	-
10	1.54	-
3	1.12	-
1	0.71	204
0	0.20	194

*Includes base density

† At D = 0.80 above total fog

Fig. 2-30 — Effect of varying Roentgen dosage on Kodak Royal-X pan film, 1000 kvp hardened x-rays

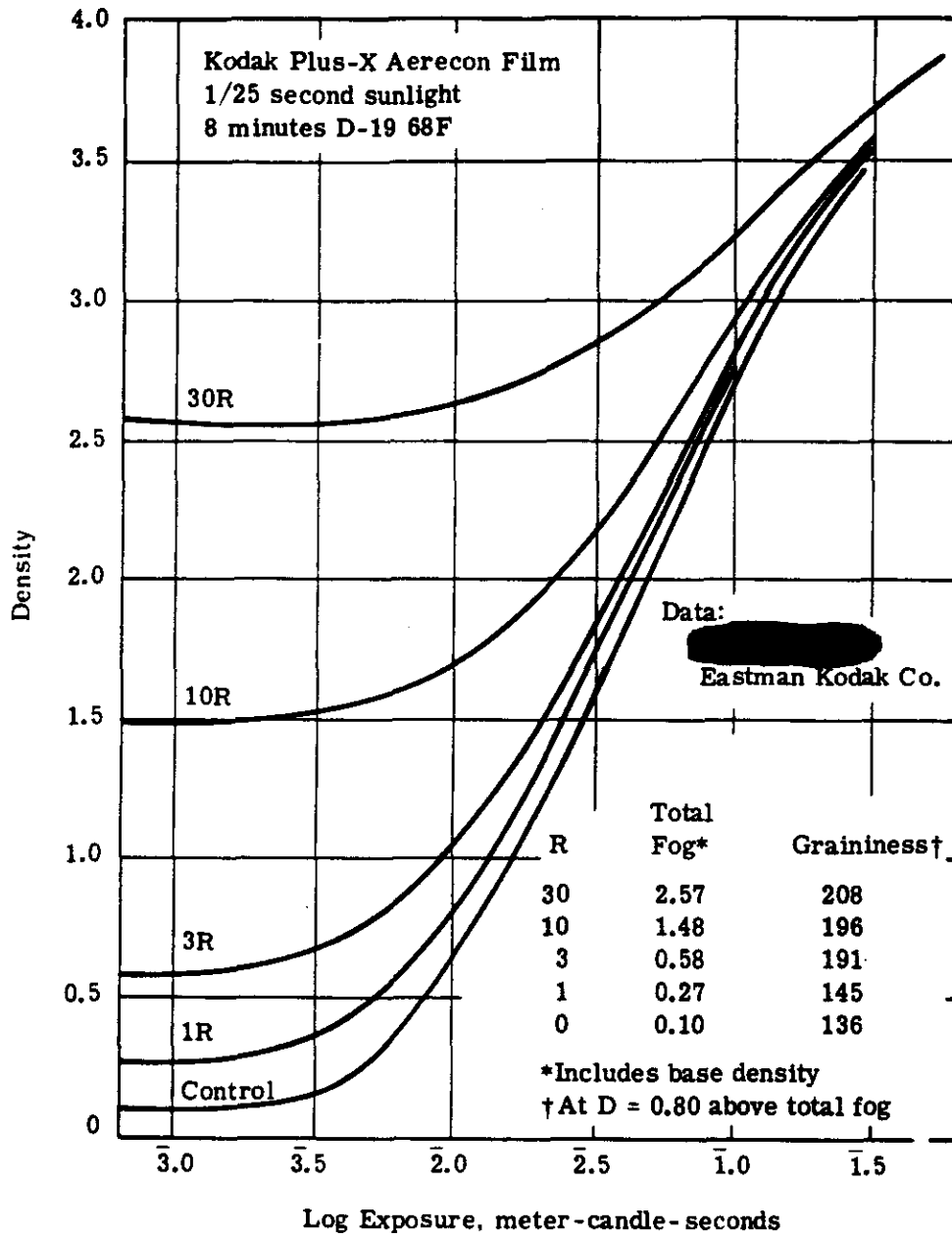


Fig. 2-31 — Effect of varying Roentgen dosage on Kodak Plus-X Aerecon film, 1000 kvp hardened x-rays

The normal stellar camera direction, nearly perpendicular to the orbital plane, gives excellent roll and yaw angle measurement but, about its optical axis, relatively poor pitch information. A stellar camera aimed forward or aft would provide the best pitch and yaw information and relatively poor roll information. In addition, this aiming angle cannot be achieved in practice because of vehicle obstructions.

At a 45-degree angle from the plane of the orbit, pitch and roll angles are measured with about equal accuracy. Yaw is measured more accurately than the other angles if the stellar camera axis lies nearly in the plane of the horizontal. Thus, a configuration of two cameras looking forward at 45 degrees out of either side of the vehicle would provide optimum results for roll and pitch measurement; this is the configuration chosen for this program. Also redundancy is provided in case of degradation of one record, and roll and pitch determinations are strengthened for the case which occurs when these two angles combine to produce rotation about one of the stellar camera axes.

2. Lens Choice

The accuracy and precision with which the angular orientations can be determined is a function of several factors. Of these, the principle sources of error are due to mensuration and the star catalogs. These two error sources are independent, and their effects may be minimized, provided that they are of a random nature, by using a large number of stars in the solution. However, star catalogs are subject to unknown systematic errors, in addition to normally distributed errors. These systematic errors cannot be reduced by statistical means, although it is possible to carry some of the stellar coordinates as loosely constrained variables to estimate the systematic components.

Data derived by Schmid for a 300-millimeter camera relates the number of stellar images used to the angular orientation precision which may be obtained. These data have been scaled for the 250-millimeter camera lens being considered and have been replotted in Figure 2-32 in log-log coordinates. According to Schmid, experience has shown that it is not sufficient to rely upon previously established camera calibrations for correcting the measured coordinates of the star images. In the program for determining orientations from measured star image coordinates, it is necessary to incorporate from four to ten parameters, depending upon the quality of the photogrammetric camera, in addition to the six geometrical parameters (three rotations and three translations) for the purpose of describing the distortion characteristics of the specific photogrammetric record at the moment of exposure. Figure 2-32 shows the number of stars which must be measured as a function of the number of additional parameters which must be carried in the solution in order to obtain a certain overall accuracy of orientation in pointing. It is based upon locating the star images in the format with a ± 3 micron standard deviation. Apparently, a minimum number of from 10 to 30 stars, depending upon the characteristics of the lens, are needed to obtain a pointing accuracy of 1 second of arc.

A wide-angle lens is desirable in order to furnish a strong angles, not because of the increased number of stars, but because of the better geometric distribution. An even more desirable solution is having two cameras oriented at 90 degrees with respect to each other. This is encompassed in the present configuration.

A large aperture lens is required to record as many stars in as short an exposure time as possible. To strengthen the orientation determination, a lens of focal length of the same order as that of the terrestrial camera system is required, with a reasonable format size to provide measurement of angular rotation about the optical axis.

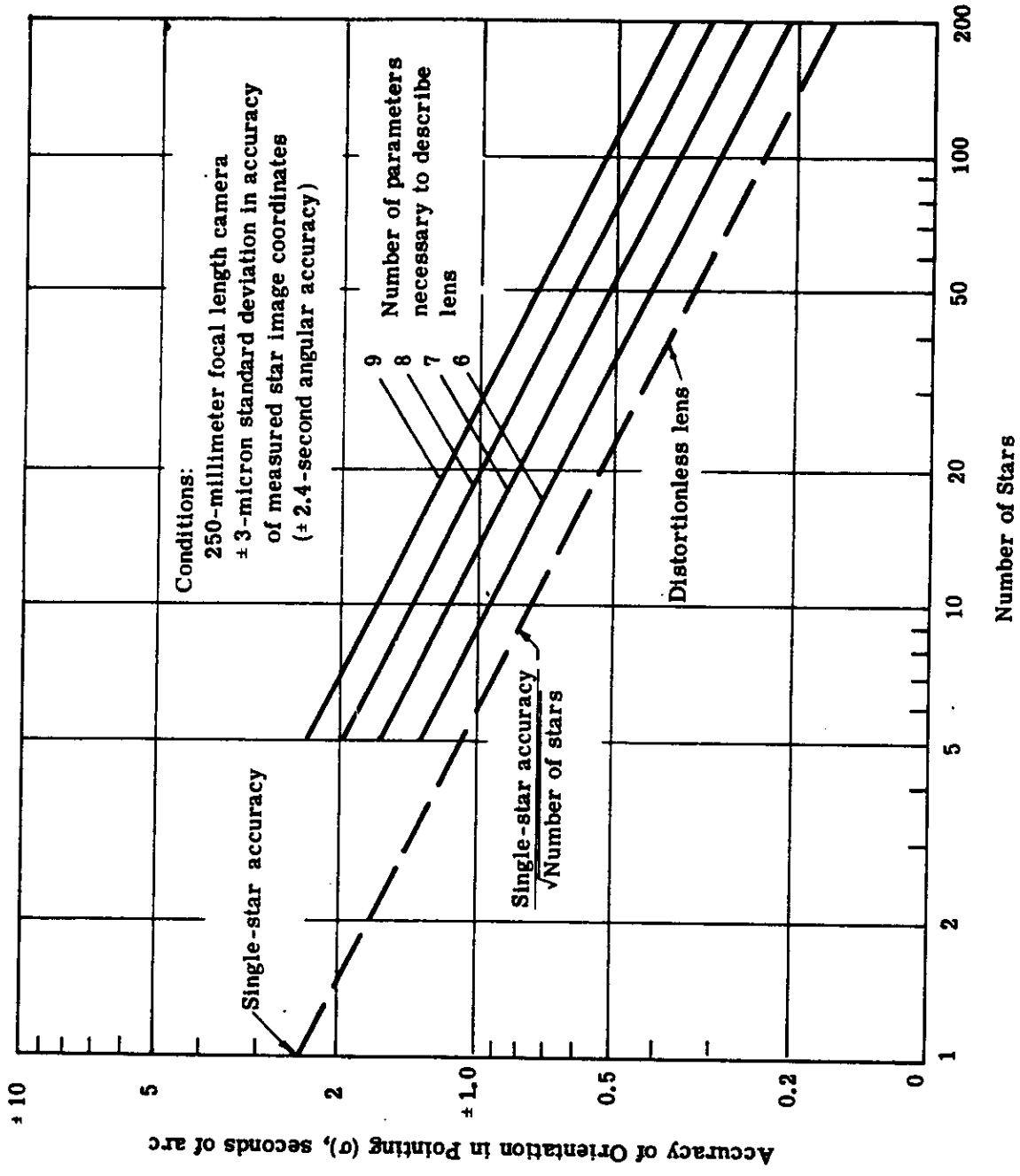


Fig. 2-32 — Accuracy of orientation in pointing determined by a stellar camera as a function of the number of stars recorded and measured

An off-the-shelf lens system, which is suitable for the stellar camera, is the Wild 250-millimeter f/1.8 Falconar (see Figure 2-33). The Wild Falconar 250 has the following significant features.

1. Focal length: $f = 248$ millimeters
2. Effective field angle: 25 degrees
3. On Gevapon 30 film, the resolution figures at high contrast were determined (see Table 2-12).
4. Optimum correction over the entire visual spectral range. The resolutions will be as listed in Table 2-13 on 3401 high contrast film.

Since stars represent high contrast objects, these resolution figures should be pertinent to the stellar measuring problem.

Based on the Falconar lens, curves have been plotted for the star magnitudes which the stellar camera can record at the edge of the format; it is here that the worst trailing velocity occurs and, for this reason, the magnitude of recordable stars is at a minimum.

The Wild Falconar lens covers a 25-degree total field. Because this lens is not normally used with a reseau plate, provision will have to be made for this change.

The insertion of a glass reseau plate in the focal plane of the 250-millimeter f/1.8 lens changes the aberration residuals. The aberration added by the plate is directly proportional to the thickness of the plate. It is also a function of the refractive index and the angle of incidence of the rays to the plate (the field angle of the lens).

The aberration contribution added by a 6-millimeter plate with index 1.517, an angle of incidence of 12.5 degrees, and a lens f/number is as follows:

The spherical aberration contribution is

$$(TSC) = 0.0234 t/f \text{ number}^3 = 24 \text{ microns blur (on axis)}$$

The distortion contribution is

$$\text{Distortion} = t \left(\tan B' - \frac{\tan B}{N} \right) = 12 \text{ microns at 12.5 degrees}$$

where B and B' = incident and refracted angles (B = 12.5 degrees maximum)
N = index of refraction

Naturally, the distortion contribution is calibrated out in initial tests.

The tangential coma distribution is

$$CC_T = \frac{3 (TSC) B}{2 (f/\text{number})}$$

$$= \frac{3 \times 24 \times 0.22}{2 \times 1.8} = 4.4 \text{ microns (at 12.5 degrees)}$$

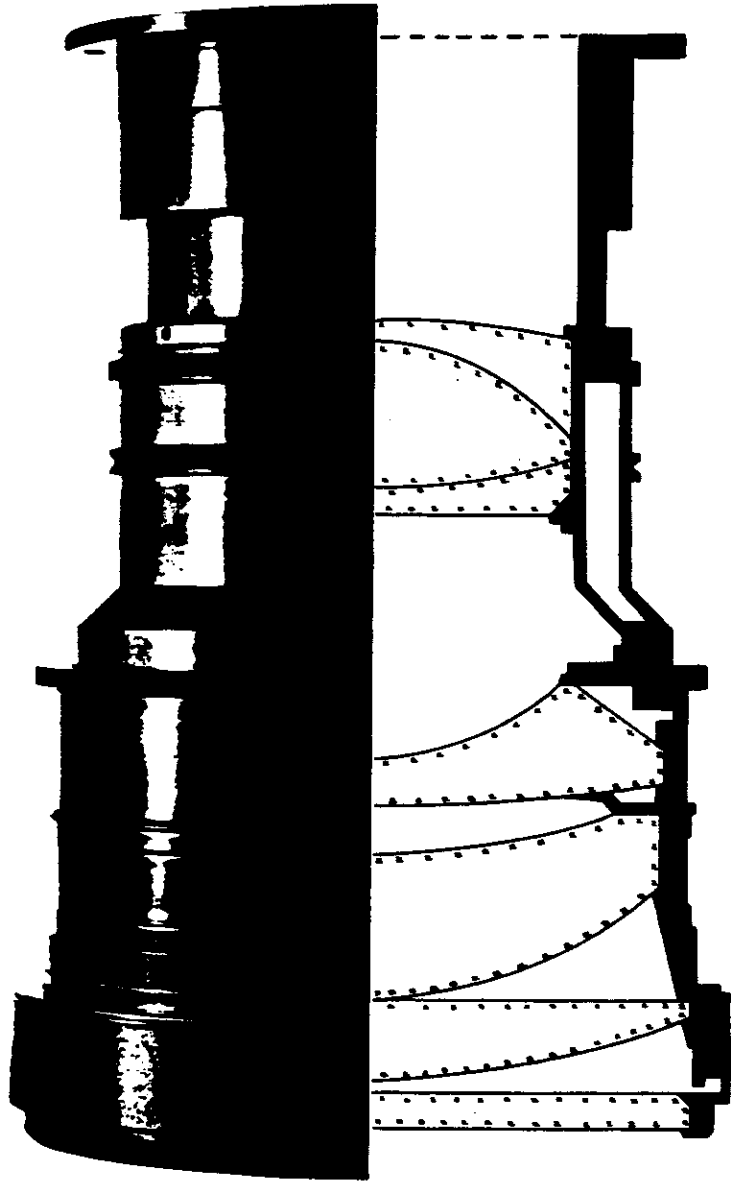


Fig. 2-33 — Wild Falconar 250 lens

Table 2-12 — Resolution at High Contrast for Gevapon 30 Film

Half Angle of Field, degrees	Radial, lines per millimeter	Tangential, lines per millimeter
12.5	25	28
10	28	28
7.5	33	33
5	45	30
2.5	46	46
0	46	46

Table 2-13 — Resolutions Obtained on EK 3401 High Contrast Film

Half Angle of Field, degrees	Radial, lines per millimeter	Tangential, lines per millimeter
12.5	22	24
10	24	24
7.5	27	27
5	36	25
2.5	37	37
0	37	37

The field curvature contribution

$$= \frac{t}{2N} \left(1 - \frac{\cos^2 B}{\cos B'} \right)$$

$$= 72 \text{ microns (at 12.5 degrees)}$$

The blur caused by this curvature is the curvature divided by the f/number or about 40 microns. The lateral color spread caused by the plane parallel plate displacement is about 8 microns.

These appear to be the main image defects caused by the insertion of the reseau in the focal plane. Their magnitudes, dictate that the Falconar lens be readjusted for use with the reseau plate.

3. Stellar Camera Motions

The predominant image motion in the stellar camera occurs as a result of the steady pitch rate of the vehicle. This rate is

$$\dot{p} = \frac{2\pi}{90 \times 60} = \frac{6.28}{5400} = 1.16 \text{ milliradians per second}$$

Since the stellar camera axis is at 45 degrees to the plane of the orbit, only a component of this steady rate will be seen by the axis.

$$\dot{p} \cos 45 \text{ degrees} = 0.82 \text{ milliradians per second}$$

This, then, is the systematic error of the axis of the stellar camera. To this we add the random variations in angular rates about roll, pitch and yaw.

These add vectorially to give a maximum of 0.14 milliradian per second for the angular motion of the axis. Adding this directly to the steady pitch rate gives 0.96 milliradian per second. This angular rate means a trailing rate for stars on the axis of 240 microns per second.

4. Number of Stars Recorded

The stellar camera can be expected to record stars up to the sixth magnitude in a 0.2-second exposure time when 3401 film is used. Figure 2-34 shows predicted performance based on experimental data and calculated trailing velocity rates. Stars up to the fifth magnitude will be recorded in 0.2 second when 3400 film is used. The star populations shown below allow an estimate of the number of stars which the analyst will have for measurement.

Magnitude	Total Number of Stars Brighter Than Listed Magnitude	Number of Stars per Square Degree of Sky
4.0	530	0.013
5.0	1,620	0.039
6.0	4,850	0.117
7.0	14,300	0.35

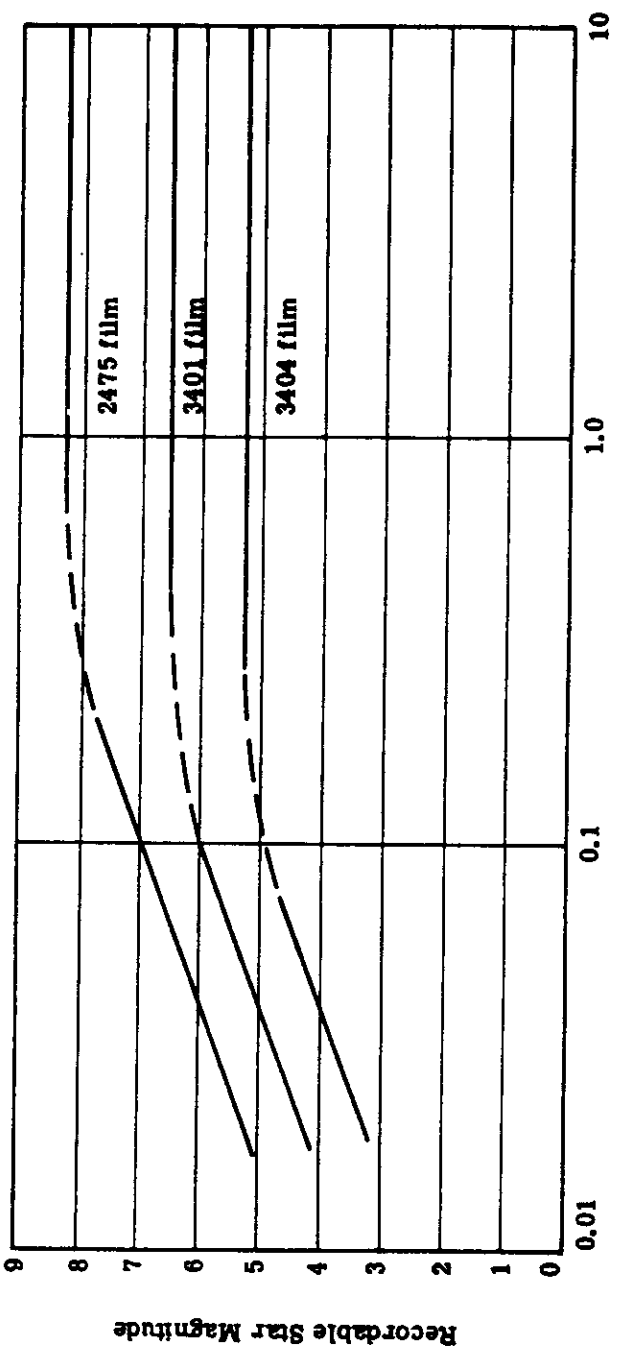


Fig. 2-34 — Recordable star magnitudes for 45-degree stellar camera orientation

The stellar camera presently planned covers a solid angle of about 290 square degrees. When 3401 film is employed to obtain sixth magnitude stars, approximately 34 stars will be recorded on each camera. With 3400 film only about 11 stars would be available (on the average).

Because of the uneven population density of stars throughout the sky, varying by a factor of about ± 3 from the nominal value, the slower film is not recommended. In fact, 2475 film (Royal-X Pan type) can be employed to record about five times as many stars if it is later found desirable. With the use of the two stellar cameras at 90 degrees to one another, the 3401 film is a good choice at this time.

2.2.1.2.3 Experimental Investigations

1. Extension of the AIM Curve

The preliminary experimental work to determine whether the AIM curve can be extended to lower modulation levels at lower resolutions through the use of high gamma printing materials has been completed. The conclusion is that through the use of high gamma printing material, the AIM curve can be extended to lower modulation levels. On low contrast imagery, this technique may prove useful for extracting additional target detail.

Type 3404 material was exposed for 0.9 second to a tungsten "point source." This exposure produced a density of 0.80 which is on the linear region of the D-log E curve of 3404. The source had a 0.6 neutral density filter placed over it. Then a high contrast resolving power target on a photographic plate was laid over the exposed 3404 material. A second exposure from the tungsten point source was made. For this case, the image contrast given to the film was 2:1, i.e., twice as much light in the target region as in the background area.

The aerial image modulation presented to the 3404 film was

$$M = \frac{2 - 1}{2 + 1} = 0.33$$

Lower modulations were subsequently obtained by repeating the procedure for separate pieces of 3404 material with additional neutral density material over the tungsten source during the exposure of the resolving power target. For instance, with a 2.4 neutral density filter added over the point source during target exposure, the target modulation was computed as follows:

Background exposure = 1.00

$$\begin{aligned} \text{Exposure in target lines} &= 1.00 + \frac{1}{\text{Antilog } 2.4} \\ &= 1.00 + 0.004 = 1.004 \end{aligned}$$

$$M = \frac{1.004 - 1.0}{1.004 + 1.0} = 0.002$$

In this way a series of 13 images was exposed on 3404 material with modulation levels down to 0.0004. Although standard Wratten neutral density material was employed in these tests, the material was measured at Itek, and the measured values were used in the modulation computation.

The 3404 material was developed for 6 minutes in D-19 to a gamma of 2.4.

To determine the value of increasing the contrast in the printing process, the 3404 material was printed on Kodalith Ortho type 3. This material was processed for 2 minutes and 10 seconds at 68 °F in Kodalith liquid developer; the gamma was 10. Because of the extreme gamma and the difficulty of controlling the exposure of the D-log E curve of the material, most of the exposures ended up near the toe of the curve, with a resultant contrast increase of less than 10. Table 2-14 shows the results of the tests.

The printing process provided a severe limitation to the highest resolution which could be obtained through the system. At the high end of the scale, the resolution appears limited to 200 lines per millimeter. Indeed, the prints do not show as much resolution as the original 3404 material until a level of 8 lines per millimeter is reached. From this point on, the print on Kodalith material shows higher resolution. It also shows imagery two steps in the series beyond the cutoff point for the 3404 material. This is a factor in modulation of about $2\frac{1}{2}$.

The results are plotted in Figure 2-35 along with the AIM curve for 3404. This relatively small factor by which the AIM curve is extended may be due to the fact that the exposures are on the tow of the curve of the printing material. In addition, the mottling in the high gamma prints makes it difficult to detect targets.

Another factor which is evident from the analysis is that the targets on the 3404 material are visible well below the contrast level (0.015) which was formerly thought to be the cutoff level. The reason for this may be that the eye is not looking at a target optically degraded into an approximate sine wave pattern, but rather at a sharp edge of low contrast. Although the modulation required by the eye for sine wave detection is about 0.035, the eye can detect step changes on the order of 2 percent or 0.01 modulation.

In the experiment, this step would be represented by a target of about 0.004. On this basis, the cutoff point for detecting the image appears more nearly reasonable.

At the present time we do not feel that this study will change our error budget for accuracy of measurements.

2. Experimental Star Recording

Much data on star recording has been generated in the past. Still, each new application of star photography, including the present system, appears to bring out a new need for data. The need here arises from the on-orbit terrestrial camera calibration. The already existing data could be extrapolated if the camera were to be used without a filter; however, a Wratten 25 filter will be used.

There are no data available on star photography through a red filter. Theoretically, a simple filter factor extrapolation with the existing films might be used. However, the existing films on which we have data with the exception of the Royal-X Pan type do not appear to have the capability of recording enough stars. In addition, Royal-X Pan has a poor filter factor for a Wratten 25 filter.

Royal-X Pan type emulsion is now available with red sensitivity similar to that of the 3400 film presently planned for the terrestrial camera. This film type 2475 is available on a four mil ester base, making it almost ideal for use as a calibration material. Because of its extreme speed, it is sensitive to radiation damage. However, an experimental investigation (see on-orbit calibration, subsection 2, page 2-64 indicates that in a 2-week period, at the altitude under

Table 2-14 — Test Results of AIM Curve Extension

Modulation	Resolution Read From 3404 Material, lines per millimeter	Resolution Read From Kodalith Print, lines per millimeter
0.639*	—	204
0.471*	—	204
0.333	—	143
0.149	—	90
0.0826	64	51
0.0476	43	36
0.0196	16	14
0.0099	6.4	8
0.0055	1	4
0.0020	0.25†	2.3
0.0013	Could not find target	1.6
0.0008	Could not find target	0.5
0.0004	Could not find target	Could not find target

*These higher contrasts were obtained by removing neutral density material from the tungsten source during target exposure.

†This point is somewhat questionable—one analyst disagreed that anything was visible.

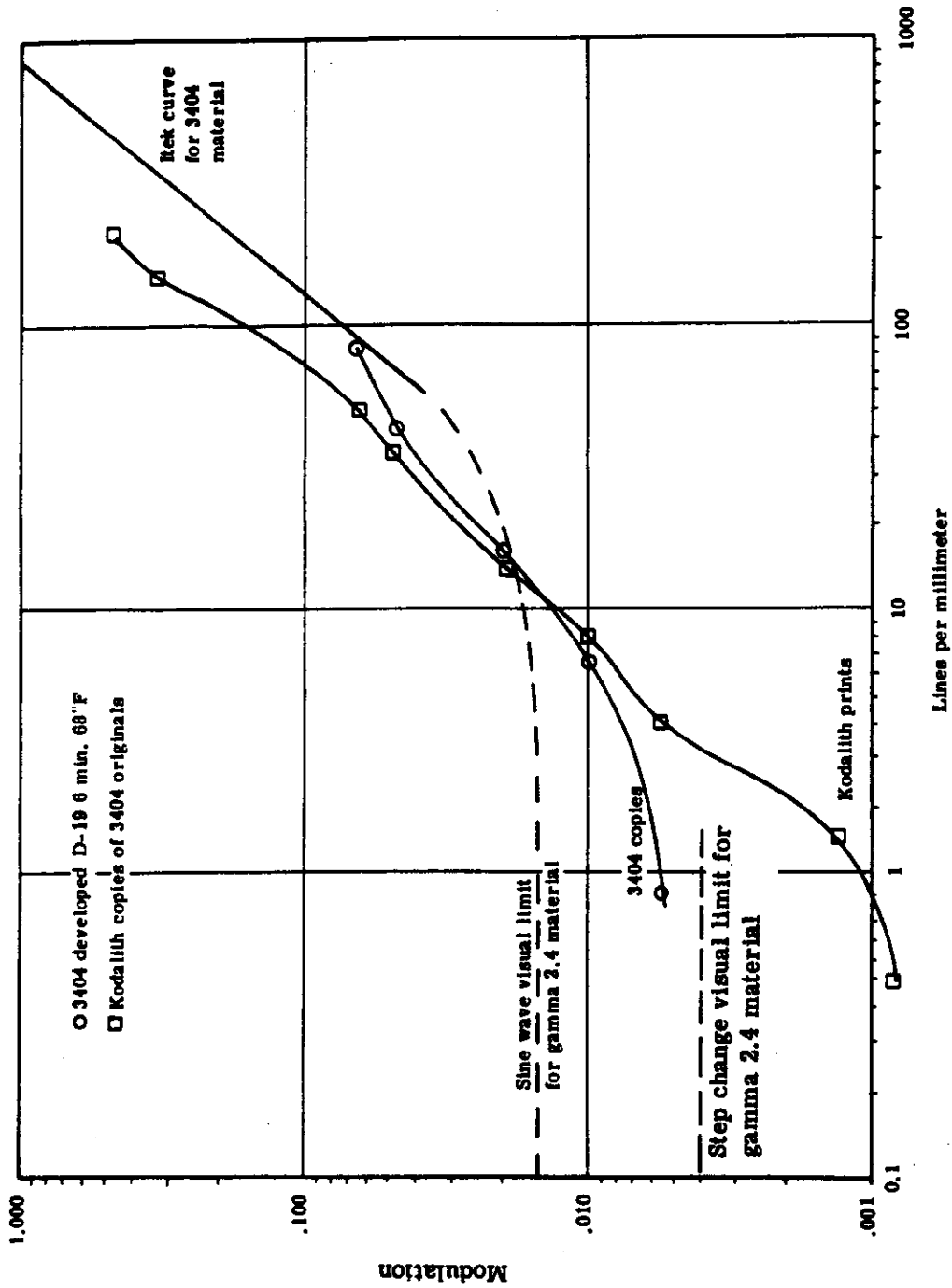


Fig. 2-35 -- Test results of AIM curve extension

consideration, it is not a risk. More work will be done on the subject to determine what, if any, shielding is required.

To determine the recording capability of 2475 film for stellar calibration of the terrestrial camera, a 12-inch focal length Tele-Rokunar lens on a Nikkorex camera was stopped down to $f/11$ and the Pleides stars were photographed. Exposure times of 10 seconds were employed with a Wratten 25 filter. The measured diameter of the entrance pupil was 1.07 inches. This lens simulates the 12-inch-focal-length $T/12$ system of the terrestrial camera in terms of its light gathering power. The $f/11$ stop plus a transmission loss in the system make it approximately $T/12$. The 10 second exposure produced an appreciable trail. For this reason, slightly shorter or longer exposure times would not have appreciably changed the recorded magnitude. On the other hand, a loss in recorded magnitude would be expected from a photographic system with an optical image quality extremely low compared to the resolving power of the film. The terrestrial camera gives a resolution level of about 40 lines per millimeter (minimum) of fine grain film at a contrast of 1.6:1. This level must be compared to the resolving power of 2475 emulsion at a contrast of 1.6:1, or about 25 lines per millimeter. On the basis of this comparison, the terrestrial camera lens should produce trails on 2475 emulsion with but little more degradation than that caused by the spreading of the light in the emulsion itself.

To test this experimentally, the 12-inch Tele-Rokunar lens was deliberately adjusted out of focus to find the loss in recordable magnitude caused by a larger blur circle. Single frame out-of-focus trails 10 seconds long (at 0.015 inch and 0.030 inch from the infinity position) and in-focus trails (with the lens at the infinity position) were recorded. Examination of frames exposed in this manner revealed only minor difference between images for the infinity setting and the 0.015-inch defocus positions. Figure 2-36 is a 12.5X enlargement of a 35-millimeter frame showing the 3 trail segments for each star. A slight degradation in the visibility of faint trails appears for the 0.030-inch defocus.

The defocusing of 0.015 and 0.030 inch with the $f/11$ setting on the Tele-Rokunar give calculated blur circle diameters of 35 and 70 microns, respectively. Such blur circles should limit resolution to about 30 lines per millimeter and 15 lines per millimeter, respectively. On the basis of these tests, it appears that the image quality of the terrestrial camera lens will not degrade the star trails as exposed on 2475 film.

Figure 2-37 shows the location of known stars in the Pleides as recorded from the star catalog, and these stars are recognizable in the photograph. Stars of 5.8 magnitude are visible on the original enlargement.

Because the trailing angular rate of the Pleides is different from the rate to be expected in the stabilized vehicle, we must make a correction. The trailing rate of the stars as photographed in the experiment was the earth's rate multiplied by the cosine of the declination angle.

$$W = 0.072 \times \cos 24 \text{ degrees} = 0.066 \text{ milliradian/second}$$

The expected vehicle residual rates during the stabilized period for the terrestrial camera is approximately 0.2 milliradian/second when we combine roll and pitch rate errors. This increase in trailing rate will give the same length of trail during the calibration time of 3 seconds that occurred in the experiment in 9 seconds. However, the effective exposure-per-unit length of trail will be down by a factor of 3. Thus the faintest recorded trails on orbit during terrestrial camera calibration will come from stars brighter by about 1.2 magnitudes. This means that the poorest

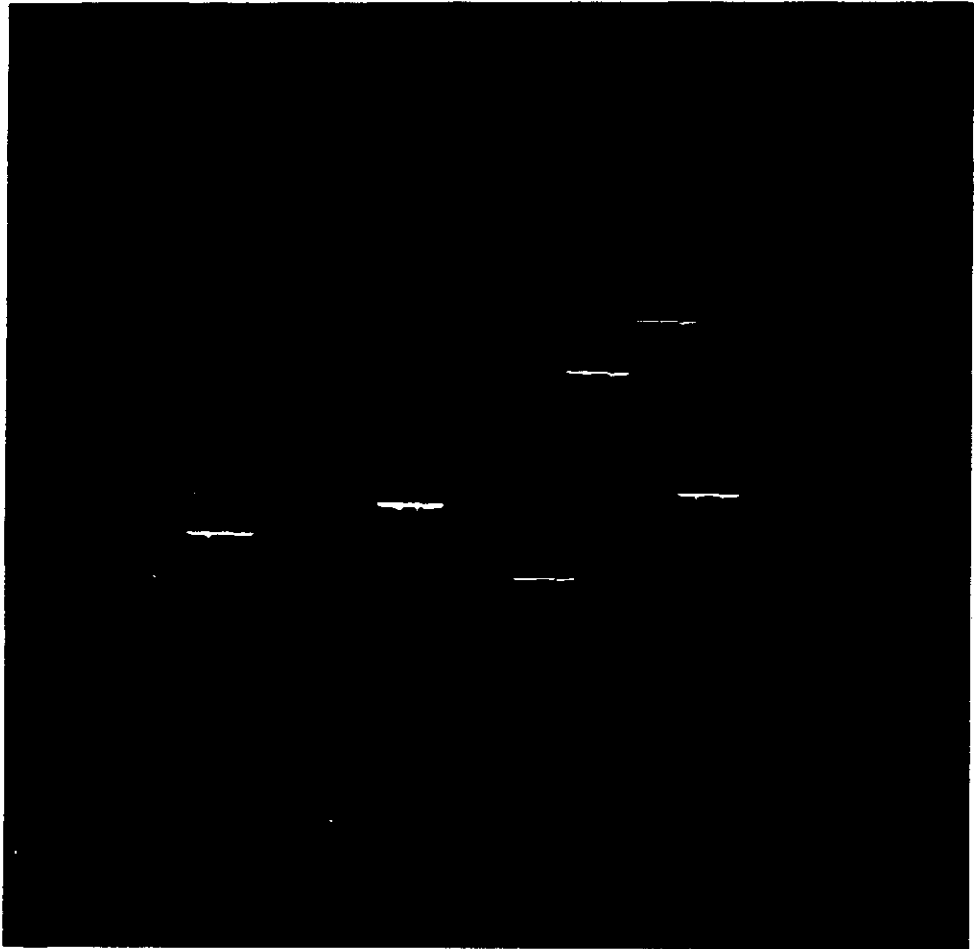


Fig. 2-36 — Photograph of stars in Pleides

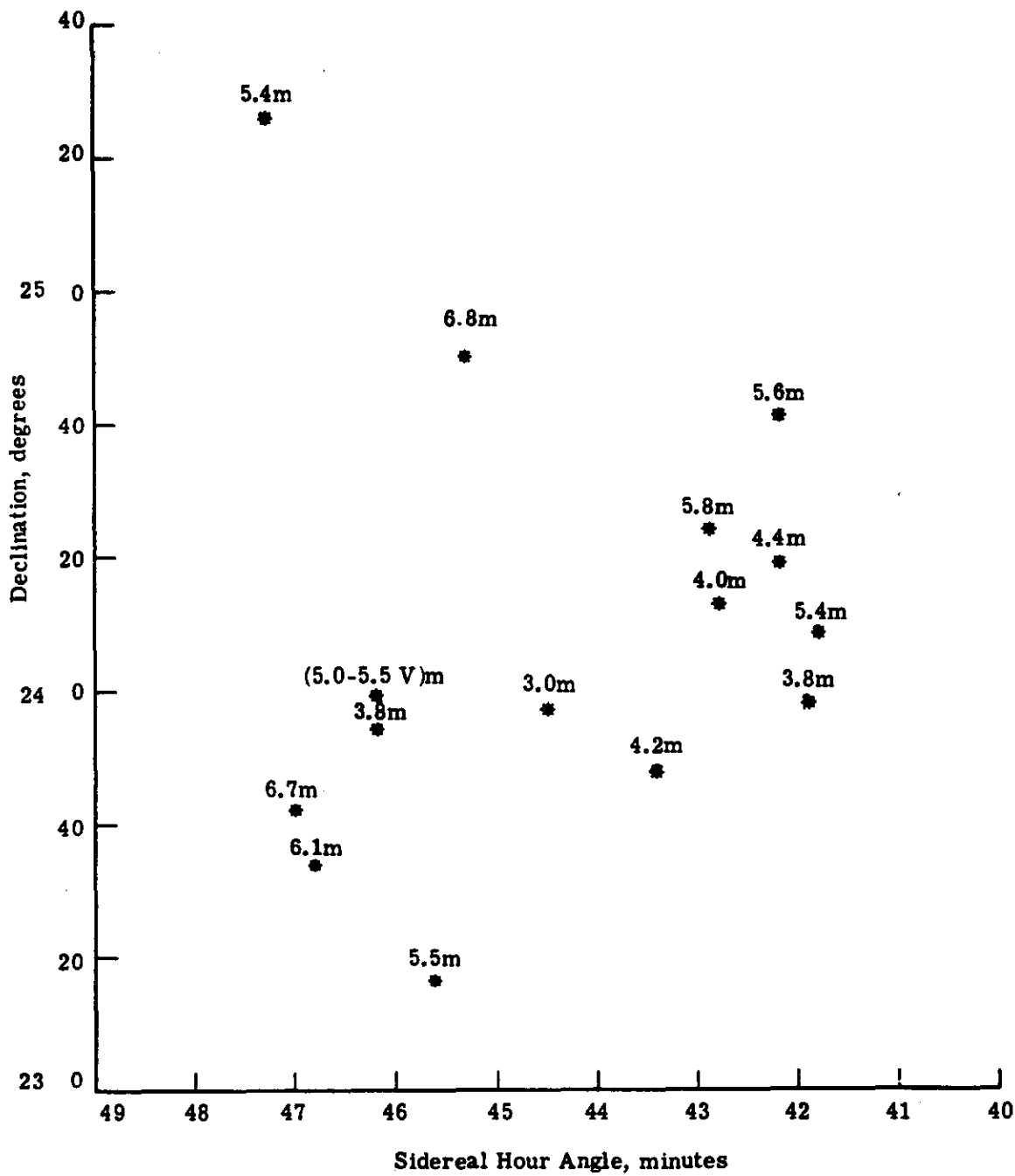


Fig. 2-37 — Stars in Pleiades from star catalog

magnitude for terrestrial camera calibration will be

$$M = 5.8 - 1.2 = 4.6$$

As pointed out in the section under terrestrial camera calibration, the same magnitude will be recorded at the edge of the field because the antivignetting filter compensates for additional motion effects.

There will be a slight benefit from the increased trailing rate in that the 2475 film will be slightly more efficient because of the shorter exposure time and smaller reciprocity loss.

These data clearly show that the terrestrial camera can capture fourth magnitude stars when photographed from the stabilized vehicle.

3. Film Flatness Test

When film is pressed against a glass platen, departures from film-to-platen contact (flatness) are observed. This lack of proper contact makes a significant contribution to the error budget of the photogrammetric system. Thus, a detailed study has been made of the combination of pressure pad material and film conditions which would give the highest degree of contact and thus, minimize its contribution to the error budget.

Since the errors are in the vicinity of a few microns, or approximately twice as many wavelengths of light, an interferometer is ideal for measuring and observing the film-platen contact. A simple interferometer was used by Isaac Newton to observe the interference pattern generated by a plano-convex lens in contact with an optical flat. The film reflects an appreciable amount of light and, when it is brought into contact with an optical flat, interference fringes are observed. The separation between each fringe corresponds to a change in optical path length of 1/2 wavelength of light. Thus, the entire fringe pattern represents a surface contour map (topograph) of the film surface to accuracies of 1/4 of a micron or better. Where the film is near physical contact with the optical flat, a dark fringe is observed.

A preliminary investigation was carried out with materials readily available in the laboratory; Figure 2-38 shows the experimental setup. A sodium arc lamp serves as a source ($\lambda = 589\mu$). An optical flat approximately 4 inches in diameter and 5/8-inch thick simulates the film platen. The film is sandwiched between the optical flat and the pressure pad. With the aid of a beam splitter, the fringe pattern generated is easily observed or photographed for a permanent record. A pressure of 0.3 psi was applied by adding lead weights to the optical flat.

Figure 2-39 shows the film topograph of 4400 film supported by a 30-diameter rubber pad under 0.3 psi. The light spots in the mottled appearance of the fringe pattern indicate departures from flatness (valleys in the film) of several microns. A statistical analysis of departures from flatness was made from this figure.

The surface shown in Figure 2-39, approximating a 3 1/2-inch diameter, was divided up into 1/28-inch squares, and the number of fringes in each square was counted. The following summarizes the results:

Flatness, microns	Population	Percent of Total Population
0 to 1.2	5328	96.32
1.5 to 1.8	137	2.47
2.1 to 2.4	67	1.21

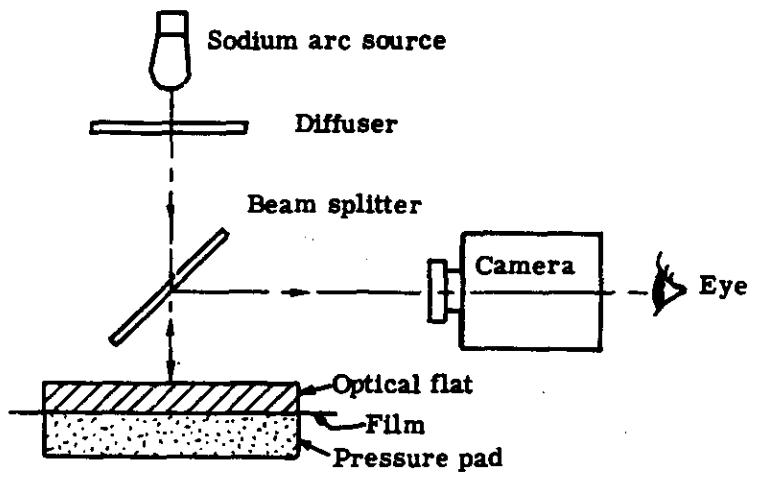


Fig. 2-38 — Experimental setup for observing film topograph

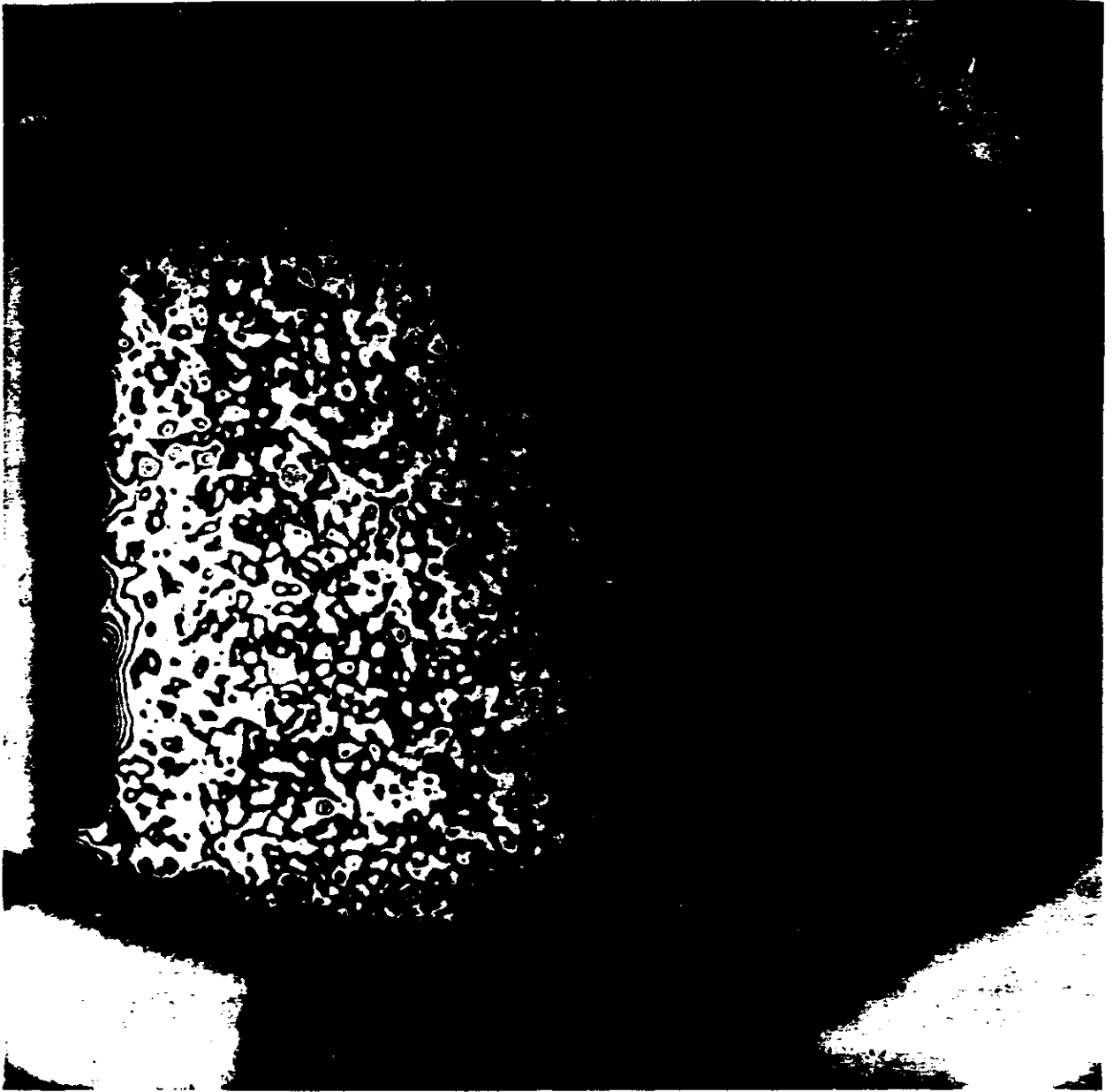


Fig. 2-39 — Film topograph of EK type 4400 film: 30 durometer rubber pressure pad; 0.3 psi pressure

It generally appears that the film topography is caused by dust, air pockets, and emulsion irregularities. Great care was taken to remove as much dust as possible. Staticmaster brushes were used to clean the emulsion surface. The uniformity of the emulsion layer was tested by making a similar test to the one described above using Eastman Kodak Ultraflat High Resolution Plate.

Figure 2-40 illustrates the results of this test which show that the largest local departure from flatness attributable to the emulsion layer is not greater than $1/4\lambda$ or approximately 0.145 micron; however, across its surface the plate departs from flatness by approximately 4λ or 1.2 microns (selected plate glass quality). Since the camera system will be used in a space environment, further tests were conducted in a vacuum.

Figure 2-41 is a diagram of the vacuum apparatus. Here the optical flat serves as both a vacuum seal and a flat against which the film is pressed. As before, a sodium arc lamp and beam splitter were used for observing the fringe pattern.

The pressure pad support and rods weight 2.156 pounds, and when a vacuum is drawn, the air pressure acting on the face of the rods exerts a net force of 2.464 pounds upward or 0.0812 psi for a surface 6 inches in diameter. The spring constant is 7.6 pounds per inch making a total of 22.8 pounds per inch for the three springs, or 0.805 psi per linear inch of spring deflection. Since 0.30 psi is required, we have:

$$0.805 \times \text{spring deflection} + 0.0872 = 0.30$$

or

$$\text{Spring deflection} = 0.265 \text{ inch}$$

One revolution of the pressure screw will deflect the springs 0.077 inch. After the springs are brought into contact with the pressure support pad, the pressure screw is advanced by 3.5 revolutions.

It is estimated that the pressure inside the vacuum chamber, after a few minutes of pumping, is approximately 5×10^{-4} millimeter of Mercury, or less than one-millionth of normal atmospheric pressure.

Figure 2-42 shows the results achieved for fresh 70-millimeter 3404 film using an 18-durometer silicone rubber pressure pad under 0.30 psi. This topograph shows the film flatness when the film is placed under approximately 1.5 psi pressure with an optical flat acting as a pressure pad. It may be compared with the topograph in Figure 2-35. Also, the reference flat, or vacuum seal deflects an appreciable amount under one atmosphere pressure, 14 psi. The flat is 1/2-inch thick and supported by an 8-inch diameter rubber "O" ring.

Film comes with several base thicknesses. The 3404 film used above is called thin-base film, and with the emulsion layer, its thickness measures about 3 mils. There is an ultrathin base film whose thickness is about 2 mils with the emulsion layer. Figure 2-43 shows the topograph of the 2-mil ultrathin base film, using an 18-durometer rubber pressure pad under 0.3 psi pressure in a vacuum.

A comparison of these results with those shown in Figure 2-38 reveals that the base material plays a minor role in keeping the film from complete contact with the glass platen. An increase in pressure beyond 0.3 psi while conducting the experiments, whose results are shown in Figures 2-42 and 2-43, did not change the film topography appreciably. Also, various pressure pad

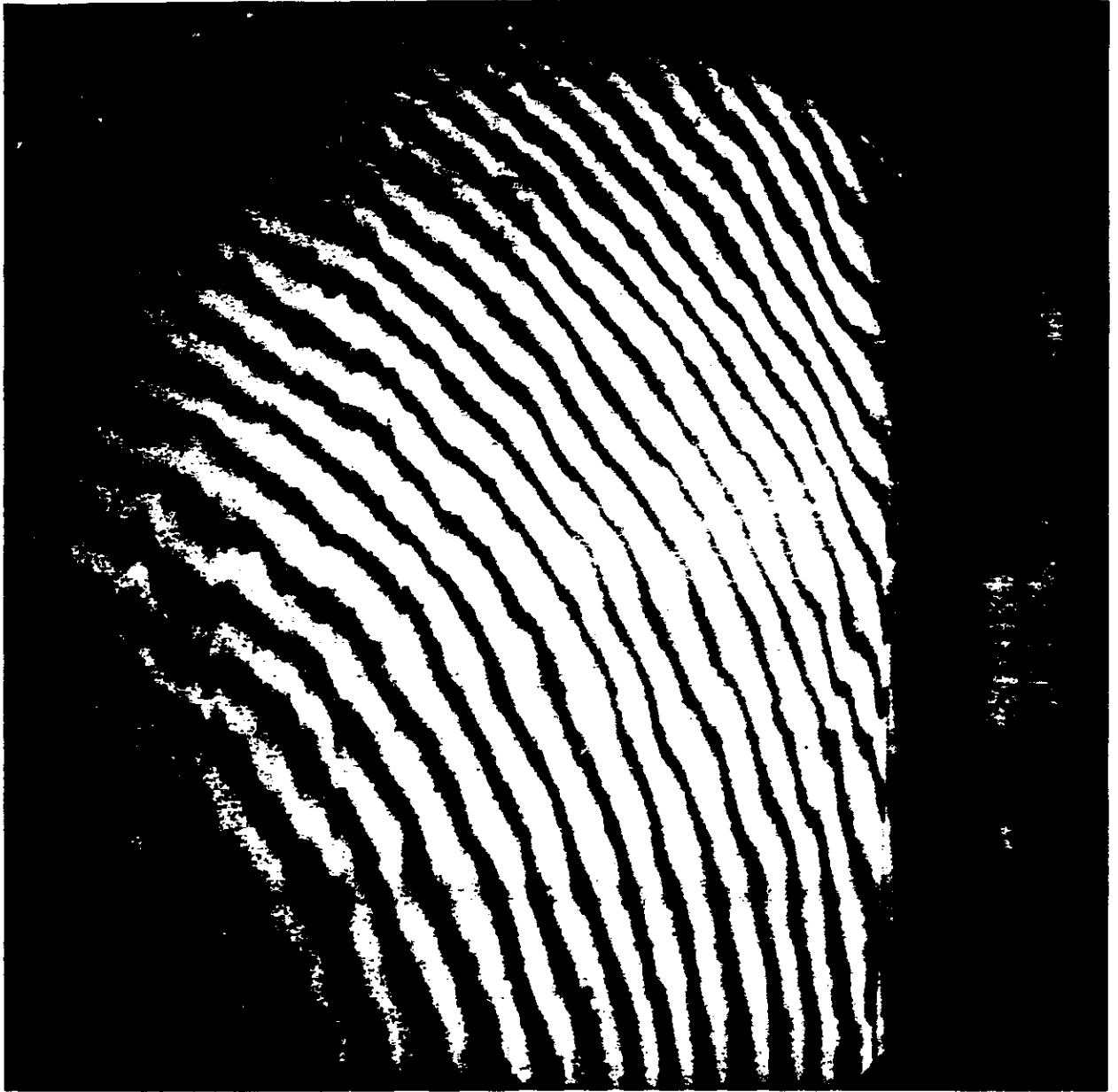


Fig. 2-40 — Topograph of EK ultraflat high resolution plate

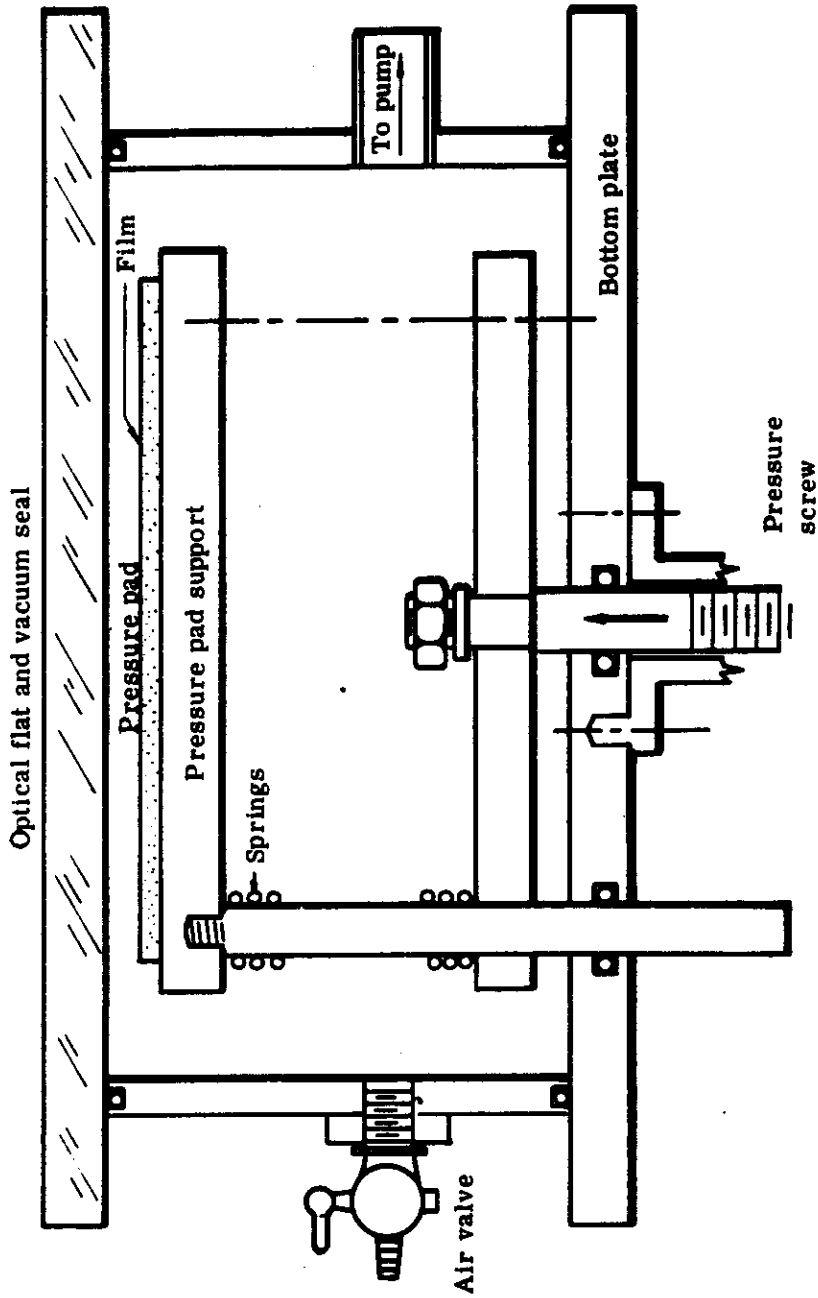


Fig. 2-41 — Vacuum test apparatus setup

~~SECRET~~

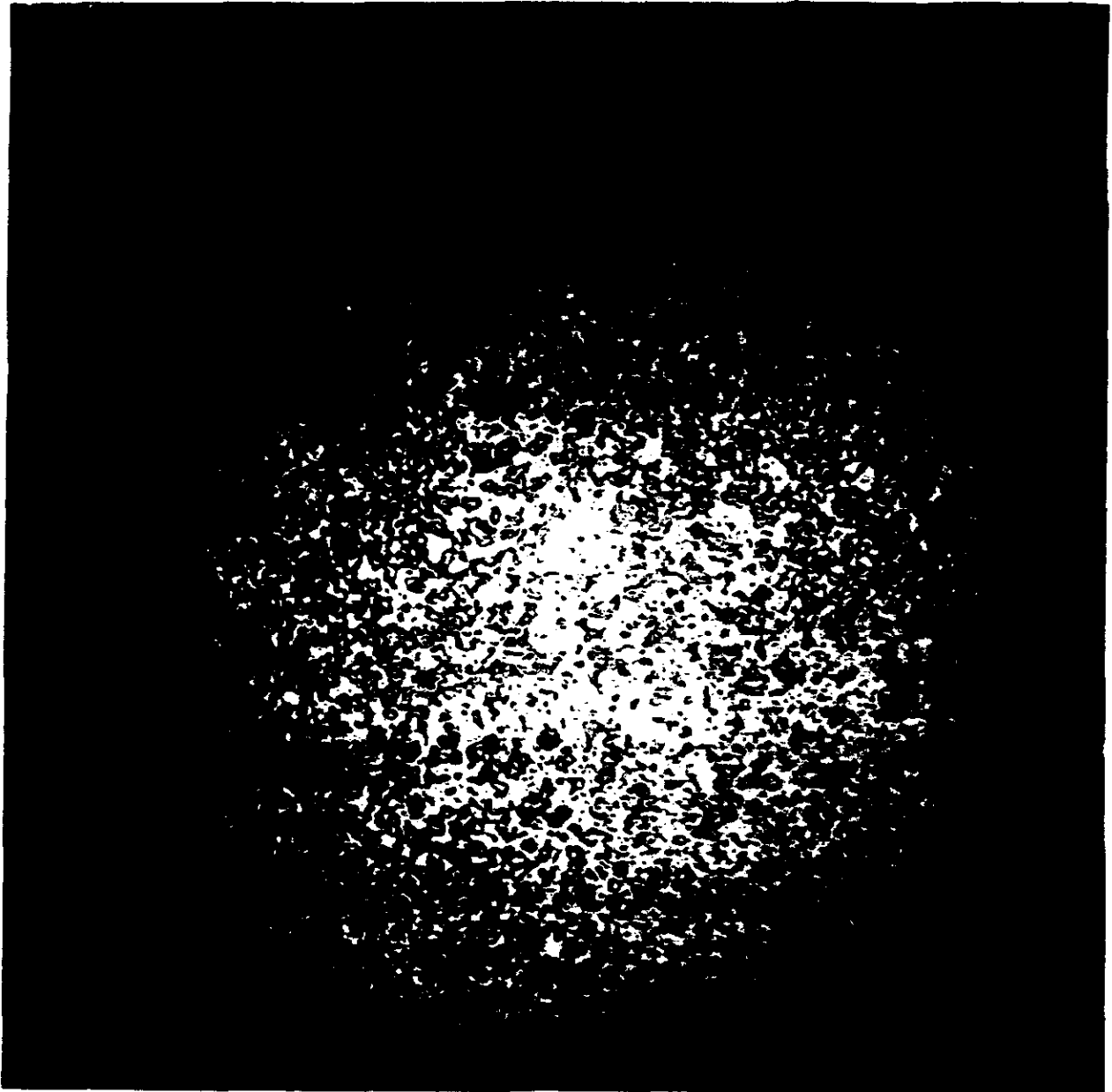


Fig. 2-42 — Topograph of 70-millimeter EK type 3404 film: 18 durometer rubber pressure pad; 0.3 psi pressure

~~SECRET~~

~~SECRET~~

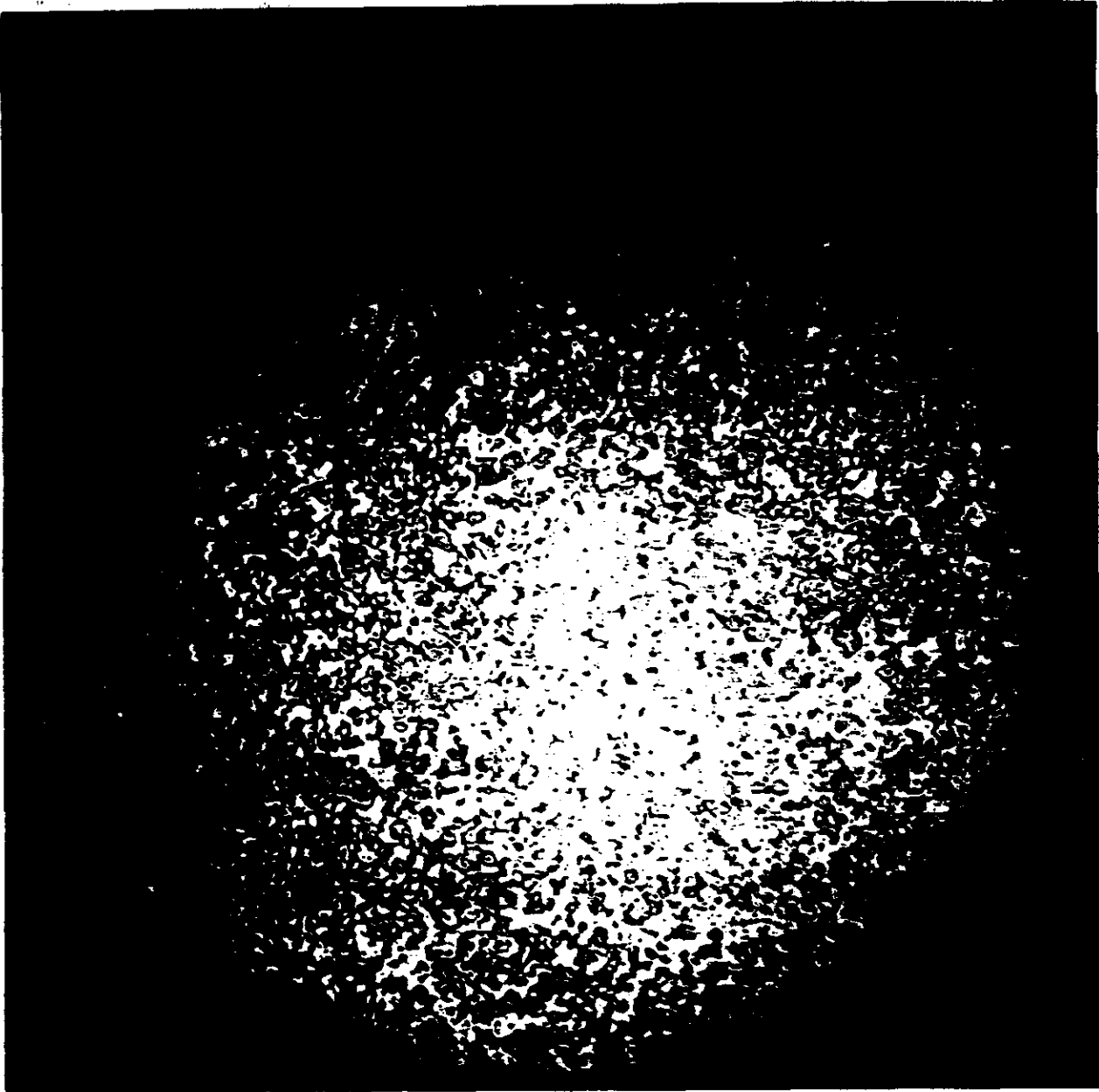


Fig. 2-43 — Topograph of 70-millimeter ultrathin base film: 18 durometer rubber pressure pad; 0.3 psi pressure

~~SECRET~~

materials such as cork, polyester foam, and felt were tried. These results are not shown here because of the very poor film to platen contact.

Figure 2-44 shows that film can be squeezed against a platen to make good contact. However, the pressures required are enormous and perhaps beyond practicability. The reason for the better flattening may be that the glass pressure plate produces large localized forces at the points where the dust prevents contact and forces the dust into the gelatin emulsion. Furthermore, the vacuum seal deflects appreciably. Perhaps this irregularity introduces enough nonuniformity in the pressure distribution to prevent good film contact. Also, the film base thickness plays a very minor role in achieving good film-to-platen contact.

Dust, surface film irregularities, and suitable pressure pad materials still present areas for further investigation. Present indications are that film/platen contact may cause a random positional error of approximately one micron.

2.2.1.2.4 Influence of Image Quality on Measurement Accuracy

A controlled laboratory experiment has been performed to find the influence of image character on measurement accuracy. Because of the magnitude of the task, only one specific area was investigated. This area was the measurement error in edge position which occurs when two photographs of different resolution are used to form the stereoscopic model.

1. Laboratory Equipment

To produce controlled photography for measurement of position errors, a simple target panel was setup and photographed in the laboratory. The target panel is shown full scale in Figure 2-45. The panel is a photographic plate with the central area a silver image, and the resolution targets taped to the plate. The objects in the central area have a contrast of 1.6:1 and a density step of 0.2.

This panel, illuminated by an aristo grid source, is photographed at an 8:1 reduction by means of an 80-millimeter, $f/2.8$ Zeiss Tessar lens. A shutter is mounted separately from the lens (see Figure 2-46). Photographic plates, held in position by a vacuum frame, record the image. All components are mounted solidly on a black granite slab to prevent accidental motion errors during the photographic series.

To provide photographs of difference resolution, the lens of the test camera is mounted out-of-focus to give a blurred image. The aperture is then decreased to provide smaller blur and better quality. The blur thus produced is symmetrical giving equal resolution in all directions. The apparatus used for this experiment is described in the following paragraphs.

Because the lens-to-film and lens-to-target distances are kept constant between photographs, the image size should remain constant. In addition, since all important image positions lie along a diameter of the field, and since the measurements are made perpendicular to this diameter, the influence of slight changes in magnification is negligible. Therefore, only the blur of the edge and its consequent effect on human judgement of edge position affect the measurement.

2. Procedure

The photographic system for the plates was set out of focus at $f/4$ to reduce the visual resolution as observed on a fine ground glass plate to about 5 lines per millimeter. Then two pictures each were taken on a grainless emulsion (649 GH) at $f/4$, $f/8$, and $f/16$ apertures.

~~SECRET~~

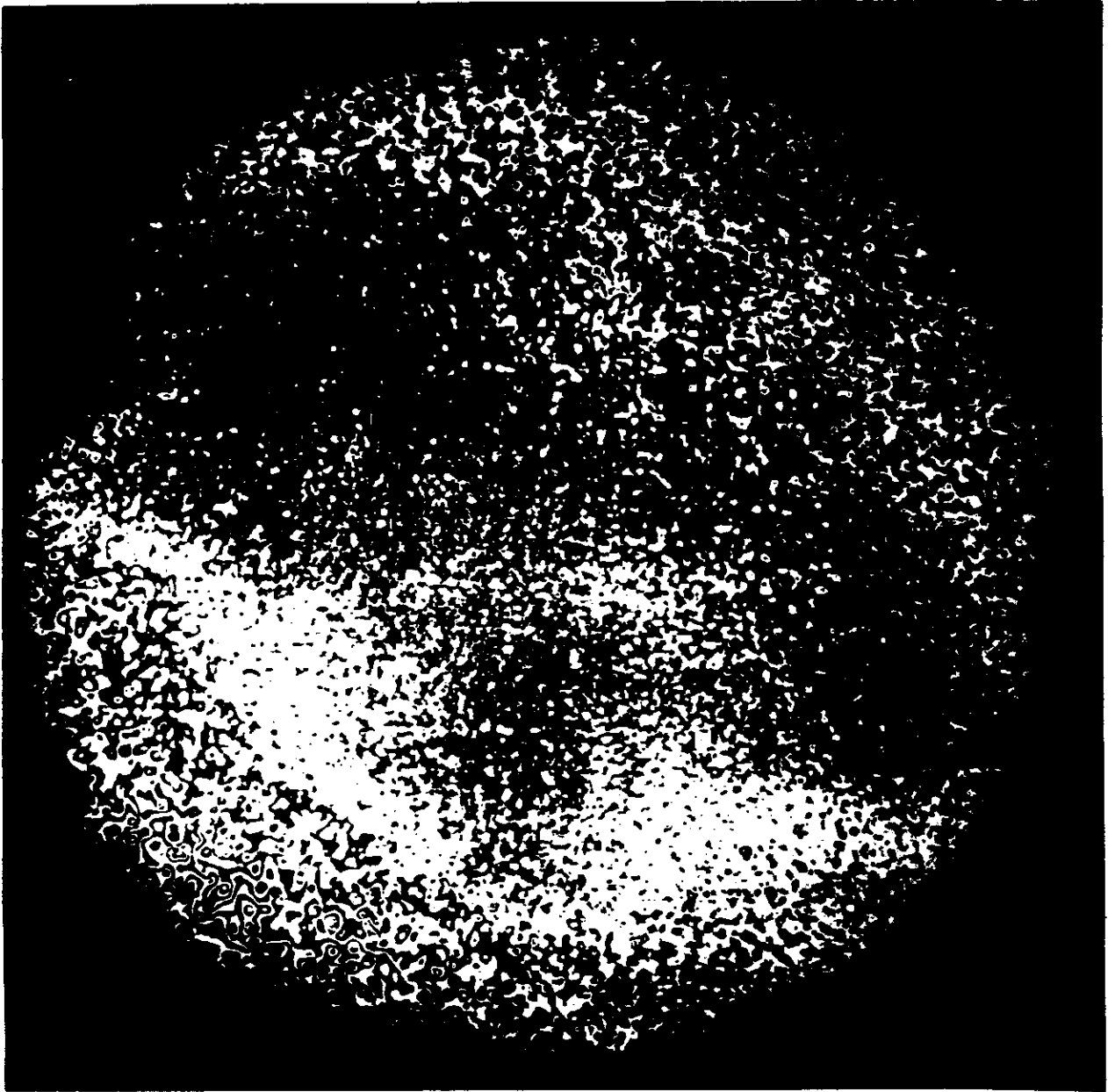


Fig. 2-44 — Topograph of EK type 3404 film: optical glass, flat pressure pad; 1.5 psi pressure

~~SECRET~~

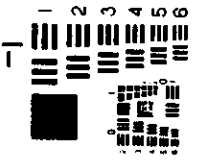
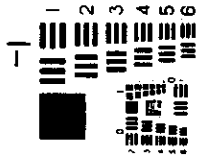
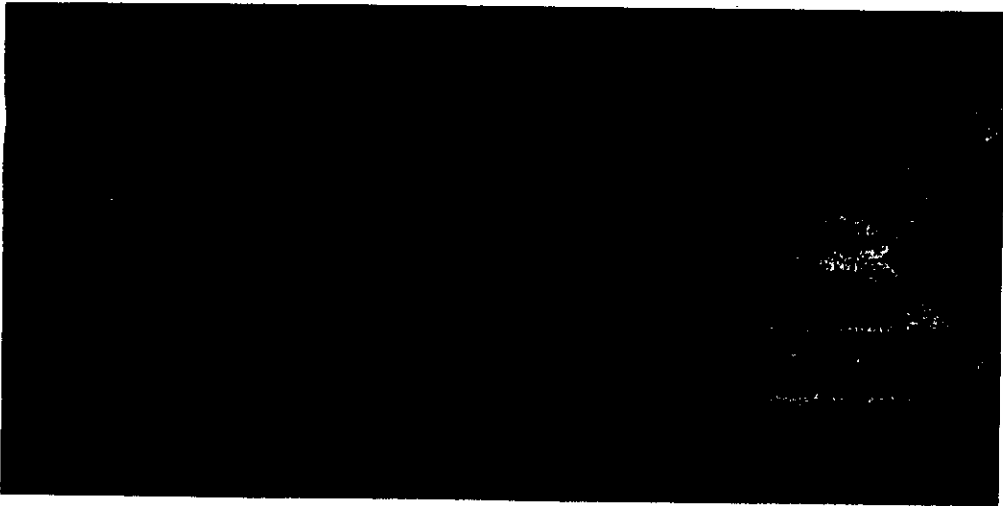
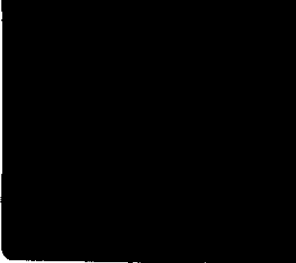


Fig. 2-45 — Contact print of target area (detail reversed right to left)



62



Notice of Missing Page(s)

Page 2-96 of the original document was missing.

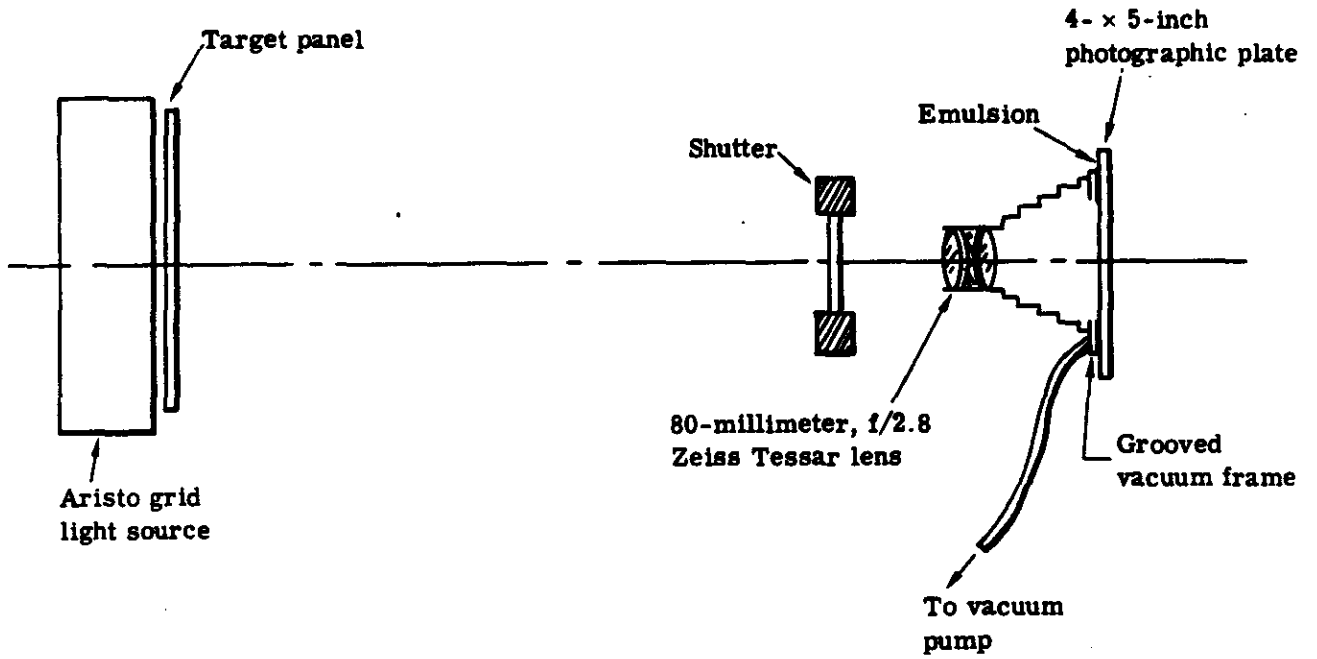


Fig. 2-46 — Diagram of photographic system

The exposure times were lengthened as appropriate to keep the image densities the same. The resolution levels as read from the resolving power target images for a 1.6:1 contrast were as follows.

Aperture	Resolution, lines per millimeter
f/4	5.0
f/8	11
f/16	23

The resolution did not vary appreciably with contrast, probably because of the rapid drop in transfer function value with frequency. This sharp drop in transfer function is caused by the fact that the main quality limitation is focus rather than aberrations. It corresponds closely to a motion blur limitation on quality except that it is omnidirectional.

The plates were processed to a gamma of 2.2 in D-76 (5 minutes at 68 °F). The gamma corresponds to that of 3404 film although, of course, the granularity is negligible.

3. Analysis

The analysis of the measurement errors caused by blur, was performed in stereo using the Wild STK-1. The following pairs of plates with their respective resolution levels were used to make a stereo model.

Pair	Left, lines per millimeter	Right, lines per millimeter	$\Delta 1/R$, microns
A	23	11	47
B	23	5	156
C	23	23	0
D	5	23	-156
E	11	5	109
F	11	11	0
G	5	5	0

The differences in resolved distance in microns represented by the resolution levels are given in the right hand column. Any measurement bias would be expected to be a function of this difference in edge blur between left and right images.







Between 6 and 14 measurement of each image point were made on the STK-1 to determine the stereo location. The positions X, Y, Px, and Py were read out automatically by the machine.

The Px setting was repeated to determine accuracy and precision. The other readings were available to aid in the analysis and, in particular, to mathematically level the stereoscopic model.

Table 2-14(a) is a listing of the significant measurements. The Px column for each pair shows the average x parallax after the model has been mathematically leveled to the plane defined by the upper and lower fiducial marks. These marks show Px = 0 for all stereoscopic pairs.

One would expect the stereoscopic pairs composed of equal quality pictures (the 23-23 pair, the 11-11 pair, and the 5-5 pair) to show no Px deviation from the plane containing the upper and

Table 2-14(a) — Stereoscopic Pair

Object and Location	23-23		11-11		5-5		23-11		11-5		23-5		5-23	
	Px	σPx	Px	σPx	Px	σPx	Px	σPx	Px	σPx	Px	σPx	Px	σPx
A  Y = 17.62mm	0	3.0	0	4.9	0	3.6	0	4.1	0	3.9	0	8.7	0	6.0
B  Y = 14.75mm	0	2.0	-2	5.0	-7	5.4	-12	5.0	-24	3.1	-78	3.7	+34	2.7
C  Y = 11.03mm	0	7.3	+9	5.6	-1	6.7	+13	4.3	+24	8.9	+27	9.6	-13	7.8
D  Y = 6.74mm	+15	6.6	-13	4.6	-12	7.6	-5	5.8	-9	9.5	-36	10.5	+33	5.6
E  Y = 2.96mm	-3	4.2	-25	4.2	-10	3.3	+1	2.8	+4	4.1	+27	5.2	-67	5.2
F  Y = 0mm	0	4.9	0	13.4	0	4.3	0	6.5	0	7.1	0	53.2	0	45.3

fiducials. In other words, the Px's should be close to zero. The actual average Px's are disappointingly far from this plane. The first possible explanation of the deviations would be observer bias. However, the deviations are not consistently in the same direction. The observer bias therefore would have to change sign with image quality level. There are too few data points to prove or disprove this possibility.

On the other hand, a clear cut and understandable deviation from the stereoscopic plane does emerge when a stereoscopic pair made up of pictures of differing quality is viewed. In pairs 23-11, 11-5, 23-5 and 5-23, the deviations from the stereoscopic plane containing the fiducials are completely consistent in sign. Also, when the pictures of a stereoscopic pair are reversed side to side, with the poorer one on the left instead of on the right as in the pair listed as 5-23, the deviations from the stereoscopic plane reverse in sign which adds credence to the measured errors.

During the measurements, the stereoscopic analyst expressed difficulty in determining the plane of the lower fiducial when the resolutions of left and right pictures differed. This difficulty is especially apparent from the standard deviation of the readings shown for pairs 23-5 and 5-23. The actual reading the analyst obtains depends upon whether he relies more heavily on the left side or on the right side of the fiducial to make his setting, since there may be more than 100 microns difference between sides. Thus, the fiducials are in the best average plane only if the observer can truly set at the point of the fiducial.

For this reason the points shown in Table 2-14(a) were plotted on graph paper with Px as a function of Y. The best straight line through the points was drawn by eye neglecting the fiducial readings. The average plus and minus deviations from this line were considered to be the average error caused by the difference in image resolution. These values are tabulated below as a function of the difference in resolved distance.

Stereoscopic Pair	$\frac{1}{R}$	Measurement Error for Single Edges Based on Average of 4 Edges, microns	Ratio, $\Delta \frac{1}{R} / \Delta Px$
23-11	47 μ	8	5.9
11-5	109 μ	15	7.3
23-5	156	36	4.3
5-23	-156	-31	5.0

Stereoscopic Pair	$\frac{1}{R}$	Measurement Precision, microns
23-23	0	≈ 3.5
11-11	0	≈ 4
5-5	0	≈ 2

In obtaining the measurement precision, the readings for the fiducial marks were disregarded since they were not used to determine measurement error. The variances of the points from the plane of best fit were averaged for the stereoscopic pairs of equal quality and the square roots of the average were taken. These were then divided by 2, the square root of the number of points, to determine the precision of the measurement. The precision of the measurement appears to justify reliance on the error determination.

Figure 2-47 shows graphically the reasons for the apparent shift of an edge under blurred image conditions. The image photometric functions for motion, focus (neglecting Fraunhofer diffraction effects), and lens aberrations (peaked distributions) are sketched.

The shift in apparent edge position arises from the fact that the eye response to light is logarithmic. That is, the sharpest portion of the blurred edge appears at the position where the eye senses the greatest fractional or percentage change in illumination. In the photometric edge function, there is a linear increase in the intensity of light as a function of distance. To the eye, which senses percentage change, the edge distribution appears sharpest at the beginning of the trace. A mathematical way of showing the sharpest apparent position in the edge trace is to plot the logarithmic edge function and look for the greatest slope. As shown in the plot, the greatest slope occurs at the beginning of the trace.

It should be noted that placing this logarithmic trace on film on the straight line portion of the D-log E curve will not affect the position of greatest log gradient. In addition, developing the film to higher gamma will only increase all gradients by the same amount, leaving the position of the maximum gradient unchanged.

For the case of focus error, the effect of blur appears to be slightly less than that of motion. And for the case of aberration with a peaked distribution, the effect might be negligible. No analytical computation has been made to determine predicted amounts. However, it is safe to say that the edge should apparently shift toward the lower density region of the image.

Because of the minimum contrast sensitivity of the eye and the eye's inability to determine the position of maximum gradient for small density changes, the error should be less for low contrast edges than for high contrast edges. In addition, the shift should decrease with observer magnification since the ability of the eye to resolve the distance over which the maximum gradient occurs decreases with magnification (the eye searches for the largest percentage change over the distance it can resolve).

Conclusions

This experiment was designed to show the maximum effect on the accuracy of measurement which could be caused through the use of a stereo model composed of two photographs of unequal resolution. The results are conclusive in that a true position error, (as opposed to a lack of precision) has been found. For the conditions of the test this position error appears to be about 1/6 of the difference in resolved distance of the photographs which make up the stereo pair. However, for the 12-inch, f/6, 9 x 18-inch camera which has been proposed, the error contribution from this source is small and may be made negligible by proper selection of image detail. The maximum error is computed as follows for the anticipated resolution of 30 lines per millimeter at the edge matched against a center resolution of 45 lines per millimeter.

$$\Delta \frac{1}{R} = 1/30 - 1/45 = 11 \text{ microns}$$

$$\Delta P_x = 1/6 \times 11 = 2 \text{ microns maximum error}$$

This error occurs only if a single edge is used in the stereo transfer process. When random detail is used in the height determination, with edges in all directions, this error should disappear. In addition, in the tri-lap area of the 9 x 18-inch format where resolutions are about equal for both sides of the model, even the worst error from using a single edge would be considerably smaller. This is an added advantage obtained with 67 percent overlap.

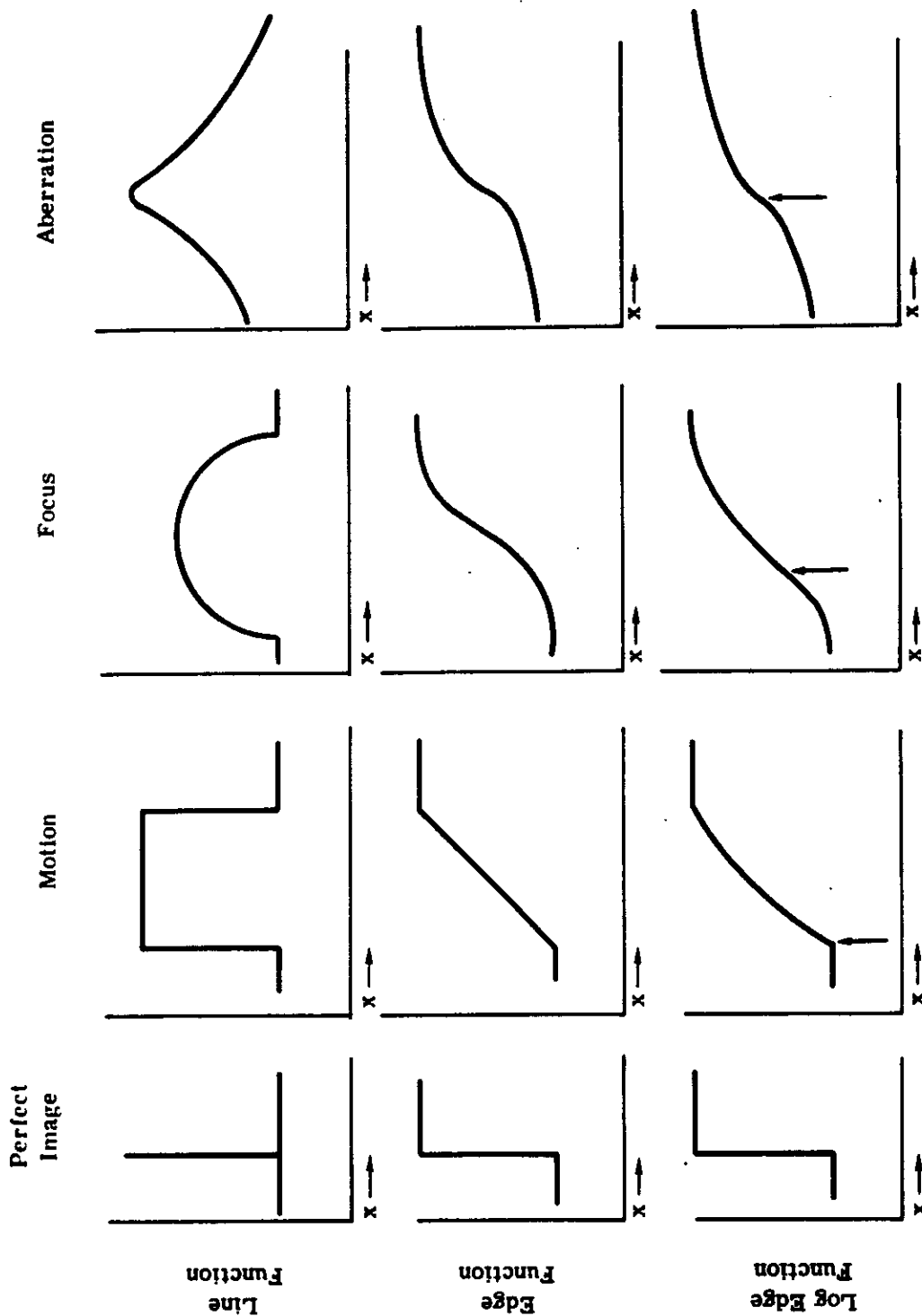


Fig. 2-47 — Image photometric functions

These conclusions have been obtained from limited data with only one object contrast (1.6:1) in the target area. The results are internally consistent for this experiment. The effects of contrast, of image blur type, and of viewing magnification have been discussed qualitatively but have not yet been tested.

2.2.1.3 Photo-Sensor Preliminary Design

Required design limits, performance characteristics, and operational requirements for the photo-sensor system were defined by the criteria developed during the photogrammetric, orbital, photo-optical, and lens design studies. These were considered in the preliminary design of the photo-sensor to assure that it capably met the photographic data gathering requirements of the GOPS System.

2.2.1.3.1 Photo-Sensor Description

The photo-sensor system consists of a terrestrial camera and a twin stellar camera which is mounted directly to the lens cell of the terrestrial camera. The stellar camera photographs star fields to provide a precise attitude reference system. The preliminary design of the photo-sensor system is shown in Figure 2-48.

The terrestrial camera consists of a 300-millimeter focal length, f/8.0 lens, shutter, IMC drive, platen assembly, film transport assembly, and connecting structure. The lens has two element groups or cells attached to a central cylindrical cell to which is mounted the shutter and a structure to mount the platen assembly and IMC drive. From this structure, two flexure mounts provide mounting for the platen and pressure mechanism assemblies. The platen support cell supports a lightweight structure to which is attached the film transport assembly and covers. Leading particulars for the terrestrial camera are given in Table 2-15.

The single-unit twin stellar camera contains two 250-millimeter focal length, f/1.8, Wild Falconar lens assemblies, two shutters, a two-platen pressure mechanism, a one-platen pressure actuator, and one film transport assembly. A single rigid structure supports these subassemblies, and has suitable access covers for assembly, maintenance, and film threading. This structure is bolted directly to the central section of the terrestrial lens cell. The combination of these structures provides the rigidity needed to maintain the calibrated knee angles between all three lenses. The stellar lenses are 90 degrees apart, ± 45 degrees from the roll axis, pointed forward, and are elevated 10 degrees with respect to the roll/pitch plane. Because the stellar lenses are centrally located within the DCM, a maximum of internal baffling is obtained, precluding baffle protrusion from the vehicle. The 10-degree elevation angle also eliminates the need for long baffles. Leading particulars for the stellar camera are given in Table 2-16.

2.2.1.3.2 Photo-Sensor Subsystems

This section describes in detail the various subsystems of the terrestrial and stellar cameras. Operation and control functions in relation to the system mission are described in Section 2.3.

1. Terrestrial Camera

This section describes the subsystems which comprise the terrestrial camera.

a. Lens

The Itek lens design for the terrestrial camera is an 11-element configuration, including an aspheric platen with an inscribed Reseau grid. The lens particulars for the final GOPSS design are as follows.

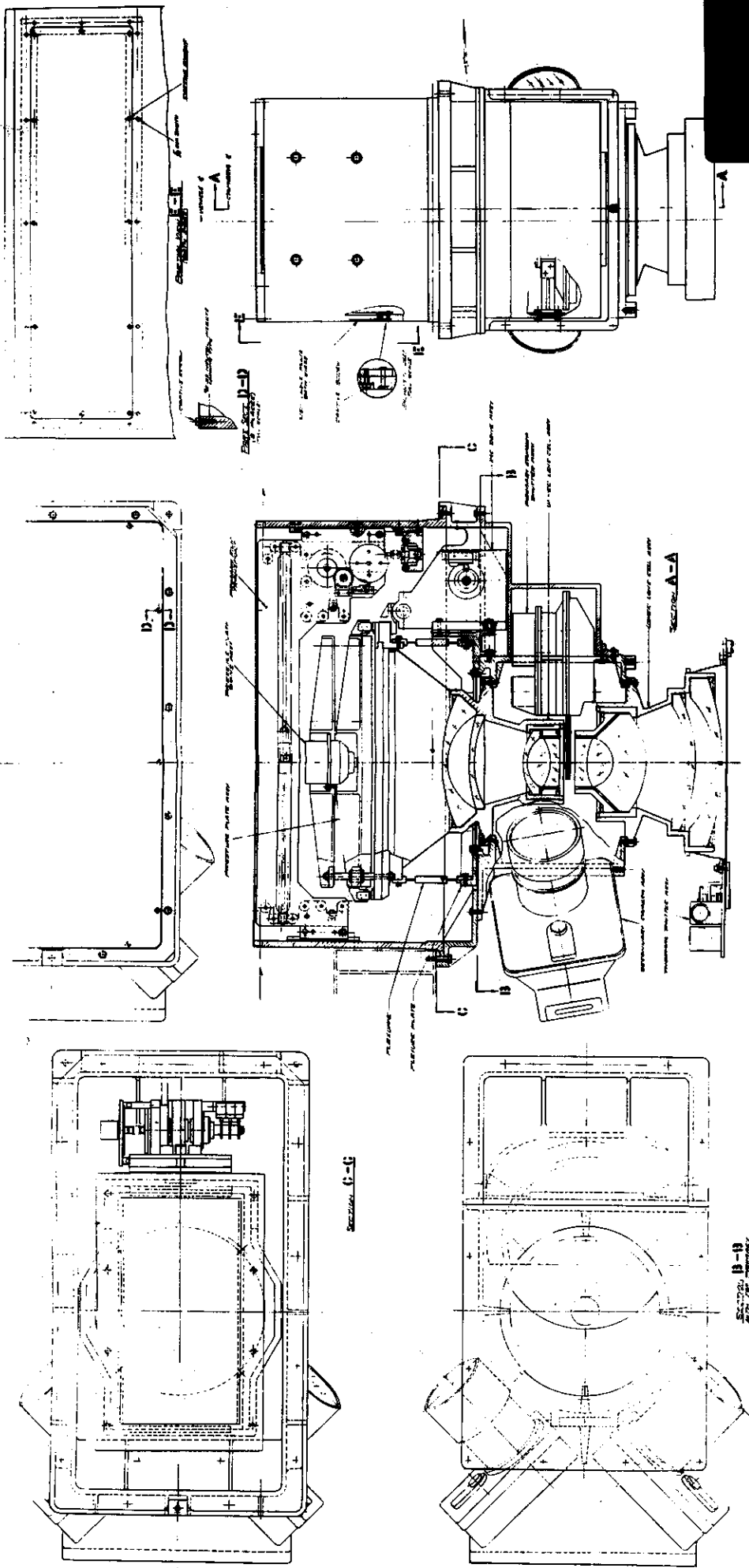


Fig. 2-48 — Primary and secondary camera assembly

~~SECRET~~

Table 2-15 — Terrestrial Camera Leading Particulars

Type: frame

Lens: 80-degree field angle, 300-millimeter focal length, f/6.0, T/12

Spectral range: 0.60 to 0.70 micron

Filter: Wratten

Film: 9.5-inch wide, thin base

Frame dimensions: 19.14 by 9.5 inches

Format: 460 millimeters along-track by 230 millimeters across-track

Data block: Fairchild light diode array imaging directly on film to record time and altitude

Additional data to be recorded: Reseau, fiducials

Overlap: fixed 70 percent

V/h range: 0.020 to 0.035 radian per second

Cyclic range: 14.5 to 22.0 seconds per cycle

Exposure times: 1/50 to 1/200 second for ground photography; 3.0 seconds for stellar calibration

IMC requirements: forward image motion compensation

Platen: 0.7-inch thick glass Reseau with 1 centimeter spacing, mounted on flexures

Shutter: self-capping, continuously rotating type

Film transport: stepping motor-driven indexing roller and shuttle to store film from continuously moving supply

~~SECRET~~

SECRET [REDACTED]

Table 2-16 — Stellar Camera Leading Particulars

Type: frame

Lens: two 250-millimeter focal length, $f/1.8$, 25-degree field, modified Wild Falconars

Platen: two 6-millimeter thick optical plates with one centimeter, Reseau spacing

Shutter: pulse operated, two-blade scissors type with integral motor drive

Exposure time: 0.200 second

Film: 70-millimeter, thin base

Frame: 70 millimeters wide by 230 millimeters long

Format: two 57 by 90-millimeter formats with a data block between them

Data block: light diode array imaging time and altitude

Additional data to be recorded: Reseau

Film transport: stepping motor-driven-indexing roller; two-frame capacity shuttle to store film from continuously moving film supply

Flare shielded for the following conditions: low altitude of 0.75×10^6 feet
altitude errors of 1.0 degree
solar elevations down to: 60 degrees across-track
10 degrees along-track

Pointing accuracy: approximately 1 arc-second with 25 stars recorded per lens

SECRET [REDACTED]

Focal length: 300 millimeters
f/number: f/6.0
T/stop: T/12
Spectral range: 0.60 to 0.70 micron
Filter: Wratten number 25
Field: flat
Format: 460 by 230 millimeters
Number of elements: 10 plus platen
Reseau: one centimeter line resseau
Aperture stop: 2.454-inch diameter
Maximum field angle: 80 degrees
Weight: approximately 125 pounds (complete assembly)

The lens is composed of a forward and a rear element group each containing five elements (one cemented triplet and two negative elements). These groups are housed in beryllium barrels which are flange-connected to the central cell. This central cell is cylindrical in shape and is made in two sections.

The element groups are centered by their flanges and bolted to and aligned by the main section of the central cell. The other section of the central cell connects to the main section in a plane parallel to the optical axis; it is removable for assembly of the shutter. The mate flanges of the two cell sections are extremely flat and smooth and drilled and dowel pinned around the flange so that, when bolted together, they appear to be structurally one piece. The shutter is mounted internally and the IMC drive (for alignment considerations) is mounted externally. A mounting surface is provided on the main section for attachment of the stellar camera.

A support ring is mounted to the upper end of the central cell, to which the platen flexures are attached. The camera support frame is bolted to this ring. This frame mounts the complete photosensor assembly to the DCM.

b. Platen and Pressure Mechanism

The platen is a rectangular glass plate supported along its edges by a metal frame which is, in turn, supported from below on two long flexure joints. (Refer to Figure 2-49.) The film side of the glass platen contains the one centimeter line resseau.

Attached to the metal frame and extending upward are eight tie rods which support a fixed structure that supports the pressure plate moving mechanism and the pressure plate. The pressure plate slides freely on four of the tie rods, and has cemented to its undersurface a 7/8 by 9 1/2-inch wide, soft silicone rubber pressure pad.

The pressure plate pressure actuator is identical to the devices used for the film spool brakes. (See Figure 2-68.) The torque motor which has an integrally mounted nut drives a lead screw axially. The screw motion compresses a spring and plunger which supply the force to the pressure plate. This force or pressure is regulated by mechanical limit stops driven from a gear train connected to the motor. In addition, cams actuate a flip-flop circuit which changes motor polarity. An ON command energizes the mechanism and applies platen pressure. When a second command is given, the platen pressure is released and the mechanism shuts itself off.

During transport of the film, chafing against either the glass platen or the rubber pressure pad must be prevented. Two spring-loaded guide rollers which travel up and down with the platen ensure the proper film positioning. A minor distortion of the image could result if a change in

tension occurred in the process of bringing the film in contact with the glass platen. To prevent this, a spring loaded "reservoir loop" is provided at each end of the platen. This mechanism causes the film to be squeezed against the glass plate with a force of approximately 0.3 psi just prior to photography. After exposure, the platen is unclamped and a frame of film is transported.

The platen, supported at its boundaries, was analyzed as a rectangular plate under uniform pressure.

A beam theory analysis of the platen bezel was made with eight tie rods located in such a manner as to minimize bezel deflection (the results were added to the results of the platen bending). Total platen deflection was determined from the algebraic sum of the platen and bezel deflections. These total deflections were considered to be the sum of a uniform and a non-uniform displacement. The uniform effect may be optically corrected. The non-uniform deflections and their instability are considered a source of calibration or scale error.

The flexures are designed to provide positive control on platen position error during IMC. This control must be verified by defining platen equilibrium positions during travel, especially during the exposure interval.

In the analysis, the flexures were assumed to obey beam theory. The platen-flexure system now becomes a spring-mass system to which a constant force is applied. The equilibrium positions of the system were determined, by means of work principles, as functions of variable spring constants and force parameters. If the variable spring constants are defined as functions of assumed machining errors, it may be shown that, for relatively loose machining tolerances, the flexures provide a platen trajectory error control well within acceptable limits.

A further stability analysis was conducted in which the member was considered a fixed-free column under combined axial and lateral loading. The flexure was shown to be a stable mount. The increased lateral deflections produced by the end loads were shown to be insignificant.

Film flatness tests were conducted to determine the suitability of the pressure pad method for holding film flat during exposure. The results showed that 96.3 percent of the area was 1.2 microns or less from being flat, 2.3 percent of the area was between 1.5 and 1.8 microns from being flat, and 1.2 percent was between 2.1 and 2.4 microns from being flat. It was felt that these errors were due largely to dust and emulsion irregularities. During Phase II, the platen will be breadboarded to provide a better opportunity for study of film flatteners and motion problems.

c. IMC Drive

The platen, moved by means of a cam and follower arm, is translated 0.040-inch longitudinally. A maximum of 0.008 inch is used for IMC during exposure. In order to achieve the positional and velocity accuracies required of the platen, a follower arm with a reduction ratio of 10:1 was selected. The forces, deflections, accuracies, control, and machineability of components have been optimized by this approach. A detail of this drive assembly is shown in Figure 2-50.

The prime mover in this mechanism is a dc torque motor which is tied directly to a shaft. A tachometer generator, which senses and controls the shaft's angular velocity as a function of V/h , two control transmitters, which correlate the shaft's angular position, and three small cams, which actuate microswitches which are part of the sequencing circuitry, are also attached.

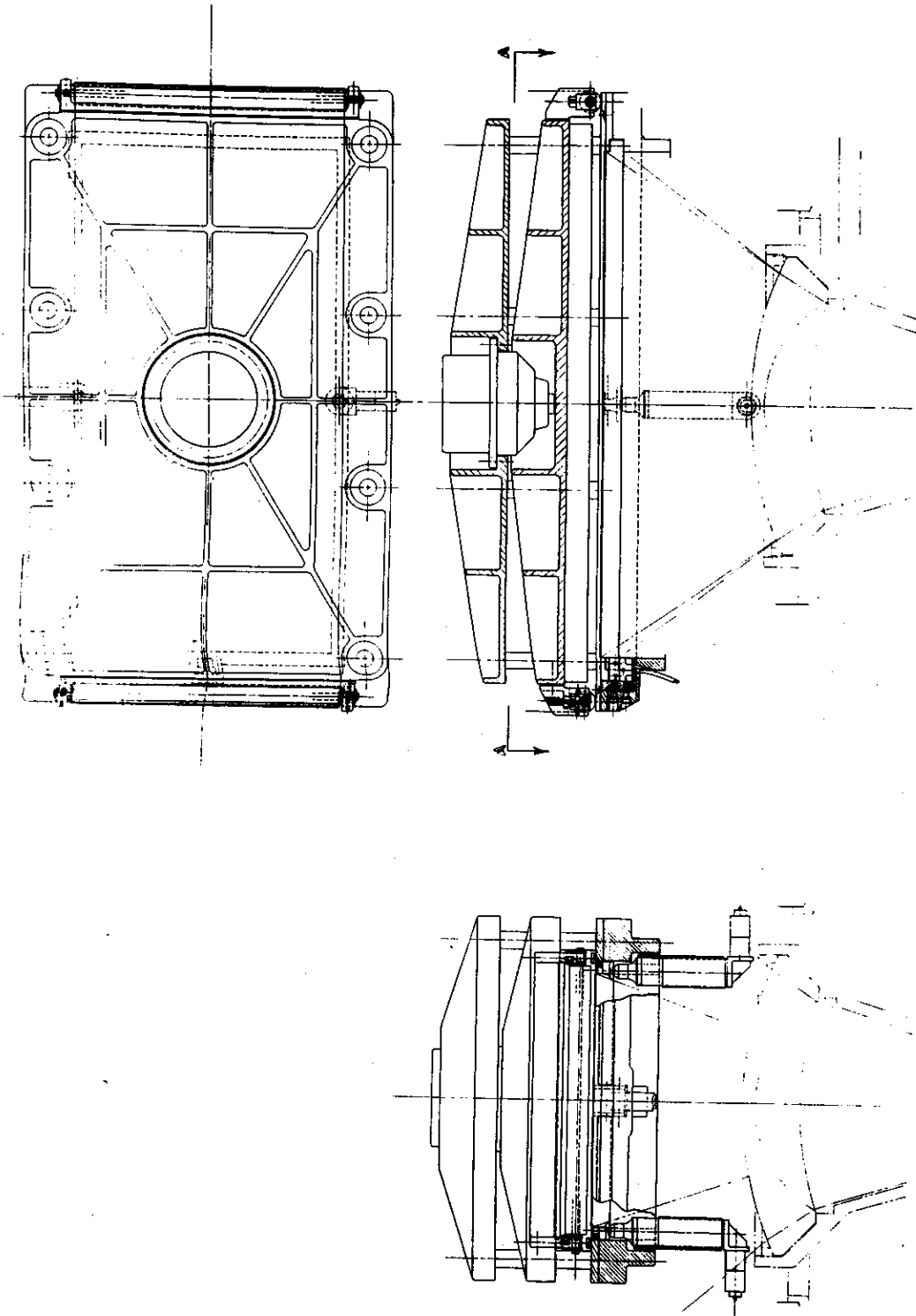


Fig. 2-40 — Flaten and pressure plate mechanism

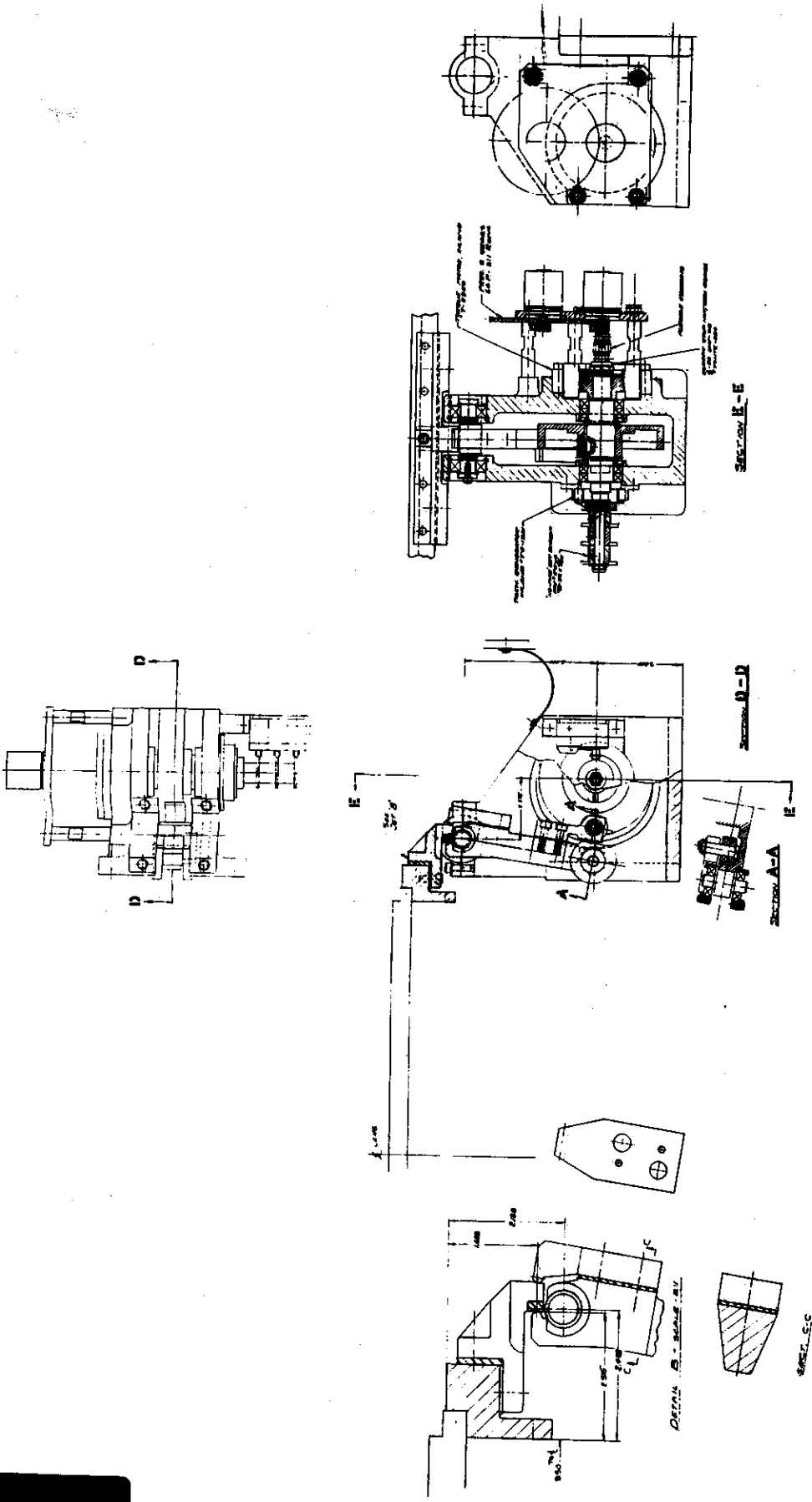


Fig. 2-50 — IMC drive assembly

~~SECRET~~

The main cam is stainless steel, hardened to RC 60, ground to within ± 0.0002 -inch accuracy, and polished to a surface smoothness of eight microinches or better. The main support bearings are precision class three and are preloaded. The supporting structure is also of stainless steel. The cam follower roll is tungsten carbide and has accuracies and smoothness similar to those of the main cam. The follower arm is stainless steel and its upper working tip is hardened, ground, and polished. Virtually all IMC drive parts are of stainless steel for stiffness and compatible coefficient of expansion, the two factors which will largely determine the performance of this subsystem.

The upper end of the follower arm pushes against the polished carbide face of a block attached to the platen bezel. The bezel itself is adequately stiff to resist deflections.

The platen is made captive to the follower arm by a spring-loaded backup finger. The contact between the cam follower roll and the cam is maintained by a long stiff spring. The entire IMC drive mechanism is mounted to the principal stainless steel supporting structure. In order to minimize temperature differentials across the lens cell, heat generated in the IMC torque motor will be conducted directly to the aluminum exterior structure heat sink by means of flexible copper strips.

d. Terrestrial Camera Shutter

(1) Operation

The terrestrial camera shutter is a complete assembly which interfaces with the lens support structure in order to locate the shutter blades between the lens of the camera (see Figure 2-51). In its operating position, the shutter housing does not become an integral part of the lens support structure, but is mounted in a manner that will minimize the effect of vibration and permit reinsertion without disturbing critical alignments.

The shutter mechanism is designed for exposure speeds which range from 0.005 to 0.020 second with a minimum efficiency of 70 percent. Much consideration has been given to the minimization of vibration, noise, and thermal shock within the shutter itself, and to the prevention of the transfer of any residual energies to the lens and its structure.

The predominant feature of the shutter mechanism is its three circular shutter blades which, on command, will be phased so as to expose the film. This is accomplished by providing relative motion of the exposure blades, an action which is described later in this report. Another feature of this mechanism is the incorporation of a photo-optical switch which will actuate, at mid-exposure, the fiducial marking mechanism. Additional equipment includes an encoder which acts both as a tachometer and position indicator, and is used for synchronization and control of the shutter mechanism. A precision encoder that monitors the position of the encoder shaft and a fiducial marking switch are also included within the mechanism. A precision servo drive system maintains constant rotational velocity of the shutter blades. An independent dc torquer provides the additional torque to the arming mechanism during the exposure interval.

(2) Operational Sequence

The terrestrial camera shutter is designed for continuous rotation at a speed established by the exposure time. The shutter has three blades rotating in such a manner as to always block the aperture. Upon command, the relative position of one of the shutter blades is changed so that the

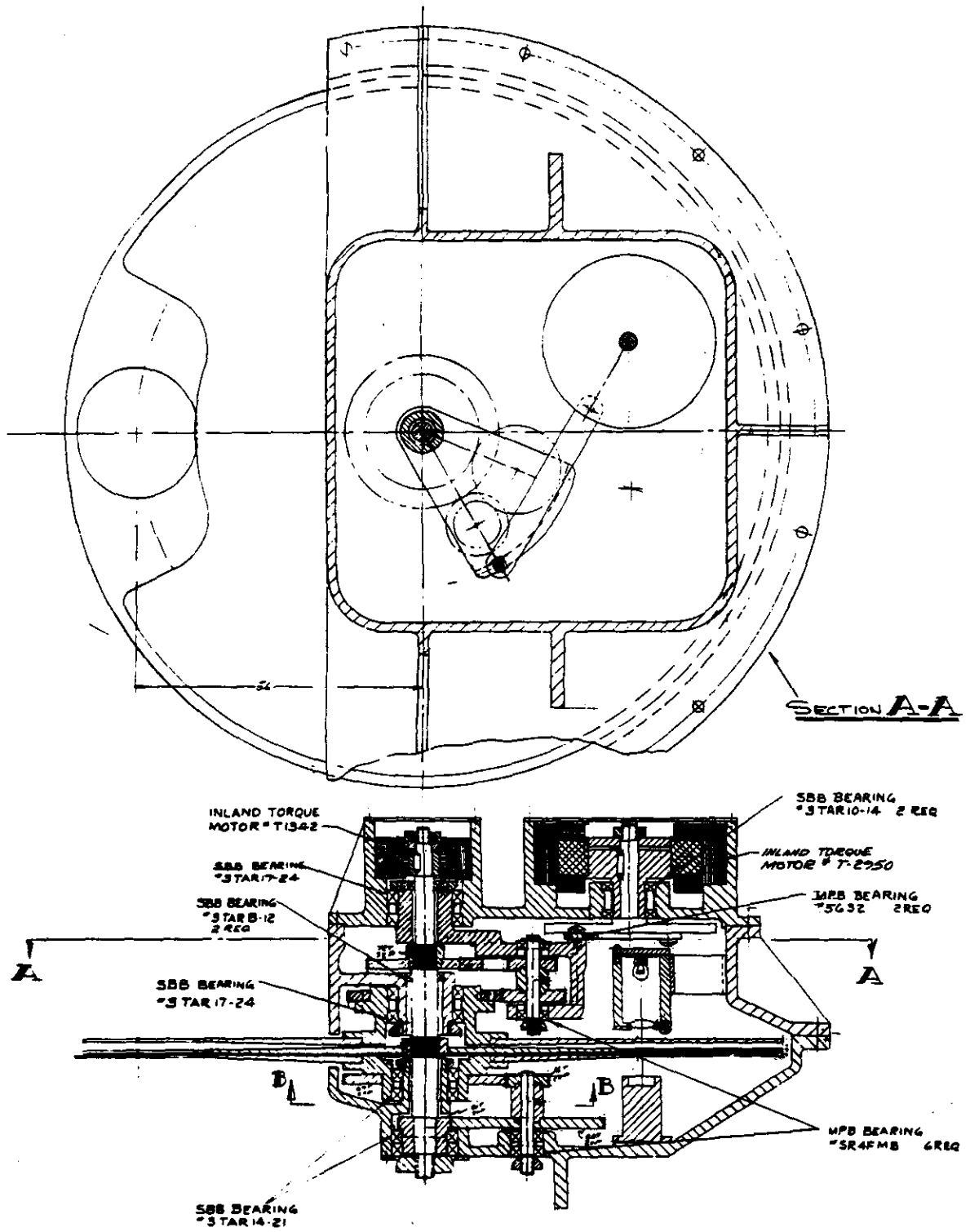


Fig. 2-51 — Terrestrial camera shutter

three shutter blade openings all coincide in the aperture, and remain coincident only for the desired exposure time. The mechanics of shutter operation is described in the following paragraphs and illustrated in Figure 2-52. Note that Figure 2-52 is a reversed representation in that the blades are transparent and the openings are black.

In this case, the shutter blades S_1 and S_2 are rotating at the same speeds but in opposite directions. The point of coincidence is at an angle of 60 degrees from that of the aperture. (See Figure 2-52(a).) Because the blades counterrotate, the aperture is always blocked by either S_1 or S_2 , even if S_3 is in the aperture. The function of S_3 is to block the aperture during the process of moving the coincident point of S_1 and S_2 into the aperture. Shutter blade S_3 revolves at 1/12 the speeds of S_1 and S_2 .

When the command is given to expose the film, the sequence of arming will begin just after blade S_3 has left the aperture. (See Figure 2-52(b).) At this point, blade S_1 , which is still revolving at ω_1 speed, will be translated so that its relative speed during translation will be reduced. At the end of the translation period, shutter blade S_1 will again have its ω_1 speed, but the coincident point of shutter blades S_1 and S_2 will now occur directly over the aperture of the camera lens. Shutter blade S_3 will still be blocking the aperture and prevent an exposure. (See Figure 2-52(c).)

With shutter blades S_1 and S_2 opening in the aperture, an exposure will take place when shutter blade S_3 is coincident in the aperture. (See Figure 2-52(d).) This occurs at the completion of 11/12ths of a revolution of blade S_3 after the command signal for arming is given. At the completion of 1/12th of this rotation of blade S_3 , S_3 will signal the mechanism to de-arm and return the coincident point of shutter blades S_1 and S_2 to their original point some 60 degrees away from the aperture. (See Figure 2-52(e).)

(3) Determination of Shutter Speeds for Given Exposure Times

The previous section described physical actions that take place to arm the shutter and make an exposure of the film. This section describes the calculations made to determine the operating speeds and the forces required to perform the described functions.

The exposure times required for the terrestrial camera shutter range from 0.005 to 0.020 second. Another requirement is that the shutter have a minimum efficiency of 75 percent. The combination of these two factors results in a one radian opening in shutter blades S_1 and S_2 . An opening in shutter blade S_3 , operating at 1/12 the speeds of blades 1 and 2, is 1/12 longer than it is wide.

With the above geometry, the operating speeds are determined as follows:

Exposure time

$$t_e = \frac{1 \text{ radian}}{V}$$

$$t_e = \frac{60}{2\pi N}$$

Then, operating speed

$$N = \frac{60}{2 t_e}, \text{ and}$$

for $t_e = 0.005$ second,

$$N = \frac{60}{2\pi(0.005)} = 1910 \text{ rpm}$$

for $t_e = 0.020$ second,

$$N = \frac{60}{2\pi(0.020)} = 478 \text{ rpm}$$

Shutter Blade	Minimum Speed, rpm	Maximum Speed, rpm
S ₁	478	1910
S ₂	478	1910
S ₃	40	159

(4) Arming Time

The arming of shutter S₁ for an exposure of the film is affected to prevent any possible double exposure. This is accomplished by completely arming shutter blade S₁ in the time required for shutter blade S₃ to make less than one complete revolution from the aperture centerline. To simplify the arming mechanism, it is designed for constant speed arming at the shorter exposure times. Another consideration is the dynamics of arming, and the allowance of sufficient time to dampen out the arming reactions. These combined factors make it necessary to perform the arming of the shutter in something less than 0.200 second, while the S₃ blade takes 0.376 second to complete one revolution at its higher speed.

(5) Torque Required for Arming

In order to arm the S₁ shutter blade in the time required, detailed servo system analysis indicates that the inertia of the complete shutter mechanism less the inertia of S₁ blade has to be 1.7 times the S₁ blade inertia, and that arming can be accomplished in 0.150 second. Thus, using the times allowed and the angles through which the arming takes place, the torque needs for arming is determined. The accompanying illustration depicts how arming is accomplished and where the torque is applied.

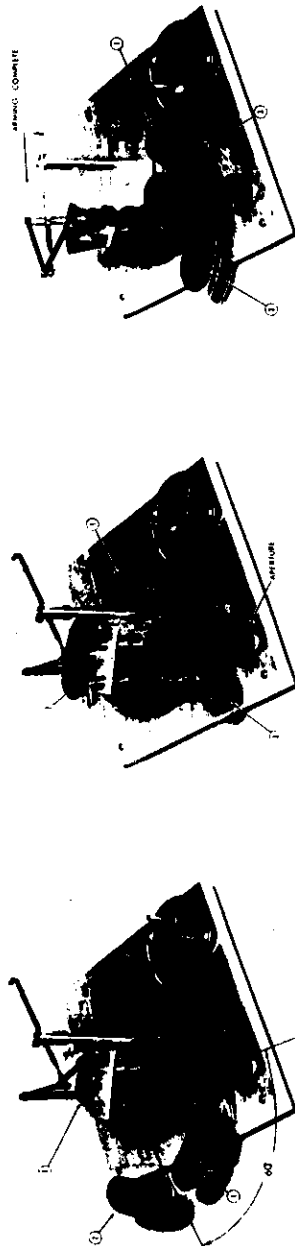
$$T_M = T_{S_1} + T_{S_2} + T_A$$

$$T_M = J_{S_1} X_1 + J_{S_2} X_2 + J_A X_A$$

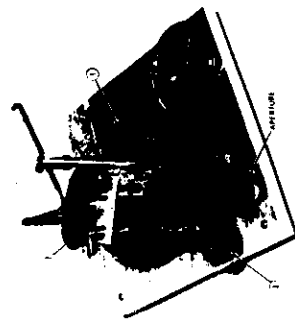
where $J_{S_1} = 0.62 p_1 = 0.037$ pound-inch²
 $J_{S_2} = 1.7 (J_{S_1}) = 0.063$ pound-inch²
 $J_A = 0.0238$ pound-inch²

$$X_1 = G_1 t^2$$

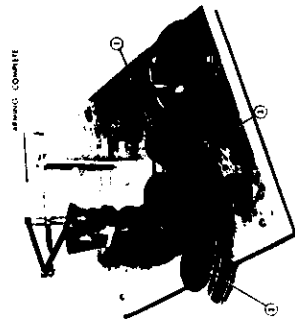
where $G_1 = 120$ degrees = 2.1 radians
 $t = 0.150$ second



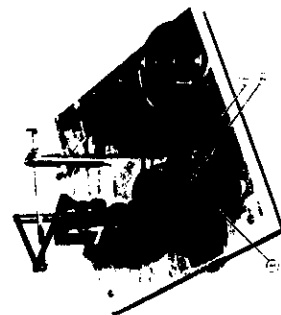
(A) Coincidence of exposure blades 60 degrees from aperture



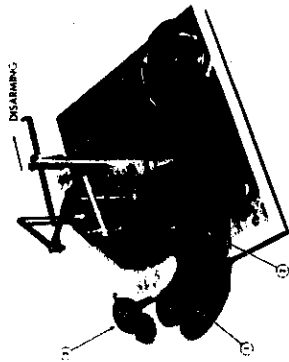
(B) Capping 3 blade passes aperture, energizing arming mechanism after receipt of fire command



(C) One revolution before exposure, blades 1 and 2 coincide over aperture, but 3 blocks aperture



(D) Exposure



(E) Disarming begins, and blades 1 and 2 move back to position 60 degrees from aperture

Fig. 2-52 — Shutter operation

$$X_1 = 2.1 (0.150)^2 = \text{rad/sec}^2$$

$$X_2 = 1/1.7 X_1 = 51 \text{ rad/sec}^2$$

$$X_A = \theta_2/t^2$$

where $\theta_2 = 60 \text{ degrees} = 1.05 \text{ radians}$
 $t = 0.150 \text{ second}$

$$X_A = 1.05/(0.150)^2 = 43.5 \text{ rad/sec}$$

Therefore,

$$T_M = (0.037)(87) + (0.063)(51) + (0.0238)(43.5)$$

$$T_M = 7.47 \text{ inch-pounds}$$

(6) Motor Selection

The selection of motors to operate the terrestrial camera shutter is based on a knowledge of the speeds at which the shutter is to operate, the torques required, and the servo analysis for dynamic system performance. The motor selected for the main shutter drive is an Inland torque motor No. T-1342, and, for the arming mechanism, an Inland torque motor No. T-2950. The reason for choosing a large motor (14.4 pound-inches) for the arming mechanism is that the application of force required becomes angular-dependent. The torque required by the motor to drive the arming mechanism reaches a value of 5.25 pound-inches. However, halfway through the cycle, dynamic breaking (current reversal) is applied in order to stop the motor smoothly. This action limits operation to half of the rated motor power. If a smaller size arming motor were used on reversal, the power surge would be enough to demagnetize the motor. Figure 2-53 depicts the loading cycle as seen by the arming motor.

(7) Fiducial Marking Switch

The fiducial marking switch is a photo-optical device which is actuated only at mid-exposure of the film. A light source is placed on one side of the shutter blades and a photocell is placed on the other side. At mid-exposure, three small holes, one in each shutter blade, are coincident and allow light to pass through. This activates the photocell which, in turn, activates the fiducial marking mechanism. At no other time are the three holes coincident to activate this switch.

(8) Reliability Considerations of Design

The following discussion summarizes the design considerations that assure high shutter reliability by considering failure of parts and shutter life. The material strengths of the terrestrial shutter are based on a main shaft operating speed of 5000 rpm. This provides all rotating parts with a 2.5 safety factor. The strength calculation results of the S_1 and S_2 shutter are shown in Figure 2-54.

(9) Vibration Analysis

Vibration analysis has been made on all rotating members of the terrestrial shutter. The analysis shows that all rotating parts are free of first critical frequencies over the operating

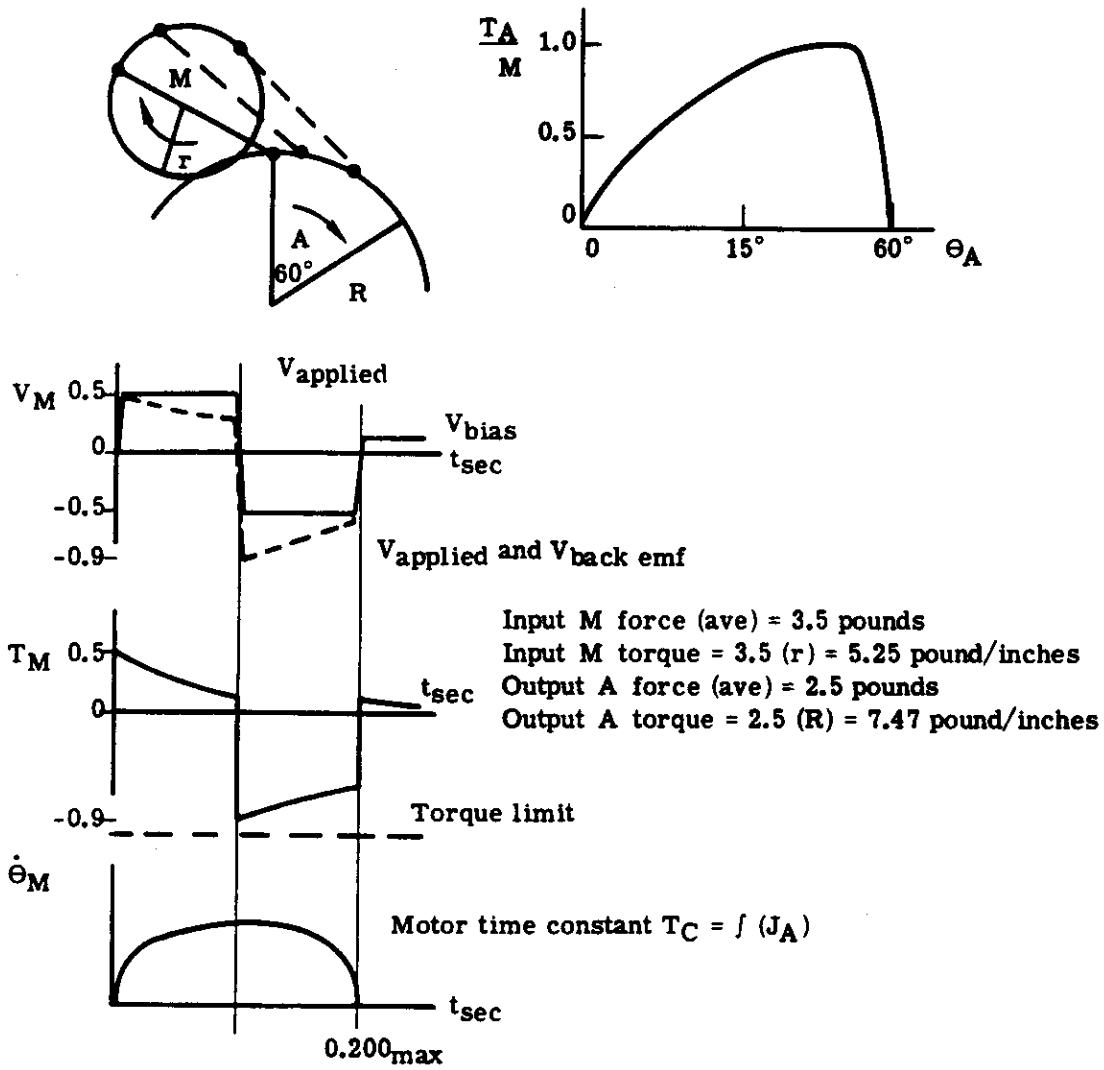


Fig. 2-53 — Arming motor loading cycle

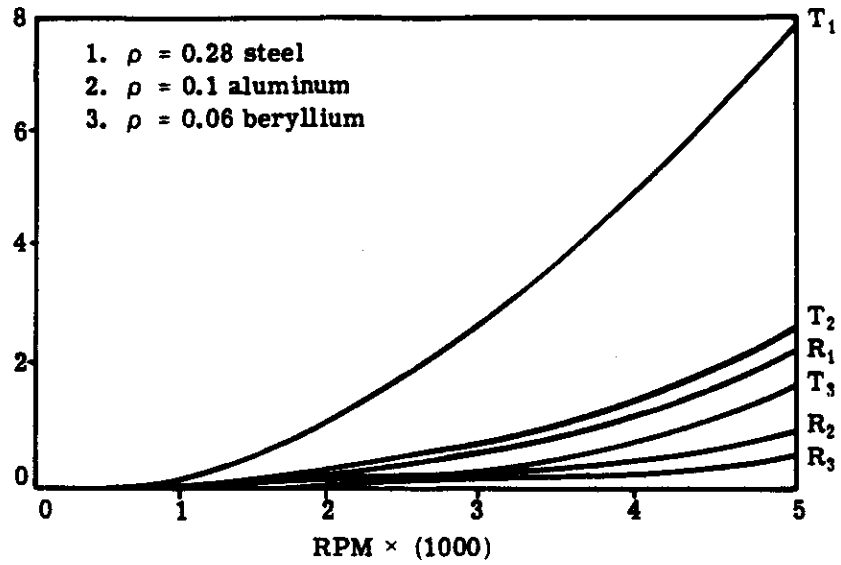


Fig. 2-54 — Stress levels versus rpm for steel, aluminum and beryllium

range. The shutter blades S_1 and S_2 did exhibit a first critical frequency close to the operating range, but these blades have since been modified. It was assumed that the shutter blades are flat disks with a small thickness-to-diameter ratio and that speeds are such that material stiffness is still a factor. The first critical frequency occurs at $2620 - 1910 = 710$ rpm above operating range. Figure 2-55 shows the location of critical frequencies associated with this shutter.

The material used in the shutter gears are 416 and 440C stainless steel, hardened to an RC of 32 to 38. They will be run together in a bench test to remove all irregularities and to polish the mating surfaces; they will then be cleaned, and a dry film lubrication such as MoS_2 , will be applied.

The gears themselves experience high loading only during an arming cycle. At this time, the gear stress is calculated at 4800 psi. With an increase to 3/16-inch in the gear face, the S_R is 3200 psi. Under these conditions, the gears have a life expectancy of in excess of 10^5 load cycles. The bearings used in this design are very lightly loaded, in many cases as low as 5 percent of rated capacity. The bearings have a life expectancy in excess of 5000 hours of continuous operation.

e. Synchronization Control System

The platen and shutter servos are synchronized with the intervalometer to accomplish three objectives:

1. Exposures are made at regular intervals upon command of the intervalometer.
2. Image motion is compensated by moving the platen at a speed proportional to the V/h ratio.
3. The center of the format is at the principal axis at the same time the shutter is at mid-exposure.

The control system which performs these tasks is shown in Figure 2-56. Principal components of the system are the intervalometer servo, the shutter servo, the platen servo, and the digital control equipment required to synchronize them. These are discussed in detail in the following sections. The intervalometer and shutter servos are sampled data control systems, and the platen servo is an analog system.

The system is controlled by the V/h and t_e signals which come from the OCV. The V/h signal is continuous over its range, whereas the exposure is selected from one of the five available discrete time intervals.

All three servos are phase-locked and run at velocities proportional to V/h . To achieve phase lock with the intervalometer, the platen and shutter make an integral number of revolutions during each frame interval. The platen servo operates its drive at 144 times the speed of the intervalometer. In order to achieve phase lock between the platen and the shutter, the shutter turns at an even submultiple of 144. Furthermore, the shutter speed is close to the selected speed to provide proper exposure. The correct submultiple is chosen by the shutter speed ratio selector. This is a logic matrix, and selects the one speed ratio (out of seven available) to give the most accurate exposure time.

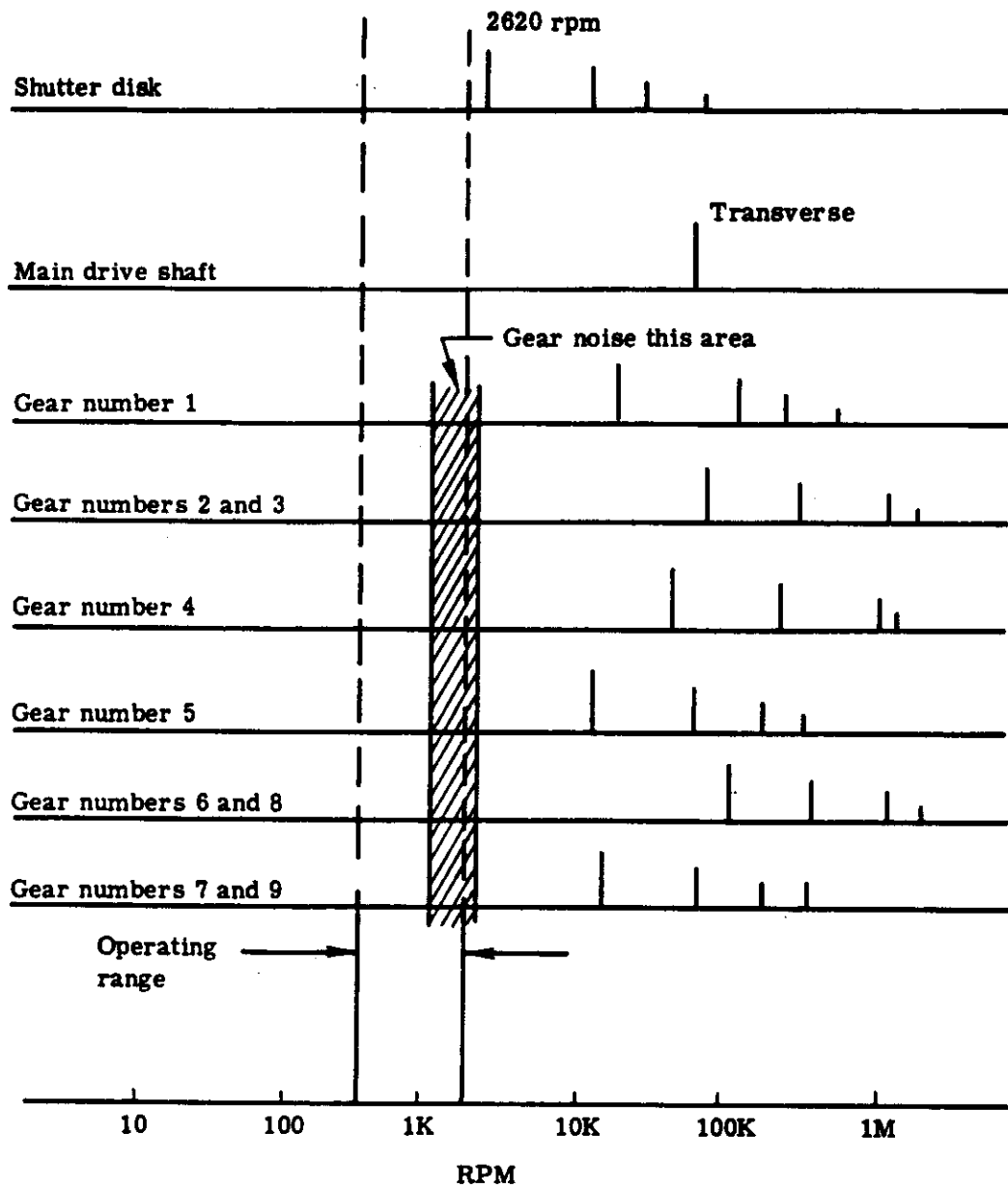


Fig. 2-55 — Location of critical frequencies, terrestrial shutter

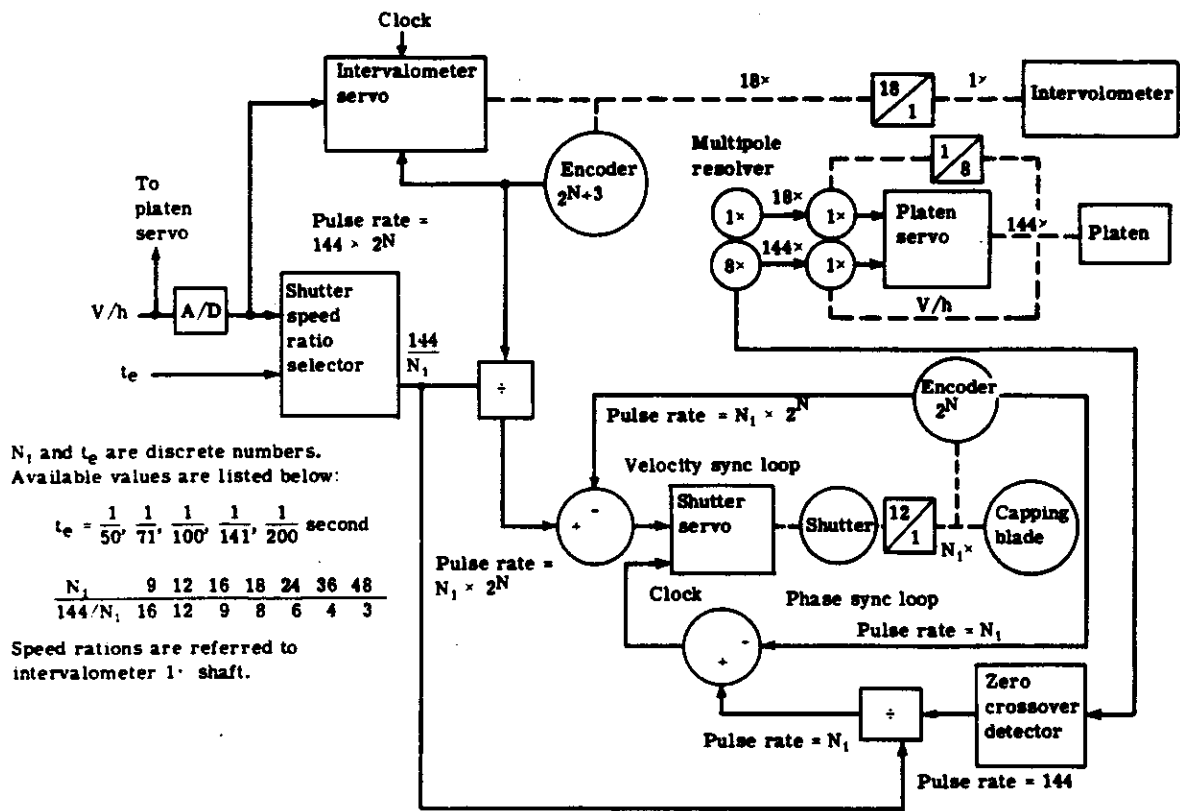


Fig. 2-56 — Synchronization and control block diagram for terrestrial and stellar cameras

The intervalometer is run by a digitally-controlled velocity servo. A binary number proportional to V/h is the reference signal for the servo. The servo is operated at the speed necessary to make the pulse rate from the $18\times$ shaft encoder equal to this number. The intervalometer cams are on the $1\times$ shaft, and turn one revolution per frame interval.

Mounted on the $18\times$ shaft is a multipole resolver with two output signals. These signals provide the coarse and fine reference inputs to the platen servo. The platen drive is intermittent and only operates for a fraction of a second when the exposure is made. Just prior to exposure, a signal from one of the intervalometer cams connects the platen servo to its reference signal. The platen builds up to speed using the coarse information. When it is at the right speed and nearly in phase with the intervalometer, the servo switches to the fine signal input which is at a frequency 144 times that of the intervalometer. The servo motor drives a cam which is shaped to give the correct linear platen motion. The result is that the platen speed is proportional to V/h , and the platen position is in phase with the intervalometer during the exposure. After the exposure is completed, the platen servo is de-energized and the motor stops until the next exposure.

The shutter servo is a digitally-controlled servo with two control loops. The velocity loop makes the shutter run at the speed chosen by the speed ratio selector. The position loop causes the shutter to synchronize in phase with the platen reference signal. The platen resolver, the multipole resolver, and the shutter encoder are all adjusted so that midexposure and the center of the platen coincide.

The quantized V/h and t_e signals are fed into a logic matrix called the speed ratio selector. The matrix output is $144/N_1$, where N_1 is the speed ratio required to satisfy the 20 percent exposure accuracy.

This number ($144/N_1$) is used to set two division registers. The first register divides the velocity reference pulse train and the second register divides the position (phase) reference pulse train.

The velocity reference pulse train comes from the encoder on the intervalometer's $18\times$ shaft. This encoder has 2^{N+3} pulses per revolution (ppr) where 2^N is the number of ppr of the shutter encoder. Since the 2^{N+3} encoder is running at 18 speed, its output is 144×2^N ppr of the intervalometer ($1\times$). When this pulse train is divided by $144/N_1$, the resulting train is at the rate of $N_1 \times 2^N$ ppr. The servo forces the shutter to run at N_1 times the intervalometer speed in order that the shutter encoder pulse rate will match the reference signal.

The position reference pulse train is derived from the fine signal output of the multiple resolver on the intervalometer's $18\times$ shaft. The fine signal is a sine wave at a frequency 144 times the intervalometer rotation rate. The sine wave nulls are sensed by a zero cross-over detector which produces one pulse per cycle of the sine wave. This pulse train (at 144 ppr of the intervalometer) is divided by $144/N_1$ to give a train at the rate of N_1 ppr. The shutter encoder produces one synchronization pulse per shaft revolution, or N_1 ppr of the intervalometer. The phase error between shutter and platen is proportional to the distance between alternate pulses from the two trains.

The shutter runs in the velocity mode (with the position loop inhibited) until it is at the correct speed. Then the position loop adjusts the phase until the shutter is in synchronization with the platen.

A digital clock and a logic circuit supply the commands required to control the digital computation circuits in the servos.

The specifications and performance requirements are listed in Table 2-17.

(1) Intervalometer Servo

The intervalometer servo is a digitally-controlled velocity servo. (See Figure 2-57.) The reference signal (V/h) is scaled appropriately so that a binary number is available which is proportional to the number of pulses from the intervalometer encoder per unit sample time. This number is inserted into a down counter once per sample period. Upon command of the sync control logic circuit, the gate opens and the pulse train from the intervalometer encoder counts the register down. The number of pulses left at the end of the sample period is proportional to the servo velocity error. This number is stored in a buffer register and held until the next sample. The buffer drives a digital-to-analog converter. Then the analog signal is amplified to the level required to drive the motor. This cycle is repeated continuously under the direction of the logic control circuit. The motor is forced to drive the encoder so that its pulse rate is equal to the input binary number.

The motor is a frameless dc torquer mounted directly on the driveshaft. The multipole resolver (for the platen reference signal), and the intervalometer encoder, are also directly attached to the same shaft. An 18:1 gear reducer drops the speed at the intervalometer cams to one revolution per frame interval. The cams actuate switches which provide command signals for the various operations in the picture-taking sequence.

The intervalometer servo is a straightforward velocity control system and is designed for essentially steady-state operation. Its most important characteristics are smooth operation and low velocity error. Since the intervalometer provides the reference signals for the platen and shutter, any drive shaft perturbations or velocity errors show up directly as errors in the IMC motion.

The intervalometer servo is designed to have a reasonably high torque stiffness in order to reduce the velocity resolution error. Furthermore, the servo bandwidth is limited in order to filter electrical and mechanical noise.

(2) IMC/Platen Servo

The platen servo is an analog position follow-up servo which moves the platen during the exposure in order to compensate for along-track image motion. The servo circuit is shown in schematic form in Figure 2-58. This servo uses dual-speed reference signals and is tachometer-stabilized.

The position reference command signals come from a dual-speed multipole resolver which is mounted on the intervalometer's 18x shaft. This resolver has two sets of windings on the same rotor and stator structure. The conventional two-pole element produces one electrical cycle per shaft revolution, and the 16-pole element produces eight electrical cycles per revolution. Each output of the multipole unit is connected to a conventional size 15, two-pole resolver on the platen drive assembly. The 1x output provides coarse information and is connected to the resolver which is running at one-eighth the speed of the platen. The 8x output connects to the resolver which is directly attached to the platen drive shaft and provides accurate, fine information required during the exposure. The outputs of the two platen synchros are position-error

Table 2-17 — Performance Specifications for the Terrestrial Camera Control System

Servo Specifications

	Capping Shutter, θ s/12	Platen	Intervalometer, 1x
Maximum velocity, radians per second	20.9	62.6	0.435
Minimum velocity, radians per second	2.57	41.3	0.286
Speed ratios	9, 12, 16, 18, 24, 36, 48x	144x	1x
Velocity error, IMC	—	—	0.3 percent
Position error, IMC	18 microns	18 microns	

Input Signals

1. $V/h = 0.023$ to 0.035 radian per second (continuous)
2. $t_e = 1/50, 1/70.7, 1/100, 1/141.4, 1/200$ second (discrete)

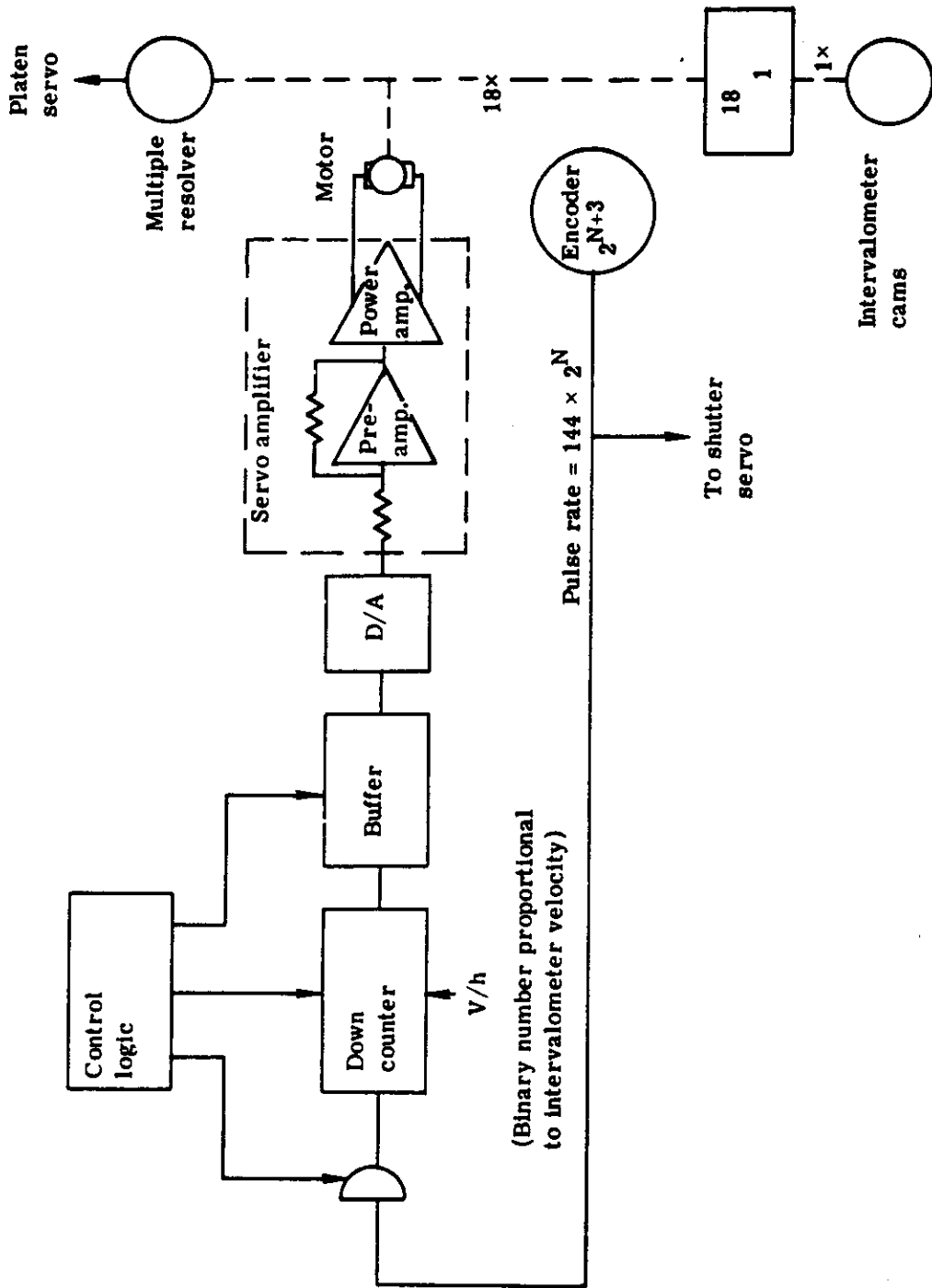


Fig. 2-57 — Intervalometer servo schematic

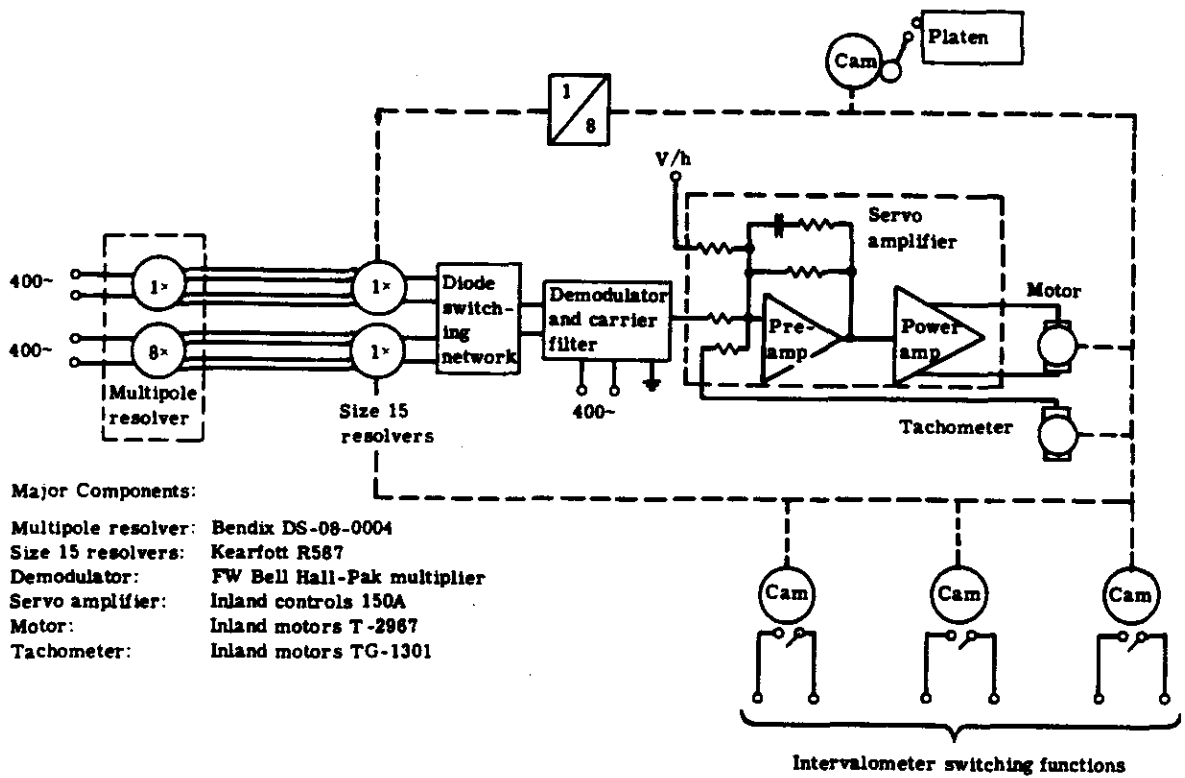


Fig. 2-58 — Platen servo schematic

commands and these signals are fed into a diode switching network. As long as the coarse error is large, the servo follows the coarse command signal; however, when the servo is approximately in synchronism with the input, the switching network blocks the coarse error signal and passes the more accurate fine error signal which is then employed for the rest of the operation. The connection of a 1x resolver on the platen with the 8x resolver on the intervalometer yields an 8:1 speed increase. Thus, this particular resolver combination acts like an electronic gear box.

The signal from the switching network is demodulated by a phase-sensitive synchronous demodulator and filtered to remove carrier frequency noise. (The carrier frequency is 400 cps.) A high gain wide bandwidth dc servo amplifier boosts the power level of the signal to drive the dc torque motor. The servo amplifier contains a preamplifier which sums the input and feedback signals through appropriate factors and a power amplifier which produces the current and voltage levels required to control the platen motions.

The drive motor is a direct-coupled dc torquer having a permanent magnet field and a wound armature. The motor is a frameless unit and mounts on the same shaft as the platen drive cam. Also mounted on the same shaft are limit switch cams and a tachometer. The tachometer is a permanent magnet dc machine similar to the motor, and it is used to provide rate feedback information to stabilize the servo.

The platen servo is basically a conventional follow-up servo with a two-speed reference signal used to provide accurate tracking data. Tachometer stabilization is used to control the transfer function of the motor-load and to increase the torque stiffness. A velocity feed-forward signal is also added to reduce the velocity following error.

When the platen servo performs IMC, it goes through two distinct modes. The servo loop is closed at the command of the intervalometer. Since the platen is not in synchronism with the command signal, there is a large error and the servo amplifier is driven into saturation. The servo motor runs at maximum acceleration until it has achieved approximate velocity and phase synchronization. While saturated, the servo is actually an open loop system whose dynamics are strictly a function of the motor-load time constant. The second mode begins when the servo is nearly synchronized and the error drops low enough to bring the amplifier out of saturation. After entering this linear mode, the servo rapidly settles and follows the input command. During this mode, the performance of the servo will be that predicted by the usual linear analysis techniques.

In order to achieve successful IMC, the servo must go through its saturated phase and settle all transients prior to the beginning of the exposure. At the time the coarse reference signal begins its last cycle prior to the exposure, the intervalometer commands the platen servo to synchronize. The platen drive motor makes several rotations while going through its synchronizing transient, then locks in and tracks the input smoothly until after the exposure, whereupon a reset switch de-energizes the servo. Each time the motor rotates, the platen moves back and forth through its travel. However, only one such cycle is actually used for taking the picture. The fact that the platen makes more than one IMC cycle per exposure, is inconsequential.

The limiting factor on the dynamic performance of the servo is the need to limit the servo bandwidth enough so that noise will cause velocity errors during the exposure. The noise can be either electrical noise (mainly on the input signal) or mechanical, due to structural resonances. In order not to excite the structure, the rate loop bandwidth should be at least a factor of three lower than the structure natural frequency. The position loop bandwidth cannot be more than

about one-third the rate loop bandwidth. The large mass of the platen plus practical limitations on the size of the spring which preloads the platen against the follower arm limit the natural frequency of the structure to about 100 radians per second. Therefore, the servo bandwidth is limited to approximately 10 radians per second. This bandwidth gives quite satisfactory attenuation of any electrical noise.

At the time of exposure, the platen servo is in the steady state. Since it is a position-control system, there are two major sources of phase error to contend with while in the steady state. The first is position resolution which is limited by the friction at the drive shaft. The inner rate feedback loop allows the torque stiffness to be increased without changing the characteristics of the outer loop. The resolution error can therefore be minimized at will. The other phase error source is the velocity-following error. The combination of high velocity and low error indicate the requirement for a rather large velocity constant. If the position loop gain is raised to the required level, rather complex integral networks are needed to compensate the gain and keep the bandwidth in the desired region. These networks tend to cause some instability during the saturated portion of the synchronizing transient, and their long settling time can cause velocity errors during the exposure. A different technique is used to obtain the desired result of low following error. This technique is called velocity feed-forward. Since the velocity of the platen is proportional to V/h and since V/h is one of the input signals to the system, there is a prior knowledge of the servo velocity. Advantage is taken of this knowledge by adding the V/h signal to the rate loop summing point. This signal forces the servo to run at the correct velocity, and the position loop reduces the following error to nearly zero. In effect, the feed-forward technique acts like an integral network, but it eliminates the problems associated with the network.

(3) Shutter Servo

The shutter servo is a digitally-controlled servo (see Figure 2-59) which synchronizes in velocity with the intervalometer and in position with the platen reference signal. The reference and feedback signals are summed in the digital circuits. The error is converted to an analog signal which is amplified to activate the drive motor.

The signal summing point is the up-down counter which operates in a velocity mode and a phase mode. In the velocity mode, the reference signal gate opens and the $N_1 \times 2^N$ ppr pulse train from the intervalometer encoder counts up for a fixed time interval. Then the input gates are switched so that the pulse train from the shutter encoder counts down for the same amount of time. The count remaining at the end of the interval is proportional to the velocity error of the shutter servo. This error is stored in a buffer register which holds it until the next sample period. The error number is converted to an analog voltage which is amplified to the power level required to control the shutter. After the error is transferred to the buffer, the counter is cleared and the cycle repeats. The servo forces the motor to drive the encoder at a speed N_1 times as fast as the intervalometer in order to make the rates of the two pulse trains equal.

In the phase mode, the synchronization pulse from the shutter encoder inhibits the velocity command, clears the counter, and opens the gate for the shutter encoder $N_1 \times 2^N$ pulse train. This pulse train counts down until the sync pulse from the zero cross-over detector arrives and closes the gate. The number in the register is proportional to the phase difference between the platen reference and the shutter. As before, the number is stored in the buffer and handled as usual. After the two sync pulses have been compared, the counter is cleared and returned to the velocity mode. The digital circuits are regulated by the sync control logic circuit which, in turn,

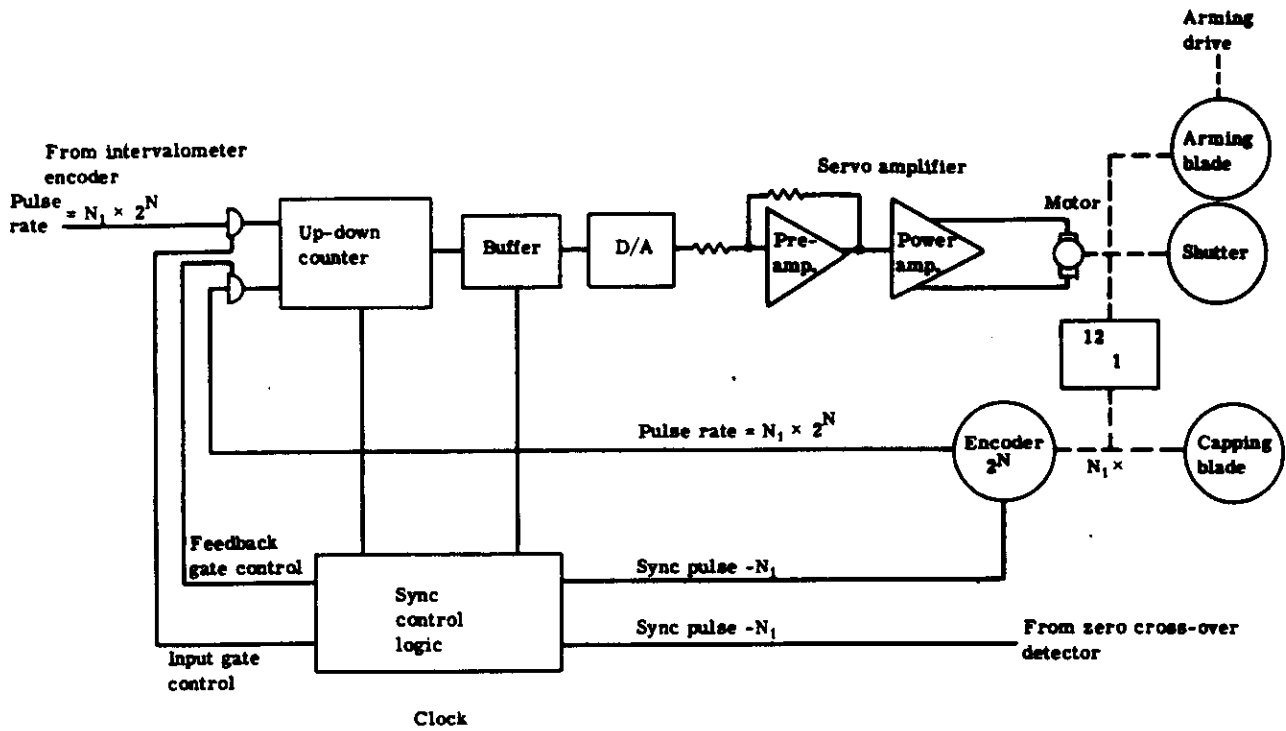


Fig. 2-59 — Shutter servo schematic

~~SECRET~~

is controlled by the clock signal. The phase loop is inhibited until the velocity error approaches null. At that time, the phase loop goes into operation and jogs the shutter until it is in the correct phase relationship.

The analog portion of the loop consists of a servo amplifier and a dc torque motor. Both items are similar to those described in the discussion of the platen servo. Note that the motor drives the main shutter blades directly, whereas the encoder is located at the capping blade. The capping blade is the element which is actually controlled, since its position determines when an exposure can be made.

The shutter servo is essentially a steady-state system. Once the servo is in both phase and velocity synchronization, the command signals will vary at a very slow rate (probably many minutes between distinguishable changes). However, the servo must overcome one severe problem. Just prior to exposure, the arming blade is switched from its standby position to its exposure position. The reaction torque from this motion tends to make the shutter change phase at the very moment when the phase error is most critical. Several approaches have been considered to suppress the arming transient. First, the inertia at the motor can be increased so that the magnitude of the reaction torque will be reduced. Second, the servo gain can be increased to improve the servo torque-stiffness. Third, the frequency response of the servo can be shaped to provide maximum possible attenuation at the frequency of the transient. All three techniques are incorporated in the design of the shutter servo. The result is a high gain, but low bandwidth system which resists all attempts to move it from its steady-state condition.

If there is a large change in the input signal (such as at startup), the servo saturates and the response of the servo is a function of the motor load time constant. The system is designed to reach maximum operating speed from standstill within one frame interval.

(4) Fiducials and Data Block

The fiducials comprise the optical/photographic time-base reference on the film. That is, the fiducials are projected onto the film from a very precisely fixed optical reference base at the exact midpoint of exposure of the shutter, and without regard to the actual position of the platen traveling in IMC.

The position of the projected fiducial image relative to the principal optical axis is maintained to within micron accuracy.

At the same time (midexposure), the signal from the shutter photocell circuit used to trigger the fiducials interrogates the system clock and the frame counter to publish the time and frame number. This data is imaged on the film by means of a light diode array. The light diode array has a mask on its frame and contacts the film, properly spacing the array. The array frame is spring-loaded to press on the film and lift off during film indexing. The light diode array has a capacity of 576 bits (see Section e., Data Recording System).

The two fiducial projectors each consist of the following principle components: an EG&G miniature strobe flash bulb and electronic unit, a condenser lens, a neutral density filter, a folding mirror, a fiducial grid projecting slide, a Bausch and Lomb (B&L) microscope objective, a target focusing device, and supporting tubes and structures necessary to maintain the extreme dimensional stability of this unit.

~~SECRET~~

The undersurface of the glass platen is relieved in the immediate vicinity of the microscope objectives to provide the necessary clearance for same. A 1-millimeter thick optically flat window is cemented over the clearance hole in the platen in this same area. The upper surface is in precisely the same film-supporting plane as the platen. The fiducial image is projected through this glass window onto the film.

Each of the projectors are rigidly tied to the upper end of the lens cell. Even though these projectors extend into the circular aperture of the main lens, this does not affect the principal photography in any way, as this is outside the rectangular format.

Figure 2-60 is a schematic of the terrestrial camera fiducial marker. Since two fiducial marks are required on the film at the time of midexposure, two independent optical systems are used.

A xenon strobe lamp serves as a light source. A 0.75-inch diameter, 1.07-inch focal length condenser system forms the image of the xenon arc source directly on the first element of a 6× microscope objective. The arc dimensions are approximately 0.3 by 0.1 inch, with the condenser located 1.4 inches from the source. The image formed 5.2 inches from the condenser is magnified by 3×, just enough to fill the entire microscope objective aperture with light. A neutral density filter is placed immediately in front of the condenser, and in front of the filter is the fiducial area mark consisting of crossed-hair lines approximately 15 microns wide formed on a glass plate 0.75-inch in diameter and located carefully in the object plane of the microscope objective. The microscope objective is a 6× B&L device having a working distance of 6.2 millimeters and a tube length of 160 millimeters. Because of the platen thickness and conjugates chosen for the objective, the working distance and the tube length of the objective are changed to accommodate the dimensions shown in Figure 2-60. The image formed is reduced in size by a factor of approximately 6, giving a 3-micron fiducial image. Given sufficient illumination, the 0.125-inch diameter ring containing the fiducial mark is easily located on the film. The exposure is sufficient to raise the density of the fiducial mark to a density of 1.0 above gross fog.

From the D-log E curve for EK4400 film processed for 9 minutes in D-19 developer at 68°F, the exposure required to obtain a density of 1.0 above gross fog is 0.05 meter-candle-second. The source (lamp) selected to produce the desired density in a 100-microsecond pulse-width is the xenon miniature flashtube.

Several possible lamps were considered. It was found that tungsten lamps required a mechanical shutter to obtain the 100-microsecond exposure, and luminescent diodes, such as the Fairchild FLC-100 and neon glow lamps, were too weak and the subsequent exposures required were much too long.

Considering the EG&G FX-31 miniature xenon flash tube in series with the optical system shown in Figure 2-60, the following characteristics are obtained:

1. Luminous efficiency: 2 lumens/watt
2. Maximum energy output: 0.2 watt/second
3. Distance (source to condenser): 1.4 inches = 3.56×10^{-2} meters
4. Percent transmission: 70 percent
5. Microscope demagnification: 6×
6. Condenser efficiency: 28.1 percent

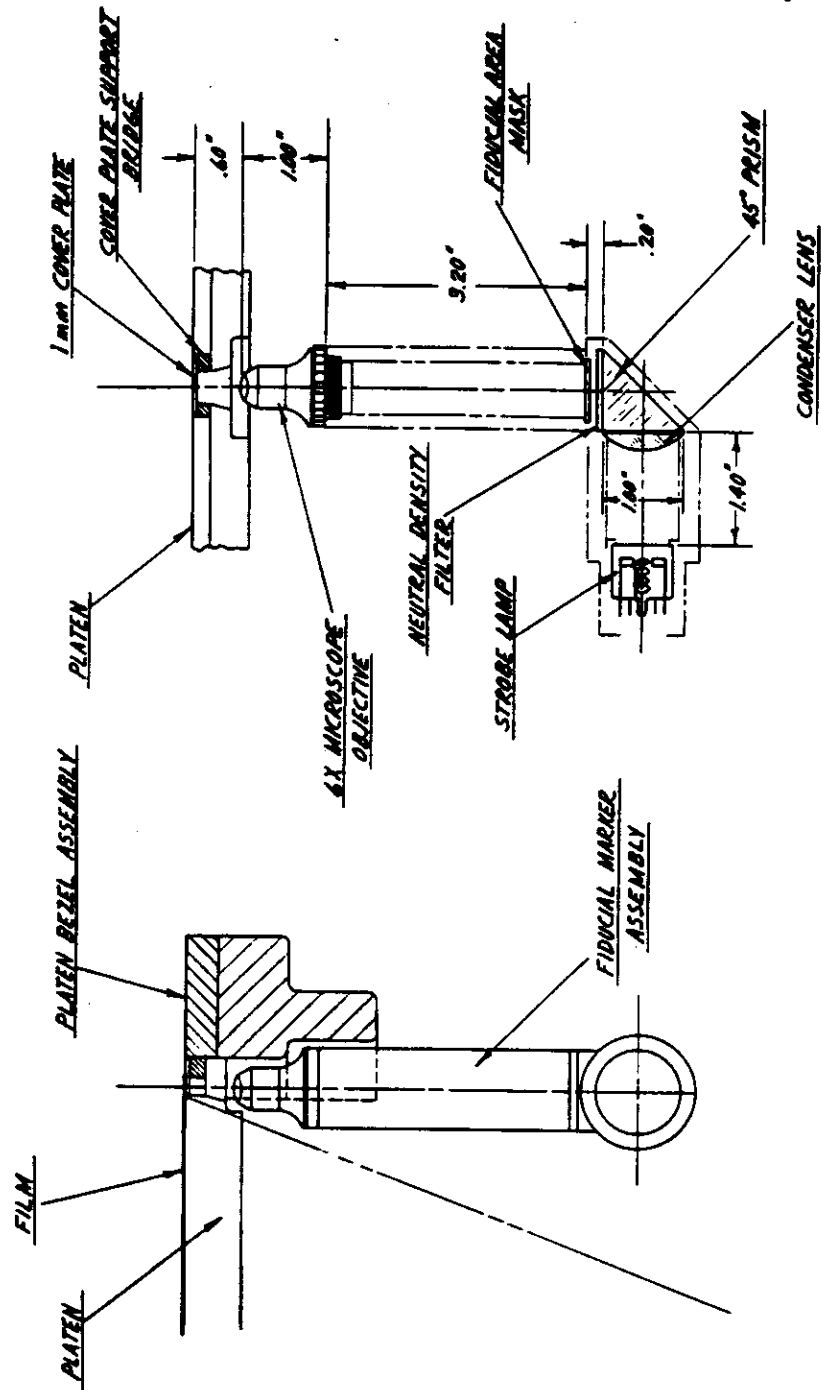


Fig. 2-60 — Terrestrial camera fiducial marker

$$\frac{2 \times 0.2 \times 0.7 \times (6)^2 \times 0.281}{4\pi \times (3.56 \times 10^{-2})^2} = 177 \text{ meter-candle-seconds}$$

Since only 0.05 meter-candle-second is required, a filter of 0.05/199 or 0.028 percent transmittance is necessary. A filter of 3.56 neutral density is used to reduce the light output.

The nominal life of this flashtube is approximately 10^8 flashes and the nominal duration of 1/3 peak at maximum input is 12 microseconds.

(5) Calibration

At predetermined intervals during the mission, the system is operated to gather photographic data that may subsequently be used to determine if in-flight changes in camera calibration have occurred, and to measure the extent of such changes.

The calibration intervals are established by splicing EK2475 recording film into the terrestrial camera film web with magnetic splicing tape. The camera system has a magnetic pickup that detects the approach of the splice to the terrestrial camera exposure area. When the programmed splice mark is detected by the pickup, the programmer is triggered to roll the vehicle so that both cameras (terrestrial and stellar) target on star-field areas, and the exposure speed of the terrestrial camera is varied so that its relative exposure is the same as that of the stellar camera.

When the roll/maneuver has been completed, both cameras are operated to make star-field exposures. This sequence continues until the magnetic pickup detects the splice that signifies the end of the calibration emulsion. The signal thus generated triggers the programmer to interrupt the calibration sequence, roll the vehicle back to its conventional flight attitude, and readjust the terrestrial camera exposure system for normal terrestrial photography.

Pre-mission planning of the location of the calibration emulsion in the film web will preclude the possibility of a coincidence wherein the calibration emulsion enters the camera during the cutdown operations; however, a safety override circuit is included in the system to make it impossible for the calibration mode to interrupt either of the cutdown modes.

2. Stellar Camera

This section describes the subsystems of the stellar camera which are illustrated in Figure 2-61.

a. Lens

The stellar camera employs two lenses for photogrammetric considerations. The lens chosen is a Wild Falconar that requires modification to accommodate a glass reseau.

Lens particulars are as follows:

1. Focal length: 250 millimeters (nominal)
2. f/number: f/1.8
3. Full field: 25 degrees
4. Format: 3.65 by 2.25 inches
5. Filter: none
6. Platen: 6-millimeter thick reseau with one centimeter spacing

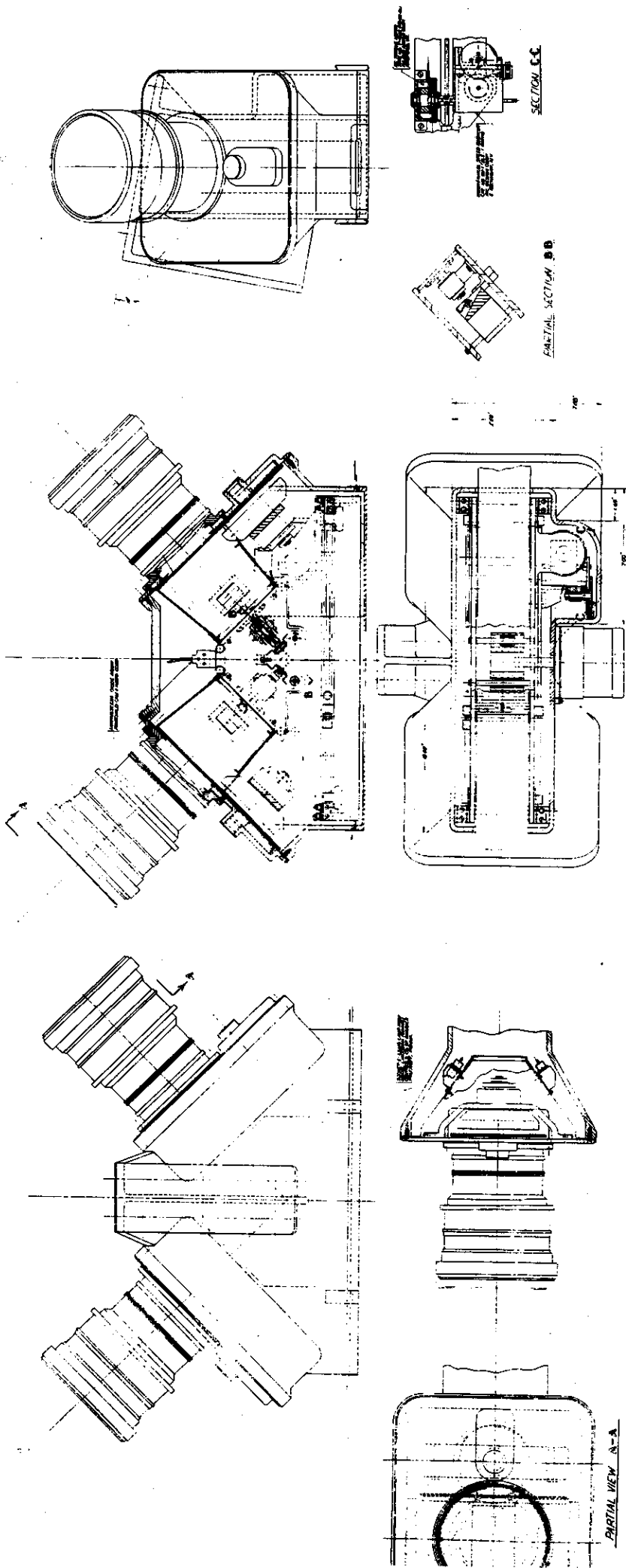


Fig. 2-61 -- Stellar camera configuration

~~SECRET~~

~~SECRET~~

7. Number of elements: 6
8. Shutter opening: 3.6-inch diameter (not at aperture)
9. Weight (with new cell): approximately 10 pounds

This lens is slightly modified for use with a 6-millimeter reseau, and in the course of redesign, the standard iris aperture stop is deleted and the elements remounted in a one-piece cell assembly. The stellar camera shutter is repositioned from the aperture location to a position between the rear element and the focal plane. Normally, this would cause image vignetting, but the system images stars over a 0.200-second exposure period, and the shutter opening and closing time is within 0.030 second. As such, only the trails of the star tracks may show the effects of vignetting.

Both lens cells are mounted to a common framework. Each cell is mounted by its base flange to a mounting plate. The reseau is mounted in a bezel and the bezel is mounted to a "stovepipe" or light, conical structure. The base of this plate is attached to the opposite side of the mounting plate. This makes a modular lens assembly that is removable from or assembled to the camera without disturbing internal alignment. The modular shutter assembly is then fixed to the mounting plate.

b. Platen and Pressure Mechanism

The platen for each lens is a 6-millimeter thick glass plate mounted in a bezel which is fixed to a metal cone mounted to the lens. The film is pressed on the platen by individual pressure pads; however, they are actuated by a common mechanism driven from a motor. The pressure mechanism consists of wedge cams, ball bearing followers, and a torque motor-driven linear actuator similar to those used on the spool brakes and terrestrial camera platen pressure mechanism. A low durometer (15) silicone rubber is used as a pressure plate facing. The platen plate has a one centimeter reseau grid on its surface which serves not only for film shrinkage control but as the camera fiducials.

c. Fiducials

When photographing a star field, there is no ambient or background light (as in the case of terrestrial photography) to image the reseau grid on the film. Reseau grid illumination is performed artificially by a pair of lamps in each platen support cone which will bounce light off the back of the shutter blades. The backs of these shutter blades will be painted white to achieve an even distribution of light. The control signals will energize the lamps just prior to a stellar exposure.

d. Shutter

The stellar shutter is a two-blade leaf type shutter whose blades open in opposite directions to provide a clear aperture for film exposure. Opening and closing times are on the order of 0.030 second; exposure time is on the order of 0.200 second with a minimum efficiency of 85 percent. A feature of this shutter is that all reaction is designed to be absorbed within the shutter itself. This is accomplished by regulation of the motor voltage and by attaching the stator of the motor to one shutter blade and the armature to the other, and using action-reaction of the motor itself to actuate the shutter. Position control for the blades is ensured by mechanical synchronization through a gear train.

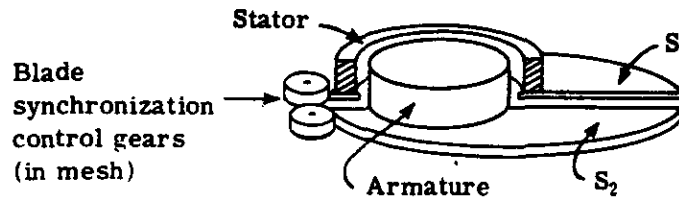
~~SECRET~~

The stellar shutter is a modular assembly interfaced with the stellar camera support structure so as to position the shutter blades immediately behind the rear lens element.

e. Operational Sequence

The principle of action-reaction is employed. Generally, reaction is minimized. In this design, the reaction is as significant as the action which caused it. This is illustrated in detail in Figure 2-62.

The general configuration of the stellar shutter is diagrammed below.



The top blade of the shutter is attached to the stator of the motor, which is on support bearings. The armature of the motor is also on support bearings and is connected to the lower shutter blade S₂. The inertias of the stator and top blade and support are closely matched to that of the armature and lower blade and support, resulting in matched acceleration rates and minimizing unbalanced forces.

To actuate this shutter, voltage regulated power is supplied to the motor brushes. The resulting electromotive forces developed by the motor cause equal and opposite torques to be applied to the stator and the armature of the motor, causing them to counter-rotate out of the lens aperture. By correctly matching the torques developed by the motor and the inertias of the various parts, the shutter blades accelerate in opening times of less than 0.030 second.

The motor selected is an Inland torque motor T-2950, with the following characteristics.

1. Inertias of armature: $J_A = 320(10^{-6})$ pounds inch-second²
2. Inertias of stator (assumed): $J_A = 320(10^{-6})$ pounds inch-second²
3. Inertia of blade (calculated): $J_B = 1223(10^{-6})$ pounds inch-second²
4. Peak motor torque: 1.2 pounds per foot, or 14.4 pounds per inch
5. Factor for back EMF: $f = 2$

The equation for motor acceleration is actually a second-order differential equation, but because of the short times involved, it is approximated by the following.

$$\ddot{\theta} = \frac{T_P}{f(J_T)}$$

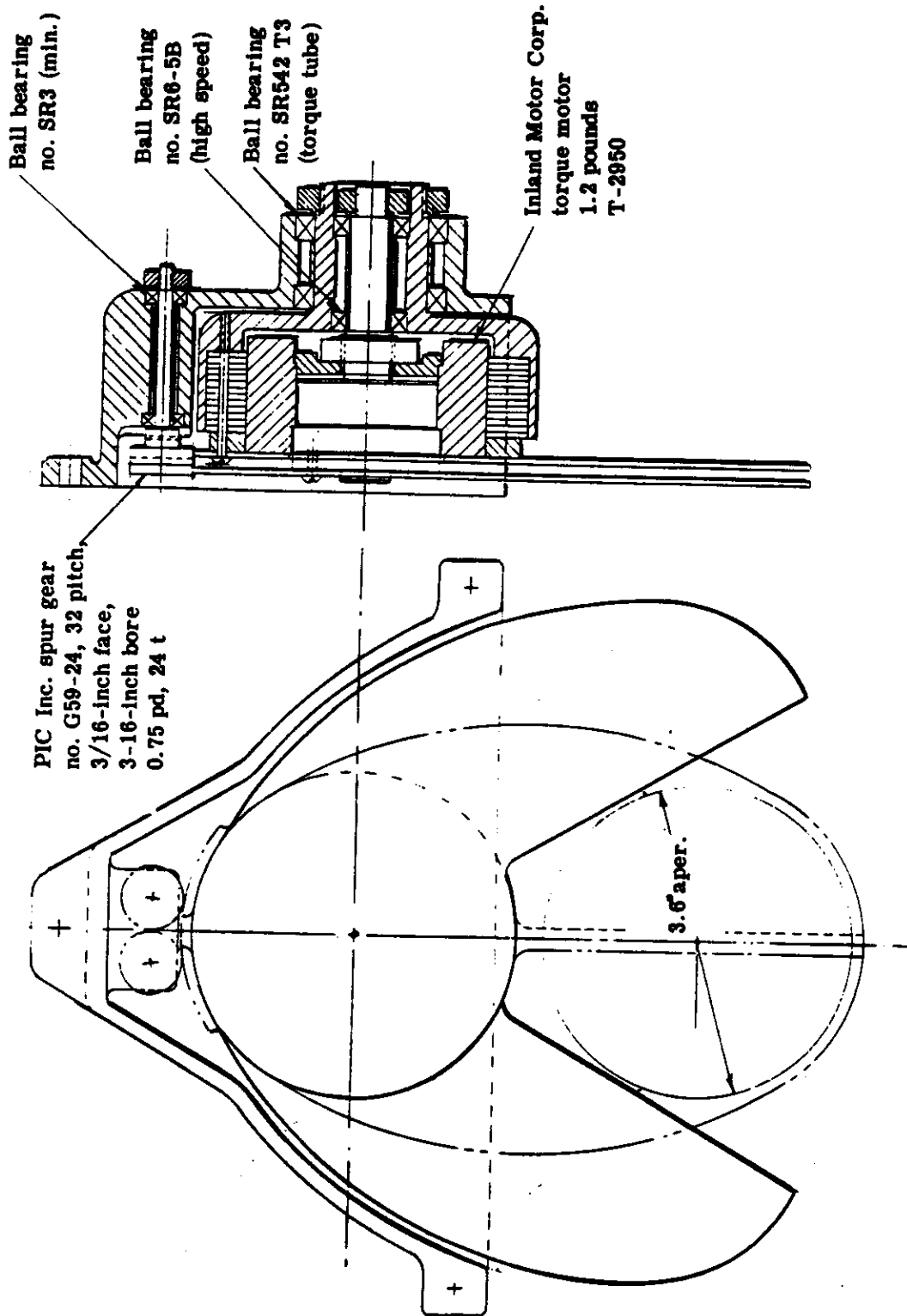


Fig. 2-62 — Stellar shutter

~~SECRET~~

where $J_T = 2J_B + J_A + J_S$

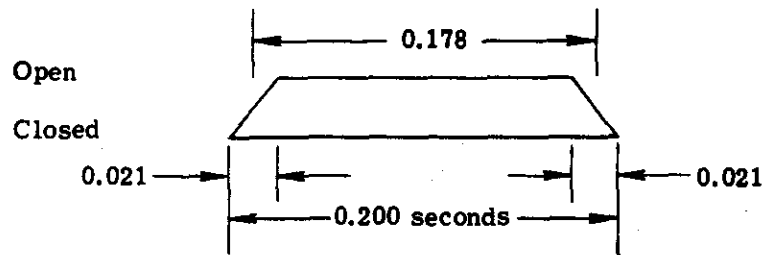
$$\ddot{\theta} = 14.4/(2)(3080)(10^{-6}) = 2340 \text{ rad/sec}^2$$

$\theta = 60 \text{ degrees} = 1.05 \text{ radians} = \text{included angle of opening or closing}$

$$t^2 = \frac{\theta}{\ddot{\theta}} = \frac{1.05}{2340}$$

$$t = 0.0212 \text{ second}$$

The efficiency for this shutter is approximated using the following diagram.



Therefore, the efficiency equals

$$\frac{0.179}{0.200} = 89 \text{ percent}$$

To prevent the motor from maintaining acceleration until stopped, the current and consequently the torque is reversed halfway through the cycle. This causes the velocity of the mechanism to be at zero when at the stop position. At this point, the motor again reverses, but at a reduced voltage level, holding the motor open and firmly against the stops during exposure. At the end of exposure, the cycle is reversed, closing the shutter. Again a low level bias voltage holds the shutter closed. During long periods when the system is inactive, any bias voltage to the secondary shutter mechanism will be shut off with the closing of the exterior thermal shutter of the stellar lens system.

To ensure that the shutter blades open as required, a mechanical synchronization control in the form of a gear train is part of the basic mechanism.

The train is designed so that one gear is engaged with one shutter blade and with the other gear. The other gear is engaged to the second shutter blade. This system provides that, if one shutter blade moves, the other shutter blade has to move through an identical angle but in the opposite direction. The advantages of this system are:

1. The shutter blades must move through identical angles and in opposite directions.
2. The shutter blades must open and close with reference to a fixed centerline, in this case the aperture centerline.
3. Slight differences in the inertia balancing of the shutter blades are allowable.

~~SECRET~~

The various elements which make up the stellar camera shutter have been analyzed for their strength properties. All elements were found to be well within the generally accepted limits of these materials.

f. Motor Selection

Selection of a motor for this shutter requires consideration of the motor inertia itself. As the power requirements increase, so do the motor inertias. It is possible for this consideration to increase rather than decrease opening times. The motor selected, the Inland torque motor T-2950, is based on the maximum acceleration available. Figure 2-63 depicts the acceleration rates of the motors considered.

g. Reliability Considerations of Stellar Shutter

The stellar shutter is designed to have as few parts as are necessary for reliable operation. However, the operational environment will require that the choice of materials and lubricants be made carefully.

The gears associated with the synchronized control of the shutter blades will be made from 416 and 440C stainless steel with dry film lubrication. Loading of the gears will be dependent upon the degree of inertia unbalance of the shutter blades and motor components. The gears will experience very light loading. Therefore, it is expected that the gear life should exceed 10^7 to 10^8 load cycles.

The bearings used in the stellar shutter to support the feedback control gears and to support the motor elements will have life in excess of 30,000 hours. The bearings supporting the motor elements will only rotate through an angle of 30 degrees. This means that the ball bearing in the smaller bearing race will make one revolution. This will be adequate for dry film lubrication but will be a problem for other lubrication methods. All bearings used in this shutter mechanism will have dry film lubrication for high reliability.

The motor elements used in the stellar shutter mechanism are designed to operate in this environment. Therefore, the life expectancy of the selected motor should be excellent.

3. Film Transport System

The film transport system includes the transport subsystems for both the terrestrial and the stellar cameras. These transport subsystems contain the supply and takeup film supply reels, shuttle mechanism, film index rollers, and electrical control systems. The supply reels are housed in the DCM structure, while the takeup reels are located in the recovery section. The supply reel of each transport is initially loaded with its full film capacity (21,300 feet of 9 1/2-inch wide film for the terrestrial, and 10,020 feet of 70-millimeter film for the stellar).

The servo systems for the supply reels consist of open-loop reverse torque controls and closed-loop tachometer rate servos. The reverse torque control sensor is a trimpot. The takeup reel drive system contains a similar trimpot, and both of these are adjusted during final systems assembly and test to provide a resultant film tension of four pounds for the terrestrial camera and two pounds for the stellar. The tachometer closed-loop rate servos have potentiometer adjustments that are set during final systems assembly and test to provide the required film velocity of 19.14 inches per frame for the terrestrial and 9.0 inches per frame for the stellar.

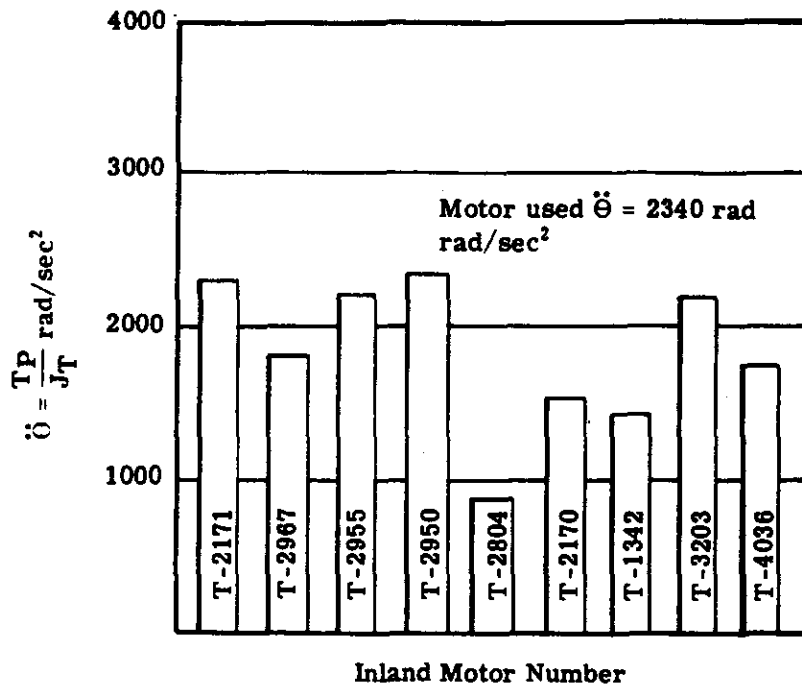


Fig. 2-63 — Acceleration rates of stellar shutter motors considered

~~SECRET~~

The reverse torque bias signal and the tachometer rate signal are fed to the input summing point along with V/h signal, and, after amplification, the resultant signal is used to drive the supply torquers.

The system intervalometer provides the V/h command signal to control the supply reel angular velocity rate.

As the film leaves the supply reel at a constant linear velocity, it is fed to the transport shuttle mechanism which provides a film storage capability within each cycle. The mechanism rides on guide tracks and derives its driving power from the takeup reel and index roller. The same amount of film is continually fed into the shuttle as is continuously extracted by the driven takeup reel. During the frame period, with the exception of the two-second "index" pulse, the shuttle mechanism accumulates film on the supply reel side. During the two-second "index" pulse, the accumulated film is transferred by the driven index roller to the takeup side of the shuttle.

a. Terrestrial Camera Film Transport

The function of the terrestrial film transport is to move 19 inches of film through the platen and the pressure plate during the "platen unlock" portion of the cycle (3 seconds). The amount of film moved is established by the 3.02-inch diameter of the index roller which is driven by a two-turn step motor. The transfer occurs once in each frame period upon command from the system intervalometer. A functional block diagram of the terrestrial film transport (Figure 2-64) shows the major electrical and mechanical components included in the present transport design. Design criterion includes the minimization of electrical power and the resultant thermal dissipation and size, and the consolidation of the supply/metering function into the supply reel servo system.

(1) Fixed Parameters

The following fixed parameters are established:

1. Supply reel core diameter: $6\frac{3}{8}$ inches
2. Film supply reel outside diameter: 32.96 inches
3. Weight of total film supply: 371 pounds
4. Frame length: 19.14 inches
5. Takeup reel core diameter: $3\frac{1}{8}$ inches
6. Film takeup reel outside diameter: $23\frac{1}{8}$ inches (2 reels required)
7. Weight of total film (takeup): 185 pounds per reel
8. Gear ratio between drive torquers and reels: 25/1
9. Film tension: 4 pounds
10. Frame time: $14\frac{1}{2}$ to 22 seconds per cycle
11. Primary power available: ± 28 vdc (unregulated)

(2) Selected Components

The following components are established for the terrestrial camera film transport:

1. Supply reel torquer: IMC T-2171D
2. Supply reel amplifier: ICC Model-50A
3. Supply reel V/h amplifier: Nexus CDA-3a

~~SECRET~~

4. Supply reel tachometer: IMC TG-2102
5. Two takeup reel torquers: IMC T-2170B
6. Takeup reel amplifier: ICC Model-50A
7. Index roller stepper motor: not as yet chosen

(3) Control Signals

Control signals required for the terrestrial film transport are as follows:

Signal	Source	Form
Index	Intervalometer	Contact closure
Unlock	Intervalometer	Contact closure
V/h	Intervalometer	Analog voltage
On/off	Mode control	Contact closure
Reel brakes	Mode control	Contact closure
Film cut	Mode control	Contact closure
Calibrate	Mode control	Contact closure

(4) Shuttle Position Sensors

The shuttle position sensors include two microswitches placed so that they are activated when a preset level of position error is reached by the shuttle mechanism. During ideally operating conditions, the transport shuttle is driven back and forth within a travel distance of approximately 9.57 inches during each frame. Actually, during the normal operating cycle, the shuttle mechanism may gradually build-up position errors that will result in a position creepage toward either end of the shuttle track.

To compensate for the gradual build-up of shuttle position errors, the shuttle mechanism is designed to include position error sensors that switch on correction voltages that are fed to the input of the tach-rate-servo system. These correction signals are applied only when the linear cam or the shuttle depresses the microswitch positioned at either end. The correction signal is removed when the shuttle mechanism is leveled, and the cam releases the microswitches. This design allows for a discrete amount of correction within each frame, maintaining the correction steps until the error is removed.

b. Stellar Camera Film Transport

The function of the stellar camera film transport is to move 9 inches of 70-millimeter film during each frame. In this case, each frame of film will contain two 70-millimeter exposures and one data block exposure. The remaining operation and timing of the stellar transport is basically the same as for the terrestrial film transport. A functional block diagram of the stellar film transport (Figure 2-65) shows the major electrical and mechanical components.

(1) Fixed Parameters

The following fixed parameters are established:

1. Film width: 70 millimeters
2. Film thickness: 0.0032 inch
3. Frame length: 9.0 inches

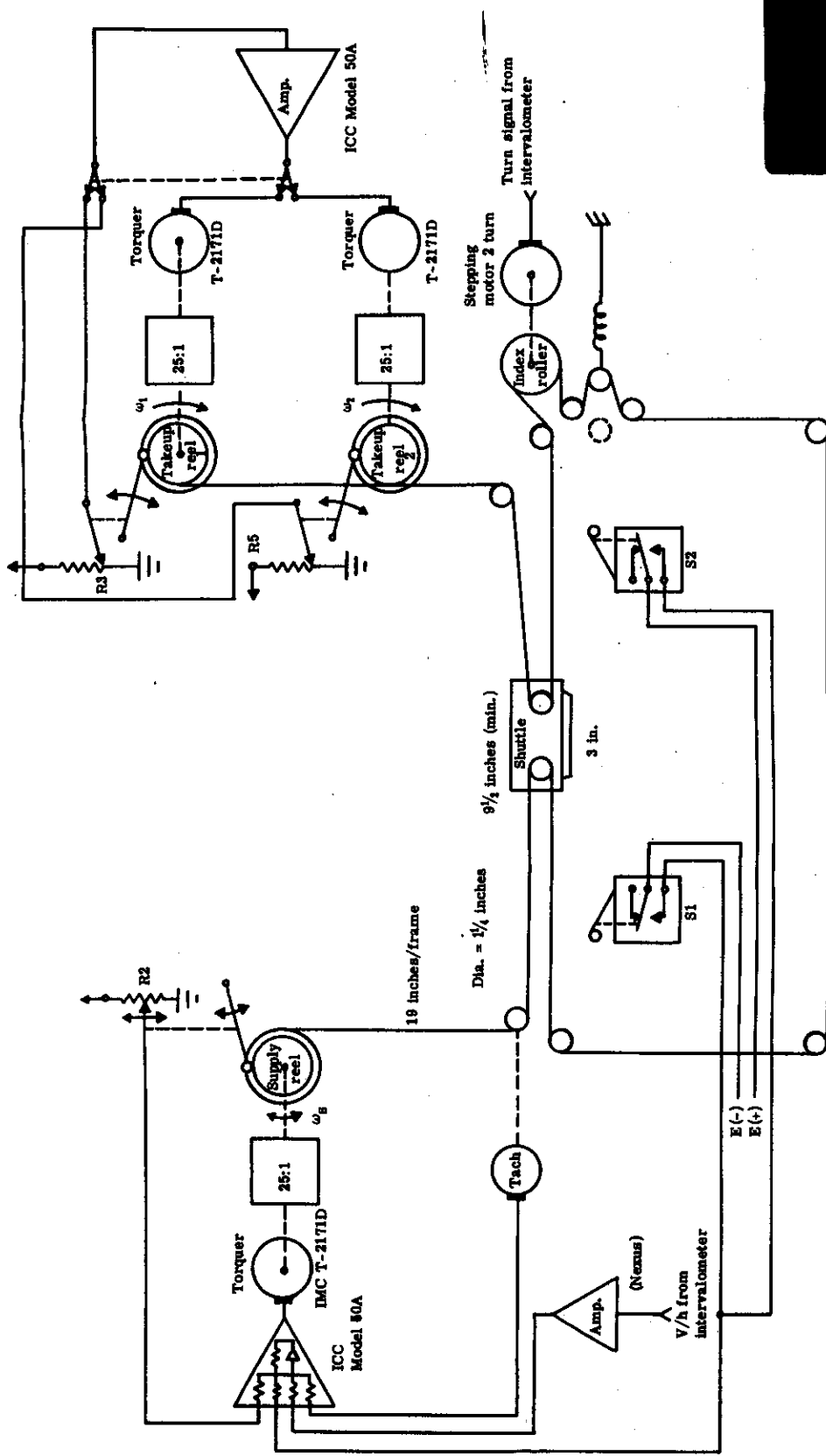


Fig. 2-64 — Terrestrial film transport system, block diagram

2-14A

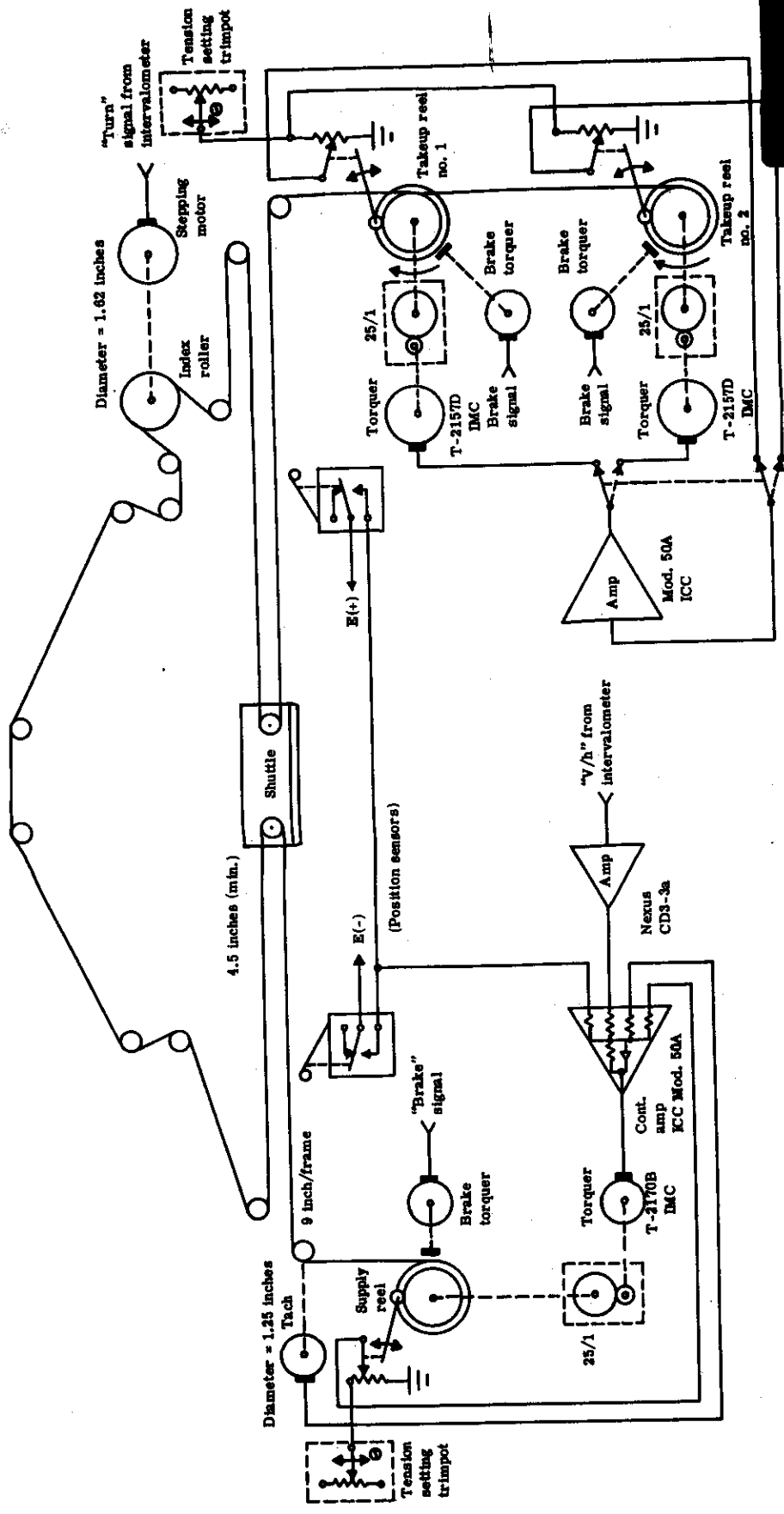


Fig. 2-65 — Stellar film transport system, block diagram

2051

4. Supply reel core diameter: 5.0 inches
5. Film supply reel outer diameter: 22.64 inches
6. Weight of total film supply: 50.0 pounds
7. Takeup reel core diameter: 3 ¹/₈ inches
8. Film takeup reel outer diameter: 16 ¹/₈ inches (2 reels)
9. Gear ratio between drive torquers and reels: 25/1
10. Film tension: 2 pounds
11. Frame time: 14 ¹/₂ to 22 seconds

(2) Component Selection

Component selection for the stellar film transport is listed below:

1. Supply reel torquer: IMC T-2170B
2. Supply reel amplifier: ICC Model-50A
3. Supply V/h amplifier: Nexus CDA-3a
4. Supply tachometer: IMC TG-2102
5. Two takeup reel torquers: IMC T-2157D
6. Takeup reel amplifier: ICC Model-50A

(3) Timing Control

The system intervalometer supplies the stellar camera with the same timing signals that it supplies to the terrestrial film transport. The timing and operation are identical with the exception of the major mode select function. The major mode selection is controlled by the intervalometer and is used to activate the various combinations of subsystems for each mode of operation.

(4) Shuttle Position Sensors

The only variation in the stellar film transport is the spacing of the microswitches. In this case, the microswitch spacing is 4.5 inches minimum. The operation of the shuttle position correction is identical to the terrestrial transport.

c. Supply Cassettes

Two films are used, namely, 21,300 feet of 9 ¹/₂-inch wide film weighing 371 pounds, and 10,020 feet of 70-millimeter film weighing 50 pounds. The two spools are mounted on a common structure which is removable from the DCM to facilitate loading, testing, and handling. The main film supply supporting structure is bolted to the longerons of the DCM. The bolting interface is provided with rollers which may be lowered in contact with the longerons, slightly elevating the massive structure, and enabling it to be easily withdrawn from the aft end of the DCM onto an adjacent ground handling dolly.

The spools are driven by a geared-down dc torque motor and timing belt. Sensor arms in contact with the outside diameter of the film roll determine the torque output of these drive motors. During launch or during extensive periods of non-photography, the flange clamping brakes prevent the spools from turning.

This overall assembly is shown in Figure 2-66. Details of the spool drives and spool brakes are shown in Figures 2-67 and 2-68.

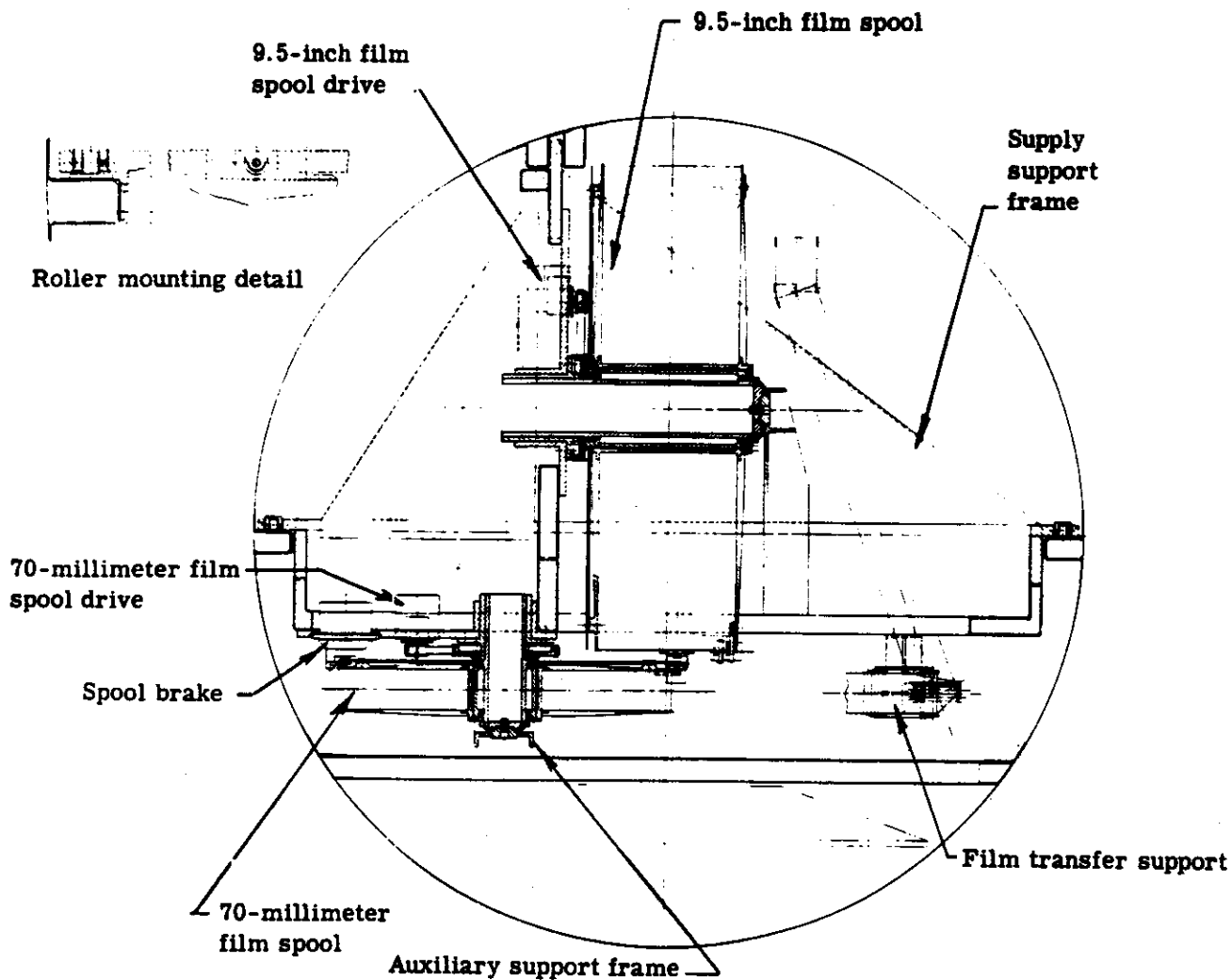


Fig. 2-66 — Supply cassette

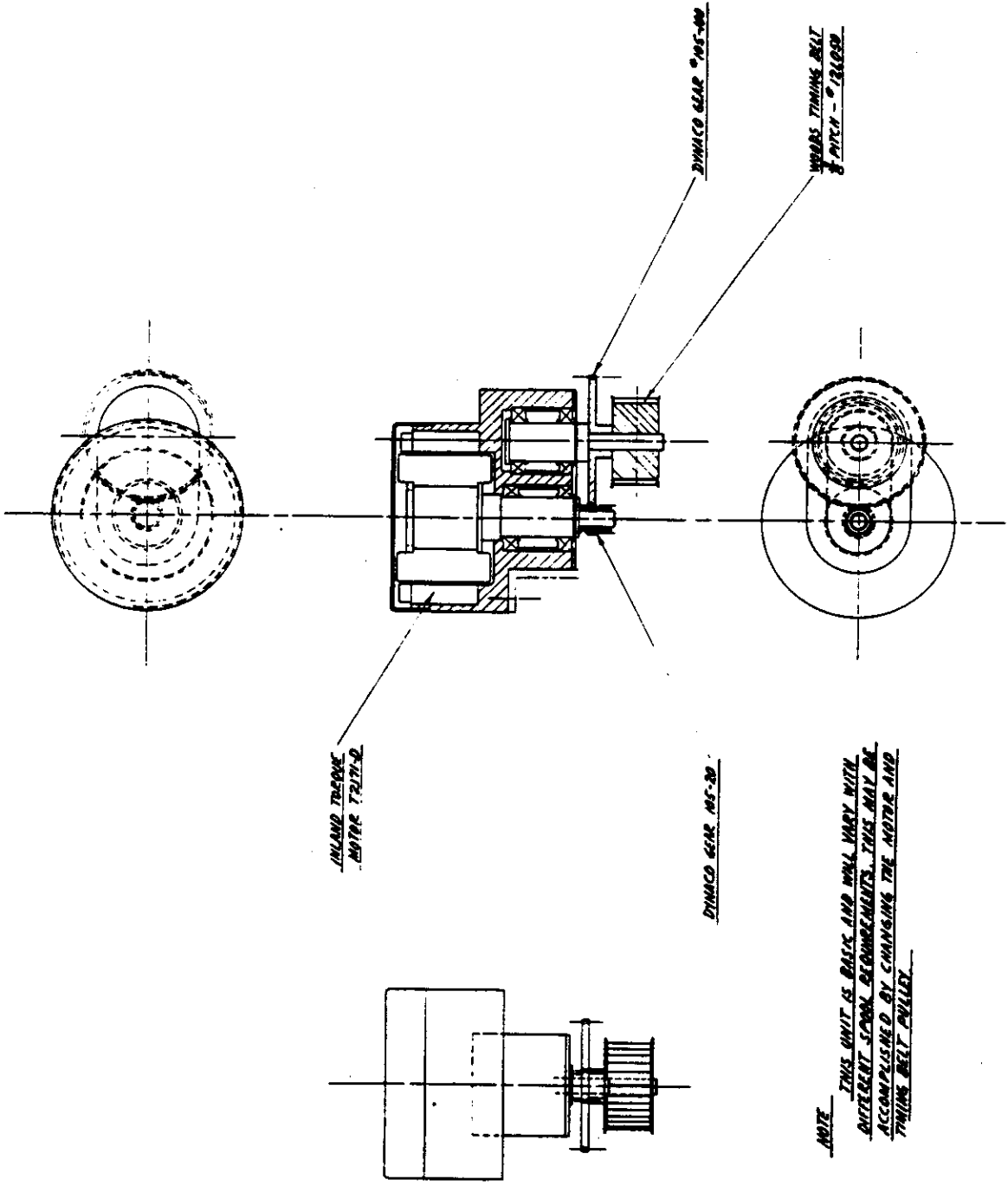


Fig. 2-67 — Spool power drive

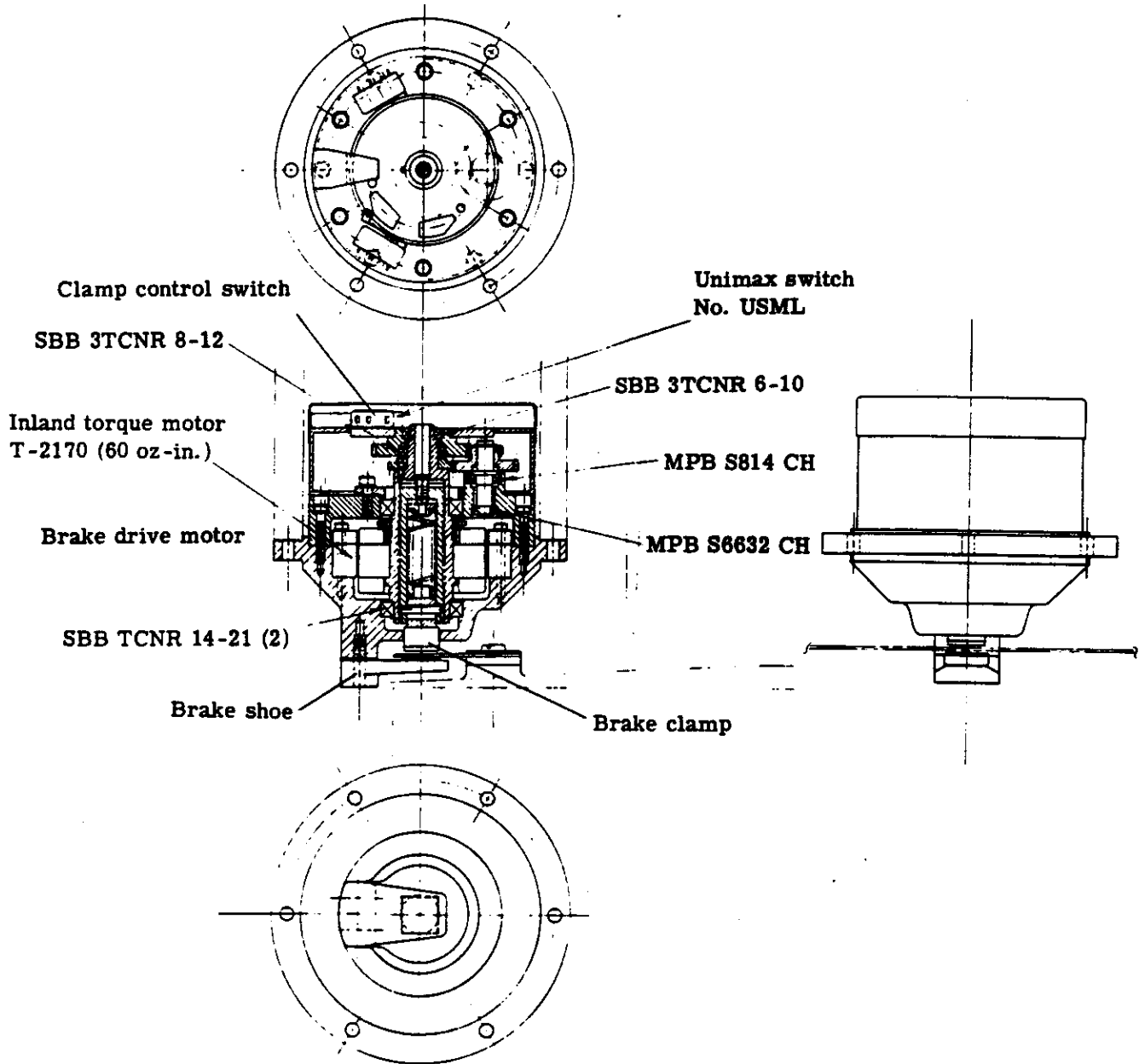


Fig. 2-68 — Spool brake system

d. Takeup Cassettes

The configuration of the takeup cassettes (see Figure 2-69) is basically determined by the compartment space within the RV and the recoverable weight limit. Each cassette has a 9 1/2-inch film reel and a 70-millimeter film reel, each having a capacity of half the mission supply. Each reel is mounted to a stationary spindle which is mounted to the cassette sides. Timing belt drives supply the reel torque from torquer drives through a 25:1 reduction ratio. The spools in the aft RV have a roller mounted in their cores so that the film path may pass on to the front RV.

The cassette side plates are the structural supports for the cassette and are bolted to the bulkhead of the RV. To these side plates the following components are mounted: spool drives, spool brakes, radius sensor arms, tape recorders, and the electronic packages for the RV control system (batteries, beacon controls, programmer, etc.).

The spool brakes clamp to rims on each spool to hold the spool stationary during non-operating periods.

At the post-mission processing station, the RV is positioned on its base. First the Marman clamp and tub structure is removed, and then the bearing caps are removed. This is followed by the slackening and subsequent removal of the two drive belts from the small pulleys. The sensor arms are then swung out of the way, and a web-type lifting sling approximately 9 inches wide is passed under the terrestrial camera spool and attached to a hoist. It is lifted sufficiently to withdraw the base structure and all associated parts. The knurled knob at the 70-millimeter film end of the shaft is then unscrewed and the 70-millimeter roll of film is slipped off. The knob at the other end of the shaft is then unscrewed, and the shaft and bearing assemblies are withdrawn from the spool. Both spools are now ready for processing.

e. Thermal Shutter

Thermal analysis (see Section 2.4.2) indicates that the front terrestrial lens element absorbs most of the incident infrared radiation. These same conditions exist for the stellar lenses. The visible light passes through and is absorbed and re-radiated by the shutter to adjacent lens elements. For a constant input flux, these adjacent elements would heat up, while the front element cools down, creating a system thermal gradient after a relatively short time period. This constant input flux would also create intolerable radial temperature gradients in the first lens element.

These conditions are reduced considerably by two design considerations: (1) the addition of a thermal capping shutter which opens for 2 seconds during the exposure period and then closes for the remainder of the cycle, and (2) a highly reflective coating on the outer surface of the first shutter disc (except around the aperture). To ensure system integrity, it may be necessary to provide heating elements on the shutter to artificially adjust its thermal characteristics.

Details of the thermal shutter assemblies for the terrestrial and stellar cameras are shown in Figures 2-70(a) and 2-70(b). The shutter consists of two semi-circular aluminum discs that are driven in a scissors action by a suitable worm gear combination. The free end of these discs is supported by a horizontal, circular track to minimize deflections.

Shutter motion is controlled by two cam-actuated limit switches and an electromechanical stop. Upon closure, the disk diameters butt against a soft rubber pad integral with one disk. Three of these shutters (two stellar, one terrestrial) are mounted to the DCM with a stiffened base assembly. Flexible, light-tight convoluted boots serve as a light seal between the shutter base and the objective end of the lens cell.

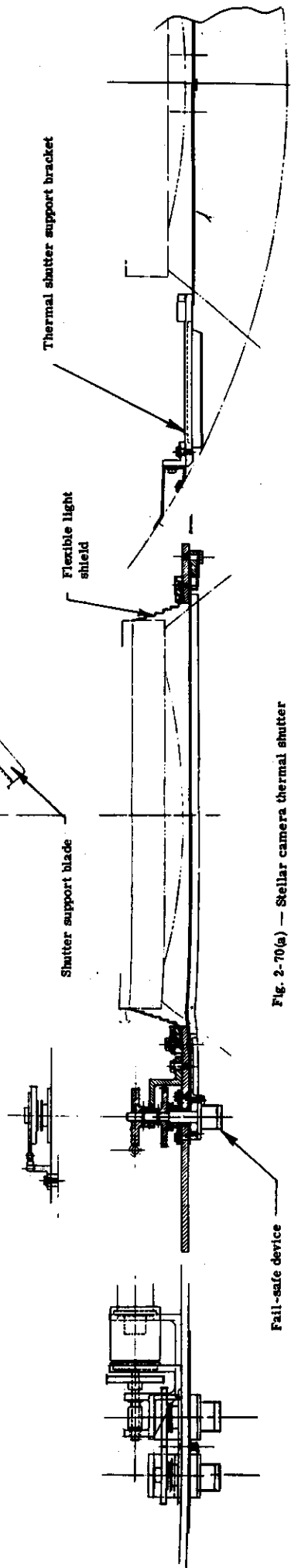
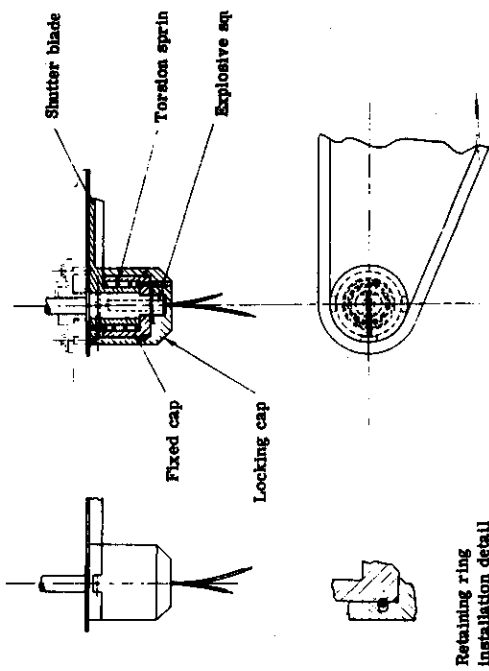
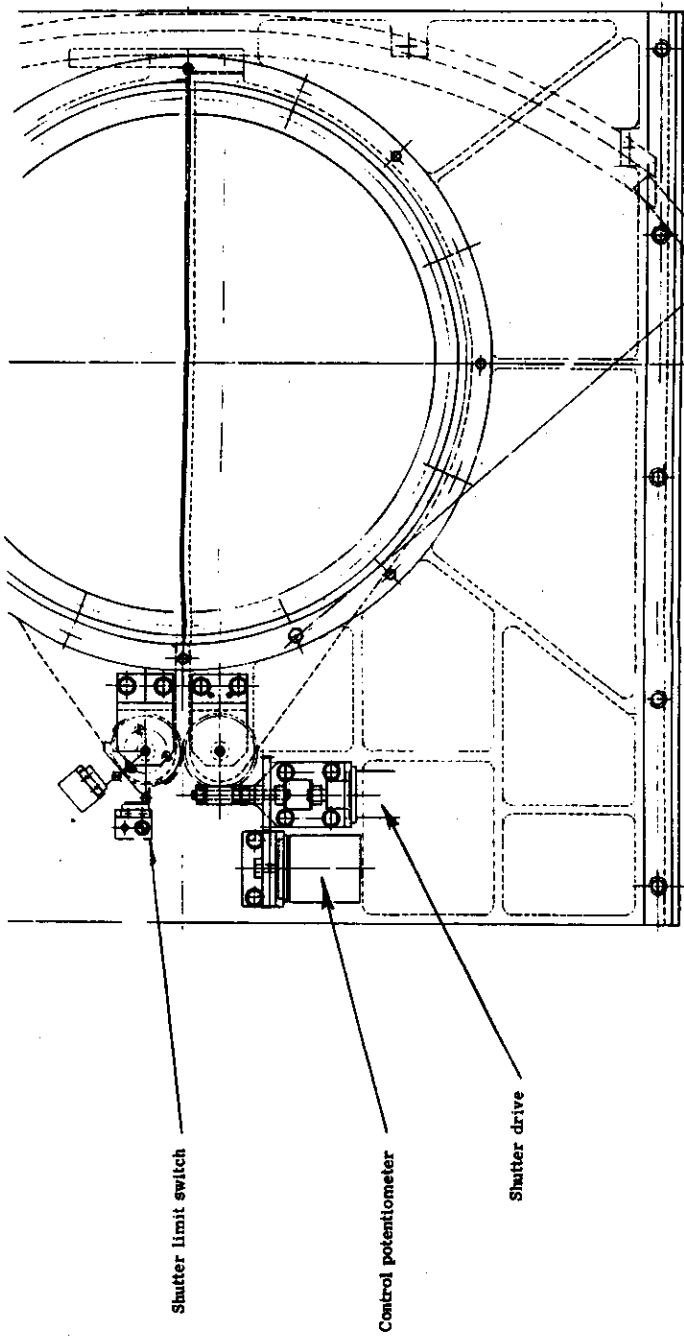


Fig. 2-70(a) — Stellar camera thermal shutter

SECRET

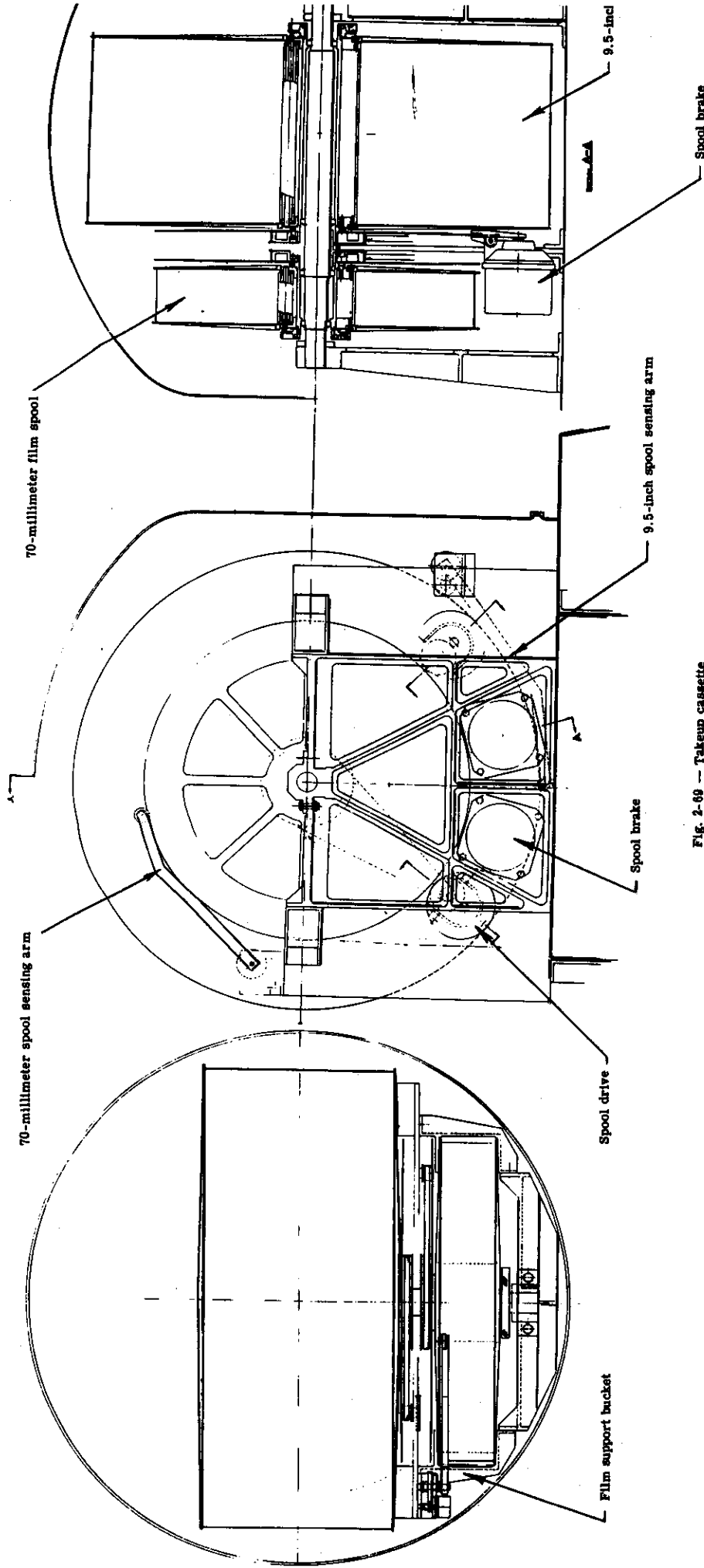
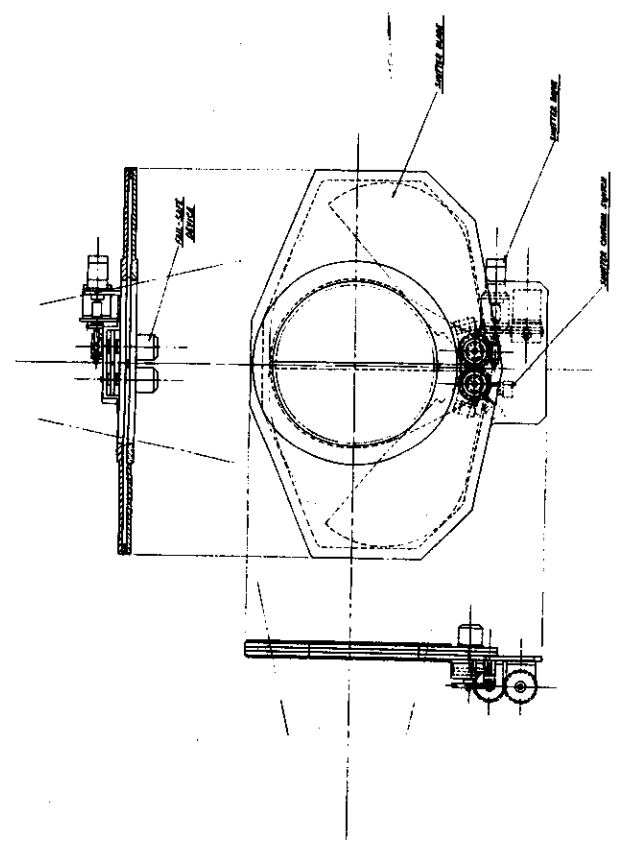
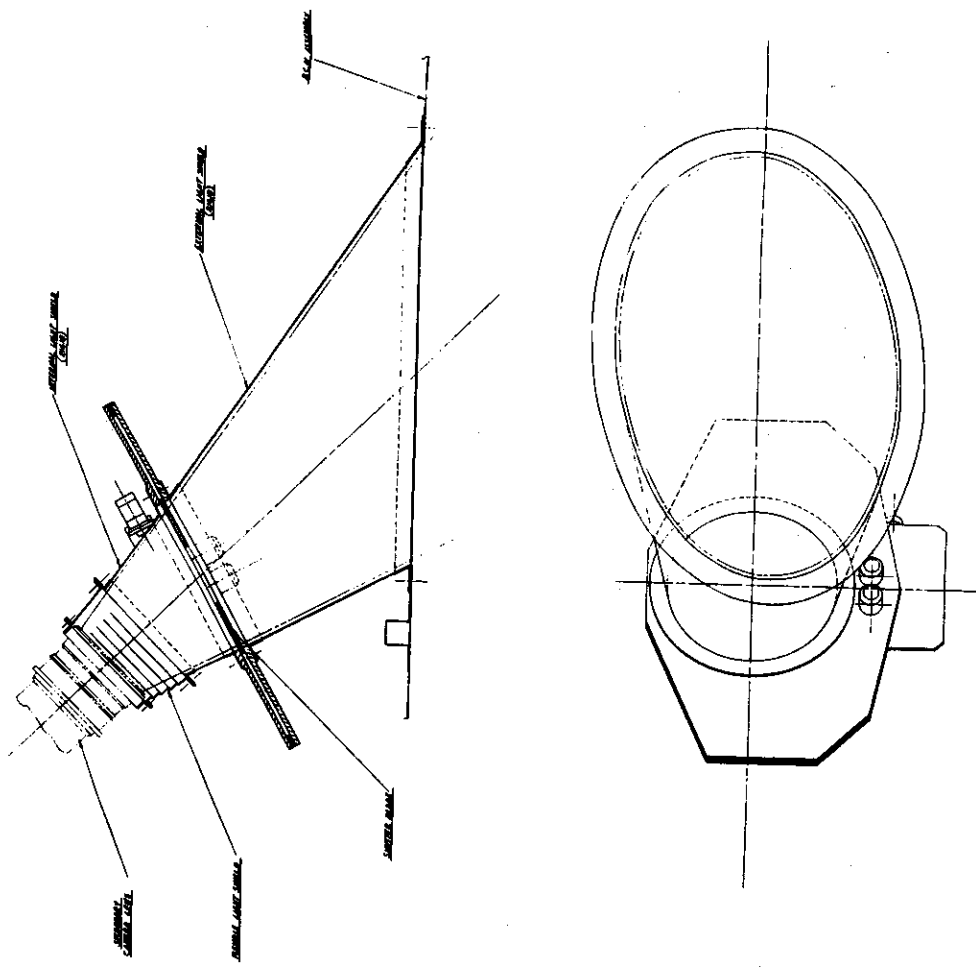


Fig. 2-69 — Takeup cassette

2-159

SECRET

~~SECRET~~



NOTE: THE OPERATIONAL POSITION OF THE SHUTTER IS SHOWN IN THE DRAWING. THE SHUTTER IS OPERATIONAL IN THE POSITION SHOWN IN THE DRAWING.

Fig. 2-70 (b) — Stellar camera thermal shutter

~~SECRET~~

Thermal shutters are, effectively, doors in the optical path. If one fails in the closed position, it prevents photography by its associated camera. Therefore, a "fail-safe" shutter has been developed, which, if it fails, can always be set to the open position. If a shutter fails in the open position, system thermal stability will be impaired, but photography will not be lost.

A device has been designed to replace the blade and shaft joint to provide a fail-safe feature. The blade shaft drives the blade through a key, collar, and a preloaded torsion spring in that order. A plastic cap holds the key in place axially and a pyrotechnic squib is placed under the key in a cored-out section of the shaft. When the telemetry system detects that a thermal shutter is not operating after a few cycles, a command is given to fire the squibs. The firing of the squibs blows off both the key and plastic cap unlocking the blade from its shaft. The preloaded torsion springs then open the blades, regardless of the position that they were stalled in, and permit photography, but under less ideal thermal conditions.

4. Control Mechanization and Module Description

This section describes the electromechanical instrumentation and the functional logic required to implement the photographic modes of operation. These modes are summarized in Table 2-18, and a detailed system description is given in Section 2.3.2.1.

Terrestrial and stellar camera operation to implement the operational requirements includes a precise control of exposure time and image motion compensation and the synchronization or sequencing of the events attendant with cyclic operation of the system. It employs a control and synchronization system, a functional block diagram of which is shown in Figure 2-71.

The key element in the operation of both systems is the intervalometer. Its output shaft, ω_0 , has an angular rate of one revolution per frame and is the system one-speed reference. The driving function for this device is the vehicle V/h ratio.

The V/h ratio is input to an error counter as a speed command through an A/D converter. During the clock interval, the intervalometer encoder output must null the counter; if it does not, an error signal proportional to the difference is generated for the next interval and the iterative process continues.

An independent operator selection of exposure time dictates that a multispeed position transmission system be employed to slave the primary shutter to the intervalometer. A digital incremental encoder servo system is thus employed. The selection of an appropriate speed position transmission to the terrestrial shutter drive is accomplished by the speed selector as a function of ω_0 and t_e . Speed selection N, the ratio of capping blade velocity to ω_0 , is made in the 9x to 48x speed range to ensure proper exposure time. As the capping blade is geared down from the shutter by a factor of 12, the shutter velocity is $108\omega_0$ to $576\omega_0$. N controls a series of gates in a down counter that ensures an output pulse for every $144/N$ input pulses. The reference pulse train on the intervalometer $18\times$ shaft generates 144×2^N pulses per frame to the down counter. The counter then generates a fine shutter position command of $N \cdot 2^N$ pulses per frame. As the capping blade encoder generates 2^N pulses per frame, its velocity is constrained to $N \times \omega_0$. Coarse position information from the intervalometer is derived by the use of an $8 \times 1 \times$ dual transmitter on its $18\times$ shaft. This device generates 144 pulses per frame. A down counter which serves as the coarse position command, allows for an output of N pulses per frame from this counter. The shutter encoder also generates N sync pulses per frame to be utilized as the coarse position response.



Table 2-18 — Photographic System Modes of Operation

Mode	Function	Operation
I	Photographic-payload operation, primary mission data gathering	Terrestrial and stellar cameras photograph their respective target areas; time and altitude data are recorded on each frame of both films; fiducial references are recorded on terrestrial film.
II	Forward RV shutdown; mission operational function	When one-half of terrestrial and stellar film supply is exposed, film is wrapped onto forward spool and forward RV is sealed; unexposed film is wrapped onto aft takeup spool for continuing photographic operation.
III	Aft RV shutdown; mission operation function	When nearly all terrestrial and stellar film is exposed, remaining film is wrapped onto aft takeup spool, and aft RV is sealed.
IV	Camera calibration; verify system calibration	Terrestrial and stellar cameras take simultaneous starfield photography to check any physical changes in the photographic system; different emulsion is spliced into terrestrial camera film web; vehicle is rolled for starfield photography.



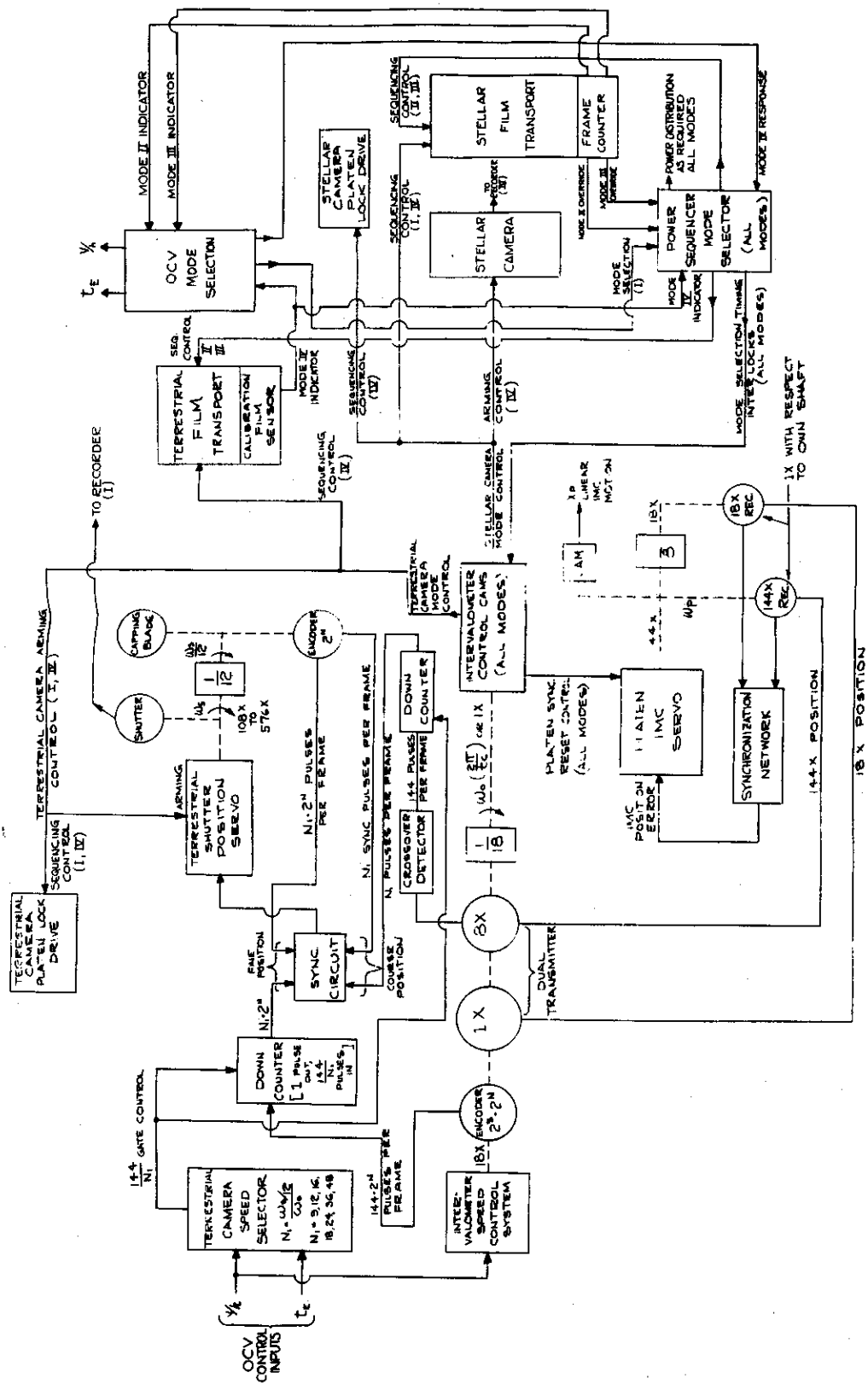


Fig. 2-71 — Camera control and synchronization system block diagram

Proper IMC dictates that ω_p , the platen IMC servo output shaft angular velocity, be $144\omega_0$. This is accomplished by coarse (18x) and fine (144x) speed position transmission from the intervalometer to the platen servo.

The synchronization system receives its constraining input from the vehicle mode selection. A power sequencer-mode selector provides for power distribution to appropriate system modules and interlocks the output electrical control signals from cam-activated switches on the intervalometer 1x shaft. Camera arming and interval sequencing of its platen pressure mechanism drive and transport system are provided during photographic operation. Usage of the takeup reels and shutdown of the camera system are initiated by the frame counter on the basis of film usage. The power sequencer-mode selection provides required control of the transport systems. Calibration is initiated by the calibration film sensor in the terrestrial camera transport system. Mode initiation is governed by the response of the vehicle operation to the indication. The system idles in the interval between indication and response.

a. Modular Functional Operation

For the purpose of system functional definition, a modular division has been established as shown in Figure 2-72.

Module 1	Terrestrial camera shutter control
Module 2	Intervalometer terrestrial shutter, IMC control logic
Module 3	Platen mode switch
Module 4	Platen IMC servo
Module 5	Stellar shutter drive
Module 6	Terrestrial camera film transport
Module 7	Intervalometer mode interval control
Module 8	Stellar camera film transport
Module 9	Terrestrial camera platen pressure drive
Module 10	Power sequencer-mode selector
Module 11	Stellar camera platen lock drive

It must be emphasized that relay coils and their associated contacts shown in Figure 2-72 are not located on the same module. This is necessary in order to reduce the number of modular interconnections shown in the figure and to facilitate the presentation of the associated system logic, i.e., a complete logical design is presented but the final electrical design of each module in terms of exact relay specification is not presented. A jack number on a module is also coincident with the module number.

System timing diagrams are presented with intervalometer design considerations governing applicable time intervals stated. The following sections provide a functional description of each of the modules.

(1) Terrestrial Camera Shutter Control (Module 1)

The terrestrial camera shutter control system receives 108x to 576x speed information from the intervalometer. This information is dependent upon the selection of exposure time for a given intervalometer rate (V/h ratio). The arming drive is subject to a mode override in Modes II and III. The shaft encoder reference pulse is utilized to generate the fiducial mark and data triggers in Modes I and IV. The terrestrial shutter arming drive is activated at the beginning of a cycle

by a cam on the intervalometer 1x speed shaft. Midexposure occurs at a sufficiently later time to ensure proper camera operation.

(2) Intervalometer Terrestrial Shutter, IMC Control Logic (Module 2) and Mode Control (Module 7)

The basic functions of the intervalometer are to provide a position reference for the terrestrial shutter drive and the platen IMC servo, to ensure the proper position correspondence of those units at midexposure and to control the timing intervals allotted for various operations during a camera cycle. As such, it is the primary command generator of the camera system. It sends 18x and 144x speed position information to the platen IMC servo. A speed ratio-selector matrix governs the speed transmission to the terrestrial camera shutter drive.

Interval control in the system is governed by a series of seven cams and limit switches on the intervalometer one-speed shaft as depicted in Module 7. The functions of the cams are as follows:

Commence frame cam—generates the arm terrestrial shutter command.

Sequence lock cam—ensures that a full indexing period is always available for the transport systems during camera operation.

Unlock platen cam—activates the platen pressure drives which, when unlocked, generate a signal to index the film in the transport systems.

Sync IMC cam—signals the platen servo to synchronize with the intervalometer 1x position to ensure proper image motion compensation at midexposure upon 144x position transmission.

Arm stellar shutter cam—ensures that stellar camera exposure is properly centered at correct intervals about the terrestrial exposure in Mode I.

Reset terrestrial shutter Mode IV cam—allows for the 3.0-second exposure interval required in that mode.

Arm stellar shutter Mode IV cam—centers the stellar exposure at the middle of the terrestrial exposure in Mode IV.

(3) Platen IMC Servo (Module 4)

The platen IMC servo can remain in a reset position or provide image motion compensation by following the intervalometer drive. Reset logic presented in Module 3 ensures that proper platen synchronization is accomplished in Mode I. In Mode IV, the platen is positioned to the midexposure position by the proper selection of the command reference on Module 1. The platen drive also provides for the removal of the terrestrial camera arming signal at a sufficient distance from midexposure to ensure proper reset of the intervalometer control signal which activated its initial arming.

The drive also provides a limit switch to shift its driving function to the proper reset reference after exposure.

(4) Stellar Shutter Drive (Module 5)

The stellar shutter drive receives its arming signal from the intervalometer cams. Proper

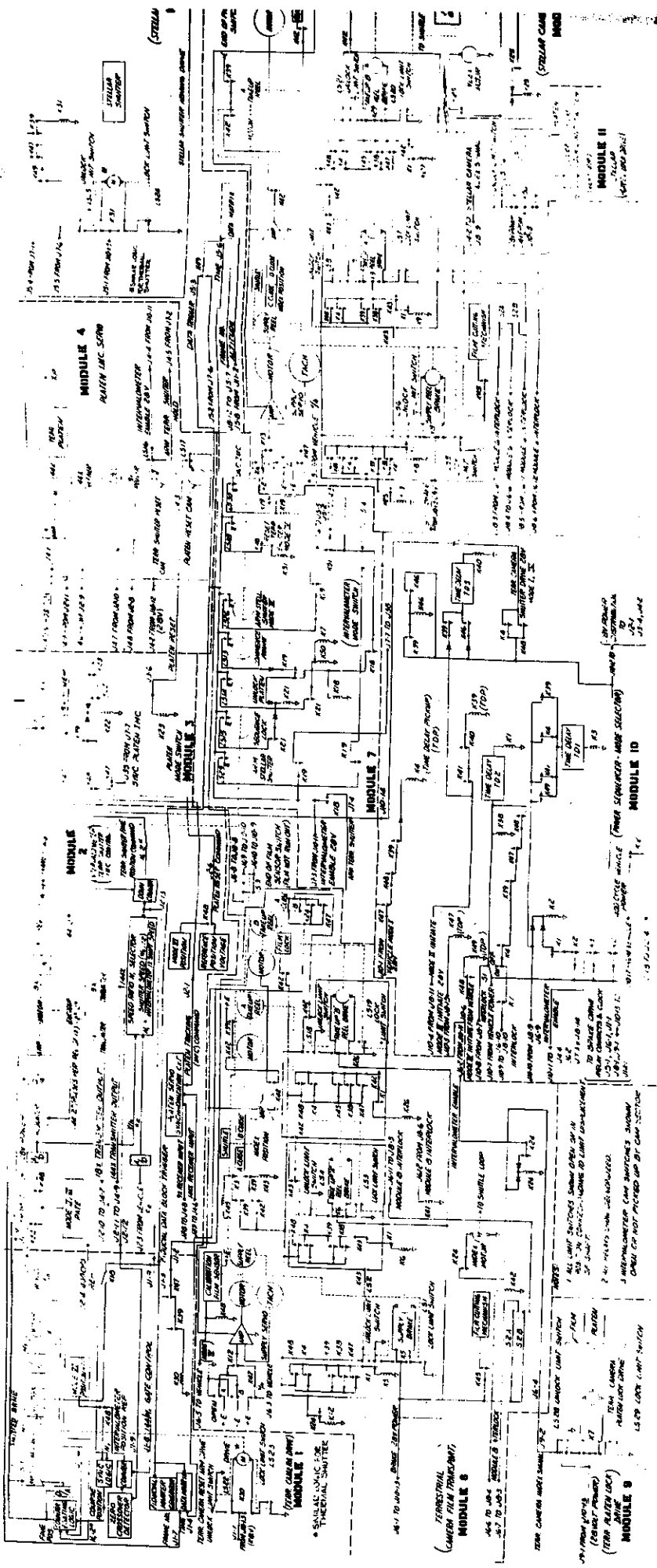


Fig. 2-72 - Camera system functional schematic

2-71

interval control for a particular mode is obtained by a selection logic at the relay which activates the drive. In all arming drives, power is removed from the drive motor when it reaches the armed position. With the control relay de-energized, the system is in the reset condition. The system is operative in Modes I and IV. Provision is made for triggers at midexposure to initiate the recording of the data matrix inputs of time, frame number, and altitude and to activate the fogging lamps.

(5) Terrestrial and Stellar Camera Film Transport Systems
(Modules 6 and 8)

The control logic of the transport systems accomplishes the following:

1. It assures that the supply and proper takeup reels are unlocked prior to commencement of cyclic camera operation.
2. It assures that the carriage is positioned at its index position before the commencement of a frame.
3. It initiates proper velocity control of the supply torquers with the arrival of the first index signal in a selected mode of operation.
4. It allows for forward RV cassette shutdown (Mode II).
5. It allows for turning off the camera system when all film has been expended (Mode III).

The power sequencer on Module 10 ensures that a suitable delay is provided so that the transport system can properly position the carriage before the start of a cycle. This is accomplished by imposing a time delay between the initiation of a mode, and the generation of the intervalometer enable signal which allows the camera system to commence cyclic operation.

The same provision is made when discontinuing operation. Contactor servo operation allows for the positioning of the shuttle to the index position prior to deactivation of the system after cyclic operation has ceased.

(6) Terrestrial and Stellar Camera Platen Pressure Drives
(Modules 9 and 11)

At a minimum of five seconds after the beginning of a frame, the intervalometer activates the relays which energize the drive motors and unlock their respective platens. When the platens have reached the unlocked position, an indexing signal for the system transport system is generated. A minimum of approximately three seconds is allowed for the transport systems to index the film. At the end of this interval, the relays are deactivated and the platen drives lock their respective platens.

(7) Power Sequencer-Mode Selector (Module 10)

The logic of the power distribution system ensures:

1. Provision of a suitable time delay for the transport systems to allow for the proper beginning and ending of cyclic operation prior to system shutdown or change in operational mode

~~SECRET~~

2. Mode selection and mode override by Modes II, III, and IV with the subsequent return to the previous Mode I
3. Power distribution compatible with required subsystem use during a particular mode
4. Automatic system shutdown if film is run out of camera or an operational mode selection is not made
5. Initiation of Mode IV when calibration film is sensed in terrestrial film transport system

b. Timing

System timing is keyed to the intervalometer shaft which makes one revolution per frame. Frame time is derived from a V/h input to the intervalometer. System timing diagrams are shown where applicable.

Terrestrial shutter velocity depends upon the selection of an exposure time with a given V/h ratio or intervalometer velocity. As the terrestrial shutter is position-synchronized to the intervalometer, a range of synchro speed transmissions (multi-speed system) is available to ensure proper terrestrial shutter exposure time. It is evident that arming of the terrestrial shutter must occur during the last turn of the capping blade before midexposure. The platen IMC servo also derives its position command from the intervalometer one-speed shaft. As the platen position at midexposure is fixed, a particular position of the intervalometer shaft must correspond to midexposure for both the terrestrial shutter and the platen IMC servos. This position has been fixed at an angular displacement of 6 degrees from the reference position (0 degrees) at which point the terrestrial shutter commences arming due to cam activation of a switch. This arrangement ensures that for the most critical condition of the fastest intervalometer speed ($t_c = 14.45$ seconds) and minimum exposure time, ample time is available for the terrestrial shutter to arm prior to exposure during the last cycle of the capping blade. These conditions are reflected in Figures 2-73 and 2-74, which depict Mode I operation at frame times of 14.45 and 22.0 seconds, respectively.

The arming and resetting of the stellar shutter is governed by a cam on the intervalometer output shaft which allows for a minimum exposure time of 200 milliseconds.

To provide proper IMC, the platen IMC servo must be run at 144x referenced to the intervalometer output shaft position. The terrestrial shutter is reset at 360 degrees of angular displacement of the IMC drive after midexposure. At 540 degrees of displacement, the platen IMC servo is reset, i.e., it no longer follows the 144x intervalometer transmission.

At a minimum of five seconds after the beginning of a frame, an intervalometer signal unlocks the terrestrial and stellar platens which generate indexing signals for their respective transport systems. Indexing film in the transport systems will require a maximum interval of two seconds. At a minimum of eight seconds after the beginning of a frame, the terrestrial and stellar platens are locked by the opening of a cam-activated intervalometer switch. (See Figure 2-73.)

In Mode IV both the terrestrial and stellar cameras operate under a special sequence of timed events. The terrestrial camera exposure time is three seconds; the stellar camera exposure time is 200 milliseconds centered in the middle of the terrestrial exposure. This unique condition is governed by a special set of cams on the intervalometer which assure proper time correspondence for the fixed intervalometer speed. The applicable timing diagram is given in Figure 2-75.

~~SECRET~~

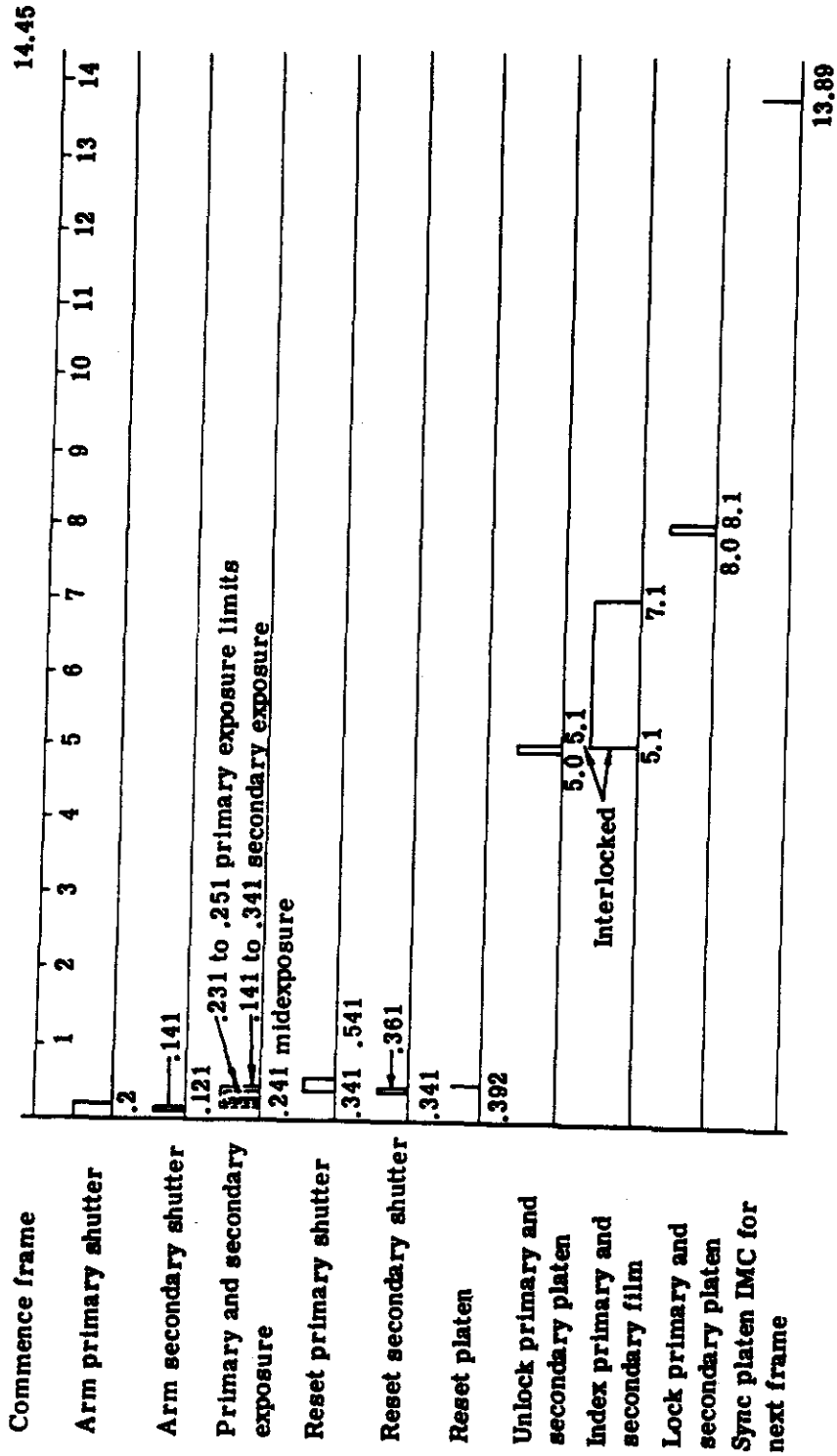


Fig. 2-73 — Mode I operation timing diagram; frame time: 14.45 seconds

SECRET

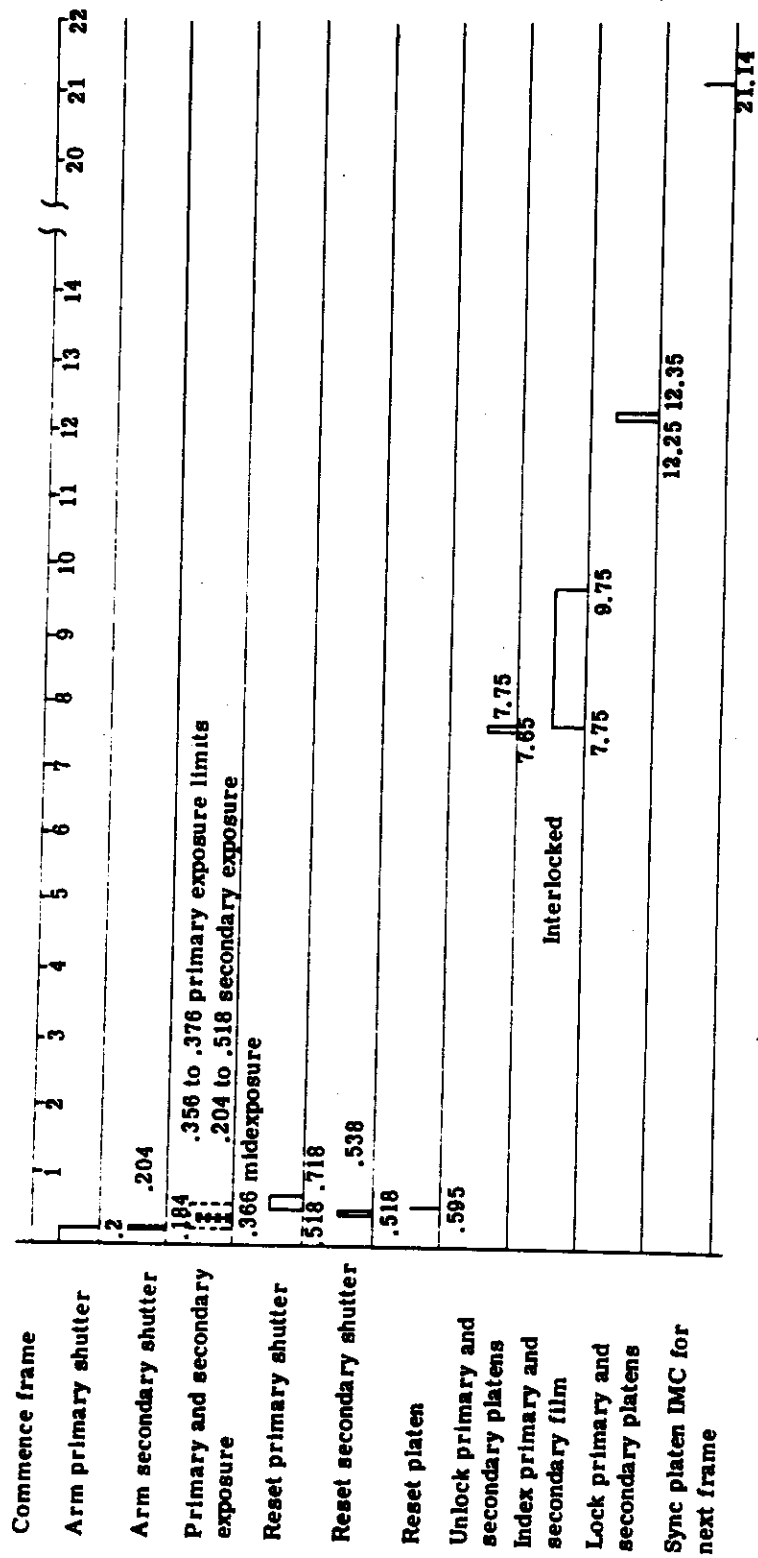


Fig. 2-74 — Mode I operation timing diagram; frame time: 22.0 seconds

SECRET

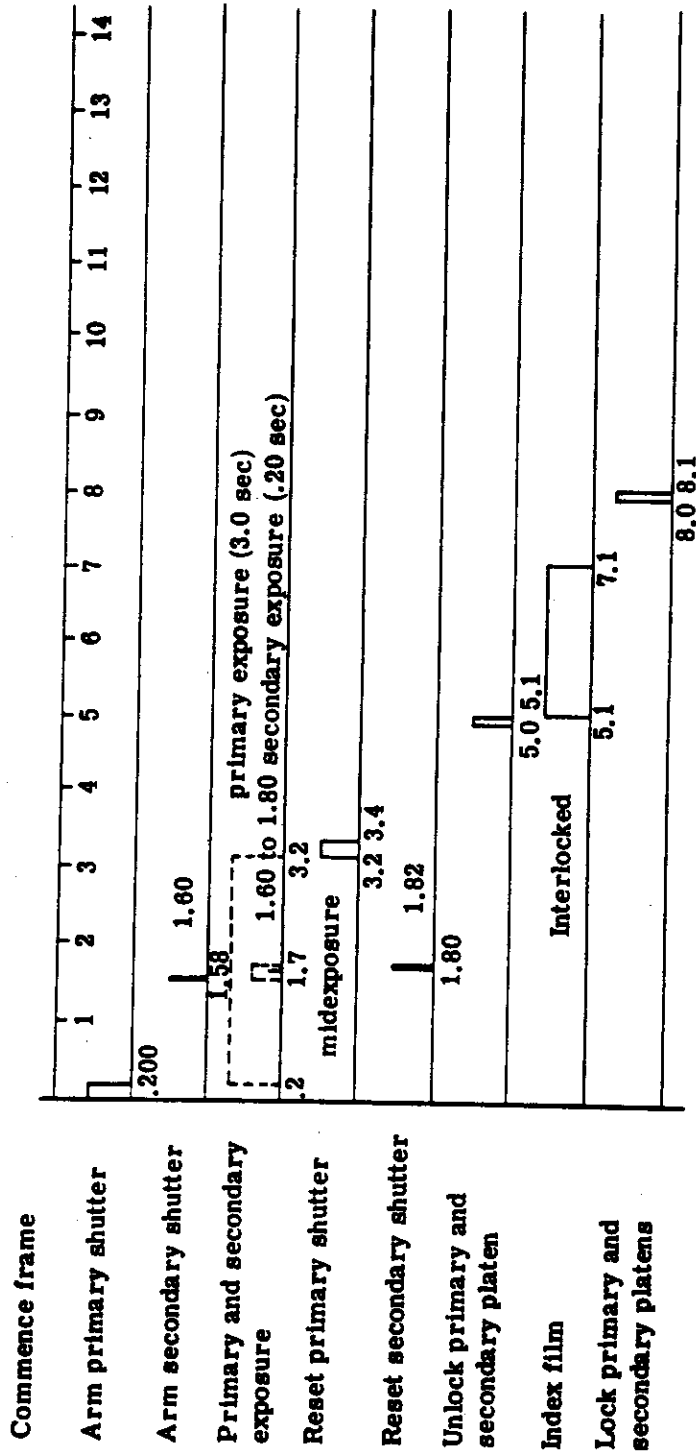


Fig. 2-75 — Mode IV operation timing diagram; frame time: 14.45 seconds

c. Electronic Packaging Concept

The design of this system lends itself to electronics which are most suitably packaged in a modular form. The camera control electronics are divided into three basic groups:

1. Drive amplifiers
2. Logic circuits
3. Relay control circuits

Commercial dc servo amplifiers modified to meet the environmental condition are used as the drive amplifiers. The intervalometer, IMC, shutter and data block logic modules are combined into a single modular assembly.

The relay control circuits are further subdivided into four modular assemblies:

1. Stellar transport control assembly
2. Terrestrial transport control assembly
3. Platen, shutter and intervalometer control assembly
4. Power sequencer and mode selector assembly

These assemblies are packaged in a similar manner. Due to the RFI/EMI consideration, the enclosure is divided into two compartments. One compartment is used to house the relays and their associated components and wiring. RFI filters and feed-through capacitors are used in the bulkhead between the two sections. A circular miniature connector is provided for connection to the system cables.

d. Photosensor Weight and Power Budget Estimates

(1) Photosensor Weight

The estimated weights for the photosensor system are listed below. The values are for those items of hardware which comprise the photosensor system are exclusive of film. A complete weight breakdown for two satellite recovery configurations is in Section 2.3.4.

Item	Weight, pounds
Camera assembly	305
Terrestrial	257
Stellar	43
Insulation	5
Film supply cassette	131
Photosensor electronics	55
Thermal shutters	14
Takeup cassettes	<u>115</u>
Total System Weight (less film)	620

(2) Photosensor Power Budget

The energy consumption of the photosensor system only is listed below for a mission at 160 nautical miles, and is 72 hours total accumulated time.

Terrestrial Camera Users	Power, kilowatt-hours
1. Shutter	0.64
2. Platen pressure mechanism	0.07
3. IMC servo	0.07
4. Supply torquer	0.22
5. Takeup torquer	0.36
6. Index drive	0.11
7. Fiducial generator	0.02
8. Relays	<u>0.14</u>
Subtotal	1.63

Stellar Camera Users	Power, kilowatt-hours
1. Shutter drive	0.05
2. Film transport	
Supply torquer	0.22
Takeup torquer	0.36
3. Index drive	0.11
4. Platen pressure mechanism	0.07
5. Electronics	<u>0.14</u>
Subtotal	0.95

Other Users	Power, kilowatt-hours
1. Thermal shutter (terrestrial)	0.06
2. Thermal shutter (stellar) (2)	0.07
3. Intervalometer	<u>0.36</u>
Subtotal	0.49

System Totals	Power, kilowatt-hours
Terrestrial camera	1.63
Stellar camera	0.95
Other	<u>0.49</u>
Total	2.07

2:2.1.4 Auxiliary Systems

Auxiliary systems are defined as that group of elements necessary to provide data (in addition to that gathered by the terrestrial and stellar cameras) to implement the GOPSS mission. Selection of these systems has been treated as a hardware determination to provide a total system feasibility based on the requirements generated by other system studies.

The auxiliary systems in GOPSS must support the mission requirements by performing the following functions:

1. Provide a means for Doppler tracking by the TRANSIT network to allow extraction of the vehicle's topocentric range rate (TRANSIT transmitter).
2. The ability to detect orbit perturbations due to non-gravitational effects in order to account for deviations in the orbit from that determined by the present Trace observational model. This accounts not only for deviations from the parameters assumed in the model, but also accounts for the effect of vehicle perturbations on measured satellite position (accelerometer package).
3. The ability to accurately record the time in conjunction with vehicle perturbation forces and altitude data (system clock).
4. The ability to evaluate additional coefficients in the gravity model (radar altimeter).
5. The ability to assess the inflight operational performance of the vehicle (system confidence module, telemetry, mission data recorder).

A functional description and the salient performance parameters of these equipments are presented in the following paragraphs.

1. Mission data recorder
2. TRANSIT transmitter
3. Radar altimeter
4. Accelerometer
5. System clock
6. System performance monitoring (confidence module)

~~SECRET~~

2.2.1.4.1 TRANSIT Transmitter

For Doppler tracking by the TRANSIT Network, the vehicle must carry a highly stable oscillator, two frequency multipliers, and two transmitters.

The heart of the system is a dual 5 megacycle, fifth overtone, oven-controlled oscillator of ultra high stability. Its ovens are also redundant, and since only one oscillator is on at a time, this allows four possible operating combinations. Switching of the oven power is normally performed in the satellite power switching, while switching of the oscillator power and the signal output is performed by the buffer/converter/switch (B/C/S). This switch also converts the 5-megacycle source to a 3-megacycle signal and supplies a buffered, low impedance, level, 3-megacycle signal at its output. This output signal level is nominally 0.5 volt peak-to-peak into a 50 ohm load, and it drives the frequency multiplier/phase modulator (FM/PM) whose input and output impedances are also 50 ohms. The FM/PM multiplies the 3-megacycle signals to 54-megacycles where two buffers are driven in parallel to supply two coherent outputs. Each of these channels then feeds into a phase modulator, which in turn drives the output buffer-amplifier, supplying an output of 7 milliwatts. The phase modulator is a pulse type modulator, advancing or retarding the phase a fixed amount when driven with the corresponding signals. It is normal practice to choose a modulation format such that no phase bias is generated. The modulator is a current-driven device whose input can be left disconnected if no phase modulation is required.

The power amplifiers differ only in the power level and output circuitry. Both multiply the 54-megacycle signal to 162 megacycles and amplify the resulting signal. The 324-megacycle power amplifier then has a varactor doubler at the output. For use in the GOPSS, the transmitters would deliver 250 milliwatts at 162 megacycles and 400 milliwatts at 324 megacycles.

At present, an entire system weighs 6.4 pounds and uses 5.7 watts of power. During Phase II of the program, it would be determined if the various oscillators of the transmitter and altimeter could be combined into a single unit. This would allow a weight and power reduction to approximately 50 percent of present levels.

Phase modulation allows telemetry information to be carried on both transmitter frequencies. When the modulation format is chosen so as to generate no phase bias, carrying telemetry information on the Doppler channels does not interfere with the accuracy of making Doppler measurements. Therefore, the Doppler transmitters need not impose power and weight beyond the needs for telemetry except for the power and weight needed for a highly stable oscillator and for two transmitters rather than one. This is the basis for charging half the total weight and power to Doppler tracking.

A TRANSIT ground station also must contain a stable oscillator and a clock driven by the oscillator. The reference frequency and the epoch time shown by the clock are monitored and corrected using very low frequency and satellite of high frequency time signal transmissions.

At the tracking station, satellite signals on two frequencies which are coherent and related by simple ratios (1:2, 3:8, for example) are received and compared with frequencies synthesized from the station's frequency standard, giving a beat frequency in the range of tens of kilocycles. The satellite oscillator is offset from 35 to about 85 parts per million to exceed the maximum expected Doppler shift, so that the beat frequency never passes through zero. The beat frequency is produced in the receiver detector and contains the desired Doppler information, phase modulation (if present), and noise. It is this signal which is presented to two tracking filters.

The tracking filters are essentially a narrow bandpass filter whose outputs are more nearly noise-free Doppler signals and modulation and timing information.

~~SECRET~~

~~SECRET~~

Signals received from the satellite have been subjected to (1) Doppler frequency shift, (2) frequency shifts due to ionospheric refraction, and (3) frequency shifts due to tropospheric refraction. Making use of the frequency dependence of the refractive effect of the ionosphere, the ionosphere refraction correction system combines the outputs of the two tracking filters in such a way as to eliminate, to first order, the refractive effects of the ionosphere. Outputs from the refractive corrector are the corrected Doppler signal and the first order refraction error signal, which is usually displayed as a tuning aid and which may be recorded for studies of the ionosphere.

The corrected Doppler output of the refraction unit is digitized. Present practice is to sample the Doppler frequency every four seconds. All of the TRANSIT stations are equipped to receive timing signals, in the form of a "timing word," from the phase modulation on Navy navigational satellites which broadcast a timing word every two minutes. When a timing word is recognized, the equipment produces a pulse at the appropriate time, which causes the station digitizer to form and punch an 11-digit satellite time data point. These time data points are recorded on five-level teletype code tape in place of a Doppler data point.

2.2.1.4.2 General Description—SCI Radar Altimeter

The radar altimeter produced by Space Craft Incorporated (SCI), is designed for application on space vehicles operating from 30 to 550 kilometers or more above the surface of the earth. The altimeter is a complete on-board tracking system designed to augment ground-based tracking systems. The data is read on-board and telemetered to the ground. Since the system is not limited by the horizon or ground-based system, tracking geometry limitations, it provides an accurate measurement of altitude where little or no coverage exists.

The altimeter determines range by accurate measurement of the time interval between the transmitted pulse from the space vehicle to the earth and the returned echo to the space vehicle. The altimeter automatically measures this interval and digitally encodes the measured altitude data.

Figure 2-76 shows the signal and data flow through the basic subsystems. Basically, the system functions as follows: the timer provides a 144 pulse per second synchronization pulse to the tracker which simultaneously produces a trigger pulse to the modulator and a 100 microsecond blanking gate to inhibit the input of the range tracker from the IF amplifier. This prevents any transmitter leakage signal from entering the tracker. The modulator produces a 1 microsecond high voltage pulse which energizes the 1610-megacycle transmitter for 1 microsecond. The output of the transmitter is directed through the duplexer to the antenna in order to beam a 5-kilowatt minimum peak signal to the earth. A small part of the transmitter output is detected to obtain a start pulse for the range tracker. The start pulse is processed in the range tracker to generate the leading edge of a counter gate which is fed to the timer. Receipt of the counter gate by the timer enable a 20 bit ripple counter (altitude accumulator) to begin counting the output of the 21.233664-megacycle clock oscillator. This counting process will continue until the counter gate is closed by the tracker.

The radar echo from the earth is received by the antenna and directed through the duplexer to the receiver. The echo is amplified in the receiver, heterodyned to 30 megacycles and fed to the IF amplifier for additional amplification, filtering, and pulse-peak detection. The video pulse from the IF amplifier is then fed to the tracker where it is processed to stop the counter gate and consequently to stop the 20 bit ripple counter. The binary work now stored in the counter represents the altitude of the altimeter above the surface of the earth.

~~SECRET~~

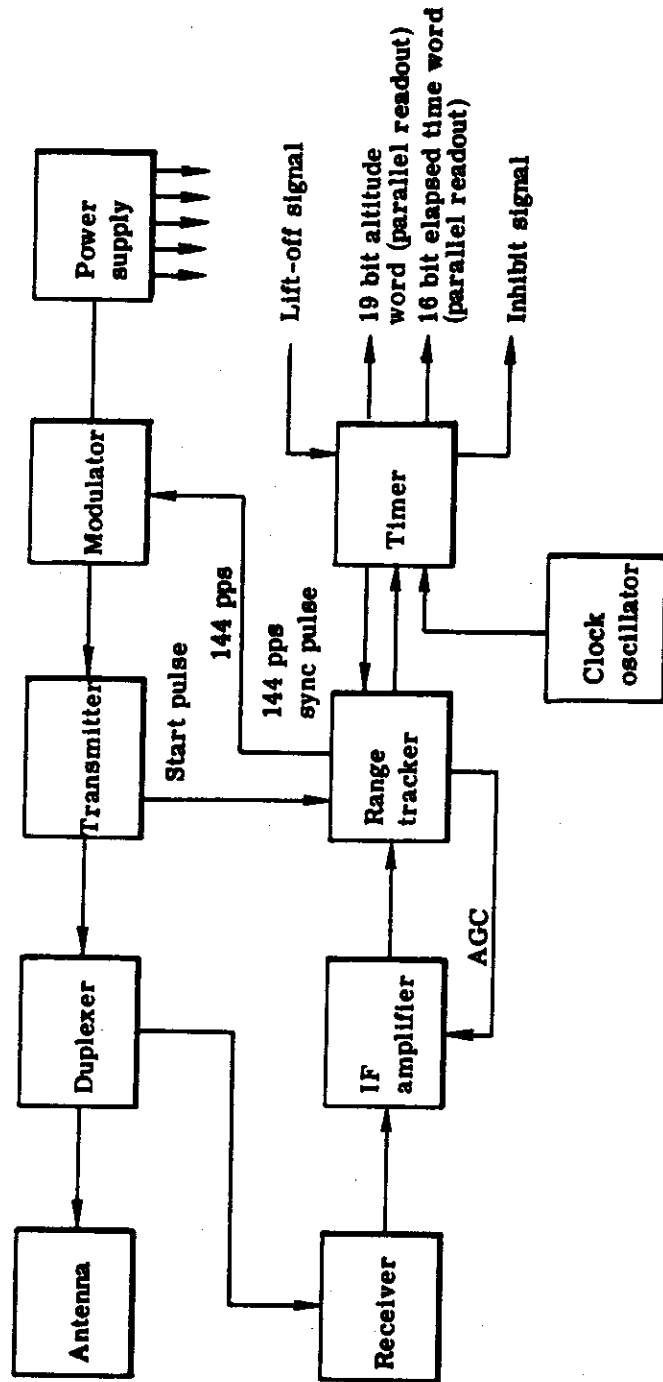


Fig. 2-76 — Radar altimeter block diagram

The output of each of the 20 flip-flops of the altitude accumulator is fed to a 20 bit storage register. The altitude accumulator is permitted to count, consecutively, four altitude words before a command is given to transfer the four accumulated altitude words to the storage registers. Immediately after data is transferred into the storage register, the altitude accumulator is cleared to begin a new data accumulation process. Note that the storing and clearing operations are performed between the trailing edge of the fourth counter gate and the leading edge of the next counter gate and that no altitude information is missed. The output of the storage register is available for telemetry as a 20 bit altitude word with parallel readouts. In the present system, only 19 bits, sufficient to record up to more than 480 nautical miles, are telemetered. The 20 bits are available because the last three modules of the altitude accumulator consist of identical modules which provide one more flip-flop than is actually needed.

Proposed Modifications

The preceding section described the existing SCI radar altimeter. To improve system accuracy, SCI proposes the following modifications: (1) modify the tracker circuitry to employ leading edge tracking in lieu of the present center-pulse tracking, (2) replace (optionally) the L-band RF subassembly with an X-band RF subassembly, and (3) provide an auxiliary output from the highly stable reference clock oscillator.

These modification will provide an optimized altimeter for the GOPSS and offers, in addition, an economic advantage in that the option for a X-band RF subassembly is less expensive than the present L-band unit.

The equipment errors predicted for the proposed altimeter may be summarized as follows:

Counter gate errors due to electronic switching noise	± 5 meters (random)
Counter gate errors due to AFC Jitter	± 1 meter maximum (random)
Error due to clock oscillator frequency drift	negligible for clock oscillator stability of 1 part in 10 ⁶
Error due to degradation of echo pulse rise time	± 15 meters, -0 meters (function of altitude can be calibrated out)
Least significant bit error	± 3.5 meters
	<hr/>
	Σ ≈ 10 meters

2.2.1.4.3 Accelerometer

Bell Aerosystems has developed a miniaturized electrostatic accelerometer (MESA) for NASA, and is producing versions of this for operational space vehicles.

The MESA is an electrostatically suspended pulse-rebalanced accelerometer. The proof mass is a beryllium cylinder with a flange at the center. The primary mechanical elements are shown in Figure 2-77. The sensitive axis is along the longitudinal axis of the cylinder. The cross-axis suspension system is passive, requiring a minimum of electronic circuitry. Along the sensitive axis, a capacitive bridge pickoff system is used to trigger a precise voltage time integral pulse each time the proof mass moves through the trigger position as a result of external

~~SECRET~~

acceleration. The cylinder proof mass is restored by the electrostatic forces derived from this precision voltage pulse. The output of the MESA is, therefore, a pulse rate proportional to the input acceleration. Each pulse signifies a discrete velocity increment that the MESA experienced. The scaling is flexible over a wide range from 0.000001 to 0.1 foot/second/pulse depending on the requirement.

The MESA permits lowering the orbital suspension voltage to the actual desired level of about 10^{-7} g by changing the magnitude of the suspension reference voltage. The null forces of the MESA are almost entirely contributed by cross-coupling from the suspension system. Lowering the suspension forces, as permitted by the g-environment, proportionally improves the null stability and repeatability. This has been verified in laboratory experiments where the suspension capability was lowered from 20 to 4 g's with a corresponding reduction in the null forces. The cross coupling of the suspension forces into the sensitive axis is typically one part in 10^5 . Hence, reducing the suspension capability in orbit to 10^{-7} g results in a null stability and repeatability from turn-on to turn-on of better than 10^{-12} g. Reduction of the suspension forces lowers the null errors at the source, eliminating all requirements for calibrating the MESA prior to launch.

The only moving part of the MESA is the lightweight but rugged cylindrical proof mass. Since there is no suspension structure to take a set, the limit of non-operating vibration and shock is set by input levels which will permanently distort the proof mass. The levels are in excess of any nominally experienced g's in a vehicle firing. The MESA can, therefore, be fired nonoperating into orbit without deterioration of performance in subsequent orbital acceleration measurements. The electronic modules have passed the extremely rigorous flight specifications of the Atlas-Agena launch environment and have been fully qualified for the program.

The instrument consists of a hollow cylindrical float which has a flange around the center. The cylinder is supported by eight electrodes arranged to act against the inner surface of the float. Each electrode is in series with a tuning inductor which exerts a voltage across the electrode-float gap which is a function of the float position. The float position determines the capacity in a series-tuned circuit and, therefore, the operating point on the series resonance characteristic curve. As a result of this situation, an attractive force develops between the float and electrode which increases as the float moves away from the electrode, causing the float to be suspended in all directions except along the cylindrical axis. The suspension system, therefore, centers the float under angular and translational accelerations. The suspensions sweep oscillator and amplifiers provide automatic suspension of the float without voltage breakdown or arcing.

Detection of the float movement is accomplished by sensing the change in capacitance between two pickoff rings concentric with the float flange. A balanced capacitive bridge circuit as shown in Figure 2-78 is excited by a carrier frequency. Displacement of the float results in a signal output from the bridge. This output is amplified and phase demodulated to produce a dc voltage whose polarity is a function of the direction of the float movement and whose amplitude is a measure of the relative displacement from the accelerometer null position. At a selected voltage level, a trigger circuit generates a dc pulse which rebalances the float. Since pulses are generated only as needed, this system is called a pulse on-command, force rebalance system.

The two outer rings shown at the left in Figure 2-77 are used to force rebalance the float. Voltage pulses of opposite polarity are applied to these rings to exert electrostatic force along the sensitive cylindrical axis. The pulses are generated by a pulse core which controls the

~~SECRET~~

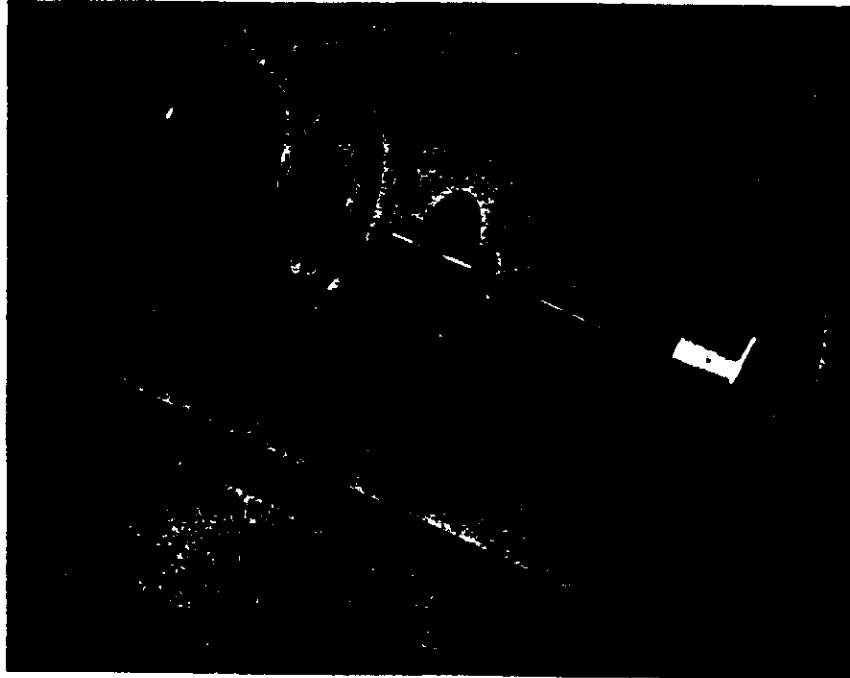


Fig. 2-77 — Primary mechanical elements - MESA

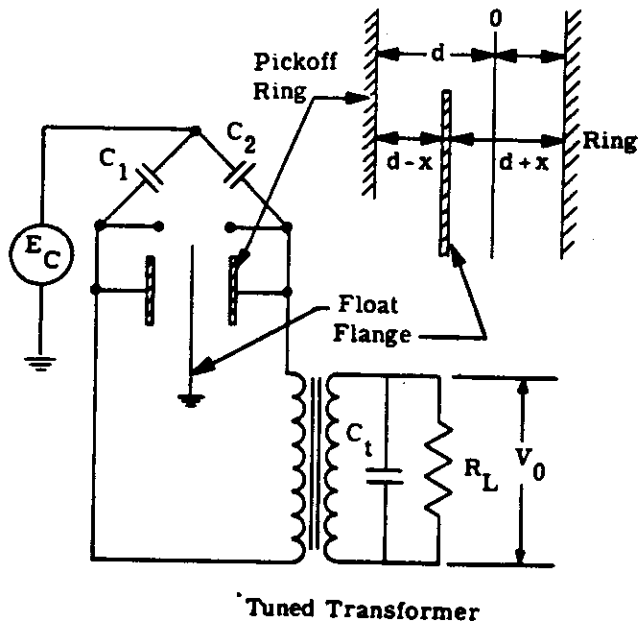


Fig. 2-78 — Pickoff system - MESA

amplitude and width of the pulse. This pulse generation technique is presently used by Bell Aerosystems on digital velocity meters for the Agena program and its accuracy and stability have been verified in over 100 space flights.

The accelerometer output is a signal whose frequency is proportional to acceleration. The output frequency is integrated to obtain velocity by the use of a digital counter.

Operational parameters for the MESA as planned to be utilized in a three-axis package for GOPSS are as follows.

g-range input: 10^{-4} to 10^{-3} g (operational)

Nominal g input: 10^{-7} g

Output: A 21 bit velocity readout to include a sign (\pm) bit shall be provided for each axis. The ability to simultaneously interrogate the digital velocity readout of each axis shall be provided.

Scale factor: The digital readout shall store 5000 counts for a velocity of 10^{-4} g foot per second. The output code shall be straight binary.

Accuracy: Velocity shall be measured with a time averaged error not to exceed 10^{-8} g foot per second. This error includes all factors except null stability.

Sampling period: The unit shall be sampled at a maximum of once every 10 seconds and at a minimum of once every 25 seconds. This read pulse interval is not maintained at a precise time tolerance. Real time is recorded, however, with a precise tolerance in other system instrumentation coincident with the read pulse.

Weight: The weight, size, and power of the accelerometer, size of power electronics, and thermal control package for a three-axis unit shall be minimized as far as practical and specified by Bell Aerosystems.

Environmental range:

1. Operating temperature 70 to 90 °F
2. Nonoperating temperature 0 to 150 °F
3. Vibration and shock

Sinusoidal

Frequency, cycles per second	Acceleration per Amplitude
5 to 14	0.5 inch
14 to 400	5.0 g
400 to 2000	7.5 g

25 minutes/axes

Random

Frequency, cycles per second	g^2 per cycles per second	Acceleration, g
20 to 200	0.01	1.34
200 to 400	0.07	3.74
400 to 2000	0.13	14.40

2 minutes/axes

Acceleration

Axis	Directions	Acceleration, g	Exposure Time, minutes
Longitudinal	2	10	5
Lateral	2	1.5	5
Normal	2	1.5	5

Shock (1/2 sine pulse):

Axis	Directions	Amplitude, peak g	Time, milliseconds	Number of Drops per Direction
Longitudinal	2	15	11 ± 1	3
Lateral	2	15	11 ± 1	3
Normal	2	15	11 ± 1	3

Null output: 10^{-9} g maximum (10^{-4} g suspension)

Scale factor stability: The scale factor stability shall ensure that an accuracy of 1 part in 1000 (0.1 percent) of the input is maintained, i.e.,

Input, g	Error, g feet per second
10^{-7}	10^{-10}
10^{-8}	10^{-11}

Mechanical interface: The input axes of the three-axis system must be orthogonal to 2 minutes of arc to include the tolerances upon the reference mounting surface. Bell Aerospace shall define the most practical mounting interface.

Electrical interface: A 17 to 28-volt, plus and minus, dc source shall be provided with application of vehicle power. The unit shall cycle itself to prepare for an operate condition. A 17 to 28-volt discrete shall be provided for the unit to assume the operate mode.

Qualification tests: Qualification tests are to be conducted upon one accelerometer package that is identical to the remaining deliverable units. The aforementioned environment shall apply.

Acceptance tests: Acceptance tests are to be conducted on each deliverable accelerometer subsystem (except the qualification model) to provide assurance that the accelerometer package performance is within the limits of applicable design parameters and the item is free from

material, construction, workmanship, and functional deficiencies. Bell Aerosystems is to specify the environments and the environmental test level for acceptance testing which is deemed necessary. A failure parameter (MTBF) shall be defined and specified.

Electromagnetic interference: Each deliverable accelerometer package shall be subjected to an electromagnetic interference test to determine conformance to MIL-I-26600.

2.2.1.4.4 System Clock

The system clock will be a 5.0-megacycle, crystal-controlled oscillator manufactured by the Sultz Division of the Tracor Corporation. The unit is housed within a double proportionally controlled oven. The oscillator stability is better than one part in 10^9 throughout the various changes to be expected during the mission. (To satisfy mission objectives of 1×10^{-3} second over a 15-day mission, an accuracy of 1×10^{-8} is required.) Specification for the oscillator unit is as follows.

Output

Frequency: 5.0 megacycles
Voltage: 1.0 volt rms, -20 percent, +50 percent into a 50-ohm load

Stability

Input voltage change, 27 ± 5.0 vdc: $\pm 1.0 \times 10^{-10}$
Load variation, 50 ± 10 ohms: $\pm 1.0 \times 10^{-10}$
Temperature variation -54 to $+65$ °C: $\pm 2 \times 10^{-9}$
During vibration of 10 to 500 cycles per second, 1 g: $\pm 1.0 \times 10^{-8}$
Shock, 50 g per MIL-STD-202A, method 202A: 1.0×10^{-8} , possible permanent shift

Input Power Requirements

Voltage: 22 to 32 vdc
Current (at 27 vdc): 450 ma at -54 °C
175 ma at 25 °C
65 ma at $+60$ °C
Frequency adjustment: course mechanical: 800×10^{-9}
fine mechanical: 100×10^{-9}
fine electrical (1 to 7 volts): 30×10^{-9}
Size: length: $4 \frac{1}{4}$ inches
width: $4 \frac{1}{4}$ inches
height: $6 \frac{7}{8}$ inches
Mounting: four 8/32 by 1/2 inch studs on $3 \frac{3}{8}$ -inch centers
Weight: 3.5 pounds

~~SECRET~~

2.2.1.4.5 Data Recording Systems

Data recording systems are required to collect data pertinent to mission performance and terrestrial and stellar camera operation.

The camera recording system utilizes a data block which is recorded on the photographic film adjacent to the pertinent frame.

For the mission data recording system, both magnetic tape and photographic film recorders were considered, and the pertinent characteristics of typical units are listed in Table 2-19. The basic requirement is for a recorder which can collect a large quantity of data in small increments over a long period of time.

The chief advantage of magnetic tape recorders is that they are standard, essentially off-the-shelf items which can be used easily with available data reduction equipment. However, they are greatly surpassed by the film recorder in the areas of average power and data density. Since the latter factors are the most significant for this mission, the photographic film recorder was selected. The system thus utilizes film recorders for both the camera and mission data recording systems.

The mission recorders consist of a film transport mechanism and a data block recording head (see Figure 2-79). The head used to record the data is an Avalanche Luminescent Diode Array which is a recent development of the Fairchild Semi-Conductor Division. The array is a matrix of siliconplanar diodes which emit light when operated in their reverse bias mode. In this mode, the diodes start to conduct via an "avalanche" mechanism at about 6 volts reverse bias. The intensity of the emitted light is proportional to the current through the diode. By gating the appropriate rows and columns of the matrix, digital data can be expressed in terms of dark or luminescent diodes. The information becomes an array of black dots or transparent areas on the processed film. Because of the high density of the diodes, only 0.1 inch of film is used for each data array. Although the film moves continuously (0.01 inch/second), the array is recorded at such a high relative speed (0.05 second) that the amount of smearing of each dot is insignificant.

Storage and reset pulses are derived for the mission recorder system from the recorder film transport drive motor shaft. Strobe pulses sample the time and altitude readouts and store these in a buffer; the strobe pulse also simultaneously gates a counter that enable successive columns of the diodes for recording. The diodes are arranged in 6 columns and 32 rows on the array. Because of its internal construction, the array must be operated in a column sequential manner, that is, one column is activated at a time. Any combination of the 32 element diodes in a column are driven simultaneously by independent, current-regulated pulse generators. The counter sets the columns in sequence for an interval dependent on the desired exposure of the film. The counter also enables the appropriate set of gates in the selection matrix so that the information in the buffers is transferred to the appropriate drivers. After the counter has cycled through the six columns, a reset pulse is generated to clean the buffers. The electronic system which drives the camera recording system is similar to that just described for the mission data recorder.

Operation of the mission data recorder is illustrated in Figure 2-80. Time, altitude, and velocity are strobed simultaneously. In addition, a set of analog temperature transducers located in the mission data system are sampled periodically by the analog-to-digital converter. Since temperature, for example, changes slowly in comparison with the data sampling interval, no

~~SECRET~~

Table 2-19 — Comparison of Data Recorders

Characteristic	Magnetic Tape		Photographic Film
	Continuous	Incremental	
Recording medium	1/2-inch tape		16-millimeter film (single sprocket)
Recording method	7-track IBM compatible spacing		Fairchild diode array data block
Record length,* feet	2400 (standard 10 1/2-inch reel)		1080
Record duration,* hours	64	127	180
Average power, watts	24	100	0.5
Readout	IBM 729 or equivalent		Special
Availability	Off-the-shelf		Special

*Assume 1 sample per 5 seconds.

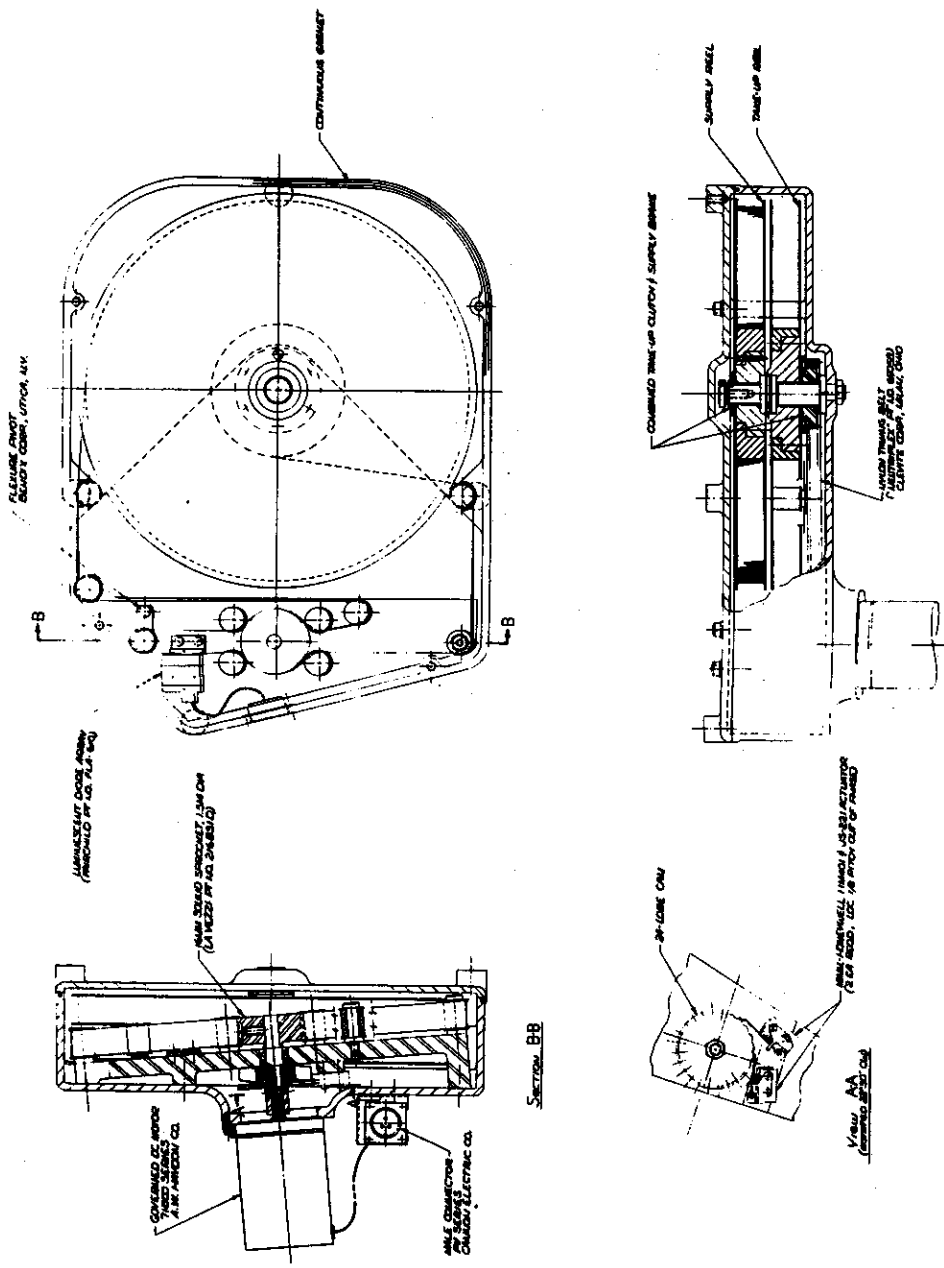


Fig. 2-79 — Optical recorder assembly

SECRET

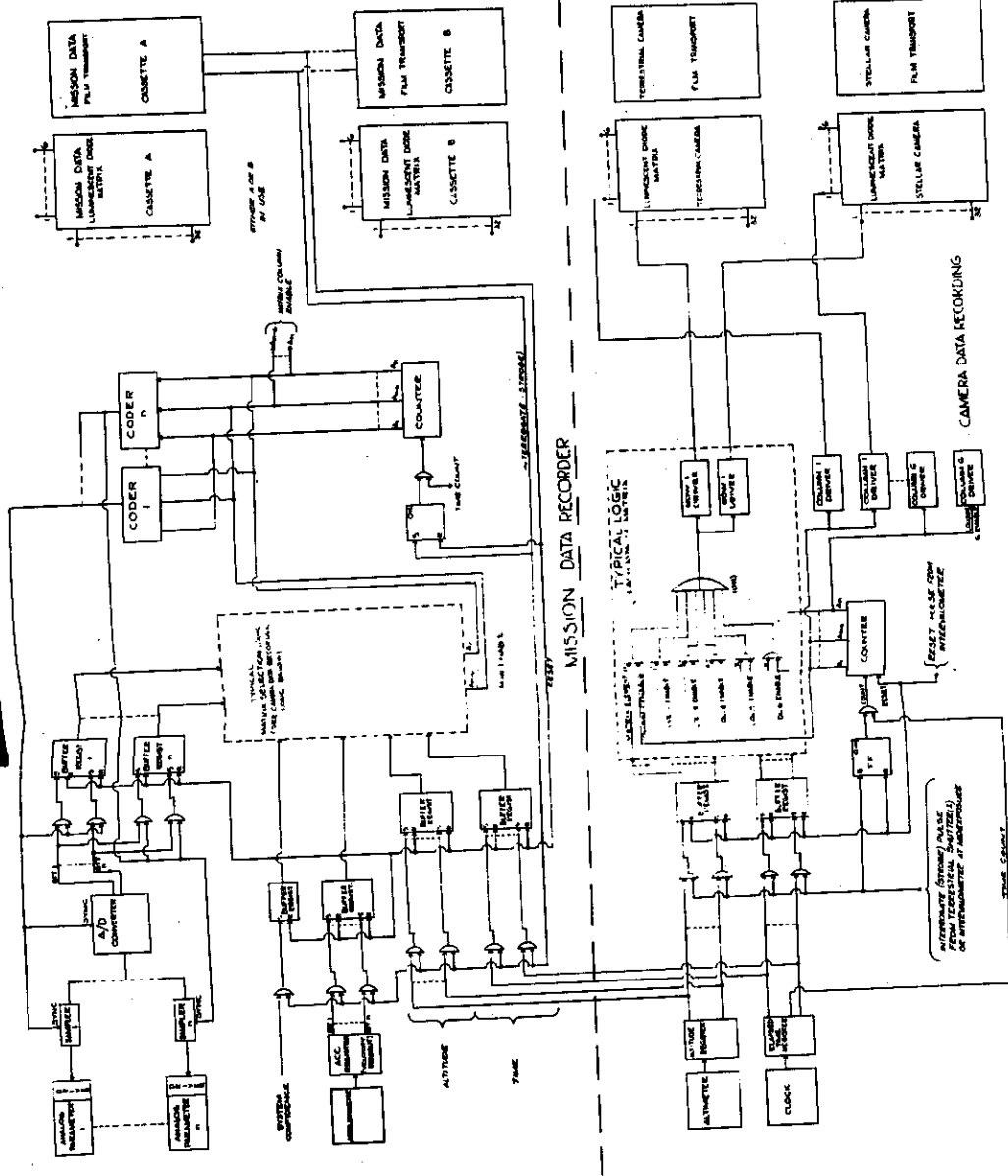


Fig. 2-80 — Mission data block recorder

SECRET

precise time correlation is made with the analog signals. The A/D converter samples sensors in the interval between recordings and stores the results in buffer registers. A coding circuit driven by the system clock provides the logic for sequential sampling of the analog devices.

At the end of the mission, the film in the mission data recorder is processed and the data converted into a tape format compatible to a computer input system. At the moment, there is no machine available to read specifically the dot array. However, existing film scanners (such as the IBM 2281 Film Scanner) could be modified to handle the 16 millimeter film.

2.2.1.4.6 System Performance Monitoring (Confidence Module)

System performance can be monitored in the preflight stage through automatic checkout circuits in the AGE equipment in order to record the sequential operation of flight hardware and its adherence to performance specification, and inflight through the use of telemetry equipment. To provide inflight telemetry data, a confidence module has been designed which utilizes flip-flops to record the events and their sequency that have occurred during operation of the photographic system. Permanent records of telemetry data are normally used for postflight evaluation of equipment performance when this type of data is available.

However, postflight evaluation of telemetry data is normally limited since this data is available only when the satellite is over ground stations. Thus, the confidence module has been designed to allow each and every cycle of photosensor operation to be read into the mission data recorder to enable a complete postflight evaluation of the entire mission. In addition, this device may be read into the AGE consoles during preflight to record operational behavior of the photographic system, and, during flight, the device may be read out at desirable times through the telemetry system.

Figure 2-81 presents the logic to obtain a Go/No-Go inflight confidence signal. Flip-flops are operated in the set-reset mode. Read and reset pulses are derived from relays shown in Figure 2-72. All relay numbers and input sources shown in Figure 2-81 are defined by reference to Figure 2-72. During the active portion of a camera cycle, flip-flops are set as the monitored operations occur. A data sequence is then present in the buffer which uniquely defines the operational status of the camera system. When an integration is required to sense the velocity limits of the terrestrial shutter, a counter is employed to count pulses, each of which is a measure of incremental shaft angular displacement. The logic is such that if the count over a specified interval is not within tolerance limits, a flip-flop is set. The mode gating signal determines the specific data sequence that is to be monitored coincident with operational requirements for a specific mode. The output flip-flop remains in the set state as long as confidence is indicated. A data sequence indicating an operational failure is required to reset FF15 in Figure 2-81.

The advantages of a data sequence defining the operational status of the camera system are as follows:

1. Interface with telemetry systems
2. Provide a base for the design of automatic checkout equipment of the AGE
3. Provide continuous in-flight monitoring of operational status by recording appropriate data sequences by the mission recorder

Events monitored during the photographic and calibration operation (Modes I and IV) are as follows:

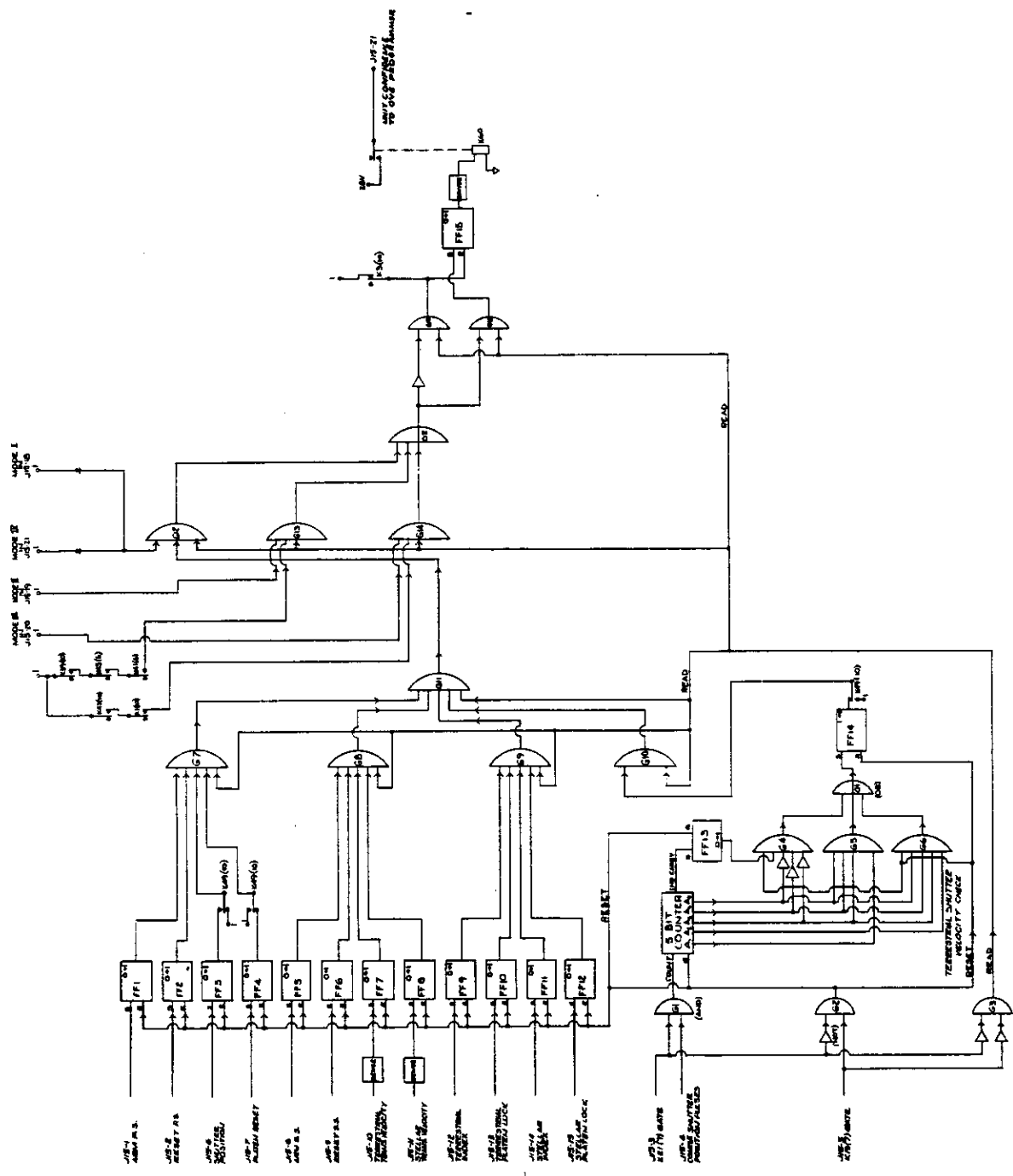


Fig. 2-81 — In-flight confidence block diagram

1. Arm terrestrial shutter/open thermal shutter
2. Reset terrestrial shutter/close thermal shutter
3. Terrestrial shutter velocity (Mode I only)
4. Terrestrial shutter position (Mode IV only)
5. Platen reset (Mode I only)
6. Arm stellar shutter/open thermal shutter
7. Reset stellar shutter/close thermal shutter
8. Terrestrial transport system velocity
9. Stellar transport system velocity
10. Terrestrial platen unlock/lock
11. Stellar platen unlock/lock
12. Power sequencer mode selector
13. Response to OCV/calibration film sensor

Events monitored during the forward and aft RV shutdown operation (Modes II and III) are as follows:

1. Power sequencer/mode selector response to mode initiation
2. Film cut
3. Radius arm position
4. Mode completion

A telemetry circuit would process analog, digital or discrete input signals into a time-multiplexed PCM format. Analog signals are quantized to a particular bit level by an A/D converter. Digital words (data sequences) and discrete inputs bypass the A/D converter and are combined into a particular output format. This circuit is the camera system interface with the space-ground link for the monitoring of system performance.

2.3 GOPSS SYSTEM INTEGRATION

Previous sections discussed the individual sensor systems and complimentary auxiliary systems which function as the "on-board" equipments. In this section, the integration of those systems into the GOPSS will be discussed from the aspects of configuration and function.

2.3.1 System Configuration

The system consists of three sections: the Orbital Control Vehicle (OCV), the Data Collection Module (DCM), and the Recovery Section (RS). See Figure 2-82. A discussion of each of these is given in the following paragraphs.

2.3.1.1 Orbital Control Vehicle

A launch vehicle consisting of a combination of an Atlas Booster and an Agena D second stage was specified at the outset of the program and has formed the basis for the configuration limitation of the payload. The Agena performs a dual role, as a second stage booster and on orbital attitude stabilizer; it is in this latter role that the Agena becomes the orbital control vehicle for the GOPSS.

The Agena D vehicle in its orbital configuration is 248 inches long and 60 inches in diameter. Its basic weight of 1490 pounds plus the required subsystems and propellant and gasses for a 15-day orbital life brings its injection weight to a 2925-pound minimum. This weight could rise to as high as 3200 pounds if additional gasses were required for stabilization. Using the 3200-pound weight for the Agena, a payload weight limit of 2800 to 2900 pounds (for 120 to 180-nautical mile altitudes at 0.10-degree orbital inclination) is possible. For this program, 2400 pounds was initially established as a design goal.

The Agena provides for a stabilized attitude "on orbit" through its gas-operated attitude control system. This system is aligned by narrow band optical horizon and wide band gyro sensors, providing a one sigma attitude pointing error of 0.0032 radian in roll and pitch and 0.0041 radian in yaw. Maximum attitude rates are 0.000105 radian per second in roll and yaw and 0.000140 radian per second in pitch.

The Agena programmer will supply operational mode signals to the payload plus V/h and exposure control signals. In addition to payload operations, the programmer operates the power and control functions of the OCV on orbit and during the recovery sequence. The Agena can deliver 19,500 watt-hours of electrical energy to the payload during its orbital life. This power would supply an unregulated voltage of 28 vdc which would drop to 23 vdc when 80 percent (15,600 watt-hours) of the energy has been consumed. The payload sensor systems operate at 20 to 18 vdc unregulated, while those payload subsystems required for control will be furnished regulated 20 vdc. Some 400-cycle ac is required, but this will be generated within the payload electronics system.

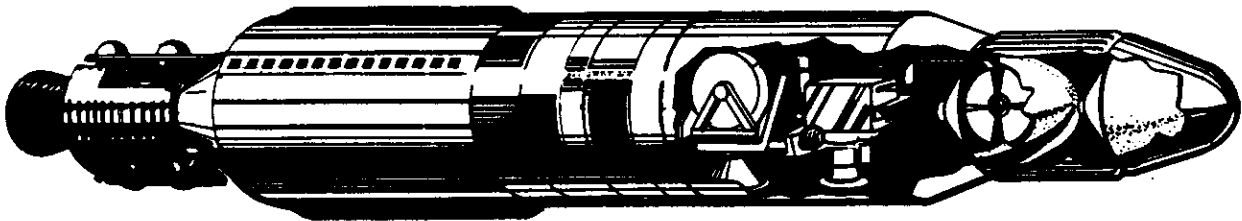


Fig. 2-82 — System configuration

The physical configuration of the Agena will be the standard one with the DCM bolted to the forward interface ring of the Agena.

2.3.1.2 Data Collection Module

The DCM section is a unitized structural assembly which contains all the sensors (except the accelerometer) and their associated electronics. (See Figure 2-83.) In the aft end of the section are housed the film supply cassette assembly and the radar altimeter antenna and electronic package. In the forward half the camera assembly is mounted with the thermal shutters, photo-sensor system electronics modules, clock, and the transit transponder. The electronic modules are secured to the outer structure of the DCM.

The structure of the DCM is a riveted semimonocoque design having five longerons that run its entire length and terminate at either end in large continuous rigid rings, with an additional ring in the central section of the structure. The remainder of the longerons in the lower half of the structure are really intercostals because they are interrupted by the forward apertures of the lenses and the antenna. The circumferential rings in the area of the apertures are also interrupted and, therefore, become intercostals. A thin aluminum skin is riveted in this framework to complete the DCM structure.

The two side longerons which run the length of the package are torsionally rigidized to accept the loads of the cassette and camera mounting structures which are bolted to them. A separate bridge structure across the lower aft end of the DCM structure accepts the radar antenna and electronics assemblies. Light cones are fastened to the structure at the skin and support the thermal shutters close to the objectives of all three lenses. Pleated rubber boots complete the light cone function by closing the gap between the thermal shutters and the ends of the lenses.

The structure is 56 inches in diameter and 86 inches long. Two thin fiberglass bulkheads at either end provide light seals for the section and act as thermal barriers. The completed preliminary thermal design dictates the following requirements:

1. Thermal bulkheads
2. Internal gold surface coating
3. Aluminized mylar insulation around cameras
4. An external paint mosaic
5. Camera mounting points to be thermally insulated with suitable bushings and washers

Both film supply cassettes and the camera assembly have been made easily removable because of their great weight. The supply cassettes are removable as a unit from the aft end to facilitate loading of fresh film, and the camera assembly is removable so that ground calibration procedures are readily accessible. Mechanization of the removal procedures is implemented by means of rollers that may be jacked down from the structure supports onto the side longerons.

Air vents are provided to permit atmospheric pressure changes but prevent light leakage to the interior of the DCM. The DCM interior is to be light sealed; however, the film path will be covered with light opaque fiberglass film chutes as an additional precaution. The light seals of the package will permit a pressure difference between the outside and inside of the DCM at operational altitudes to permit leakage of an inert gas and maintain a partial pressure internally to reduce the affects of corona.

There are three separate harness systems within the DCM. One harness passes through the DCM, connecting the recovery vehicle with the OCV for operation of the RV's. A second harness is employed to interconnect the functioning sensor elements of the DCM, i.e., photo-sensor

~~SECRET~~

system and auxiliary sensors. A third harness is used to connect those points in the functioning systems which serve as telemetry or monitoring points to the confidence module telemetry equipment in the OCV and preflight test connector. This harness is functionally separate so that it may easily be shielded from spurious signals.

2.3.1.3 Recovery Section

The recovery section consists of two 430-pound Mark VIII recovery vehicles and a support structure. Both vehicles contain film takeup cassettes, each capable of accepting approximately 210 pounds of film.

An alternate to either of two Mark VIII recovery configurations is a dual Mark V recovery system. The Mark VIII recovery systems are designed around a recovery vehicle capable of returning 225 to 250 pounds of film per vehicle for a system total of 450 to 500 pounds. The Mark V is a smaller but operational recovery vehicle and returns approximately 110 pounds of film per vehicle or a system total of 220 pounds in a dual configuration. This configuration could be attached to the DCM in much the same manner as the Mark VIII inline arrangement previously shown.

The dual Mark V recovery system capacity of only 7000 frames of terrestrial photography, therefore, would require operation at higher altitudes to provide the necessary system coverage (i.e., 113×10^6 nm² coverage at 220 nm altitude at 70 percent overlap).

Two support configurations have been considered. Both configurations cantilever the vehicles from the forward DCM interface ring and are designed to locate the recovery vehicle centers of gravity on the Agena roll axis. Overall system length is approximately 10 feet in both cases.

The first arrangement allows an inline recovery vehicle configuration, with both vehicles facing forward. (See Figure 2-84.) A truncated conical shell structure is rigidly attached at its base to the forward DCM interface ring. The forward end of this shell is flanged to support the aft recovery vehicle. An intermediate cylindrical fairing envelopes the aft RV, supports the forward RV, and is tied to the DCM through the conical shell. Therefore, the external configuration may be considered an aerodynamic fairing capable of serving as a thermal shroud.

The second arrangement, which appears to be preferable from a mission reliability aspect, allows a canted recovery vehicle configuration, with both vehicles facing aft and canted 60 degrees from the Agena roll axis. (See Figure 2-85.) This configuration is supported by a welded tubular steel truss. The base of the truss is cantilevered from a rigid DCM interface ring. Integral with the truss are two canted rings to which the aft sections of the recovery vehicles are rigidly tied. The truss also supports all ejection guides and release mechanisms.

Past studies have indicated the suitability of the canted RV arrangement over the inline arrangements; this is based on a mission reliability aspect, in that the satellite system would fly forward in the canted arrangement always at an attitude or angle suitable for recovery. In the inline arrangement, the aft end of the satellite would be in the flight direction and, to accomplish recovery operations, the satellite would have to be pitched down to approximately 60 degrees to start recovery. This requires a fully operative attitude control system; in addition, failure to eject the forward RV precludes recovery of the aft RV. Both have been included here because the inline arrangement is a flight proven concept, and it imposes less of a weight penalty.

This configuration will also incorporate a thermal shroud enveloping approximately 240 degrees of the truss, allowing control over the effects of direct solar radiation on the otherwise exposed recovery system.

~~SECRET~~

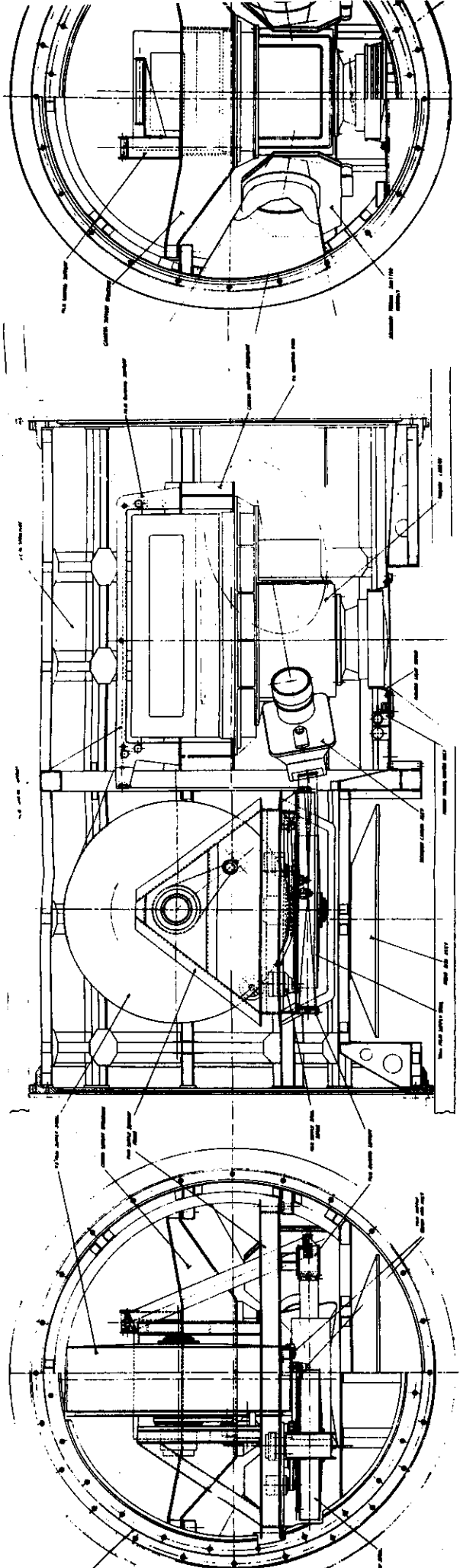


Fig. 2-83 — Data collection module (DCM)

2-205

~~SECRET~~

SECRET

2-207

SECRET

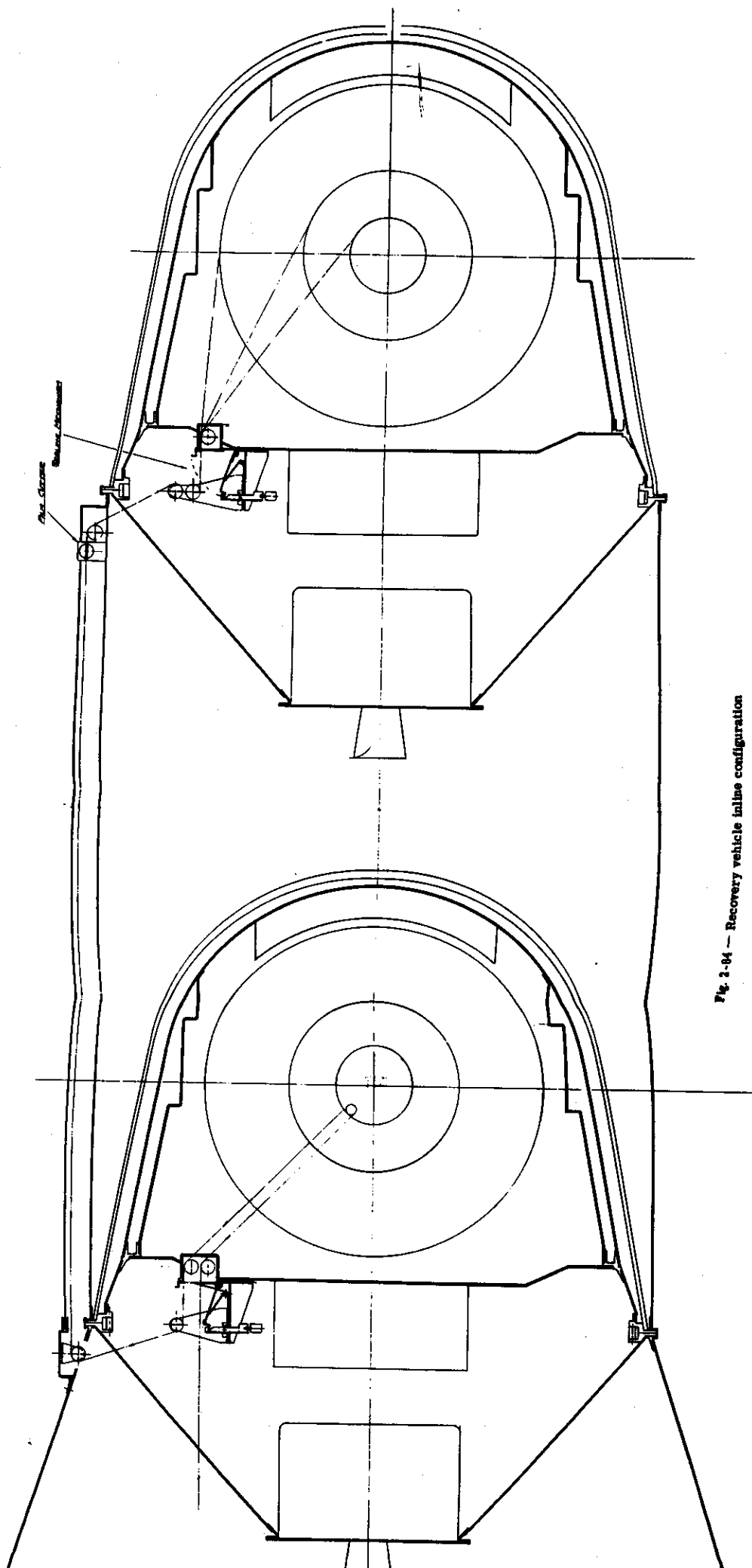


Fig. 2-04 — Recovery vehicle inline configuration

~~SECRET~~

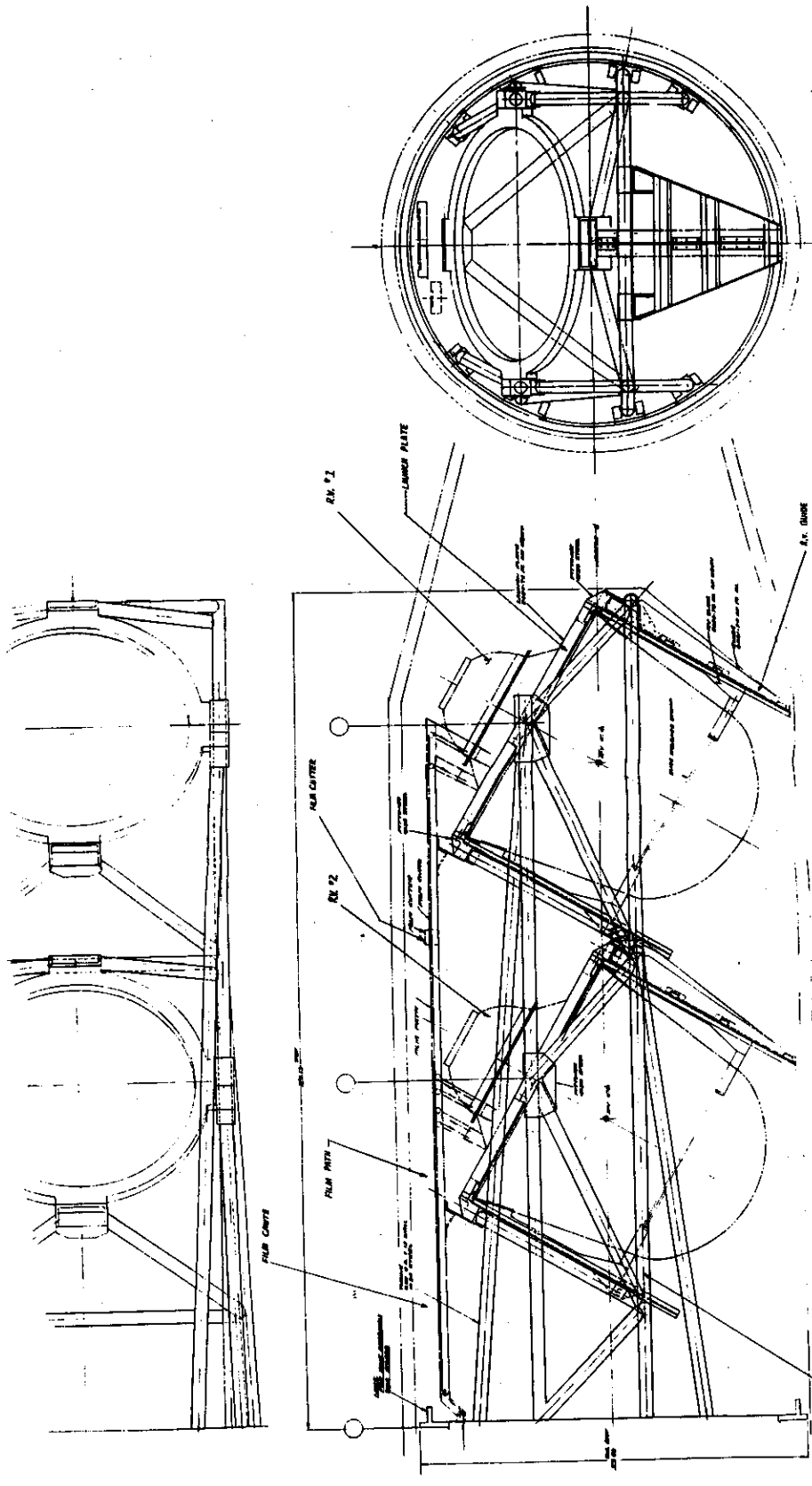


Fig. 2-85 — Recovery vehicle, canted configuration

SECRET

The film path through the two styles of recovery sections is functionally the same. The 9 1/2-inch wide and 70-millimeter film pass from the DCM through chutes to the aft RV. In the aft RV, the film passes around a roller onto the cores of the takeup spools and back out of the RV along film chutes to the forward RV. The two mission recorders are located in the RV's, one in each of the side frames of the cassettes.

The films shall pass through a cutter/sealer assembly to be mounted on a bulkhead in the RV. (See Figure 2-86.) This assembly shall have a two part operation and shall be energized by means of two separate signals, one "cut" the other "seal". This solenoid-actuated assembly shall consist of a slotted conical or tapered cutter through which the film shall pass. The gap between the tapered cutter and its housing shall be 0.001 to 0.002 inch wide. This gap shall serve as the shear spacing during the cutting process. The cutter shall be preloaded by means of a torsion spring and restrained by a solenoid actuated pin. On actuation, the cutter rotates, shearing the film, and comes to rest with its slot rotated 90 degrees from its original position. After this cutting action has taken place, the slots in the cutter and housing do not line up, nor do any portions of the openings line up. Now the seal command is given and a second solenoid releases a pin which permits the cutter to move axially, under spring loading, and mate with the female taper in the housing, thus tightly sealing the film path opening.

2.3.2 Mission Operation and Coverage

The GOPSS on-orbit operations have been described, in part, throughout this report. In this section, the designed operations and functions of the system are summarized.

There are two basic limitations to the duration and coverage of the GOPSS mission.

1. The mission is limited to 13,300 frames of terrestrial photography. This is gated by the recoverable weight capacity of the dual Mark VIII recovery vehicle system.
2. The mission is limited to 19,500 watt-hours of payload power. This limit is imposed by the standard battery pack of the Agena D. Judicious design of electrical components and the choice of auxiliary sensors preclude the necessity of extra battery packs to maintain line voltage above 20 vdc.

The OCV programmer is the key element to mission control; it is intended to provide programmed V/h and exposure control signals and the "on" and "off" signals for the photo-sensor system modes in addition to those required for Agena and recovery vehicle functions. Continuously operating systems of the GOPSS (transit, radar altimeter) may be controlled directly from the ground through the OCV receiver.

2.3.2.1 Mission Modes

The programmed intermittent operations comprise four operational modes of the photo-sensor system.

Mode I Photo-Payload Operation

In Mode I, the terrestrial and stellar cameras operate simultaneously to photograph the desired targets. Time and altitude data are recorded on each frame of both films, and fiducial references are recorded on each frame taken by the terrestrial camera. During the mode, the vehicle is maintained in its conventional flight attitude. The purpose of Mode I is to gather primary mission photodata.

SECRET

~~SECRET~~

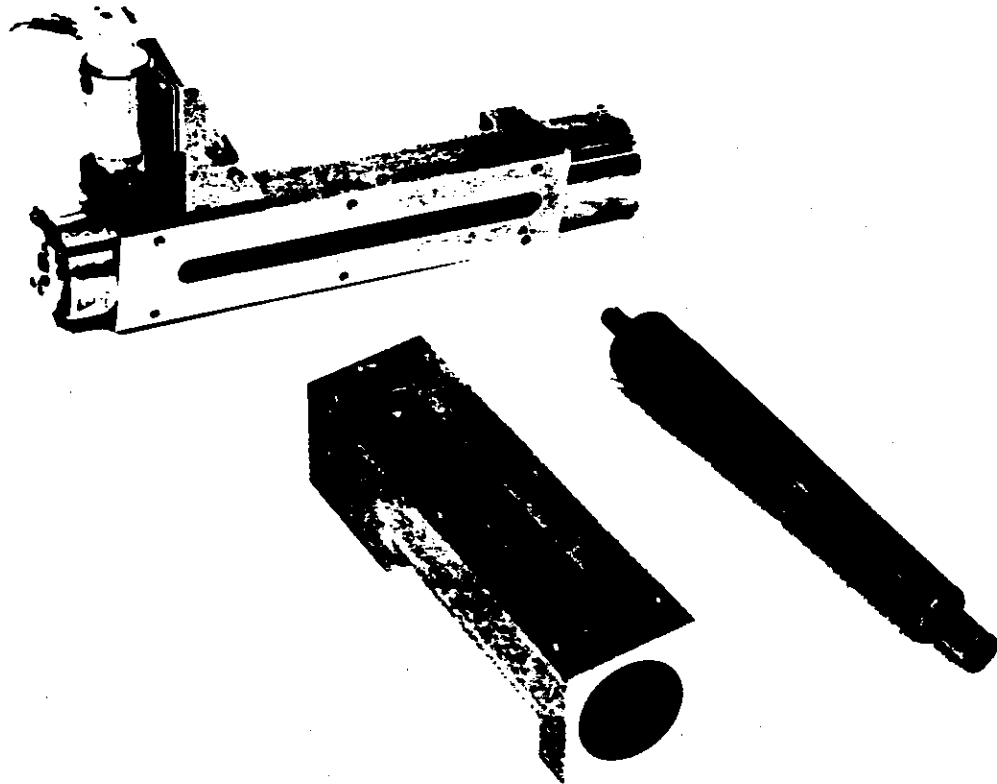


Fig. 2-86 — Cutter/sealer assembly

~~SECRET~~

Mode II Forward RV Shutdown Operation

Mode II is a programmed operation which initiates the cut and wrap operation when approximately one-half of the mission film supply has been exposed and wrapped onto the forward takeup spool. The programmer ensures that photography is not interrupted; this operation only occurs during transit of the dark part of the earth. The film webs (stellar and terrestrial) are cut between the forward and aft cassettes, the trailing edge of the cut films are wrapped onto the forward spool, and the forward RV is sealed. While the final wrapping and the sealing of the forward cassette is progressing, the leading edge of the cut film is wrapped onto the aft takeup spool. When the aft cassette has thus been readied for operation, operation can be reactivated with film now being taken up in the aft RV. Mode II is an operational function that does not gather mission data.

Mode III Aft RV Shutdown Operation

Mode III interrupts the mode currently in progress when the mission film supply has been completely, or nearly completely, exposed. Photography is halted and all of the remaining stellar and terrestrial film (or in some cases a predetermined length) are wound onto their respective aft takeup spools. The cutters are activated (whether or not film remains in the film track), and the takeups remain activated for a predetermined period to assure the complete winding of any remaining trailing edge onto the spools. After the winding period, the aft RV is sealed and the payload photo system is shut down. Mode III is an operational function that does not gather mission photo or orbital data (although ground tracking may continue).

Mode IV Camera Calibration (In-Flight)

In Mode IV, the terrestrial and stellar cameras operate to take simultaneous starfield photography which is subsequently cross-checked with the original calibration records to determine if any inflight physical changes have occurred in the photographic system. This mode will occur only at the beginning and the end of the mission, according to present philosophy.

An emulsion, different from the terrestrial camera normal film (EK type 2475), is spliced with magnetic tape into that camera's film web at predetermined intervals, and the location of the special emulsion in the web serves to activate a programmer which starts and ends the calibration cycle.

A signal indicating the magnetic splice interrupts the mode in operation, rolls the vehicle for starfield targeting by both cameras, varies the exposure speed of the terrestrial camera, and starts the calibration exposure sequence. Another signal, generated by the end of the calibration emulsion, halts the calibration sequence, rolls the vehicle back to the conventional attitude, and re-initiates the interrupted operational mode.

A typical mission profile is as follows:

1. After Agena Burn (launch shroud has been ejected) and the satellite has achieved orbital altitude, the auxiliary sensor systems are turned on and the OCV programmer is turned on.
2. The OCV programmer initiates Mode IV operation (camera calibration) after several orbits (20) to achieve thermal stabilization. The satellite is rolled 180 degrees and de-pitched (i.e., pitch rate is zero) and stabilizes the satellite at that attitude. Six to twelve calibration frames are taken with each camera and then the calibration film sensor indicates the end of the calibration film and Mode IV is automatically shut down.

3. The OCV programmer then begins operating the photo-sensor system in Mode I for predetermined lengths of time. The altimeter, clock, transit transponder and accelerometer are running and the data is being recorded in the mission data recorder.

4. At that point in the mission when the forward cassette reels are filled (a radius arm sensor indicates this condition), the OCV program turns off the camera systems going into the "night" phase of the orbit, and Mode II is initiated. After Mode II is completed, the camera systems are ready to run using the aft cassette.

5. When the photographic mission is near completion, the calibration film sensor indicates the start of the last piece of calibration film and Mode I operation is automatically shut down. Mode IV is initiated and the "end of mission" calibration pictures are taken. When Mode IV is completed, Mode III is initiated and all the film is slewed from the camera system into the aft RV. If the mission is to be terminated prior to the use of all the terrestrial film and if calibration photography is desired, then a variation in Modes III and IV is utilized. Mode III is initiated and film is slewed until the calibration film sensor stops Mode III operation and initiates Mode IV. After Mode IV completion, the system reverts to Mode III for final shutdown of the aft RV.

6. Auxiliary data may be continually acquired until recovery operations are begun. Signals from the OCV programmer control recovery operations ejecting the forward RV first, followed by the aft RV ejection.

2.3.2.2 Mission Coverage

To achieve total coverage of all land masses with the GOPSS, the system must have an estimated coverage capability of 114×10^6 square nautical miles. To provide a frame of reference, the earth's surface is nominally 141×10^6 square miles, of which 41.8×10^6 square miles is land mass.

In the near polar orbits proposed for this mission, redundancy of coverage increases with the secant of the latitude, limited only by the total number of photographic passes. With precise sequencing of the camera system, this redundancy will be minimized to maintain a reasonable balance between the complexity of the required sequencing and the optimization of redundant coverage.

In the computation of the required coverage, allowances have been made for the coverage required to photograph groups of islands, variation of sidelap with latitude, and variation in the land mass area as a function of latitude.

The effective coverage of the GOPSS at 200 nautical miles altitude with a dual Mark VIII recovery system is:

$$C = 40.9 (1-V) h^2 w \text{ square nautical miles}$$

where V = 70 percent overlap

h = 200 nautical miles

w = 440 pounds of film

C = 215×10^6 square nautical miles

Table 2-20 shows the coverage characteristics of the dual Mark V recovery system. Table 2-21 shows the coverage characteristics of the Mark VIII system designs, trying to achieve a minimum of 114×10^6 nm² coverage.

Table 2-20 — Dual Mark V Recovery System Coverage

Altitude, nautical miles	Coverage/Frame, square nautical miles	Total Coverage, square nautical miles
160	8,500	58.8×10^6
180	10,500	73.5×10^6
200	13,300	93×10^6
220	16,200	113×10^6
240	19,200	135×10^6

Table 2-21 — Dual Mark VIII Recovery System Coverage

Altitude, nautical miles	Coverage/Frame, square nautical miles	Total Coverage, square nautical miles
160	8,500	137×10^6
180	10,500	174×10^6
200	13,300	215×10^6
220	16,200	260×10^6
240	19,200	362×10^6

2.3.3 System Power Budget

In the previous section, a typical mission profile was presented. The power consumed by the sensor equipments cannot exceed the basic Agena supply capability of 19,500 watt-hours and, during the study, consideration was given to the choice and design of the subsystems so that they would not exceed 80 percent of this value. (The high altitude missions will consume more energy because the camera systems require more running time before all the film is expended).

Energy is computed on a cyclical and a continuous basis. For those components in the camera system which run on a cyclical basis, the average power consumption per cycle is multiplied by the total number of frames or cycles (13,300) to get the mission power consumption. The average power consumption of those camera system components which run continuously during Mode I is computed by multiplying the average power by the total running time. The total running time is computed as follows:

$$T = t_c \times \text{number of frames}$$

$$\text{where } t_c = \text{cycle time} = \frac{(1 - \text{overlap})(\text{format length})}{V/h \times \text{focal length}}$$

$$\text{overlap} = 0.67$$

$$\text{format length} = 460 \text{ millimeters}$$

$$\text{focal length} = 300 \text{ millimeters}$$

$$V = \text{orbital velocity}^* = 25,450 \text{ feet per second}$$

$$h = \text{altitude in nautical miles}$$

As example for $h = 160$ nautical miles, $T = 72$ hours

A typical power consumption tabulation for a 160 nautical mile altitude is as follows:

Terrestrial Camera

1. Shutter (9 watts × 72 hours)	648 watt-hrs
2. Platen $(18 \text{ watt-sec} \times \frac{13,300}{3,600})$	66
3. IMC $(19 \text{ watt-sec} \times \frac{13,300}{3,600})$	70
4. Supply Spool Drive (3 watts × 72)	216
5. Takeup Spool Drive (5 watts × 72)	360
6. Index Drive $(30 \text{ watt-sec} \times \frac{13,300}{3,600})$	111
7. Fiducials $(5 \text{ watt-sec} \times \frac{13,300}{3,600})$	18
8. Data Block $(0.057 \text{ watt-sec} \times \frac{13,300}{3,600})$	0
9. Electronics (2 watts × 72)	<u>144</u>
Subtotal	1633 watt-hrs

*This assumes an error in V of ±0.8 percent from $80 \leq h \leq 200$ nautical miles.

Stellar Camera

1. Shutters $(14.5 \text{ watt-sec} \times \frac{13,300}{3,600})$	54 watt-hrs
2. Supply Spool Drive (3 watts \times 72)	216
3. Takeup Spool Drive (5 watts \times 72)	360
4. Index Drive $(30 \text{ watt-sec} \times \frac{13,300}{3,600})$	111
5. Platen $(18 \text{ watt-sec} \times \frac{13,300}{3,600})$	66
6. Data Block $(0.057 \text{ watt-sec} \times \frac{13,300}{3,600})$	0
7. Electronics (2 watts \times 72)	<u>144</u>
Subtotal	951 watt-hrs

Thermal Shutters

1. Terrestrial $(15 \text{ watt-sec} \times \frac{13,300}{3,600})$	55 watt-hrs
2. Stellar $(2 \times 10 \text{ watt-sec} \times \frac{13,300}{3,600})$	<u>74</u>
Subtotal	129 watt-hrs

Intervalometer (5 watt \times 72 hrs)

360 watt-hrs

Total for Photosensor System

3073 watt-hrs

Auxiliary Systems

1. Altimeter (10 percent duty cycle) (12 watts \times 360 hrs)	4320 watt-hrs
2. Accelerometer (15 watts \times 360)	5400
3. Clock (5.5 watts \times 360)	1980
4. TRANSIT Transmitter (4.7 watts \times 360)	1692
5. Mission Recorder (0.6 watts \times 360)	<u>216</u>
Subtotal	13,608 watt-hrs

GOPSS Payload (160 nautical miles)

16,681 watt-hrs

Grand Total

16,681

The previous example was for a full film capacity and a total mission time of 15 days. The following formular may be used to determine the power consumption for varying mission durations, film capacities, and altitudes.

$$E = 0.047 \times n + 11.6 \times h \times n \times 10^{-4} + 38 \text{ tm}$$

where E = payload power consumption, watt-hours
n = number of frames
h = altitude, nautical miles
tm = total mission operating time, hours

The terms in the above equation reflect the number of variables in the mission profile; they may be used in mission planning to preclude a power failure due to over consumption.

2.3.4 System Weight and Balance

This section provides a summary of the weights, centers of gravity, and inertias for both the inline and canted RV arrangements.

2.3.4.1 System Weight

A summary of the weight of the two GOPSS configurations is given in Table 2-22 for the canted RV arrangement, and in Table 2-23 for the original inline RV arrangement. Although the "canted" is desirable from a mission reliability standpoint, a clear-cut weight difference is shown to be in favor of the "inline" arrangement. The assumed error on the totals is ±100 pounds. Structural weights are assumed to be high because they reflect the weight of the first designs which will not be optimized until Phase II.

The launch shroud weight has not been included in the system weight because it was not designed as part of this phase. However, it is assumed to have a 550-pound gross weight and, at a 3:1 exchange, its net or effective payload weight is assumed to be 184 pounds.

2.3.4.2 System Centers of Gravity and Inertias

Using a right-handed coordinate system, with X on the Agena roll axis and positive aft, Y is the pitch axis and Z is the yaw axis (positive earthward). For both the inline and the canted configurations, Station 116.0 will coincide with the forward end of the forward DCM interface ring.

During the mission, the centers of gravity will undergo continual displacements due to film transfer. These relocations are tabulated, allowing the forward recovery vehicle to fill first.

Canted Configuration
(\bar{Y} and \bar{Z} , inches)

	Launch	1/4 Mission	1/2 Mission	3/4 Mission	Full Mission
\bar{X}	104.1	97.0	89.9	85.2	80.4
\bar{Y}	-0.1	-0.2	-0.4	-0.5	-0.6
\bar{Z}	-0.8	-0.1	+0.5	+1.3	+2.0

Inline Configuration
(Y and Z, inches)

	Launch	1/4 Mission	1/2 Mission	3/4 Mission	Full Mission
\bar{X}	118.4	108.1	99.9	95.5	89.9
\bar{Y}	-0.1	-0.2	-0.4	-0.5	-0.7
\bar{Z}	-0.9	-0.7	-0.3	+0.0	+0.3

The total system inertias (pound-inches²) are given about the three axes for the launch configuration only.

Canted Configuration

I_{xx}	I_{yy}	I_{zz}	k_{xx}	k_{yy}	k_{zz}
527,588	11,586,066	11,422,927	14.4	67.5	67.0

Inline Configuration

I_{xx}	I_{yy}	I_{zz}	k_{xx}	k_{yy}	k_{zz}
466,325	8,571,859	8,506,402	14.2	60.9	60.7

~~SECRET~~ [REDACTED]

Table 2-22 — System Weight—Canted Configuration

Data Collection Module

Camera assembly

Terrestrial	257.4	
Stellar	43.2	
Insulation	<u>5.0</u>	305.6

Film supply cassette 131.3

Film

9 1/2-inch	371.0	
70-millimeter	<u>50.0</u>	421.0

Photosensor electronics 54.1

Auxiliary data equipment

Radar electronics	24.0	
TRANSIT transmitter	6.4	
Transmitter antennas	4.0	
Altimeter dish	20.0	
Accelerometer	<u>4.5</u>	59.9

Structure 260.0

Subtotal 1231.9

Recovery Subsystem

Forward recovery vehicle 430.0

Aft recovery vehicle 430.0

Forward takeup cassette 57.8

Aft takeup cassette 57.8

Recovery system support structure 319.0

Auxiliary data equipment (recorders) 16.0

Subtotal 1309.6

Total System Weight 2542.5

~~SECRET~~ [REDACTED]

Table 2-23 — System Weight—Inline Configuration

Data Collection Module

Camera assembly

Terrestrial	275.4	
Stellar	43.2	
Insulation	<u>5.0</u>	305.6

Film supply cassette 131.3

Film

9 1/2-inch	371.0	
70-millimeter	<u>50.0</u>	421.0

Photosensor electronics 54.1

Auxiliary data equipment

Radar electronics	24.0	
TRANSIT transmitter	6.4	
Transmitter antennas	4.0	
Altimeter dish	20.0	
Accelerometer	<u>4.5</u>	59.9

Structure 243.0

Subtotal 1214.9

Recovery Subsystem

Forward recovery vehicle 430.0

Aft recovery vehicle 430.0

Forward fairing 64.0

Aft fairing 39.0

Forward takeup cassette 57.8

Aft takeup cassette 57.8

Auxiliary data equipment (recorders) 16.0

Subtotal 1094.6

Total System Weight 2308.5

2.4 SUPPORTING STUDIES

2.4.1 Payload Structural Study

Due to the nature and duration of powered flight shock loading, the system response approximates the response to the static equivalent of these loadings. Since the shock loading represents the maximum acceleration loadings, it is reasonable to design the system to withstand the effects of these shocks applied as static loads.

The g loadings are defined as follows:

Axial	± 10.0 g
Lateral	± 5.0 g

These loads are limit loads, so the "Margin of Safety" is defined as:

$$\text{M.S.} = \frac{\text{Ultimate Allowable Stress}}{1.25 (\text{Actual Stress})} - 1.0 \geq 0.0$$

All components have been designed to have a first natural frequency in excess of 25 cps. Two notable exceptions are the truss-configuration recovery section and the film supply cassette. In both cases, the application of the above criterion will cause prohibitive weight problems. However, it is felt that the structural integrity of the system can be maintained if the frequency criterion for these two components is relaxed to 12 to 15 cps.

2.4.1.1 Recovery Section

The canted recovery section consists of two 430-pound recovery vehicles, appropriate support structure, film chutes, cutters, and ejection system. Integral with each vehicle is a 58-pound cassette assembly capable of accepting approximately 210 pounds of film. When mounted to the support structure, these vehicles are facing aft and canted 60 degrees from the Agena roll axis.

The basic support structure is a welded steel (4130) tubular truss. The tubing shall be 2.0 inches outside diameter, with a 0.125-inch wall. Integral with the truss shall be two rigid canted RV support rings. Truss loadings shall consist of the previously defined limit loads applied at the centers of gravity of the unloaded RV's. Under the loads defined, minimum member margin of safety is +0.84 with the maximum deflection at the free end of 0.19 inch. It is shown that all members are stable in all modes.

Due to the "cantilever-canted" configuration, support structure weight would become prohibitive if any effort were made to achieve a first natural frequency above 25 cps. Results of a dynamic analysis show the first natural frequency to be 12 cps. This value is felt to reasonably

~~SECRET~~

approximate the minimum acceptable component natural frequency. A more rigorous analytical effort may provide a slightly lighter, stiffer structure. This will be presented in Phase II.

2.4.1.2 Data Collection Module

The Data Collection Module contains the terrestrial camera, stellar cameras, film supply cassette, auxiliary data systems, and photo sensor electronics. The structure will carry the inertia load of the above components and of the Recovery System, during ascent, and shall provide environmental control on orbit.

The structure consists of an internally stiffened cylindrical shell with appropriate longitudinal supports for the camera assembly and film supply cassette. Interface loads are applied to the cylinder from the Recovery System through a forward interface ring, and are reacted at a bolt circle within the Agena OCV skin-line through an aft interface ring. The cylinder, after installation of appropriate bulkheads, shall form a lighttight enclosure for the film path.

The primary structure has been designed for a maximum loading of 10 g axially and 5 g laterally.

A stiffened, 0.080-inch-thick aluminum skin will remain stable under this loading. It is necessary to use appropriate intercostals to minimize panel dimensions, as panel instability is the controlling parameter. All longerons and rings are shown to be structurally compatible with the loading from the Recovery System. The camera assembly and film supply cassette supports have been provided with high torsional rigidity to minimize DCM shell loading.

Data system and electronic component supports shall be designed to resist the maximum expected vibratory response.

The camera system is removed through the forward end of the DCM, while the film supply cassette is removed through the aft end. Both components roll on appropriate support rails. Access is provided through load-bearing doors in the outer shell to allow minor adjustment after integration of the system.

2.4.1.3 Camera Support

The camera system support structure consists of two main load-carrying members. Structural cross braces, combined with shear resistant panels, separate and stiffen these main members. The camera is hung from the support at three points such that the camera center of gravity is in the plane of the support. The support spans the DCM and is tied to two suitably stiffened longerons at several attachment points. All support members are structural aluminum shapes, although not necessarily standard shapes.

The camera is assumed to weigh 304 pounds, to which is applied 10 g axially and 5 g laterally. To ensure a camera support system natural frequency of above 25 cps, the structure becomes deflection limited with no significant stresses.

It is shown that the support system has an axial, first natural frequency of 202 cps, and a lateral first natural frequency of 54 cps, with maximum deflections of 0.0024 inch and 0.017 inch respectively.

Initial location of the camera mounts with respect to the Agena OCV interface need not be made to an accuracy closer than 0.5 degree, which can easily be attained with normal fabrication tooling.

~~SECRET~~

2.4.2 Thermal Analysis

2.4.2.1 Summary

To develop a thermal design philosophy and a method of approach, the functions of the thermal analysis and control system must be cited; these are as follows:

1. Maintain the optical elements at a uniform temperature throughout the mission
2. Minimize temperature gradients in the lens elements
3. Prevent defocusing and scale changes of the optical system caused by thermal expansion or contraction of the lens support structure
4. Maintain the temperature of the electrical components within specified limits
5. Prevent mechanical and structural failure

The thermal analysis must show that these functions can be performed throughout the mission.

2.4.2.2 Results

It is possible to point out some of the design features and temperature responses of the camera system, although the entire system and the mission analysis will not be completed until the detailed design phase. These are as follows:

1. A thermal shutter is required for the terrestrial camera. By opening this cover only when the system is in use, the temperature gradients in the lens elements will be minimized.
2. With a thermal-shutter cycle of two seconds open, twelve seconds closed, the radial temperature gradients in lens number 1 of the terrestrial camera will be well within acceptable limits.
3. The temperature differences from lens to lens in the terrestrial camera will be maintained within acceptable limits.
4. A thermal shutter, possibly with a heater on the inside surface, is required for the stellar camera.
5. The installation of the shutter drive and arming motors will have to be modified so as to re-distribute the heat generated by them.
6. Preliminary analysis of the thermal interaction of the DCM shell and camera box indicates that the camera box temperature can be passively maintained at $70 \pm 10^\circ\text{F}$.

2.4.2.3 Analytical Methods

2.4.2.3.1 Nodal Program

The purpose of the analytical portion of the analysis is to predict the temperature response of the various elements and components of the system during the entire mission. From the viewpoint of the thermal analysis, the system being investigated has a rather complex configuration. To determine the desired temperature responses, it was necessary to make some simplifications.

2.4.1.4 Film Supply Cassette

The film supply cassette is a riveted aluminum structure which utilizes structural shapes for load carrying members. Two main load-carrying members are stiffened by appropriate cross braces and loaded, through a stiffened film support structure, by the film g loading. The support spans the DCM and is tied to two suitable stiffened longerons at several attachment points.

The 9 1/2-inch film, with spools and drives, is assumed to weigh 410 pounds while the 70-millimeter film, with spools and drives, is assumed to weigh 60 pounds. The design g loading (10 g axially, 5 g laterally) is applied at the appropriate centers of gravity. As in the camera support, the structure becomes deflection limited to satisfy the frequency criterion (15 cps for the cassette).

The configuration as described, with a full load of film, has an axial first natural frequency of 17 cps, and a lateral first natural frequency of 16 cps, with the riveted construction providing high damping. Maximum deflections are 0.23 inch and 0.25 inch respectively.

All members are 7178-T6 aluminum. Since the system is deflection designed, primary stresses are relatively low, with a minimum margin of safety of +0.65. It is further shown that no instability of any form exists in any member under the applied loading.

Due to the relatively high deflections in the overall system, it may be necessary to provide a means of relieving excessive film tension during ascent. Should this not be provided, it may be extremely difficult to verify system structural integrity.

2.4.1.5 Terrestrial Camera Platen and Pressure Mechanism

The platen is analyzed as a rectangular plate under uniform pressure, simply supported at its boundaries. Standard plate equations yield maximum platen deflection.

Analysis of the bezel is accomplished utilizing beam theory. The eight tie-downs are considered as deformable supports of equal rigidity and are located in such a manner as to minimize bezel deflection. Standard beam theory yields bezel deflections at given points.

Total platen deflection is determined from the algebraic sum of the platen deflections and the bezel deflections. These total deflections shall be considered as a uniform displacement plus a nonuniform displacement. Since the uniform effect may be optically corrected, only the non-uniform deflections are considered. Analysis indicates in-plane platen deflections within allowable limits.

The flexures are designed to provide positive control on platen trajectory error during IMC. It is necessary to verify this control by defining platen equilibrium positions during its travel, and, in particular, during the exposure interval.

In the analysis, the flexures are assumed to obey beam theory, thus allowing calculations of the flexural spring constants. The platen-flexure system now becomes a spring-mass system to which is applied a constant force. Using work principles, the equilibrium positions of the system may now be determined as functions of variable spring constants and force parameters. If the variable spring constants are defined as functions of assumed machining errors, it may be shown that, for relatively loose machining tolerances, the flexures provide a platen trajectory error control well within acceptable limits.

The flexure is further analyzed for stability, in which the member is considered a fixed-free column under combined axial and lateral loading. The flexure is shown to be a stable mount. The increased lateral deflections produced by the end loads are shown to be insignificant.

Therefore, a numerical method was used in which it was assumed that the structure and optical elements were divided into discrete elements or nodes, coupled thermally, each with a uniform temperature at any given time. The nodal analysis performed for this design utilized an existing Itek digital computer program and is based on the heat balance equation:

$$\frac{dT_n}{d\theta} = \frac{1}{a_n} \left[\sum_{n=1}^N \sum_{m=n+1}^N b_{nm} (T_m^4 - T_n^4) + \sum_{n=1}^N \sum_{m=n+1}^N C_{nm} (T_m - T_n) + (\alpha_{1n} \kappa_{1n} + \alpha_{2n} \kappa_{2n}) - \sigma (\epsilon_n A_{\epsilon n} + \beta_n A_{\beta n}) T_n^4 + k_n f_n(\theta) \right]$$

- where
- T_n = temperature of node (n)
 - T_m = temperature of node (m)
 - θ = time
 - $a_n = wc_p$ = weight \times specific heat
 - σ = Stefan-Boltzmann constant = 0.171×10^{-8}
 - b_{nm} = radiation conductance factor from (n) to (m)
 - C_{nm} = conductance from node (n) to (m)
 - α_{1n} and α_{2n} = absorptivity
 - κ_{1n} and κ_{2n} = incident flux
 - ϵ_n and β_n = emissivity
 - $A_{\epsilon n}$ and $A_{\beta n}$ = nodal area
 - $k_n f_n(\theta)$ = joule heating

The equation above is simply a heat balance for each node which considers the heat capacity of the node, radiation interchange between the node and all others, incident heat fluxes, electrical heat dissipation from within the node, and radiation heat loss. Since the temperature of each node is dependent on the temperature of the other nodes in the system, the solution of (n) simultaneous equations is required to yield the temperature and time histories of each node.

Physical representations of the terms in the equation are as follows:

1. The term on the left represents the rate of change of energy stored in node (n).
2. The first term on the right represents the net exchange of radiant energy between node (n) and all other nodes within the system.
3. The second term on the right represents incident energy on node (n), e.g., from earthshine or albedo.
4. The third term on the right represents incident energy on node (n), e.g., from earthshine or albedo.
5. The fourth term on the right represents heat lost by node (n) to space.
6. The fifth term on the right represents joule heating of node (n).

2.4.2.3.2 Nodal Models

The ability of this computer program to predict the temperature response of the optical and structural members is a strong function of several factors. The first, and most basic, is the nodal model. That is, the nodal arrangement (or model) must adequately represent the actual configuration if meaningful results are to be obtained. The arrangement and number of nodes selected is generally based on a compromise between what is felt to be an accurate thermal

representation of the system on the one hand, and on the other, what can be analyzed within the time and economic restraints of the program.

1. Terrestrial Camera

Three different nodal models were utilized in the analysis of the terrestrial camera. These are shown in Figures 2-87, 2-88, and 2-89; they vary in complexity and the degree to which they represent the actual camera configuration.

The first and simplest model (Figure 2-87) was assumed to consist of the lens elements, a single shutter disc, and a black massless surrounding structure. Since the aim of the calculations for which this model was used was to determine gross temperature changes rather than detailed temperature gradients within each lens, each element was considered to be one node.

The second model (Figure 2-88) includes a conical extension at the outside of lens element number 1 which restricts the field of view to 80 degrees. Also, the shutter consists of three closely spaced discs, instead of one, which are thermally linked to the system in the following manner. It was assumed that the energy interchange between the front (rear) of the first (third) shutter disc and adjacent nodes involved a 4-inch diameter area of the shutter. Energy interchange between the shutter discs was considered; however, energy interchange between the shutter and the surrounding housing was ignored.

The third nodal scheme (Figure 2-89) is the most complex and also comes closest to the actual configuration of the camera. In this model the black massless structure is eliminated and the actual lens cell is included. In addition, not only are the three shutter blades included, but also the complete shutter mechanism, drive and arming motors and housing are included.

2. Stellar Camera (Figure 2-90)

This system consists on the lens elements, the surrounding structure, and a conical extension.

3. Data Collection Module (DCM)

A relatively simple model (Figure 2-91) was devised in order to examine the interaction of the DCM shell and the camera box. The DCM was assumed to be a ten-sided aluminum prism with fiberglass ends. A box representing the terrestrial camera was suspended inside. In order to simulate the energy exchange between the camera and the external environment, lens number 1 and the 80-degree conical extension were mounted in one side of the box. It was considered that the camera box was covered with aluminized-mylar multi-layer insulation (NRC-2) and that the inside surface of the shell was covered with a reflective coating.

2.4.2.4 Environment

The ability of the design analysis to simulate the temperature response of the camera system is also strongly dependent on the validity of the environment considered. Unlike many other systems the response of the lenses to a thermal environment depends not only on the magnitude of the heat flux, but, also on the wavelength. When subjected to incident energy whose wavelength is above 2.5 to 3.0 microns, the glass behaves as a black body, thereby absorbing all of the energy. On the other hand, it is transparent to radiation in between about 0.3 to 3.0 microns. Therefore, when the incident flux is solar or albedo the glass passes about 85 to 90 percent of the energy.

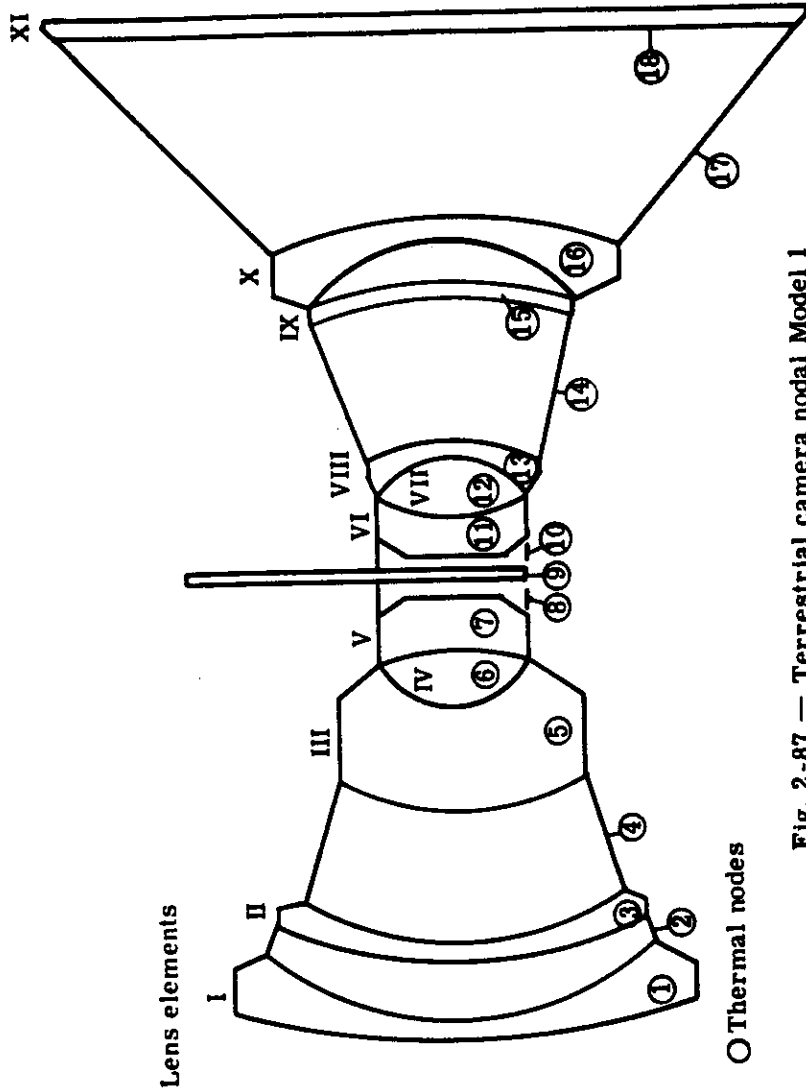


Fig. 2-87 — Terrestrial camera nodal Model 1

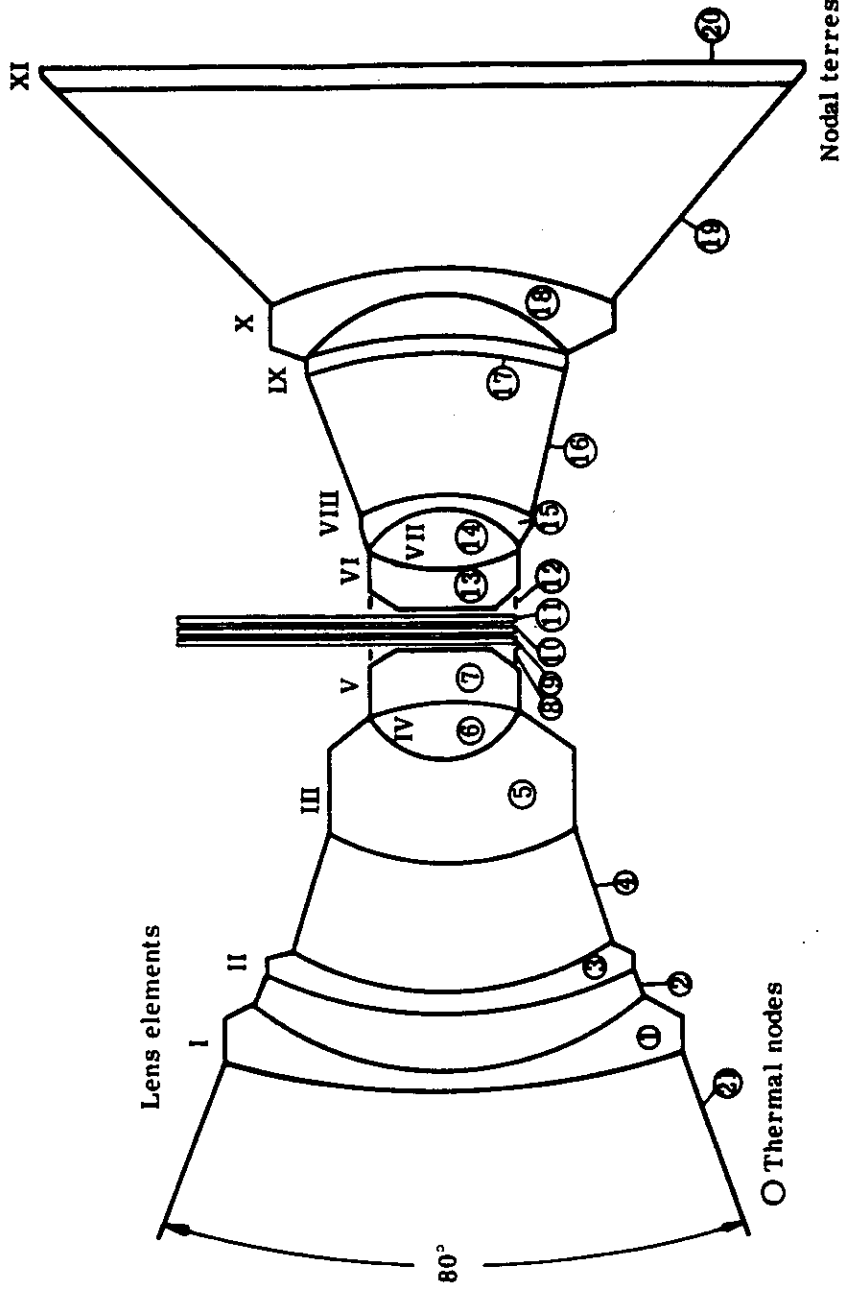


Fig 2-88 — Terrestrial camera nodal Model 2

~~SECRET~~

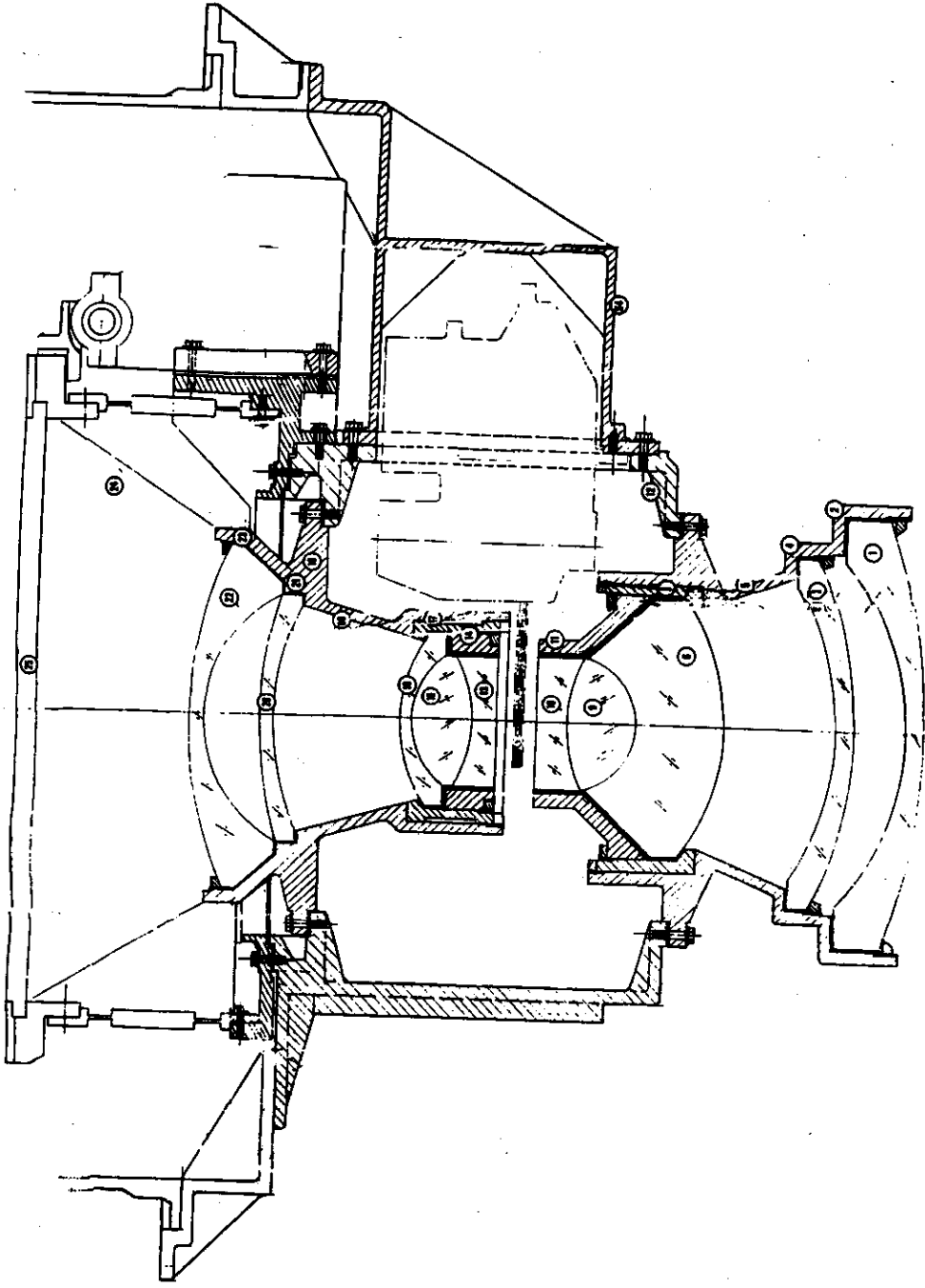


Fig. 2-89(a) — Terrestrial camera nodal Model 3, primary; see 112
(circled numbers indicate nodal points)

~~SECRET~~

SECRET

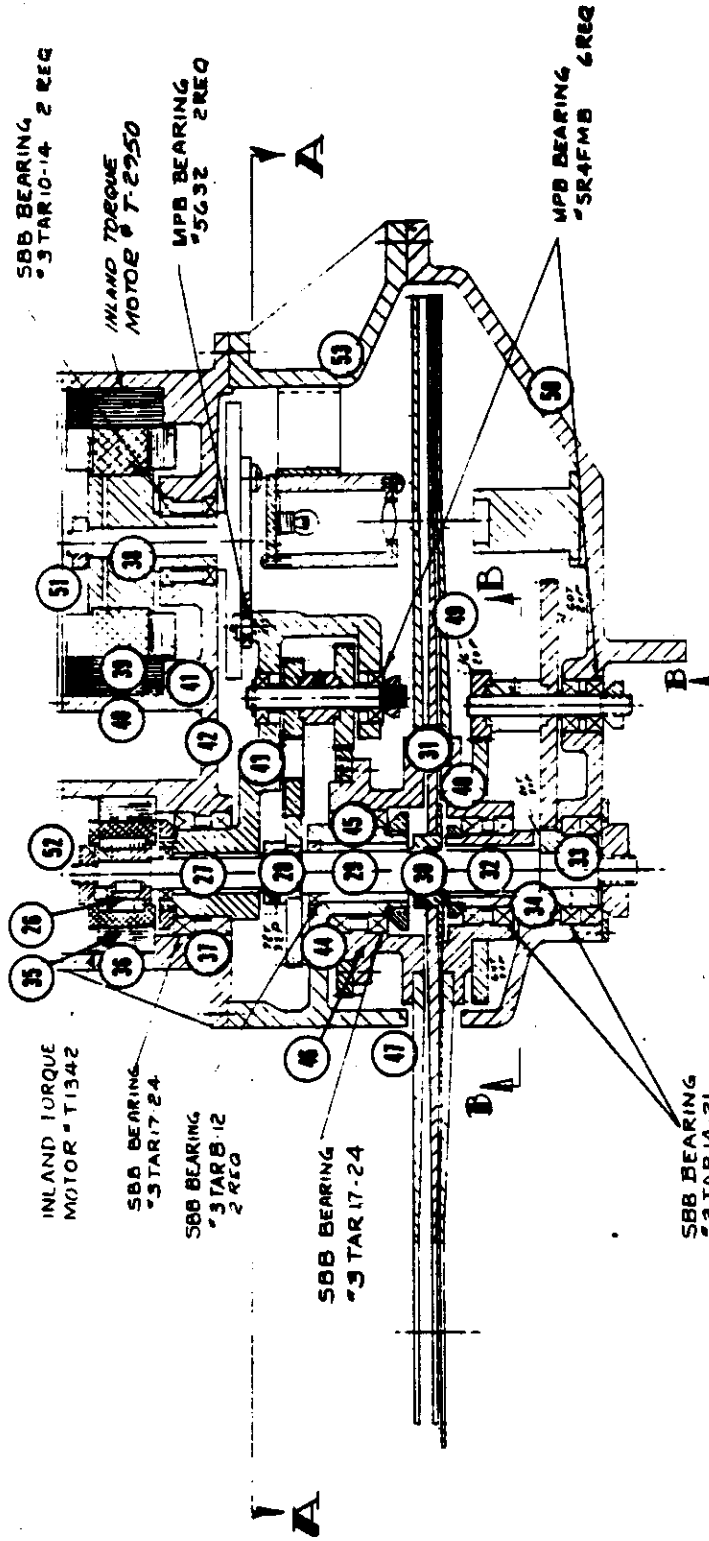


Fig. 2-89(b) — Terrestrial camera nodal Model 3, primary shutter (circled numbers indicate nodal points)

SECRET

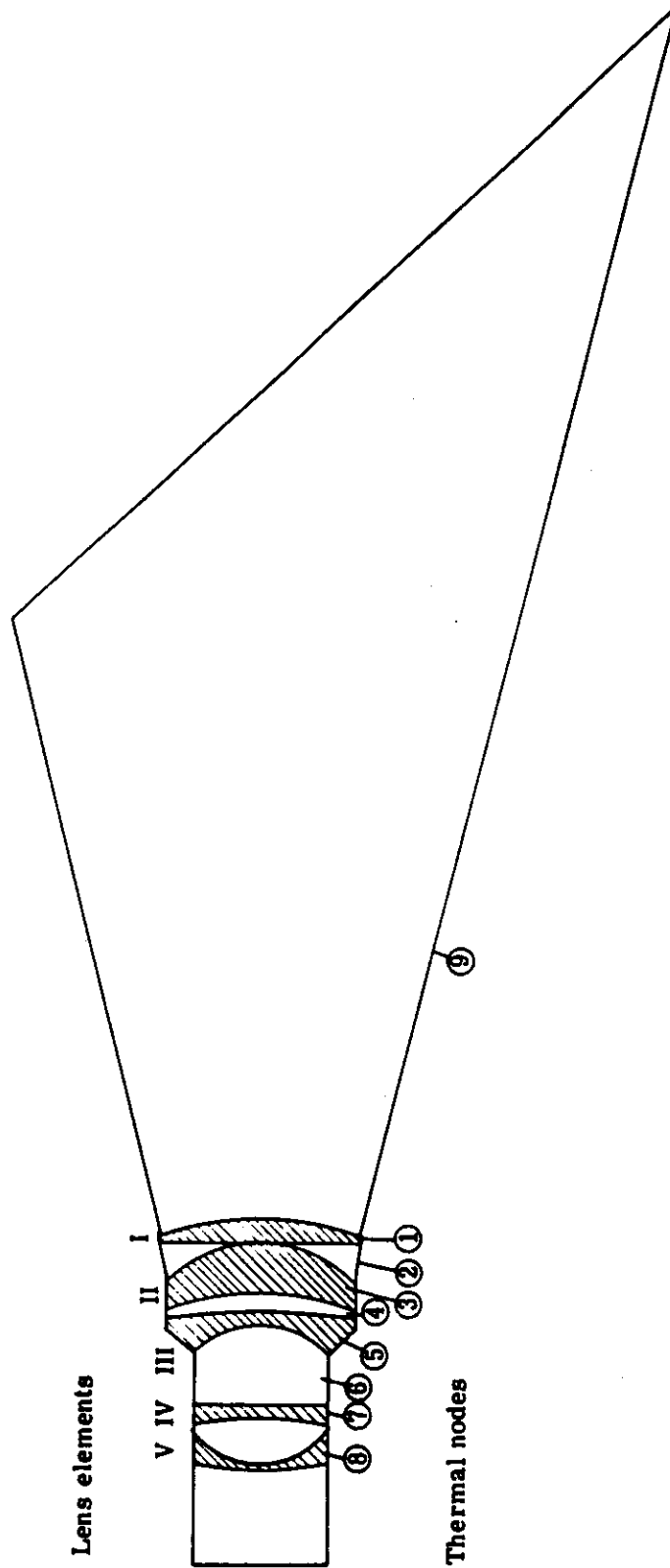


Fig. 2-90 — Stellar camera nodal model

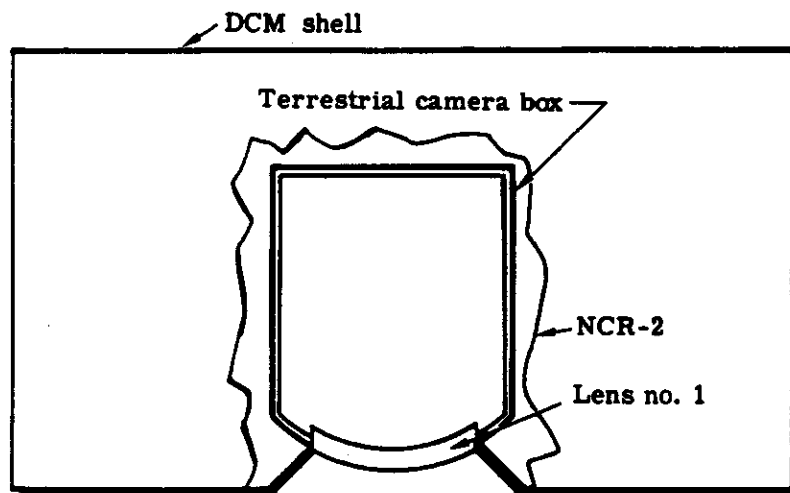


Fig. 2-91 — Simplified DCM thermal model

SECRET

In the absence of a specified thermal environment, the temperature responses of the lens elements have been determined for several assumed conditions. It was assumed, in some cases, that the incident flux was constant with time, with wavelength being above 3.0 microns. Since the glass is opaque, all energy exchange with surrounding space occurs at the first lens element. In other cases a variable cyclic flux with frequency below 3.0 microns was superimposed on the other flux. This means (in the case of the terrestrial camera) that some of the incident energy passes through the first five lens elements until it encounters the shutter.

2.4.2.5 Analytical Studies

2.4.2.5.1 Terrestrial Camera

The first configuration examined is shown in Figure 2-87. This system consists of the lens elements, a black massless surrounding structure and a single shutter disk. The purpose of this portion of the analysis was to determine system temperature response as a function of incident heat flux. When the lower wavelength (ultraviolet) fluxes were included, it was assumed that all energy passing through the first element was intercepted by a 4-inch diameter area on the shutter. It was further considered that energy loss from the shutter is from this area only (both sides) and that the material has an infinite conductivity. Detailed numerical results of this analysis are shown in Figures 2-92 through 2-95, and are described below.

Figure 2-92 shows the temperature decay in the first element after 0.5 and 1.0 hour as a function of heat flux when this element is subjected to a constant magnitude infrared source. For example, with a flux of 60 Btu per square foot per hour the temperature drops to about 524 °R in the first 1/2 hour and to about 512 degrees in 1 hour. Since the initial temperature was 530 °R, the change is significant. The reason for the decay is that the heat loss at 530 °R is about 135 Btu per square foot per hour. Therefore, for any lower flux there is a net loss in energy from the first elements.

Figures 2-93 through 2-95 show the temperature response of several of the lens elements when the thermal environment consists of a constant infrared flux of 100 Btu per square foot per hour and a cyclic ultraviolet flux. It may be seen from these curves that if the aperture remains open, the temperature gradient through the system will increase with time. Even for the minimum flux case (Figure 2-95) the temperature difference between the first and fifth elements would be about 22 °F after a period of 6 hours (approximately four orbits). There is a twofold reason for the gradient increasing with time. The temperature of the first element is decreasing because of a net loss in energy while the temperature of the fifth element is increasing because of energy being absorbed from the shutter.

The most significant conclusion to be drawn from these curves is the requirement for a thermal cover to be used over the first element when the system is inactive. Regardless of the environment, there would be a substantial temperature change in most of the lens elements if the system is allowed to face a space environment for extended periods of time.

In the next analysis, the nodal model described above was modified by adding an 80-degree extension to the outside of lens element number 1 and changing the shutter disk to three closely spaced disks instead of one. This model is shown in Figure 2-88. As in Figure 2-93, the thermal environment consists of a constant infrared flux of 100 Btu per square foot per hour, and a cyclic ultraviolet flux. The results of this analysis are shown in Figure 2-96. In order to readily determine the effect of the extension, the terminal temperatures from Figure 2-93 are indicated.

SECRET

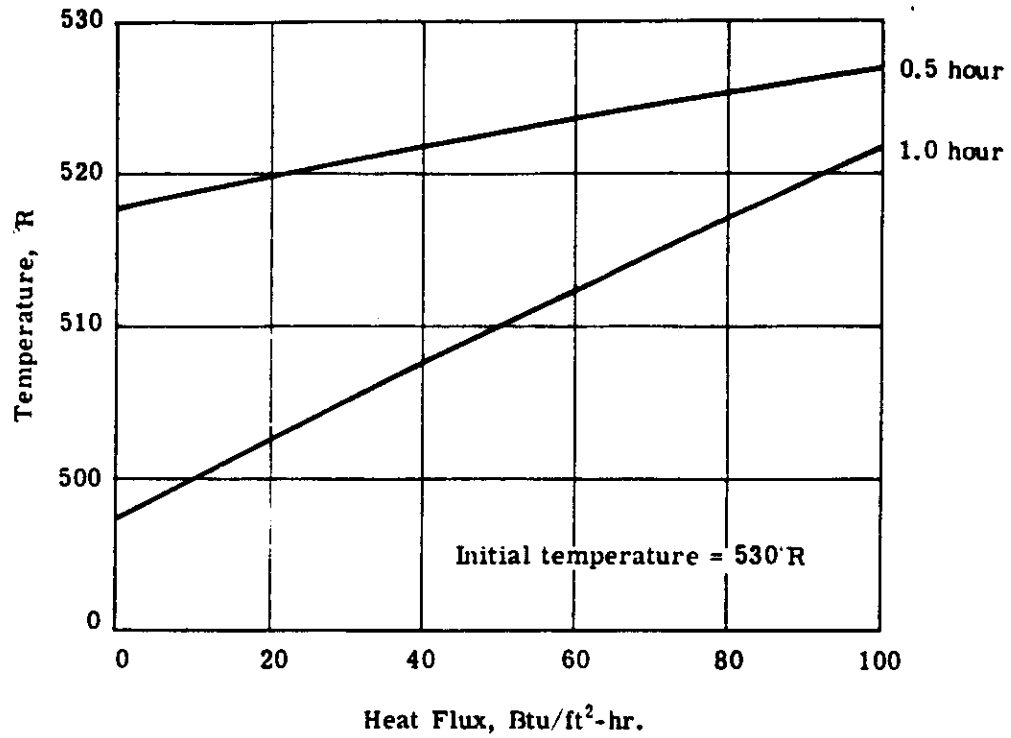


Fig. 2-92 — Temperature of element number 1 when subjected to infrared heat flux

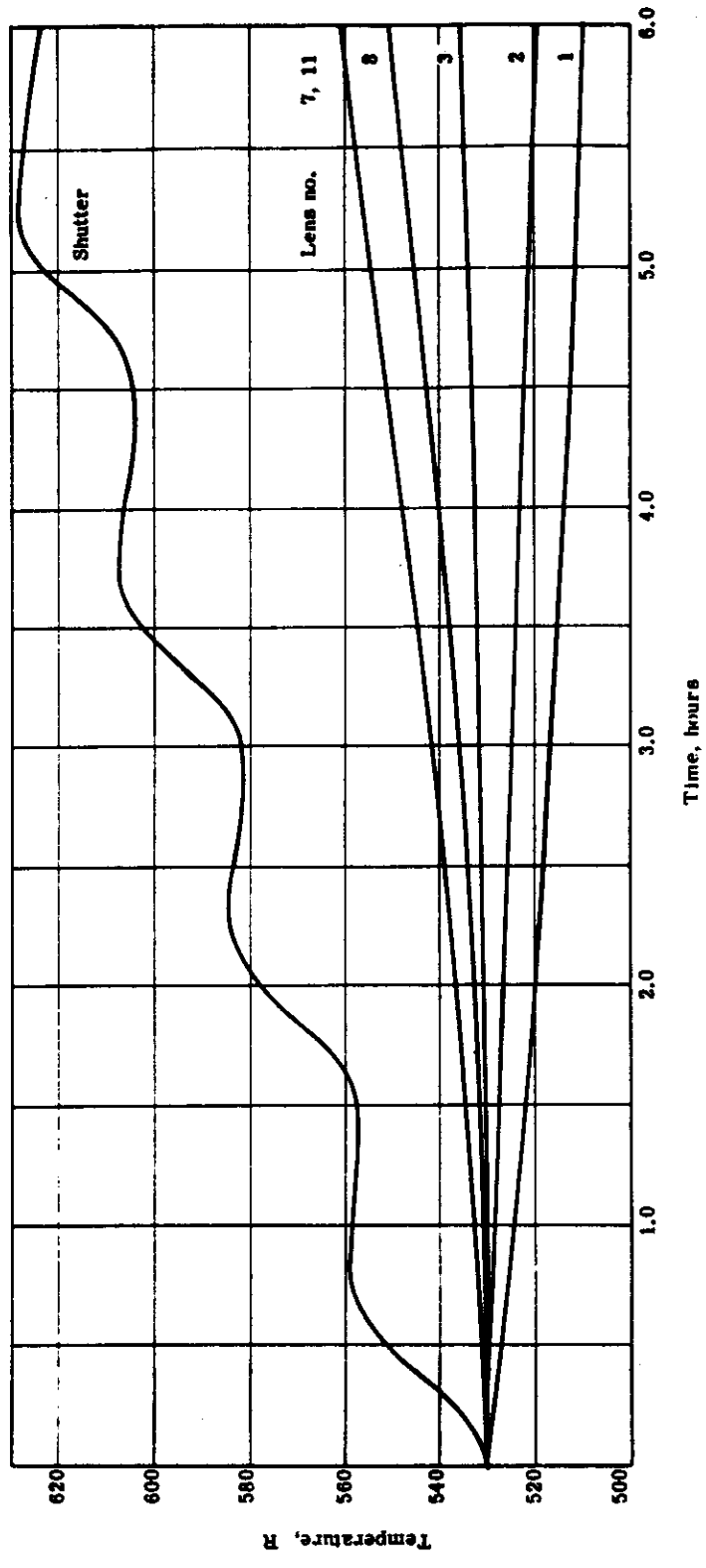
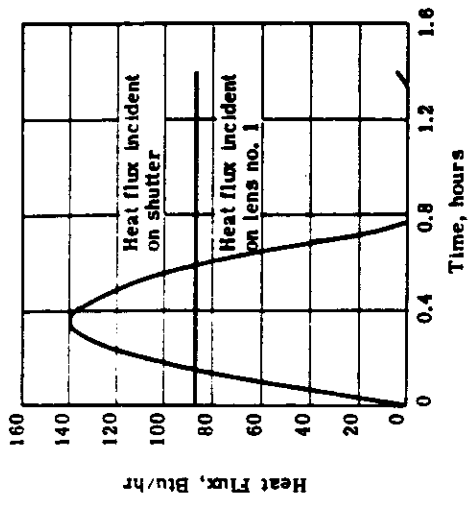


Fig. 2-93 — Lens system temperature response for Model 1 (Fig. 2-87)

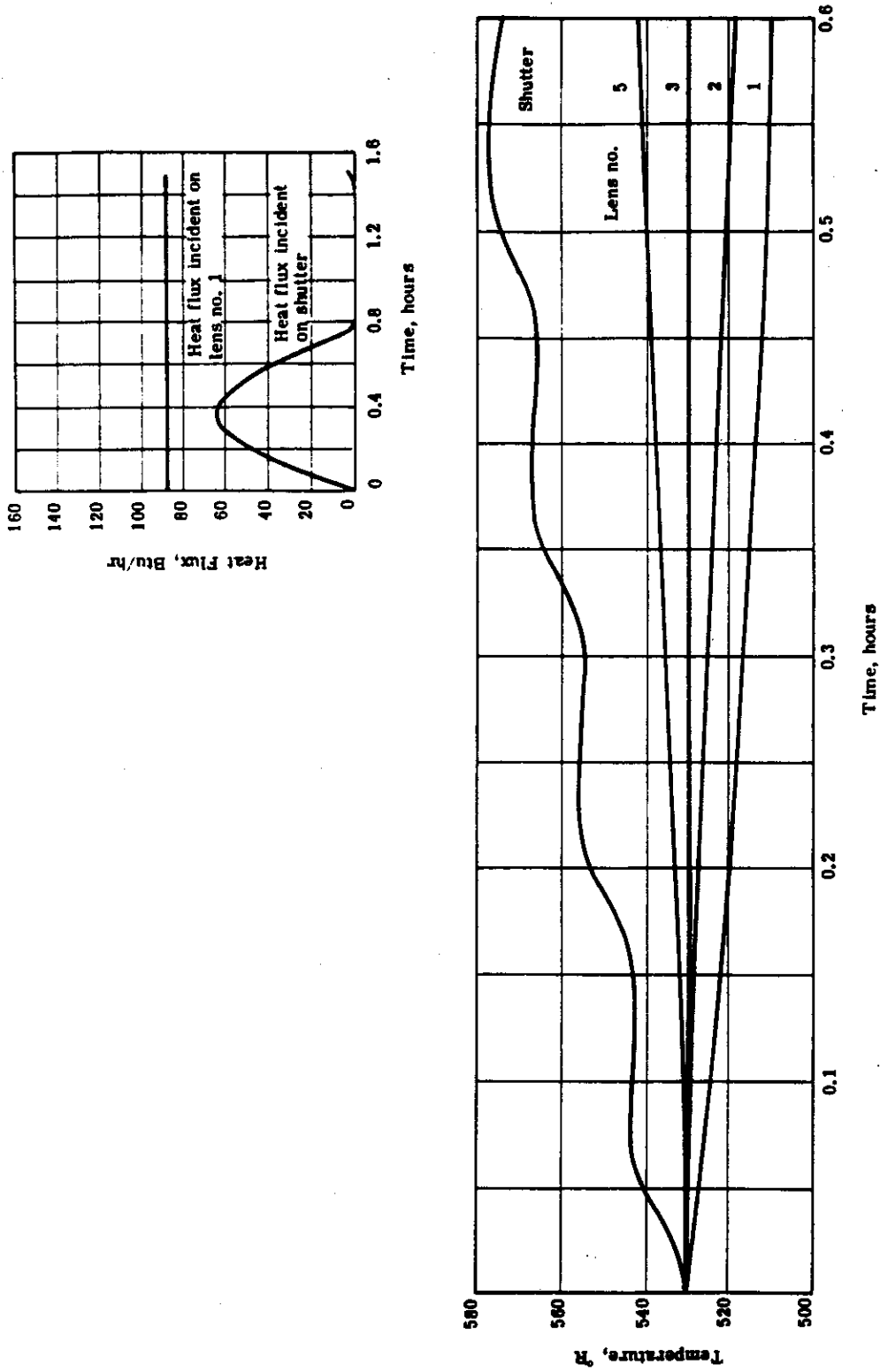


Fig. 2-94 — Lens system temperature response for Model 1 (Fig. 2-87)

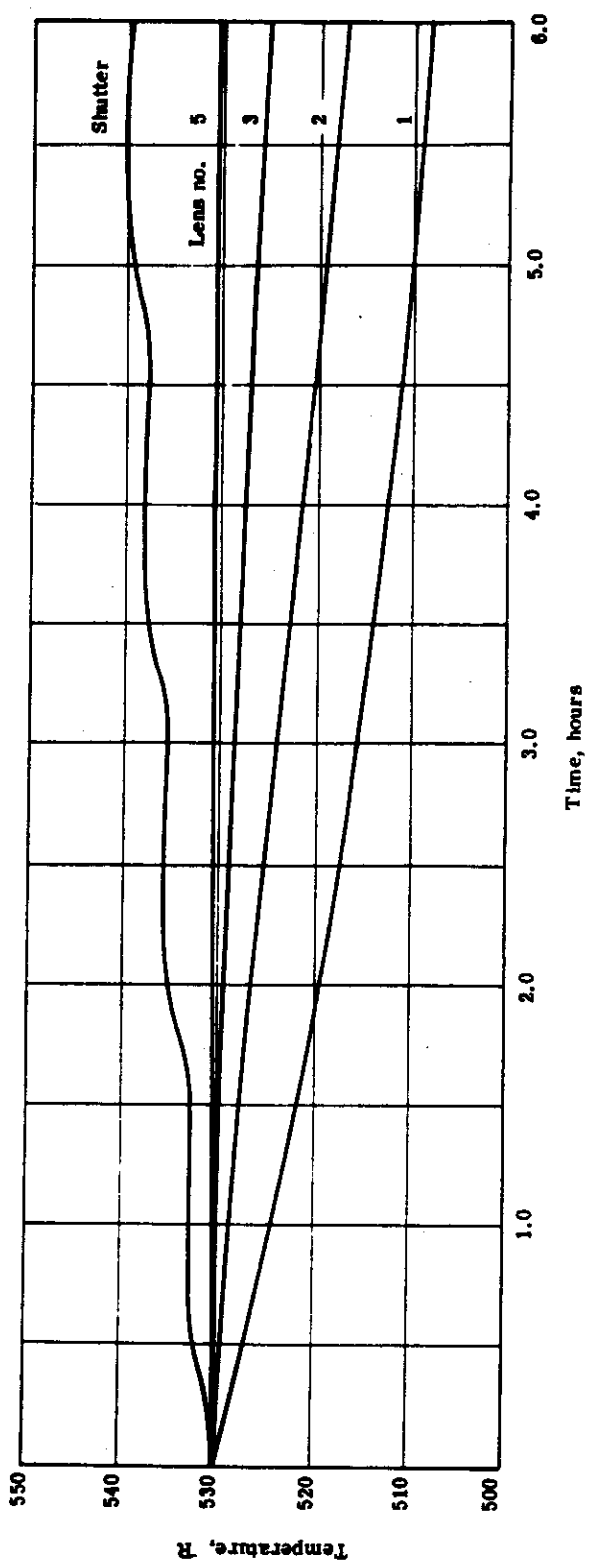
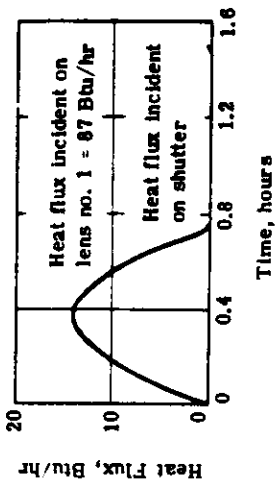


Fig. 2-95 — Lens system temperature response for Model 1 (Fig. 2-87)

~~SECRET~~

Without Extension

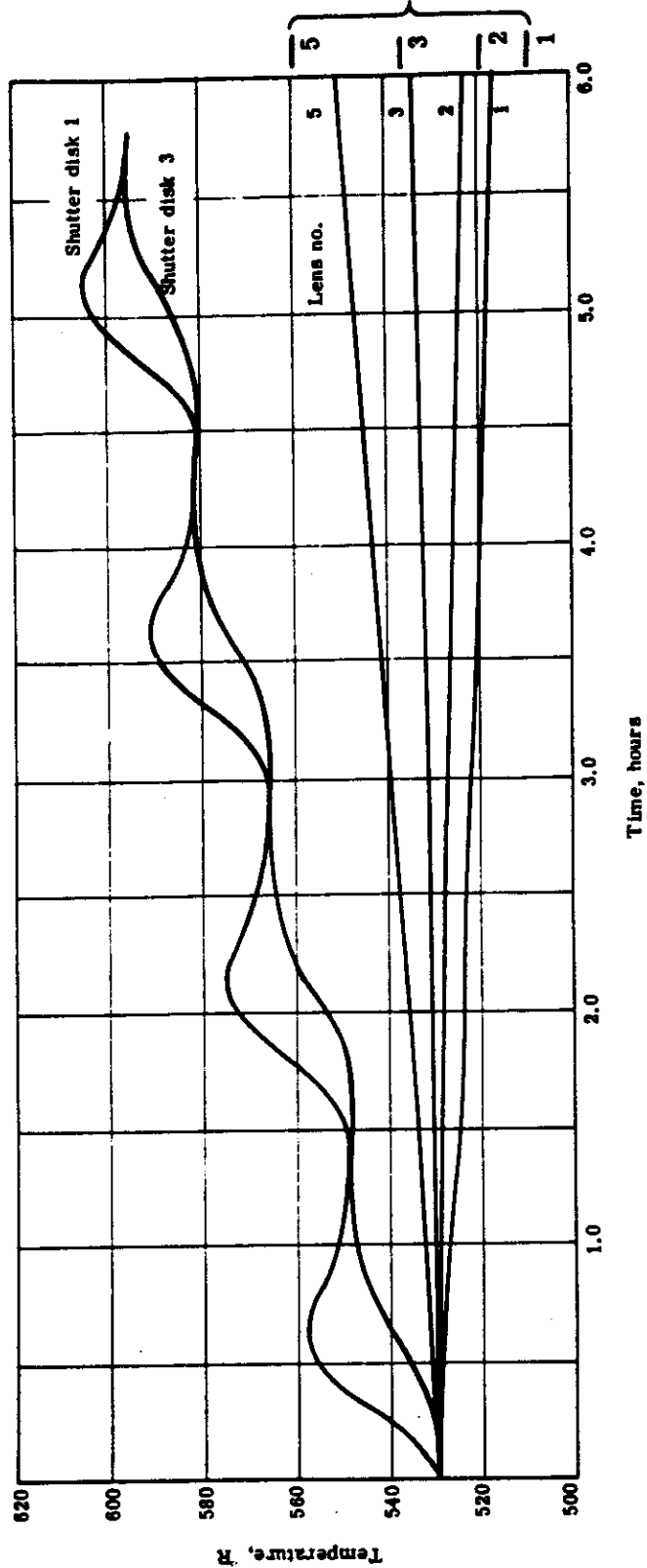


Fig. 2-96 — Lens system temperature response for Model 2 (Fig. 2-88)

~~SECRET~~

~~SECRET~~

Even though the conical extension has damped the lens temperature variations somewhat, it may be seen that after 6 hours there is still a differential between lens number 1 and lens number 5 of about 22 °F. This decrease in the temperature differential results from the fact that the conical extension decreases the net energy loss from lens number 1 while also decreasing the heat flux to the shutter. The gradient has not, however, decreased sufficiently to negate the requirement for a thermal shutter.

The effect of opening and closing the thermal shutter upon the temperature response of the lenses was also investigated, and two cycles were analyzed. The first consisted of an open period of 42-minutes (with the same environment as above) and a closed period of 48 minutes. The system temperature responses for this condition are shown in Figure 2-97. Although the temperature variations are damped somewhat, the gradient through the system is still greater than allowable. In addition, it is apparent that the system does not come back to its initial temperature during the closed period.

The second cycle consisted of a 2-second open period and a 12-second closed period for 40-minutes followed by a 50-minute closed time. Table 2-24 shows the lens element temperatures at several times during this cycle and after the 50-minute closed period. The system temperature gradients appear to be quite small after one cycle. The ΔT from lens number 1 to lens number 5 is about 0.8 °F. However, a final determination of the adequacy of this cycle to maintain specified temperatures depends on the numbers of cycles per mission and the difference between the assumed and actual environment.

The most realistic results were obtained from the analysis of the third nodal model (Figure 2-89) since it is an accurate representation of the terrestrial camera. Unlike the previous analyses, the thermal environment considered is one which exists for a 150-mile circular noonday orbit. That is, an earthshine infrared flux of about 66 Btu per square foot per hour and an albedo of about 35 percent of the solar flux was utilized.

The operating cycle was the same as the previous case, namely a 2-second open period and a 12-second closed period for 40 minutes followed by a 50-minute closed period. Table 2-25 shows the lens element and lens cell temperatures at several times during the operating portion of the cycle and after the 50-minute inactive time. The temperature gradient across the lens cell after one orbit is quite small, as are the temperature changes in the individual lens elements. That is, the temperature difference from lens number 1 to lens number 5 is about 0.3 °F and the maximum individual lens temperature change is about 0.2 °F. Since the camera will be operated in this mode for a minimum of 120 orbits (based on 40-minutes of operating time per orbit), the fact that the temperatures have decreased even slightly during one orbit may at first appear to be of some concern. There are several reasons why this is not a problem:

1. Although the complete camera has been analyzed when subjected to a realistic thermal environment, it has been isolated from the DCM. This is the same as assuming that the camera is perfectly insulated. Under this condition the camera will suffer a net loss in energy whenever the thermal shutter is open. In actuality, the camera is thermally coupled to the DCM shell. By proper selection of the DCM shell's external coating, and a number of layers of aluminized-mylar surrounding the camera, this deficit can be made up.

2. The temperature decrease in lens number 1 cannot be extrapolated to 120 orbits since it is not to be expected that this decay will be linear, but, rather that it will decrease with time.

3. The camera will not operate for 40 minutes every orbit, i.e., it may operate for only a few minutes on some orbits and not at all during others. During this "off time" the temperatures will tend to stabilize.

~~SECRET~~

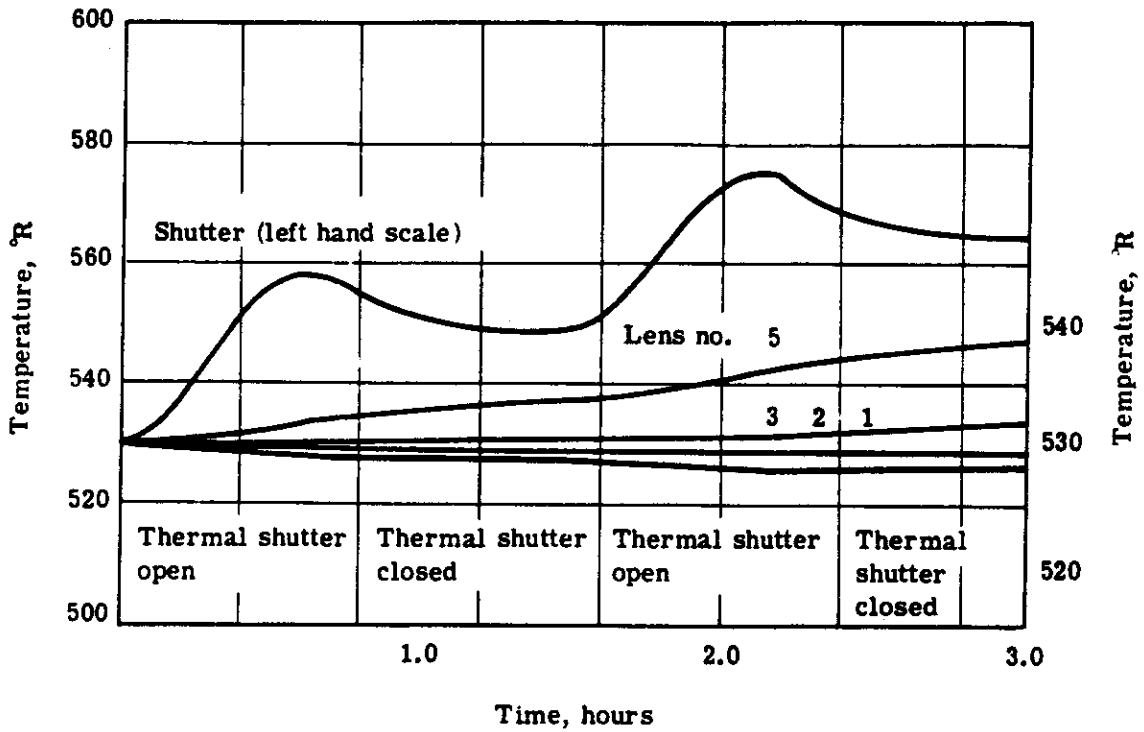


Fig. 2-97 — Lens system temperature response with thermal shutter

Table 2-24 — Terrestrial Camera Lens Temperatures
with Thermal Shutter Cycling

Temperatures, °R

Time, hours	Lens Number 1	Lens Number 2	Lens Number 3	Lens Number 4	Lens Number 5
0	530.00	530.00	530.00	530.00	530.00
0.167	529.74	529.98	529.99	530.00	530.01
0.335	529.72	529.96	529.99	530.00	530.06
0.502	529.71	529.95	529.99	530.02	530.16
0.670	529.65	529.93	529.99	530.05	530.27
0.8 (after closing)	529.67	529.86	530.03	530.22	530.51

Table 2-25 — Terrestrial Camera Lens and Lens Cell Temperatures
with Thermal Shutter Cycling

Temperatures, °R

Time, hours	Temperatures, °R					Lens Cell	
	Lens Number 1	Lens Number 2	Lens Number 3	Lens Number 4	Lens Number 5	Node 2	Node 11
0	530.00	530.00	530.00	530.00	530.00	530.00	530.00
0.107	529.75	529.99	529.99	530.00	530.02	529.98	530.00
0.335	529.61	529.96	529.99	530.00	530.09	529.94	529.99
0.502	529.53	529.93	529.98	530.00	530.17	529.91	529.99
0.670	529.43	529.90	529.98	530.04	530.21	529.89	529.99
0.8 (after closing)	529.77	529.88	529.98	530.04	530.10	529.96	530.05

4. Even if detailed analysis of the camera in the DCM indicates too large a temperature drop in the first lens regardless of insulation and coating selection it could be minimized by installing a heater on the thermal shutter.

The temperature responses of several nonoptical parts of the camera are shown in Figure 2-98. These curves point up to a problem area, namely, the shutter drive and arming motors. It may be seen that as they are currently installed that they will reach excessive temperatures. The drive motor reaches a maximum temperature of about 640 °R during operation which then decays to 567 °R during the 50-minute nonoperational time. During the same period the arming motor temperature reaches 543 °R and then decreases to about 538 °R. There are several possible solutions to this problem which can be examined during the detail design phase. The motors could be relocated outside the insulated housing by lengthening the shaft. Inside-out torquers could be used so that more of the energy generated by the motor would be transferred to the housing. Or still another possibility would be to actively cool the motors through use of cold plates.

There are three temperature criteria which are pertinent in the case of the lens elements. These are: the bulk temperature of each lens element, the temperature difference between the lenses, and the temperature gradient within the elements. For this report the radial temperature gradients in element number 1 of the terrestrial camera were analyzed. Only this element was examined at this point since a gradient in this lens element would be more deleterious to system performance than a gradient in the others.

The thermal model used in this analysis is basically the same as in Figure 2-88. The difference is that element number 1 (node 1) was subdivided into 3 nodes (see Figure 2-99) namely, a center disk and two concentric rings. Conduction between these nodes, as well as the radiant energy interchange between each part of the lens element and the surrounding nodes was considered. The thermal environment was the same as considered in previous cases.

In the first case analyzed, the thermal shutter was allowed to remain open for 40 minutes and was then closed. Figure 2-100 shows that the temperature difference from the edge to the center of the lens is about 3.5 °F after 40 minutes. As expected, the lower temperature is at the center. This occurs primarily because the capacity for heat-loss to space relative to the nodal mass is much greater for the inner disk than for the outer ring, that is, the ratio of the product of nodal for the outer ring. The decay of temperature gradient with time is shown in Figure 2-100. It should be noted that the gradient decreases exponentially to one-half the initial value in about 0.29 hour. Even though it has decreased to a tolerable level in less than 50 minutes this mode of operation would not be acceptable since the gradient would be too steep during the 40-minute open period.

From the above results, an approximation has been made of the radial gradient which would exist for a cycle consisting of a 2-second open period and a 12-second closed period, which continues for 40-minutes and is followed by a 50-minute closed period. A conservative estimate of this was derived in the following manner. During the 30-minute open-close part of the cycle the thermal shutter is open for a total of approximately 350 seconds. A conservative value of the gradient (because the 12-second closed periods are ignored), after the first 40-minute cycle, is obtained from Figure 2-100, and is found to be about 0.18 °F. Following this procedure, the radial gradient as a function of 90-minute cycles was obtained, and is shown in Figure 2-101.

2.4.2.5.2 Stellar Camera

A preliminary analysis has been made of the temperature response of the stellar camera when the aperture is facing deep space. The nodal model for this system was shown in Figure 2-90.

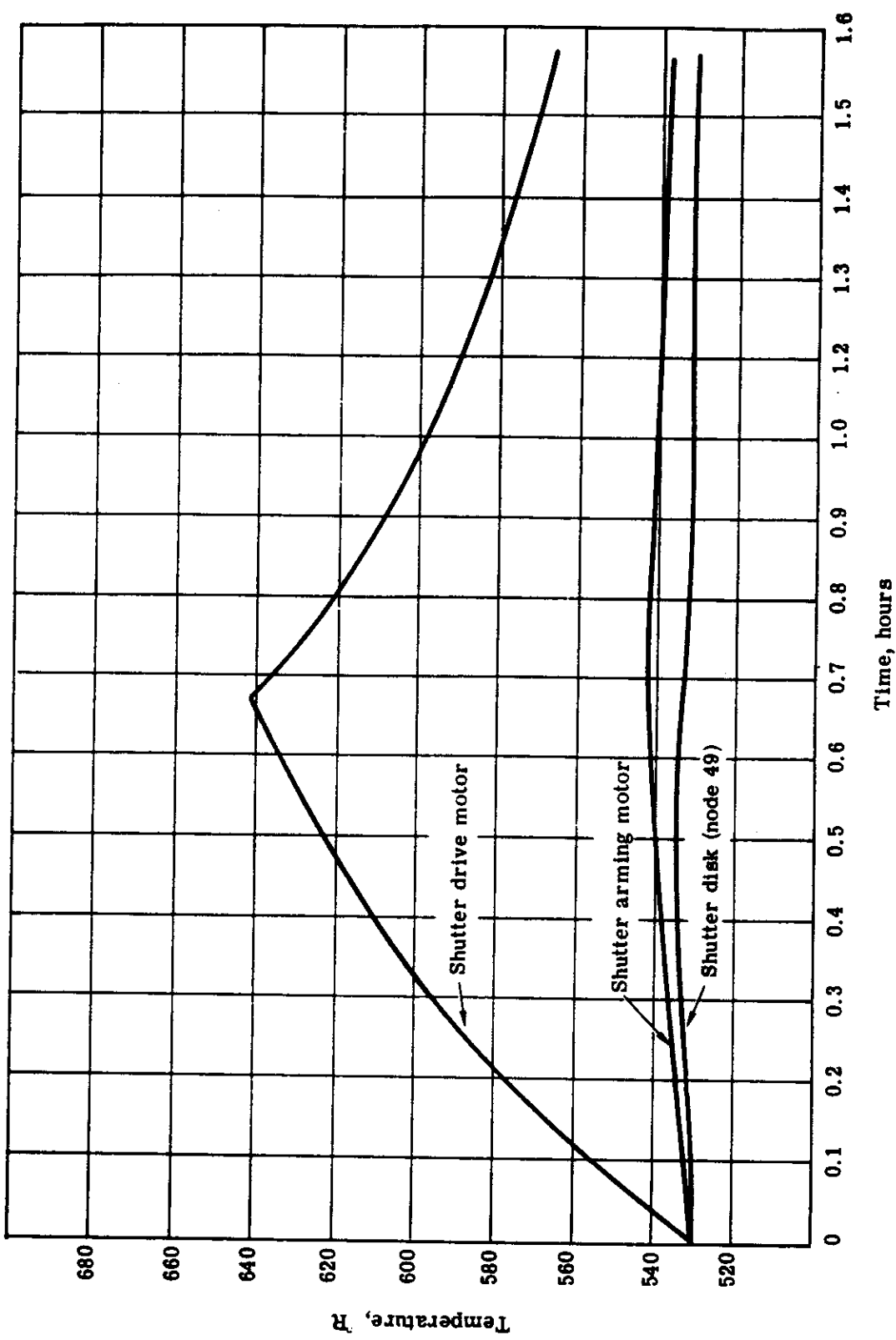


Fig. 2-98 — Terrestrial camera shutter and motor temperatures

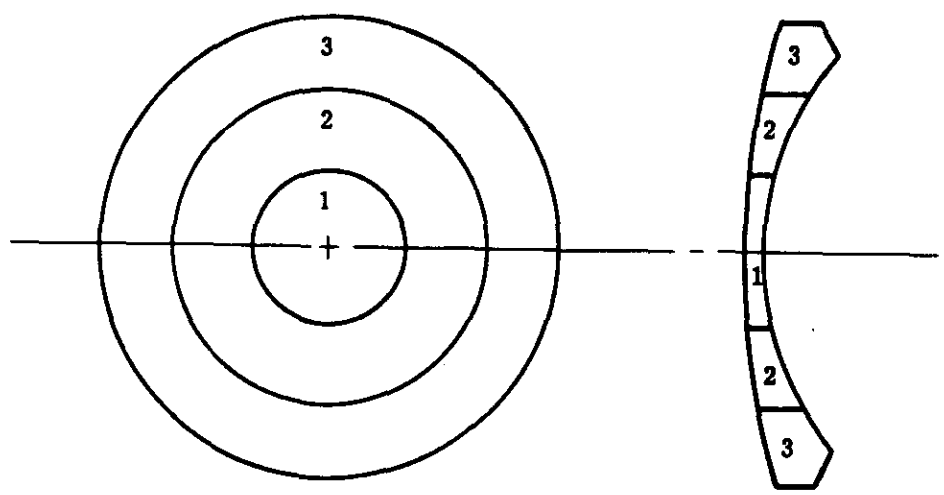


Fig. 2-99 — Lens element 1 nodal scheme

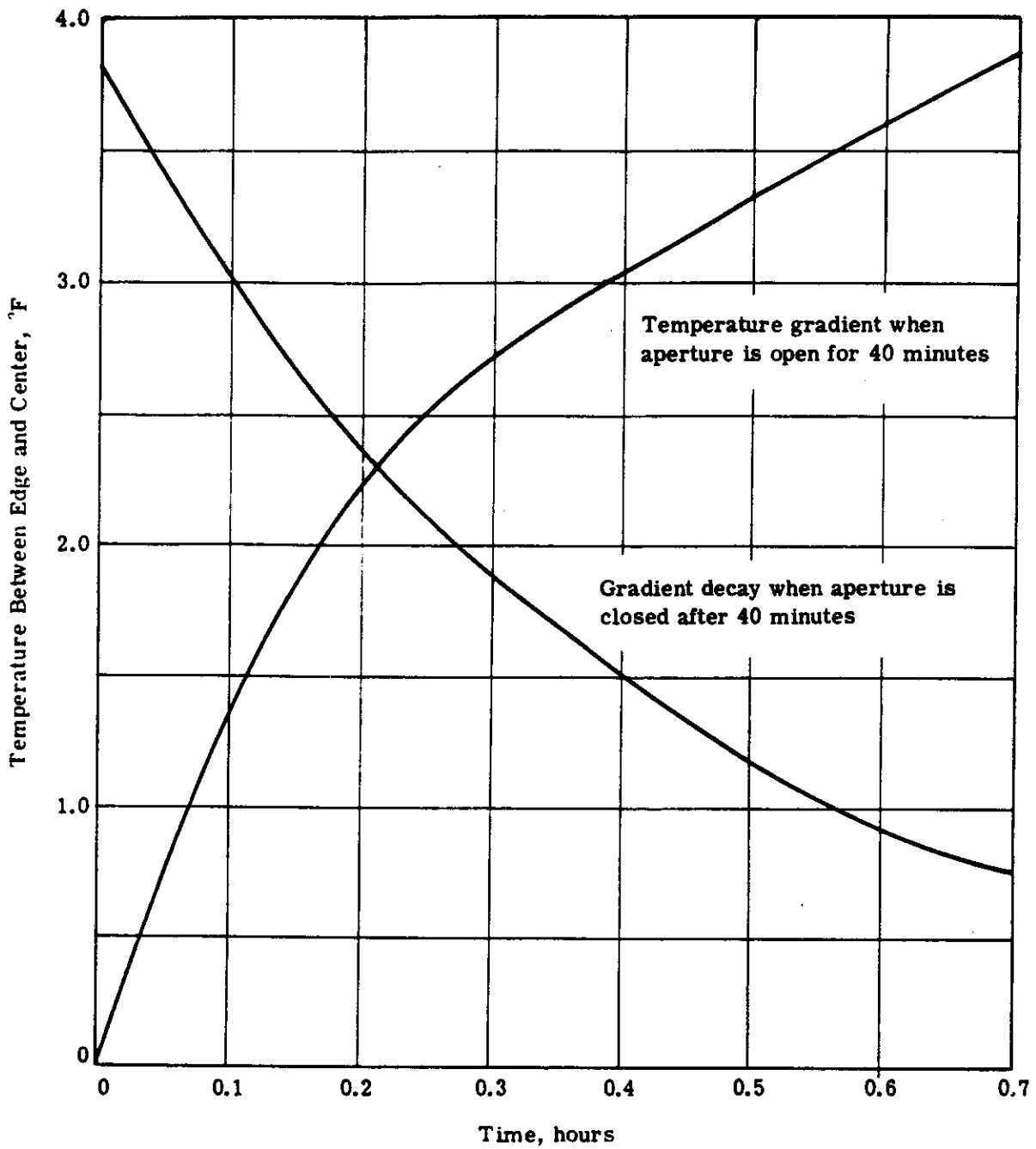


Fig. 2-100 — Lens element 1 radial temperature gradients

It consists of the lens elements, the surrounding structure, and a conical extension. Even though the temperature limits on the lens elements are fairly broad, it is necessary to include a thermal cover at the end of the conical extension to minimize temperature decay, since there is no thermal energy entering the system.

In this analysis it was assumed that the stellar camera operates on the same cycle as the primary, i.e., open for 2 seconds and closed for 12 seconds for a period of 40 minutes. It may be seen that after only one 40-minute period the temperature of lens number 1 has dropped 5 °R. The temperatures of the lens elements were found to be as shown in Table 2-26. When the cover is then closed for 50 minutes, the temperature of lens number 1 will be partially restored. It is likely, however, that in order to avoid too large a temperature drop, energy will have to be added to the system during the closed portion of the cycle. This might be accomplished by putting a heater on the inside of the thermal cover.

2.4.2.5.3 Data Collection Module (DCM)

The analyses presented up to this point have not considered the vehicle or DCM, but rather have been concentrated on the terrestrial camera. A detailed analysis of the complete system (DCM containing terrestrial and stellar cameras, film spools, etc.) during a full mission must await Phase II. It was felt, however, that even some limited preliminary results would be of value at this point.

The main purpose of this analysis was to test the assumption that the camera box can be passively maintained at 70 °F ± 10 °F. The configuration considered was previously described and is shown in Figure 2-91. In order to determine the heat flux incident on the DCM shell, it was assumed that the vehicle was in a 150-mile circular orbit oriented such that the earth-sun line falls within the plane of the orbit (a noonday orbit). Both the direct solar flux and earthshine can be accurately determined, however, this is not so for the albedo flux. The average earth albedo is found to be from about 34 to 40 percent of the solar flux; therefore, in these calculations a value of about 36 percent was used.

Since this is an order-of-magnitude calculation, the camera operating cycle of 2-seconds open and 12-seconds closed was not used. The same ratio of open time to closed time was maintained; however, the cycle was changed to a 1-minute open and 6-minutes closed. It is expected that this will yield approximately the same results while considerably reducing required computer time.

In this analysis the variables which have the strongest effect on the camera box temperature are the ratio of absorptivity to emissivity (α/ϵ) of the DCM external coating and the number of layers of aluminized-mylar covering the camera. Calculations were performed for three sets of these variables as indicated below.

	Number of Orbits	Layers of NRC-2	α/ϵ
1	5	5	1.1
2	5	3	1.1
3	1	3	1.2

The results of these calculations are shown in Figures 2-102, and 2-103. It can be seen that even though the shell temperature undergoes wide variations with time, the camera box temperature has changed by only about 0.3 °F during five orbits, thereby indicating the effectiveness of the aluminized-mylar in damping out temperature oscillations. When it is considered that no attempt was made to optimize the absorptivity-emissivity ratio (α/ϵ) or the number of layers of NRC-2 it seems evident that the camera box can be passively maintained at the desired temperature.

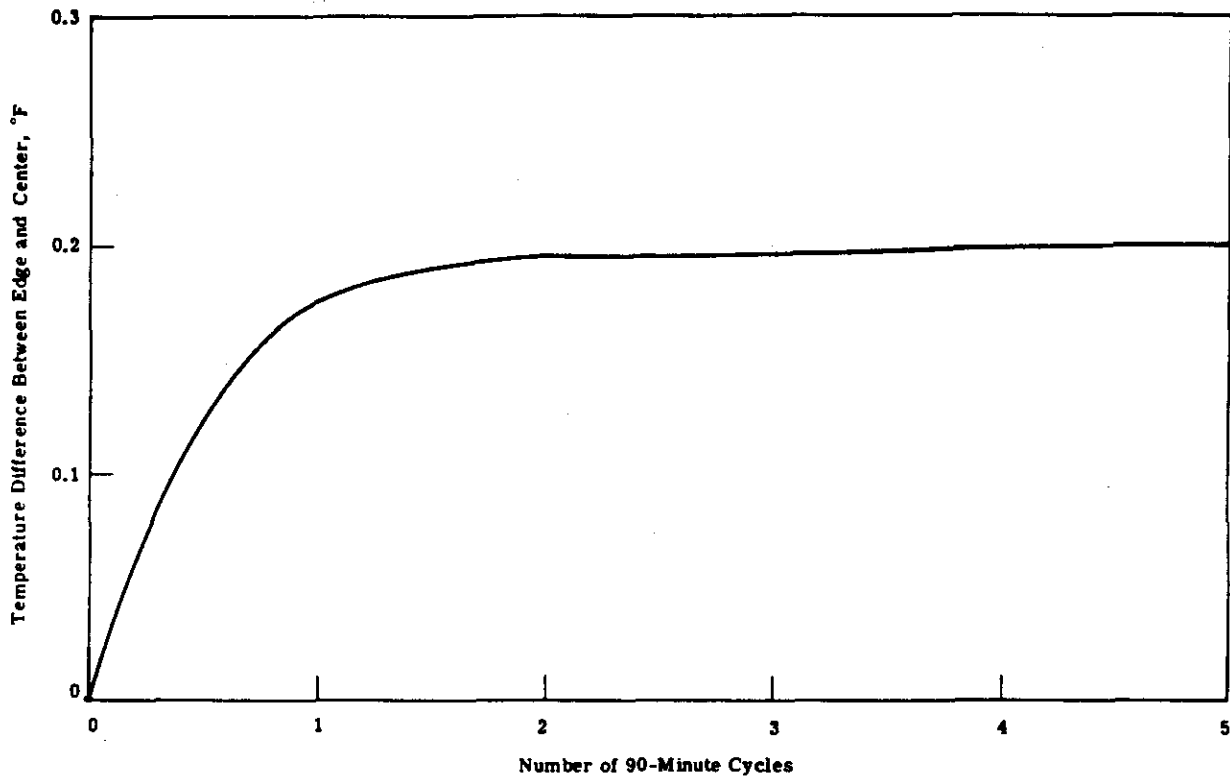


Fig. 2-101 — Lens element 1 temperature gradient after each 90-minute cycle

Table 2-26 — Stellar Camera Temperatures

Lens Number	Temperature, °R
1	524.99
2	529.54
3	529.95
4	529.97
5	529.97

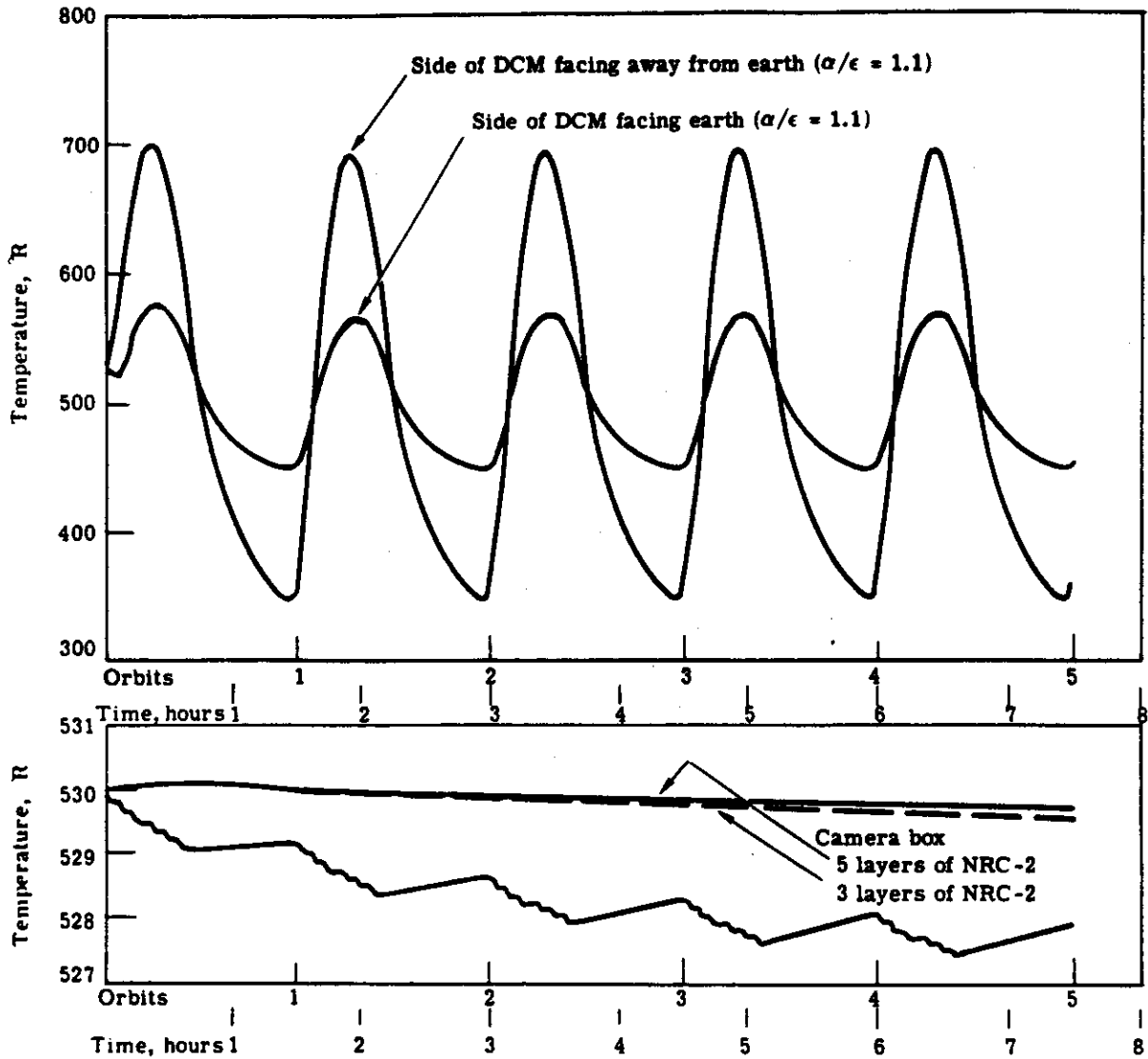


Fig. 2-102 — Camera box temperature response, case 142

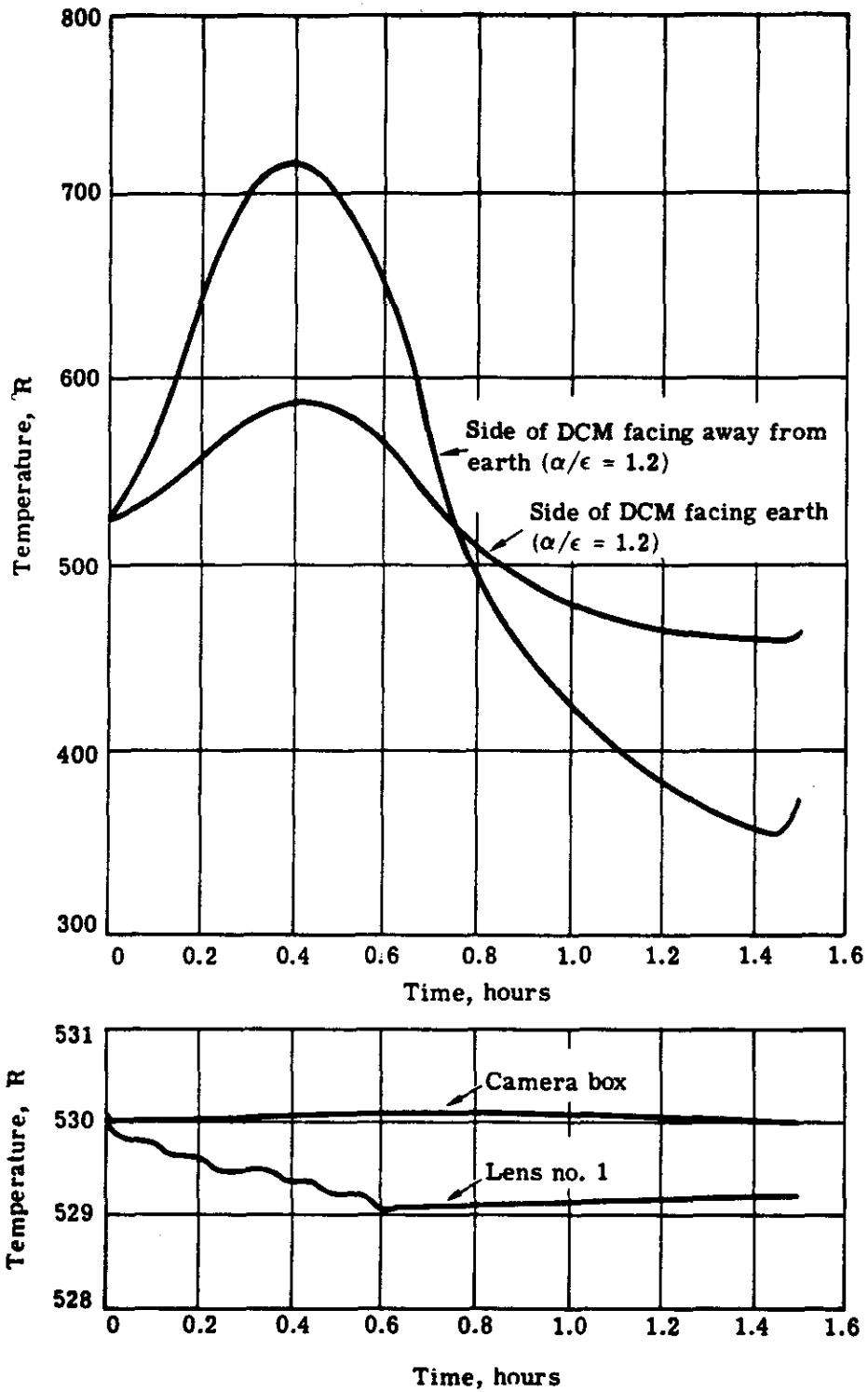


Fig. 2-103 — Camera box temperature response, case 3